ISSN 0003-2670

ANALYTICA CHIMICA ACTA

International monthly devoted to all branches of analytical chemistry
Revue mensuelle internationale consacrée à tous les domaines de la chimie analytique
Internationale Monatsschrift für alle Gebiete der analytischen Chemie

ELSEVIER SCIENTIFIC PUBLISHING COMPANY

AMSTERDAM

Anal. Chim. Acta, Vol. 89, No. 2, 231–433, April 1977

Published monthly

Completing Volume 89

ANALYTICA CHIMICA ACTA

Publication Schedule for 1977

Vol. 88, No. 1	January 1977	
Vol. 88, No. 2	February 1977	**(completing Vol. 88)**
Vol. 89, No. 1	March 1977	
Vol. 89, No. 2	April 1977	**(completing Vol. 89)**
Vol. 90	May 1977	**(complete in one issue)**
Vol. 91, No. 1	June 1977	
Vol. 91, No. 2	July 1977	**(completing Vol. 91)**
Vol. 92, No. 1	August 1977	
Vol. 92, No. 2	September 1977	**(completing Vol. 92)**
Vol. 93,	October 1977	**(complete in one issue)**
Vol. 94, No. 1	November 1977	
Vol. 94, No. 2	December 1977	**(completing Vol. 94)**

Subscription price for 1977 (Vols. 88–95): Dfl. 920.00 plus Dfl. 112.00 postage (approx. U.S.$421.22 inclusive of postage). Claims for issues not received should be made within three months of publication of the issues; if not, they cannot be honoured free of charge. Subscribers in the U.S.A. and Canada receive their copies by airmail. Additional charges for airmail to other countries are available on request. For advertising rates apply to the publishers.

Subscriptions should be sent to:
Elsevier Scientific Publishing Company, P.O. Box 211, Amsterdam, The Netherlands.

GENERAL INFORMATION

Languages

Papers will be published in English, French or German.

Detailed information

Authors should consult Vol. 73, p. 435 for detailed instructions. Reprints of this information are obtainable from Dr. Macdonald or from: Elsevier Editorial Services Ltd., Mayfield House, 256 Banbury Road, Oxford (Great Britain)

Submission of papers

Papers should be sent to:

Prof. Philip W. West,
Coates Chemical Laboratories,
College of Chemistry and Physics,
Louisiana State University,
Baton Rouge 3,
La. 70803 (U.S.A.)

or to:

Dr. A.M.G. Macdonald,
Department of Chemistry,
The University,
P.O. Box 363
Birmingham B15 2TT (Great Britain)

Reprints

Fifty reprints will be supplied free of charge. Additional reprints (minimum 100) can be ordered at quoted prices. They must be ordered on order forms which are sent together with the proofs.


Suprapur®
Ultrapure
reagents

Analytica Chimica Acta, 89 (1977) 231—239

AUTOMATED CATALYTIC ULTRAMICRODETERMINATION OF MANGANESE IN NATURAL WATERS WITH A MINIATURE CENTRIFUGAL ANALYZER

T. P. HADJIIOANNOU*, S. I. HADJIIOANNOU, J. AVERY and H. V. MALMSTADT
School of Chemical Sciences, University of Illinois, Urbana, Illinois 61801 (U.S.A.)
(Received 9th October 1976)

SUMMARY

The application of a miniature centrifugal analyzer to trace analysis by kinetic methods has been studied. A spectrophotometric reaction-rate method based on the potassium periodate—diethylaniline reaction which is catalyzed by manganese has been developed. Ultramicro amounts of manganese in the range 0.13—3.4 ng in 45 μl of sample were determined with relative errors and relative standard deviation of about 2%. The method was applied to the determination of manganese in natural waters.

Analysis of natural waters for the trace metal manganese is usually performed colorimetrically by oxidation with persulfate or periodate to form permanganate [1] or by forming colored products with formaldoxime [2, 3]. Most of these methods require large samples and are time-consuming. Sensitive kinetic methods, based on the catalytic oxidation of diethylaniline by potassium periodate in the presence of traces of manganese, have been developed. The absorbance of the colored product is measured at a fixed reaction time and manganese is determined from suitable calibration curves [4—6]. In these procedures errors associated with absorbance measurements taken while the reaction is in progress are inevitable. In an automatic reaction-rate method based on the periodate—diethylaniline reaction, the time required for the reaction to produce a small fixed amount of yellow product is measured automatically and related directly to the manganese concentration [7].

To reduce substantially the sample size and increase the sample throughput rate, the automatic method was adapted for use on a miniature centrifugal analyzer. In this paper, the modified method for the ultramicrodetermination of manganese in water is presented and the potentialities of this miniature centrifugal analyzer in trace analysis by kinetic methods is demonstrated.

Centrifugal analyzers were conceived and developed by Anderson and coworkers in the Molecular Anatomy group at Oak Ridge National Laboratory

*Visiting Professor of Analytical Chemistry, from the Laboratory of Analytical Chemistry, University of Athens, Athens, Greece.

[8—13] and have been used successfully for microanalytical work, mainly in clinical analysis. These instruments incorporate a rotating multiple-cuvet sample disc and single-beam photometer to obtain the chemical data. Centrifugal force is used to mix aliquots of a reagent directly with several discrete samples and to propel these reaction mixtures radially into the cuvets which are equally spaced on the outer edge of the sample disc. Classical absorption spectrophotometric principles can be employed for encoding the quantitative chemical information into analog electronic signals with subsequent digitization for data processing. A miniature centrifugal analyzer, based on the original Oak Ridge design [10], but incorporating extensive modifications [14] to the measurement and data acquisition system, has been developed and used for the determination of alcohol in blood and of phenobarbital and diphenylhydantoin in serum [15, 16]. The reaction rate in each cuvet is determined by fitting the absorbance values measured over specified time intervals to a least-squares line. Unknown concentrations may then be calculated by the computer either from working curves or from standard addition data.

The automatic method as adapted to the miniature centrifugal analyzer is simple, rapid, accurate, and requires much smaller quantities of sample than conventional methods. Ultramicro amounts of manganese in the range 0.135—3.38 ng in 45 μl of sample can be determined with relative errors and precision of about 2%. The method can be applied for the determination of manganese in natural waters.

GENERAL CONSIDERATIONS

Basic considerations concerning contamination, pH control, and stability of reagents are similar to those previously reported [7]. By adjusting the conditions the reaction is made pseudo first-order with respect to manganese.

The composition of the standard manganese solutions should be similar to that of the samples or the standard addition method should be used [7, 17].

To accomplish thorough mixing and to allow for the reaction induction period the acquisition of data is delayed for 20 s. This results in absorbance data being taken during the period of maximum reaction rate. The computer program allows any subset of up to fourteen samples run on a single disc to be included in the calculation of a least-squares line of rate vs. concentration, from which the concentration of unknown samples can be determined either by a normal working curve method or by more sophisticated standard addition techniques.

EXPERIMENTAL

Instrumentation

The experimental setup is the same as that for the determination of alcohol in blood [15] except that a 470-nm second-order interference filter is used. The entire system is automated with a PDP-8/f minicomputer as a

control, communication, data acquisition, and data reduction device. Operator interaction is accomplished by means of a teletypewriter and an oscilloscope display. In each analytical run 20 absorbance measurements are made during a measurement time of 25 s after delay of 20 s, which includes a 17.1-s mixing cycle. At the end of a data acquisition cycle, the computer processes the data and outputs results, displays and/or prints the absorbance—time plot, displays the working curve, etc., according to responses to an initial dialog.

Reagents

All solutions were prepared with triply distilled water from reagent-grade materials.

Citrate—phosphate buffer, pH 7.1. Mix 100 ml of 0.5 M H_3PO_4 and 100 ml of 0.3 M citric acid, dilute to about 700 ml, neutralize with 3 M NaOH and dilute to 1 l with water.

Potassium periodate, saturated aqueous solution. Dilute with the citrate—phosphate buffer, 1 + 4 and 1 + 9, fresh every day, to give composite reagents 2X and X, for procedures A and B, respectively.

Manganese standards. For the stock solution (100 p.p.m. of manganese) dissolve 0.3076 g of $MnSO_4 \cdot H_2O$ in 1 l of water.

Prepare working solutions (100 p.p.b., 2 p.p.m. and 8 p.p.m. of manganese) from the stock solution by dilution. The 2 and 8 p.p.m. solutions are used for the addition of known amounts of manganese to the water samples. Prepare working standards containing 3, 8, 15, 20, 50, and 75 p.p.b. of manganese from the 100 p.p.b. solution by dilution. Prepare fresh standards daily.

Diethylaniline hydrochloride, 0.020 M. Dissolve diethylaniline (0.298 g) in 20 ml of 0.1 M HCl and dilute to 100 ml with water. Keep this solution in amber bottles; it is stable for several weeks at 4° C. Prepare the 0.0040 M diethylaniline hydrochloride freshly from the 0.020 M solution by dilution; dilute this solution with working manganese standards, 3, 8, 15, 20, 50, and 75 p.p.b. of manganese, 1 + 9, to give composite manganese standards Z_3, Z_8, Z_{15}, Z_{20}, Z_{50}, and Z_{75}, respectively.

Preparation of water samples

In the standard addition method, measurements are taken for 3 solutions, either S_0, S_1 and S_2 (procedure A) or S_0, S_3 and S_4 (procedure B). Solution S_0 is a composite containing the unknown water sample and diethylaniline; solutions S_1, S_2, S_3 and S_4 contain in addition 4.45, 8.9, 17.8, and 35.6 p.p.b. of manganese, respectively. To prepare solution S_0, pipet 1.00 ml of the 0.0040 M diethylaniline hydrochloride solution (DEA) into a 10-ml volumetric flask and dilute to the mark with the water sample. To prepare solution S_2, transfer 1.00 ml of the 0.0040 M DEA solution and 40 μl of the 2 p.p.m. manganese solution into a 10-ml volumetric flask and dilute to the mark with the water sample. Prepare solution S_1 by mixing 2 ml of each of solutions S_0 and S_2. Solution S_4 is prepared as solution S_2 except that the 8 p.p.m. manganese solution is substituted for the 2 p.p.m. manganese

solution. Prepare solution S_3 by mixing 2 ml of each of solutions S_0 and S_4. For the determination of manganese only 0.100 ml of solutions S_1, S_2, S_3, and S_4 are needed for an analysis in duplicate; however, larger quantities are prepared so as to permit sedimentation of suspended impurities and to facilitate sample handling and preparation of composite reagents.

A summary of directions for the preparation of reagents and water samples for the standard addition method is given in Table 1.

Operating procedure

Procedure A, for the range 3—20 p.p.b. of manganese. Pipet 50 μl of water into both cavities of the first (reference) cuvet, using a Pipetman P200 pipet. Pipet 50 μl of potassium periodate solution 2X into all 14 remaining outer cavities of the disc (the second cuvet is not counted since it is used for a background reading). Pipet 50 μl of composite manganese standards Z_3, Z_8, and Z_{15}, each in duplicate, into 6 of the inner cavities of the sample cuvets, and 50 μl each of the samples in duplicate in the remaining inner cuvets. Use the teletypewriter to set the following operating parameters: mixing time 17.1 s during which 4 rapid acceleration and braking operations take place, delay time 30 s, and measurement time 25 s during which 20 absorbance readings are taken. Place the loaded disc on the rotor. The analysis is started and run under computer control. After the analytical run has been concluded, the disc is removed, emptied by applying a vacuum, washed thoroughly with distilled water and allowed to air dry. No disc carryover or memory effects were observed when going from more concentrated to dilute samples such as 150 p.p.b. to 3 p.p.b. manganese.

Procedure B, for the range 20—75 p.p.b. of manganese. Procedure B is similar to procedure A, except that the potassium periodate solution X and the Z_{20}, Z_{50} and Z_{75} composite manganese standards are used.

Data reduction

The maximum reaction rates in each cuvet are automatically determined by a special least-squares program [18]. The unknown concentrations are calculated either by reference to a normal working curve or by analysis of standard addition data.

The slope and y-intercept of the normal working curve are calculated by fitting concentrations and average rates of the manganese standards to a straight line. These values are used to calculate the concentrations of unknown samples from the rates.

In the standard-addition technique, the x-intercept (concentration) is determined for the line fit through values obtained from either S_0, S_1, and S_2 or S_0, S_3 and S_4. The concentration of the unknown is determined by subtracting from this x-intercept the blank, i.e. the x-intercept of the normal working curve. This subtraction compensates for the uncatalyzed reaction, for manganese present as contaminating agent in the reagents used, and for possible manganese adsorption.

TABLE 1

Preparation of reagents and water samples for the standard addition method

Reagent no.	Reagent or sample	Procedure A	Procedure B
1	Phosphate—citrate buffer, pH 7.1		
2a	KIO_4 solution, saturated		
2b	Composite KIO_4 solution 2X	Reagents 2a + 1 (1 + 4)	
2c	Composite KIO_4 solution X		Reagents 2a + 1 (1 + 9)
3	Diethylaniline hydrochloride, 0.0040 M		
4a	Working manganese solution, 2 p.p.m.		
4b	Working manganese solution, 8 p.p.m.		
4c	Working manganese standards, 3, 8, 15 p.p.b.		
4d	Working manganese standards, 20, 50, 75 p.p.b.		
5a	Composite manganese standards, Z_3, Z_8, Z_{15}	Reagents 3 + 4c (1 + 9)	
5b	Composite manganese standards, Z_{20}, Z_{50}, Z_{75}		Reagents 3 + 4d (1 + 9)
6	Composite water samples: S_0	1 ml reagent 3 + 9 ml sample	1 ml reagent 3 + 9 ml sample
	S_2	1 ml reagent 3 + 40 µl reagent 4a + 8.96 ml sample	
	S_1	2 ml S_0 + 2 ml S_2	
	S_4		1 ml reagent 3 + 40 µl reagent 4b + 8.96 ml sample
	S_3		2 ml S_0 + 2 ml S_4

RESULTS AND DISCUSSION

Various initial concentrations of periodate and diethylaniline can be used. By running the various mixtures in parallel on a single disc and using arbitrary subsets of the samples in the construction of the normal working curve, the effects of different reagent and sample concentrations on working curve linearity and slope can be observed and the optimal concentrations chosen. Several combinations of periodate—diethylaniline were tried, in the ranges $5 \cdot 10^{-5}$—$2 \cdot 10^{-3}$ M diethylaniline and about $8 \cdot 10^{-4}$—$8 \cdot 10^{-3}$ M periodate (the saturated potassium periodate solution is 0.02 M at 25° C), with the ratio of periodate concentration to diethylaniline concentration ranging from 1 to 80. The most accurate results were obtained with the combinations $4 \cdot 10^{-3}$ M periodate—$4 \cdot 10^{-4}$ M diethylaniline for the range 3—20 p.p.b. of manganese (procedure A), and $2 \cdot 10^{-3}$ M periodate—$4 \cdot 10^{-4}$ M diethylaniline for the range 20—75 p.p.b. of manganese (procedure B), and these reagent concentrations were chosen as the optimal for the analysis of water samples.

On the basis of rate curve displays on the oscilloscope a delay time of 20 s and a measurement time of 25 s were chosen as the optimal time parameters, so that at least 10 of the 20 absorbance measurements are taken with the rate at the maximum and the effects of curvature due to induction delay or reagent depletion are minimized.

The temperature of the spinning rotor should be monitored and controlled within narrow limits. Work on incorporating a better temperature monitoring and control system into the miniature centrifugal analyzer is in progress. However, even without good temperature control accurate results were obtained because reference materials were included among the samples in each disc. If a single normal working curve is to be used for a series of runs throughout the day the temperature should be controlled and held constant within 0.1° C.

The effect of various ions on manganese determination with the periodate—diethylaniline reaction has been reported [7].

Analysis of aqueous manganese solutions of known concentrations using the working curve method gave the results shown in Table 2. The data indicate that ultramicro amounts of manganese in the range 0.135—3.38 ng (45 μl samples of solutions containing 3—75 p.p.b. of manganese) can be determined with relative errors of about 2%. The relative standard deviation ranged from 0.8% to 3.0%, which includes pathlength variation, pipetting and other instrumental factors. Under the selected conditions for procedure A the reaction is pseudo first-order with respect to manganese in the range 3—25 p.p.b. of manganese; for procedure B the range is 20—75 p.p.b. of manganese. The slopes of the working curves decrease at higher concentrations and therefore the manganese concentrations of the samples should be brought in the aforementioned ranges by appropriate dilution.

The average slopes of working curves obtained according to procedure B on 2 alternate days were $0.954 \cdot 10^{-4}$ (s_r = 1.7%, n = 7) and $0.951 \cdot 10^{-4}$ (s_r = 2.3%, n = 6). The average slopes of working curves obtained according to procedure A on 2 days one week apart were $0.277 \cdot 10^{-3}$ (s_r = 5.7%, n = 6). The large difference in slopes (ca. 12%) in the second case is probably due to temperature differences and concomitant differences in saturated potassium periodate concentrations. The data indicate the feasibility of using a single working curve for a series of runs, provided they are performed at the same temperature and an accuracy of about 5% is acceptable.

As a test of the method, several samples of treated and natural waters from various parts of Illinois, U.S.A., were analyzed by both the working curve and standard addition methods, by procedures A and B. Some of the samples had to be diluted with distilled water to bring their manganese concentrations to the appropriate values, which for the standard addition method are less than 15 and 40 p.p.b. of manganese for procedures A and B, respectively. These samples had also been analyzed by the periodate method [1] at the Illinois State Water Survey. Typical results are shown in Table 3. Given that the analyses were performed in singles by the spectrophotometric method

TABLE 2

Results for aqueous manganese solutions

Manganese Concentration, p.p.b.							
Taken	Found	% error	s_r (%)[a]	Taken	Found	% error	s_r (%)[a]
Procedure A[b]				*Procedure B*[c]			
3.00	2.99	−0.3	1.7	20.0	19.2	−4	3.0
6.00	5.77	−3.8		25.0	25.5	+2	
10.00	10.2	+2		30.0	30.4	+1.3	
15.0	14.9	0.7	1.9	50.0	51.5	+3	
20.0	19.8	−1		75.0	74.6	−0.5	0.8

[a]The values for which relative standard deviations (s_r) are given are based on samples in 4 cuvets, and all others are the average of samples in 2 cuvets.
[b]The Mn standards, 3.00, 8.00, and 15.00 p.p.b. gave rates of 0.597, 2.12, and 4.30 mA s^{-1}, respectively, and the working curve slope was 0.309 mA s^{-1} p.p.b.$^{-1}$ and the intercept was −0.339 mA, and correlation coefficient squared was 0.9999.
[c]The Mn standards 20.0, 50.0, and 75.0 p.p.b. gave rates of 1.79, 4.55, and 6.70 mA s^{-1}, respectively, and the working curve slope was 0.089 mA s^{-1} p.p.b.$^{-1}$ and the intercept was 0.038 mA, and correlation coefficient squared was 0.9997.

and the results for manganese were reported in mg l^{-1},with an uncertainty of 0.01 mg l^{-1}, i.e. 10 p.p.b. of manganese, there is satisfactory agreement between the results obtained with the two methods.

If the rate of the reaction in all water samples was the same for the same manganese concentration, the working curves obtained with pure manganese solutions and those obtained with natural waters would have the same slope. However, this is not the case. Thus, whereas the average slopes of the normal working curves obtained according to procedures A and B with manganese standards were $0.243 \cdot 10^{-3}$ (range: $0.232 \cdot 10^{-3}$—$0.265 \cdot 10^{-3}$) and $0.951 \cdot 10^{-4}$ (range: $0.926 \cdot 10^{-4}$—$0.987 \cdot 10^{-4}$), respectively, the average slopes of the working curves obtained with natural waters by the standard addition method during the same runs were $0.198 \cdot 10^{-3}$ (range: $0.123 \cdot 10^{-3}$—$0.245 \cdot 10^{-3}$) and $0.769 \cdot 10^{-4}$ (range: $0.623 \cdot 10^{-4}$—$0.912 \cdot 10^{-4}$). The difference in slopes of the two kinds of working curves and the large variation in slopes for working curves obtained with natural waters are due to interfering substances that affect the rate of the reaction. Any substance that oxidizes diethylaniline or reduces periodate under the conditions of the procedure, constitutes a potential interference. To compensate for the effect of interfering substances the composition of the standard manganese solutions should be similar to that of the samples. However, since interfering substances may be present in different amounts in the various samples, it is not feasible to prepare such standard manganese solutions. It is therefore concluded that the use of a normal working curve obtained with pure solutions of manganese sulfate in distilled water can often lead to erroneous results (Table 3) and that the standard addition method should be applied.

TABLE 3

Comparison of spectrophotometric and catalytic method results for the determination of manganese in water (Results are given as p.p.b.)

Sample no.	Origin[a]	Manganese Concentration, p.p.b.						
		Spectrophotometric method[d]	Catalytic method[e]					
			Procedure A			Procedure B		
			Standard addition method			Standard addition method		
			With 3 points	With 2 points and average blank	Working curve	With 3 points	With 2 points and average blank	Working curve
1	Fairfield[b]	$266 \cdot 10^1$	2900	2650	2895	2740	2780	2570
2	Rend Lake at Benton[c]	0	10.4	10.2	10.7	6.3	5.9	9.6
3	Colchester	$3 \cdot 10^1$	19.9	19.5	19.5	18.1	18.3	12.6
4	Colchester	$1 \cdot 10^1$	17.0	17.4	13.1	15.9	16.1	12.9
5	Colchester	0	7.0	6.9	5.8	8.4	7.7	7.8

[a] Natural waters from Illinois. [b] Farm pond. [c] Treated sample. [d] Single analysis; results reported on mg l^{-1} with an uncertainty of 0.01 mg l^{-1} [1]. [e] Average of 2 values.

It was found that the blank value does not vary significantly from run to run. It is therefore possible to determine the blank once a day and use this value for subsequent runs. It is also possible to use only 2 solutions in the standard addition method, S_0 and S_2 for procedure A and S_0 and S_4 for procedure B. Thus, the accuracy is slightly decreased, but the number of samples per run is increased by 50%. Results calculated with 2 points and the average blank of 6 runs are given in Table 3 and they agree with those obtained with 3 points and a different blank for each run (sample).

Although the application reported here deals with the determination of manganese in water, the scope of the method is intended to be more general. A basic procedure and general considerations for the determination of manganese are given, so that the method can be adapted to many specific cases, e.g., tissues, bones, serum. In conclusion, the results of this study show that the miniature centrifugal analyzer can successfully be applied to trace analysis by kinetic methods.

The authors express their appreciation to Laurel Henley of the Illinois State Water Survey for supplying water samples. This research was supported in part by NIGMS, NIH Grant HEW PHS GM 21984-01.

REFERENCES

1 Standard Methods for the Examination of Water and Wastewater, 13th edn., APHA, AWWA, WPCF, New York, 1971, p. 206.
2 A. Heriksen, Analyst (London), 91 (1966) 647.
3 J. J. Delfino and G. F. Lee, Environ. Sci. Technol., 3 (1969) 761.
4 E. Kun, J. Biol. Chem., 170 (1947) 509.
5 S. G. Oradoviskii, Zh. Anal. Khim., 19 (1964) 864.
6 F. Dittel, Z. Anal. Chem., 229 (1967) 193.
7 T. P. Hadjiioannou and T. A. Kephalas, Mikrochim. Acta (Wien), (1969) 1215.
8 N. G. Anderson, Amer. J. Clin. Pathol., 53 (1970) 778.
9 N. G. Anderson, C. A. Burtis, J. C. Mailen, C. D. Scott and D. D. Willis, Anal. Lett., 5 (1972) 153.
10 C. A. Burtis, J. C. Mailen, W. F. Johnson, C. D. Scott, T. O. Tiffany and N. G. Anderson, Clin. Chem., 18 (1972) 753.
11 C. D. Scott and C. A. Burtis, Anal. Chem., 45 (1973) 327.
12 C. A. Burtis, W. F. Johnson, J. C. Mailen, J. B. Overton, T. O. Tiffany and M. B. Watsky, Clin. Chem., 19 (1973) 895.
13 T. O. Tiffany, CRC Critical Reviews in Clinical Laboratory Sciences, October 1974, p. 129.
14 J. Avery, R. P. Gregory IV, T. Woodruff, B. W. Renoe and H. V. Malmstadt, Clin. Chem., 20 (1974) 942.
15 T. P. Hadjiioannou, S. I. Hadjiioannou, J. Avery and H. V. Malmstadt, Clin. Chem., 22 (1976) 802.
16 S. D. Brunk, T. P. Hadjiioannou, S. I. Hadjiioannou and H. V. Malmstadt, Clin. Chem., 22 (1976) 905.
17 H. Flaschka and D. Paschal, Anal. Lett., 6 (1973) 101.
18 J. Avery, P. Dryden and H. V. Malmstadt, Anal. Chem., in preparation.

Analytica Chimica Acta, 89 (1977) 241—254

FLOW INJECTION ANALYSIS
PART VIII. DETERMINATION OF GLUCOSE IN BLOOD SERUM WITH GLUCOSE DEHYDROGENASE

E. H. HANSEN, J. RŮŽIČKA and B. RIETZ

Chemistry Department A, The Technical University of Denmark, Building 207, DK-2800 Lyngby (Denmark)

(Received 18th October 1976)

SUMMARY

The flow injection principle is used for enzymatic determination of glucose in blood serum with glucose dehydrogenase. Methods based on single-point determination on deproteinized serum samples, single-point determination comprising continuous flow dialysis, and two-point kinetic assay, are described and discussed. Special consideration is given to optimizing the flow parameters in order to minimize reagent consumption, yet to maintain a high sampling rate. Thus, for the single-point determination, a sampling rate of 120 samples per h was achieved at an expenditure of 3.12 g-units of glucose dehydrogenase per sample.

In enzymatic procedures for the determination of either substrates or enzymes, automated batch and stop-flow systems are usually preferred to continuous flow systems. The reason is that the course of the chemical reaction, the kinetics of which is being followed, can be monitored continuously, and the linear part of the recorded response curve can then be used for evaluation of the analytical result. The presence of lag phase, product inhibition and blank value is easily detected and corrected for in each individual sample.

Although inherently much simpler, continuous flow systems cannot compete with the reliability of batch or stop-flow measurements, because the use of a single flow cell, through which the monitored stream passes continuously, merely permits a single-point measurement to be made on each sample. Therefore, unless an ideal situation is encountered (Fig. 1, curve A) in which the enzymatic reaction on mixing the sample and reagent reaches immediately a velocity proportional to the maximum velocity, the presence of a lag phase and/or product inhibition will invalidate the measurement by affecting the linearity of the read-out. Furthermore, opalescent and coloured solutions, which are often encountered in clinical analysis, may exhibit variable blank values which will adversely affect the single-point assay. The two-point assay (Fig. 1, curves B and C) would obviously give more reliable results as the incubation intervals could be varied by placing the measuring stations at a suitable distance along the line, so that only the linear portion of the response curve which corresponds to the maximum rate would be used for evaluation.

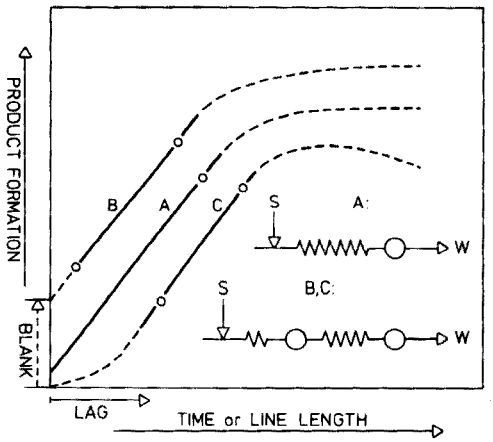

Fig. 1. Single-point (A) and two-point (B, C) kinetic assays in the presence or absence of blank and lag phase. Note that product inhibition at longer reaction times causes a non-linear rate of product formation.

On air-segmented streams, this concept of two or multipoint kinetic assay is not simple to execute as the bubbles influence the absorbance and disturb the continuous read-out. In the SMAC instrument, which presently is the only one capable of multipoint kinetic assay [1], this problem has been solved by precisely dispensing the volume of air injected into the stream at regular intervals, and by computerizing out the disturbances of the read-out caused by the bubbles [2].

In the flow injection system, multipoint kinetic assay should be — because of the absence of air segmentation — inherently simpler to execute. Additionally, the incubation intervals could be more precisely timed as, in the absence of air, the pulsation of the stream is minimized and the travel pattern of the sample from the point of injection to the measuring stations is better defined. The purpose of the present work was therefore to test the utility of the flow injection method in kinetic assays, and to compare various approaches to blank correction with regard to their precision and accuracy and their time and reagent consumption.

The determination of glucose in blood was chosen as an example, as it is the most frequently performed assay in the clinical laboratory. Most chemical procedures applied for the determination of glucose rely on the reducing action of this sugar, so that other reducing compounds cause high results. Various enzymatic reactions have therefore become more commonly used. Although in principle these are more specific than inorganic redox reactions, redox-type interfering mechanisms may still be encountered, e.g., in the procedure suggested by Hugget and Nixon [3] where the method is based on the use of glucose oxidase (GOD) and peroxidase (POD).

$$\text{D-Glucose} + H_2O + O_2 \xrightarrow{\text{GOD}} \text{D-gluconic acid} + H_2O_2 \qquad (1)$$

$$H_2O_2 + DH_2 \xrightarrow{POD} D + 2H_2O \quad (2)$$

in which the liberated hydrogen peroxide oxidizes the reduced form of the *o*-dianisidine dye (DH_2) into D, the colour of which is measured at 436 nm. The quantity of the oxidized dye-form is inevitably affected by reducing species like ascorbic acid, uric acid and creatinine [4]. Replacing *o*-dianisidine with another chromophore such as 2,2′-azino-di-(3-ethylbenzthiazoline)-6-sulphonate is said to improve the selectivity of the method [5].

Most recently, a specific reaction of glucose dehydrogenase (GDH) with β-D-glucose has been investigated and employed successfully by Banauch et al. [6] for assay of biological materials.

$$\alpha\text{-D-Glucose} \xrightarrow{\text{mutarotase}} \beta\text{-D-glucose} \xrightarrow[NAD^+]{GDH} \text{D-glucono-}\delta\text{-lactone} + NADH + H^+ \quad (3)$$

The rôle of the mutarotase is to accelerate the conversion of α- to β-glucose, while the nicotinamide adenine dinucleotide (NADH) acts as a chromogen which can be measured at 340 nm. As the enzymes have now become readily available from commercial sources [7], this enzymatic reaction was adopted for the flow injection system.

To avoid the problems associated with the variable blank value in blood serum samples, it was decided to test and compare the following approaches:

1. single-point determination with deproteinized serum samples;
2. single-point determination with continuous flow dialysis;
3. two-point kinetic determination.

EXPERIMENTAL

Reagents

All reagents were of p.a. quality and distilled water was used throughout.

The enzyme-containing buffer solution was prepared on the basis of the commercially available enzyme set System Glucose from Merck (Cat. No. 14.055). The set consisted of two types of freeze-dried solutions, one containing glucose dehydrogenase (β-D-glucose: NAD-oxidoreductase, EC 1.1.1.47) and mutarotase (aldose-1-epimerase, EC 5.1.3.3), and one containing the coenzyme NAD (β-nicotinamide adenine dinucleotide, β-NAD^+). One bottle of each solution was dissolved in 500 ml of 0.15 M sodium chloride containing 0.12 M ammonium hydrogenphosphate buffer of pH 7.66, yielding a final concentration of the enzymes of 5.2 kU l^{-1} glucose dehydrogenase, 0.11 kU l^{-1} mutarotase and 1.1 mmol l^{-1} NAD, respectively.

Glucose standards were prepared by dissolving D(+)-glucose monohydrate (Hopkin and Williams Ltd., England) in distilled water.

The serum samples were two serum pools (University Hospital of Copenhagen) of normal and elevated glucose value, respectively, and three commercially available freeze-dried serum standards: Technicon SMA Reference Serum 2; Monitrol I (Dade, Lot No. LTD 131 A,B); and Monitrol II (Dade,

Lot No. PTD 39 A,B). Each of these sera was dissolved in the solvent supplied with the serum and prepared according to the manufacturer's instructions.

In the measuring procedure calling for deproteinization of the serum samples before analysis, deproteinization was effected by taking 0.5 ml of serum and diluting it with 0.33 M perchlorate solution (Merck, Cat. No. 9431; pH 1.1) in the ratio 1:10 or 1:16, in centrifuging tubes. After careful mixing, the mixture was centrifuged for 20 min at 6000 r.p.m., whereupon the supernatant was used for analysis.

Apparatus

The flow injection analyzer systems used were essentially similar to those described previously [8, 9]. Reagents were pumped (here with a Technicon AutoAnalyzer Model II peristaltic pump) into the manifold into which the sample was also introduced, either by manual or by automatic injection [8, 9] (cf. measuring procedures below, and Figs. 2—4). After reaction the mixture went through a flow-cell situated in a Beckman DB-GT spectrophotometer fixed at a wavelength of 340 nm, and from there to waste. Polyethylene tubing (0.75 mm i.d., unless otherwise stated) was used throughout for making mixing coils, transmission, reagent and waste lines. The signal from the spectrophotometer was continuously registered with a Radiometer Servograph recorder furnished with a REA input unit.

Two flow-through cells were used, one of 10-mm light path (Helma, type 178-QS, volume 80 μl) and one of 20-mm light path (Helma, type 178-OS, volume 160 μl). To minimize the dead volume, the connecting tubes were in both cases inserted all the way into the terminals of the cells, so that the orifices of the tubes were as close as possible to the light path. The use of flow-cells of smaller aperture would reduce the carry-over, since cells of 3-mm aperture as used in this work connected to 0.75-mm tubing represent a rather large hold-up volume.

The dialysis unit used was similar to the long unit described previously [8] except that the groove of the 75-mm long dialysis path was half-rectangular,

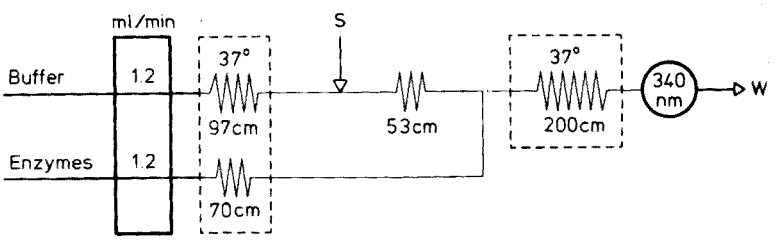

Fig. 2. Single-point assay manifold used for determination of glucose in deproteinized serum samples. All tubes 0.5 mm i.d. The acidic deproteinized serum sample is injected (S, 100 μl) into a preheated phosphate buffer of pH 7.66 and neutralized in the 0.53-m mixing coil before being joined with the enzyme solution. After passing through the 2.00-m thermostated reaction coil the absorbance of the solution is measured at 340 nm, whence the solution is led to waste (W).

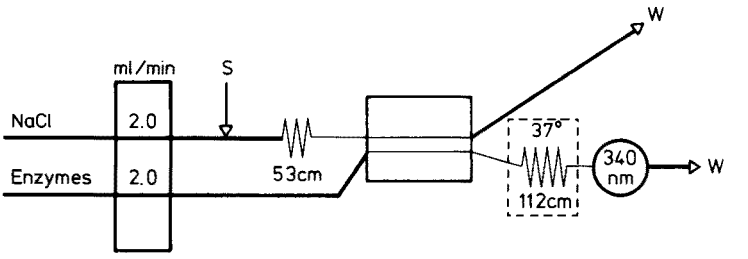

Fig. 3. Single-point assay manifold with continuous dialysis. Thin lines denote tubes of 0.5 mm i.d. The 100 μl samples is injected (S) into a solution of 0.14 M sodium chloride and after mixing in the 0.53-m coil glucose is dialysed into the pH-buffered enzyme-containing recipient stream. The increase of absorbance due to the NADH formed in the 1.12-m reaction coil is measured at 340 nm.

2 mm wide and 0.3 mm deep, thus resulting in a 150-mm^2 surface area and a volume of 45 μl. Two membrane materials were used, Technicon Type C and Cuprophan Type 150 PM (Enke Glanzstoff AG, Germany).

Measuring procedures

Single-point determination with deproteinized serum samples. The system used is shown schematically in Fig. 2; in this case 0.5-mm i.d. tubing was applied. The sample (100 μl) of deproteinized serum (S) was injected into the preheated 0.15 M sodium chloride containing 0.12 M ammonium hydrogenphosphate buffer of pH 7.66. After being neutralized in the 0.53-m coil, the sample was then mixed with the preheated enzyme-containing buffer solution before entering the 2.00-m thermostated reaction coil, whereupon the colour of the $NADH^+$ product formed was measured in a 10-mm flow-cell at 340 nm.

Before analysis, the aqueous glucose standards, which comprised a concentration range of 3—20 mmol l^{-1}, were diluted with the 0.33 M perchlorate solution in the same ratio as the serum samples, i.e. 1:10 or 1:16. The blank value was measured by injecting 100 μl of distilled water diluted similarly with perchlorate solution.

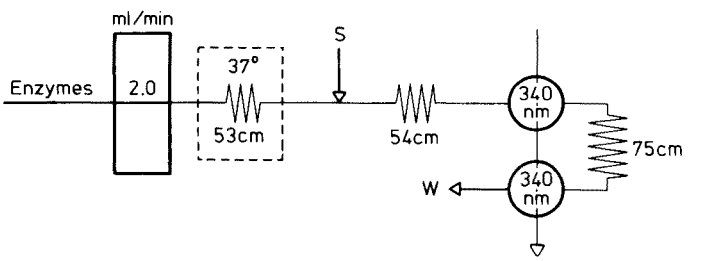

Fig. 4. Two-point kinetic assay manifold used for direct determination of glucose in serum. After mixing in the 0.54-m coil the injected sample (S, 100 μl) enters the first flow-cell from which it passes through the second reaction coil (0.75 m) to the second flow-cell.

Single-point determination with continuous flow dialysis. The system used is shown in Fig. 3; 100 μl of serum sample or aqueous glucose standard was injected at point S into a 0.14 M sodium chloride solution containing 2 % glycerine. After passing through the 0.53-m mixing coil, the solution entered the dialysis unit where the dialyzed material was mixed with the enzyme-containing buffer solution. The colour-forming reaction then proceeded in the 1.12-m mixing coil placed in the thermostated waterbath. Because of the low yields of dialysis, a 20-mm flow-cell was used for monitoring the solution.

Two-point kinetic determination. This procedure was effected with the system depicted in Fig. 4; two 10-mm flow-cells were placed in the same optical path of a single spectrophotometer adjusted to 340 nm. Serum sample or aqueous glucose standard (100 μl) was injected at point S into the pre-heated enzyme-containing phosphate buffer solution. After mixing in the 0.54-m mixing coil, the solution was passed through the first flow-cell, and from there via the 0.75-m mixing coil back to the spectrophotometer through the second flow-cell, after which the solution was led to waste.

RESULTS

Manifolds for all three procedures used (Figs. 2—4) were designed on the basis of preliminary experiments where the yield of the enzymatic reaction versus line length and residence time of the sample was investigated as described previously [8, 9], with a simple straight, thermostated reaction line of variable length. The results of these experiments are summarized in Fig. 5, which shows the increasing yield of the enzymatic reaction with increasing line length (or residence time) at a pumping rate of 2 ml min^{-1}

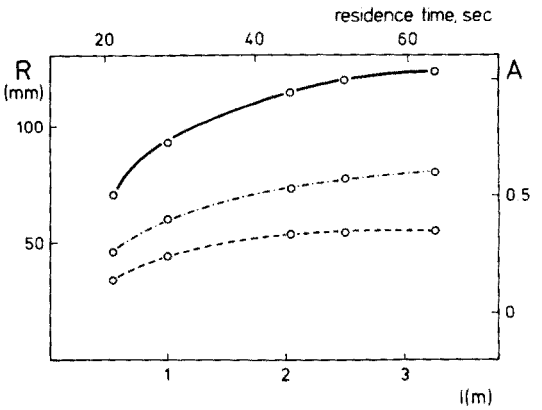

Fig. 5. The product formation of the glucose—mutarotase—dehydrogenase—NADH reaction sequence, monitored at 340 nm, as a function of line length and/or residence time. 20 mmol l^{-1} glucose sample, prior to analysis diluted with distilled water in ratios 1 : 10 (——); 1 : 16 (—·—·—); and 1 : 20 (— — — —).

(i.d. of tubing, 0.75 mm). As the line length is defined as the tube length between the point of injection and the point of measurement, the time of 13 s at length coordinate zero thus corresponds to the residence time of the sample in the measuring cell (i.e., use of smaller flow-through cells would be advantageous as it would allow higher sampling rates). Based on these observations, the position of the measuring station(s) was chosen in such a way that the shortest possible residence time of sample in each of the systems used was attained.

In the single-point determination of glucose in serum samples, two approaches were adopted: deproteinization and dialysis, the purpose of both operations being to eliminate the interference of proteins and minimize the blank value. In the deproteinization procedure, relatively large amounts of perchlorate solution of pH 1.1 are used; neutralization is then necessary before the enzymatic reaction, but this is done automatically in the flow injection system of Fig. 2. A recording of a series of glucose standards and four serum samples is shown in Fig. 6(b) along with a high paper speed recording of a single standard (Fig. 6(a)). By comparing the time span between the point of sample injection (S_1) and sample read-out (R), it is seen that 25 s elapses from sample introduction until the analytical result is available. Provided that the maximum permissible carry-over allowed is 1%, the next sample can be introduced at point S_2, i.e. 5 s after R. This results in an overall sampling rate of 120 samples per h. Statistical evaluation of the calibration graph of Fig. 6 yielded a straight line with a regression coefficient r of 0.999

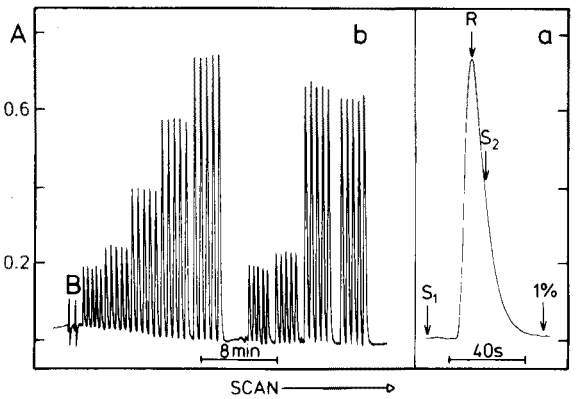

Fig. 6. (a) High paper speed recording of a single glucose peak obtained with the manifold shown in Fig. 2 (S: 20 mmol l^{-1}, 100 μl, dilution 1 : 10). S_1, point of injection; R_1, read-out position; S_2, point of injection of the next sample. 1% refers to the time at which 1% of the maximum absorbance colour of the previous peak (R_1) is left in the flow cell. (b) Series of glucose standards (3.0, 5.0, 10.0, 15.0 and 20.0 mmol l^{-1}) preceded by a blank (B) and followed by four serum samples (serum pool, normal value; Monitrol I; and two different serum pool samples of elevated values). Sample volume 100 μl; dilution 1 : 10; all samples injected in quintuplets. Sampling rate, 120 per h.

and a standard error of 2%. It is interesting to note that despite the deproteinization procedure a blank value corresponding approximately to 1 mmol l^{-1} was encountered. However, this is acceptable for routine analysis. Routine analysis of various samples gave the results shown in Table 1. As various dilution ratios of serum with perchlorate solution are used in the deproteinization procedure [6], a series of dilution ratio 1:16 was investigated in addition to the 1 : 10 series mentioned above. Practically identical results were obtained for both series (Table 1), the regression data for the 1 : 16 series being similar to those obtained for the 1 : 10 series.

To reconfirm the selectivity of the present procedure, the method was checked (a) by adding potentially interfering agents [10] to a serum sample initially containing 10 mmol l^{-1} of glucose, and (b) by standard addition of various amounts of glucose to a serum sample originally containing 20 mmol l^{-1}. In both cases, the 1 : 10 deproteinization procedure was used. No elevation of the recorded glucose values was observed in the presence of ascorbic acid, creatinine or uric acid when these each were added at a level at 10 mmol l^{-1}. The standard addition reconfirmed the selectivity of the method (Fig. 7) and at the same time verified that the linearity of the calibration extends up to 40 mmol l^{-1}.

The procedure involving dialysis was effected in a manifold of the type shown in Fig. 3. Unpretreated serum samples or aqueous standards could be analyzed in this system at a rate of ca. 45 samples per h provided that the maximum carry-over allowed was maintained at a level of 1%. The sampling rate is relatively low because a fairly long residence time of the sample in the dialyser is needed to ensure a sufficient yield of dialysis. Although a 20-mm flow-cell was used, a signal of only ca. 0.1 A.U. was obtained for a normal serum. However, the calibration curve yielded a straight line over the range of 2—20 mmol l^{-1} with a regression coefficient of 0.999 and a standard error

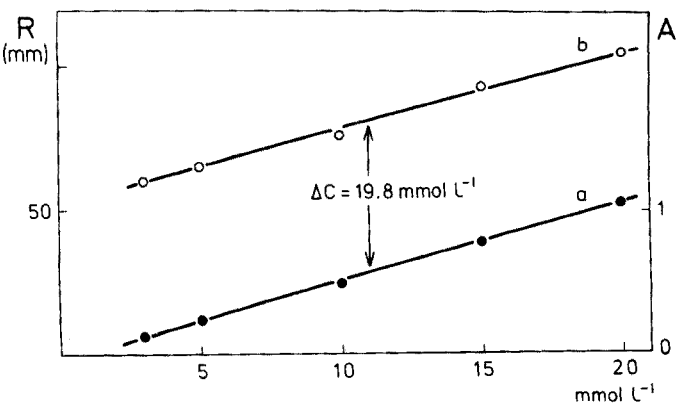

Fig. 7. Standard addition of various amounts of glucose to a sample originally containing 20 mmol l^{-1} of glucose, the experimental conditions being those of Figs. 2 and 6. Dilution ratio 1 : 10. R, peak height in mm; *A*, absorbance.

TABLE 1

Determination of glucose in serum (All results expressed in mmol l^{-1})

Sample	Single-point determinations				Two-point determinations			Reported or assigned values
	Deproteinization and dilution		Dialysis with membrane		Predilution of samples			
	1 : 10	1 : 16	Cuprop.	Techn.	1 : 10	1 : 16	1 : 20	(±2 r.s.d.)
Monitrol I	5.0	5.0	6.4	5.4	4.8	4.5	4.8	5.1 ± 0.5[a]
Monitrol II	12.3	12.4	13.4	13.7	10.6	9.3	10.8	11.9 ± 0.7[a]
Technicon SMA-2	15.1	15.5	13.0	12.8	—	—	—	11.7
Technicon SMA 6/60	—	—	—	12.2	12.2	12.2	13.2	12.6
Serum, normal[b]	4.6	5.0	4.3	—	—	—	—	4.2 — 5.4
Serum, elevated[b]	19.7	19.3	—	20.0	20.8	18.4	18.9	18—20
Reynolds number	102		56		56			
Sampling rate, samples per h[c]	120		45		60			
Enzyme consumption per anal. (g-units)[d]	3.12		13.7		10.4			

[a] Values reported for AutoAnalyzer procedure.
[b] Human serum from University Hospital of Copenhagen.
[c] Allowing max. 1% carry-over between successive samples.
[d] AutoAnalyzer: 12.6 g-units per sample.

of ca. 2%. Furthermore, the values obtained for the serum samples analyzed were satisfactory (Table 1). Comparison of various dialysis membranes showed no significant differences between their behaviour.

For the two-point kinetic measurement procedure, the manifold used was as shown in Fig. 4; the distance between the two measuring cells was 75 cm, corresponding to a residence time of 11.5 s (cf. Fig. 5). By testing this manifold through injections of methyl orange (aqueous 0.00125% solution of pH 3; measuring wavelength 480 nm), the dilution factor D was established to be 0.8 (Fig. 8(a)), the residence time between the two peaks R_1 and R_2 (Fig. 8(b)) corresponding to 12 s which is in excellent agreement with the value obtained from Fig. 5. When the two-point kinetic measurement is used in this arrangement the first read-out (R_1) occurs 17 s after the point of injection (S_1), while the second read-out value (R_2) appears 29 s after S_1. If the criterion of 1% carry-over is maintained, i.e., the signal of R_2 must only constitute a level of 1% of sample S_2 at the time when it reaches cell no. 1, it might appear that ca. 60 s are required between injecting sample 1 (S_1) and the subsequent sample (S'_2). However, because there is a momentary increase of the pumping rate at the instant of injection of the 100-μl aliquots, the wash-out time of the previous sample is decreased by approximately 17 s; thus, the time required to reach the 1% level, and therefore the retardation time needed before injection of the next sample, are shortened accordingly. In fact, the second sample can be injected at point S_2, readily allowing a sampling rate of 60—70 samples per h to be maintained (Fig. 8(c)); a decrease of the volume of the flow-through cells would clearly allow higher sampling rates. A typical calibration record is shown in Fig. 8(d) and a series of serum samples is depicted in Fig. 8(c). Before analysis, the serum samples were diluted with water in three different ratios (1 : 10, 1 : 16 and 1 : 20) in order to keep the response curve within the linear range (cf. Fig. 1). The calibration curves for these three dilution series are shown in Fig. 9. It is interesting to note that the difference between the peak height values of R_1 and R_2 for the samples lowest in glucose content is negative, which reflects the fact that the dilution occurs between cells 1 and 2 (compare Figs. 8(a) and 9). Thus, there is no colour formation when the lowest glucose standards are injected, because at this level the recorded peak difference merely reflects the blank-lag phase combination.

The results of the two-point assay of serum standard materials are summarized in Table 1, which shows that irrespective of the dilution ratio used satisfactory results are obtained. It should be pointed out, however, that the 1 : 20 dilution series exhibits linearity over the largest range (r = 0.998; s = ca. 2%), and from Fig. 9 it is therefore apparent that this procedure, along with the 1 : 16 dilution, is preferable in practical analysis.

DISCUSSION

It has been reconfirmed that the glucose determination based on the glucose dehydrogenase reaction [6] is highly selective, as demonstrated by

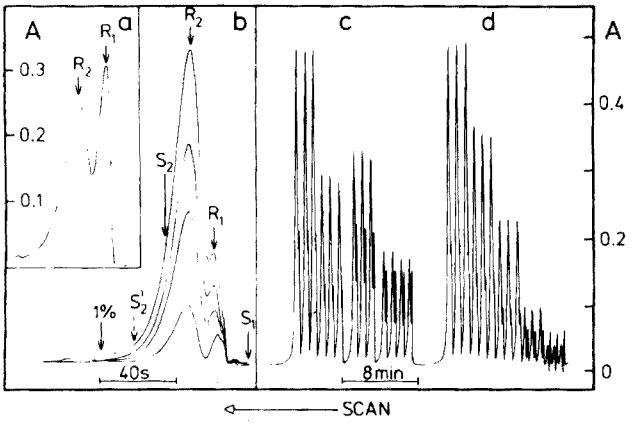

Fig. 8. Two-point kinetic assay of glucose with a manifold of the type shown in Fig. 4. (a) Verification of the dilution factor D by injection of 100 μl of 0.00125% methyl orange solution (480 nm); the decrease in peak height R shows the dilution of colour caused by the carrier stream on the way from flow cell 1 to 2. (b) Assay of 5.0, 10.0, 15.0 and 20.0 mmol l^{-1} of glucose recorded at high paper speed. S_1 sample injection; R_1 and R_2, respective read-outs of cells 1 and 2. S_2 and S'_2, point of injection of next sample (for details see text). (c) Four serum samples (from right to left: Monitrol I; Monitrol II; Technicon SMA 6/60; and serum pool, elevated). (d) A series of glucose standards (3.0, 5.0, 10.0, 15.0 and 20.0 mmol l^{-1}) analysed by the two-point procedure. Dilution ratio 1 : 16; sample volume, 100 μl.

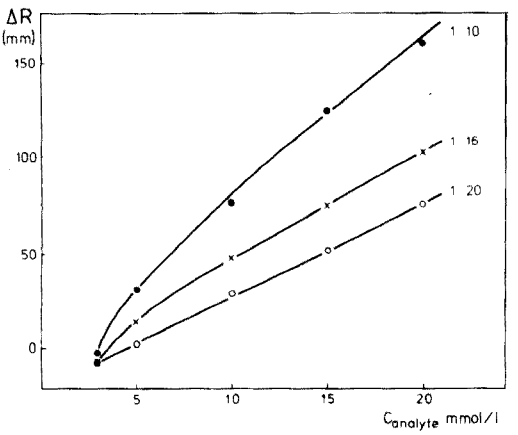

Fig. 9. Calibration curves obtained by the two-point kinetic assay method for various glucose dilution ratios. ΔR is the difference between R_1 and R_2 (cf. Fig. 8 and text).

the standard addition method (Fig. 7) as well as by assaying glucose in the presence of species which interfere in other glucose methods [4, 6, 10]. By analyzing various serum standard materials, the precision and reproducibility of all three approaches was found satisfactory. Therefore the choice between the single-point assay involving either manual deproteinization or continuous dialysis, and the two-point assay performed directly on diluted serum sample must be based on factors such as speed of analysis, labor expense and disposable sample volume. Here the two-point assay, although yielding a much lower sampling rate (60 samples/h), compared with the single-point assay without dialysis (120 samples/h), appears an obvious first choice, as the time- and sample-consuming manual deproteinization is not necessary. The only other aspect which might reverse this choice is the case where it is required that the serum samples for glucose determination are preserved by perchloric acid immediately after collection; for this would result in deproteinization.

Continuous dialysis has once again [8] turned out to be the least practical approach; it does not yield visibly better correlation between the assigned and found values on standard serum samples than the other two methods, yet it is more complicated to execute because the dialysis membrane has to be changed periodically. In contrast, the two-point assay inherently eliminates the blanking problem which otherwise might prove troublesome on some opalescent serum samples.

The successful adaptation of the glucose method is the first enzymatic assay performed by flow injection and it is therefore useful to point out the special aspects of this work compared to the techniques described in the previous papers of this series [8, 9, 11—15]. Save the design of the flow system, where the arrangement of the flow cells in series was found superior to the previously suggested parallel arrangement (chloride determination [14]), the modest reagent consumption is the most important aspect of this work.

The relatively high pumping rates used in the earlier described flow injection methods were employed in order to create a near turbulent flow in the reaction coils, as it was believed that this was necessary in order to reduce band spreading. This is the usual approach [16] devised on the basis of the profiles of the flow velocities across the tube, which are nearly constant for the turbulent flow, while in the laminar flow the fluid in the centre of the tube moves at twice the mean fluid speed. Therefore, at high Reynolds numbers

$$\mathrm{Re} = 127\, Q/d$$

(where Q is the fluid flow in ml s^{-1} and d is the i.d. diameter of the tube, in cm), the peak spreading should be less and so should be the carryover from one sample to the next. It has been recognized [8, 9], however, that the velocity profile is not the main factor influencing the band spreading, as the tube length and tube diameter have a much more profound effect than the pumping rate, the increase of which in fact increases the peak spreading. Therefore, the relatively high pumping rates used in the first parts of this

series (phosphate determination [12] 20 ml min^{-1}, Re = 450; ammonia determination [13] 17 ml min^{-1}, Re = 380) were later replaced by more moderate ones (chloride determination [14] 8 ml min^{-1}, Re = 170; determination of potassium, sodium and nitrate [9] 4 ml min^{-1}, Re = 85) and further decreased in the present work (to 2 ml min^{-1}, Re = 56), so that the relatively expensive enzyme solutions are consumed at an economical rate. In fact, the present system requires a smaller amount of reagent than the corresponding Auto-Analyzer glucose determination [6] (Table 1). Instead of air segmentation, spreading of the peak zone is limited by a careful design of length and diameter of the reaction line between the point of injection and the flow cell. Then the pumping rate is chosen in such a manner that it still allows a convenient rate of manual sampling, resulting in a residence time of 30 s. Thus, with one sample in the system at a time, there is no need for sample identification as the readout closely follows the sample injection, which may be effected at a rate of 120 samples per h.

Besides glucose, other substrate determinations could be adapted for flow injection, provided that the enzymatic reaction proceeds at a rate about the same as, or faster than, the glucose dehydrogenation. Of clinically important methods, transformation of uric acid by uricase (E.C. 1.7.3.3)

$$\text{Uric acid} + 2H_2O + O_2 \xrightarrow{\text{uricase}} \text{allantoin} + CO_2 + H_2O$$

could be considered, based on a two-point spectrophotometric measurement of the decrease in the uric acid concentration at 293 nm. Urea could be determined either by the following sequence of reactions

$$\text{Urea} + H_2O \xrightarrow[\text{E.C. 3.5.1.5}]{\text{urease}} 2\,NH_3 + CO_2$$

$$\text{2-Ketoglutarate} + 2\,\text{NADH} + 2\,NH_4^+ \xrightarrow[\text{E.C. 1.4.1.3}]{\text{glutamate dehydrogenase}} 2\,\text{L-glutamate} + 2\,NAD^+ + 2\,H_2O$$

by monitoring the decrease of the NADH absorbance at 340 nm, or by monitoring the increase of ammonia by a colour reaction or by a gas sensor. Besides the substrate determination, the determination of enzymes, such as alkaline (E.C. 3.1.3.1) and acid (E.C. 3.1.3.2) phosphatase, could readily be considered. Because of the reasonably rapid speed of these types of enzymatic reactions, the flow injection procedure based on two- or three-point measurement might be an interesting approach with a fair chance for successful development.

CONCLUSION

The flow injection system has proved to be suitable for enzymatic determination of glucose in blood serum which, based on the two-point kinetic assay, can be performed at a rate of 60 samples per h with a very modest reagent consumption. The limiting factor in the present study was the requirement that both cells must be washed out at least to the 1% R_1 absorbance level before the next sample is read out, because a one-channel spectro-

photometer was used for measurement. In a two-channel instrument, where the cells do not share the same optical path, the sampling rate could be almost doubled and the reagent consumption further decreased. Because of the absence of air segmentation, it is easy to perform two (and perhaps multiple) point measurements as the signal monitored by flow cells, placed in series along the carrier stream, is not disturbed by passage of air bubbles. By recognizing the parameters which influence spreading of the sample zone at laminar flow, it was possible to design the flow path and conditions in such a way that the carryover became negligible, even at high sampling rates.

Apart from kinetic assays, the experimental arrangement in which two (or perhaps several) measuring stations are placed in series on the same carrier stream could conceivably be used for blanking or differential measurement of two components in the same sample. Because of the regular flow pattern in the absence of air, reproducible measurements could be expected not only in the simple conduit arrangement used in this work, but also if an additional stream joined the main carrier stream in between the monitoring stations.

The next paper of this series will be devoted to a novel way of performing titrations by the flow injection system with potentiometric as well as photometric flow-through detectors.

The authors wish to thank Inge Marie Johansen for conscientious technical assistance; Dr. H. Schröder of Merck, Denmark, for donating the System Glucose enzyme set; and Dr. J. Melchior Rasmussen of the University Hospital of Copenhagen for providing the serum pool samples.

REFERENCES

1 S. Morgenstern, R. Rush and D. Lehman, Advances in Automated Analysis, 1972, Techn. Int. Congr. Vol. 1, Mediad 1973, p. 27.
2 H. Diebler and M. Pelavin, Advances in Automated Analysis, 1972, Techn. Int. Congr. Vol. 1, Mediad 1973, p. 19.
3 A. Hugget and D. A. Nixon, Biochem. J., 66 (1957) 12 P.
4 W. T. Caraway, in N. W. Tietz (Ed.), Fundamentals of Clinical Chemistry, W. B. Saunders, Philadelphia, 1970, p. 159.
5 W. Werner, H. G. Rey and H. Wielinger, Z. Anal. Chem., 252 (1970) 224.
6 D. Banauch, W. Brümmer, W. Ebeling, H. Metz, H. Rindfrey, H. Lang, K. Leybold and W. Rick, Z. Klin. Chem. Klin. Biochem., 13 (1975) 101.
7 W. Brümmer and W. Ebeling, Kontakte, Nr., 2 (1976) 3.
8 E. H. Hansen and J. Růžička, Anal. Chim. Acta, 87 (1976) 353.
9 J. Růžička, E. H. Hansen and E. A. Zagatto, Anal. Chim. Acta, 88 (1977) 1.
10 S. Addanki, W. K. Wolf and P. Golding, Advances in Automated Analysis, 1972, Techn. Int. Congr. Vol. 1, Mediad 1973, p. 183.
11 J. Růžička and E. H. Hansen, Anal. Chim. Acta, 78 (1975) 145.
12 J. Růžička and J. W. B. Stewart, Anal. Chim. Acta, 82 (1975) 79.
13 J. W. B. Stewart, J. Růžička, H. Bergamin Filho and E. A. Zagatto, Anal. Chim. Acta, 81 (1976) 371.
14 J. Růžička, J. W. B. Stewart and E. A. Zagatto, Anal. Chim. Acta, 81 (1976) 387.
15 J. W. B. Stewart and J. Růžička, Anal. Chim. Acta, 82 (1976) 137.
16 V. Pretorius and T. W. Smuts, Anal. Chem., 38 (1966) 274.

Analytica Chimica Acta, 89 (1977) 255—266

NON-DESTRUCTIVE PROTON ACTIVATION ANALYSIS FOR NITROGEN IN REFRACTORY METALS

K. STRIJCKMANS, C. VANDECASTEELE* and J. HOSTE

Institute for Nuclear Sciences, Rijksuniversiteit Gent, Proeftuinstraat 86, B-9000 Gent (Belgium)

(Received 17th September 1976)

SUMMARY

The non-destructive determination of nitrogen in some refractory metals was studied by activation analysis with the $^{14}N(p, n)^{14}O$ reaction. The samples were irradiated with 12-MeV protons from a cyclotron. The proton beam intensity was normalized by means of a copper flux monitor. After chemical etching, the ^{14}O activity (E_γ = 2313 keV, $T_{1/2}$ = 70.5 s) of the sample was measured by means of a Ge(Li) or NaI(Tl) detector. Standardization was carried out by the "average cross-section" method with nylon 6 as a nitrogen standard. The method gives a sensitivity of 0.4—30 $\mu g\ g^{-1}$ for analysis of Ta, W, Nb, and Ti, and 2000—4000 $\mu g\ g^{-1}$ for Zr, Ni and Mo.

The refractory metals dissolve nitrogen at high temperatures. The nitrogen settles in interstitial spaces of the crystal structure, thus influencing the physical, mechanical and chemical properties of the refractory metals [1].

For the determination of nitrogen in metals, charged particle and photon activation analysis can be applied. Table 1 summarizes the most important nuclear reactions. Reactions 1—4 have been used thus far; they yield pure β^+-emitters of relatively short half-life, so that a fast radiochemical separation is nearly always necessary. Interfering reactions are sometimes difficult to avoid by the selection of an appropriate particle energy.

This paper reports the possiblities for a non-destructive determination of nitrogen with the $^{14}N(p,n)^{14}O$ reaction. In this method ^{14}O is measured selectively by means of its 2313-keV γ-ray. The excitation function of the reaction is given by Kuan and Risser [7]. When 12-MeV protons are used, interferences do not arise, as the threshold of the $^{16}O(p,t)^{14}O$ reaction is 22 MeV.

STANDARDIZATION

Nylon 6 (12.38% nitrogen) is used as a nitrogen standard. If the incident proton energy is the same for the standard and the sample, the concentration in the sample is given by

*Aspirant of the N.F.W.O.

TABLE 1

Nuclear reactions for the determination of nitrogen in refractory metals

Reaction	Threshold (MeV)	Radiation emitted	Half-life	Interfering reactions	Threshold (MeV)	Refs.
(1) $^{14}N(\gamma, n)^{13}N$	10.5	β^+	9.97 min	$^{16}O(\gamma, t)^{13}N$	25	2, 3, 4, 6
				$^{19}F(\gamma, \alpha\ 2n)^{13}N$	25.4	
(2) $^{14}N(p, \alpha)^{11}C$	3.1	β^+	20.4 min	$^{11}B(p, n)^{11}C$	3.0	3, 4, 5, 6
(3) $^{14}N(d, n)^{15}O$	5.8	β^+	2.05 min	$^{16}O(d, t)^{15}O$	10.6	2, 3, 4
(4) $^{14}N(d, \alpha\ n)^{11}C$	5.9	β^+	20.4 min	$^{10}B(d, n)^{11}C$	$Q > 0$	3, 4, 5
				$^{12}C(d, t)^{11}C$	14.5	
(5) $^{14}N(p, n)^{14}O$	6.345 ± 0.015 (7)	β^+, γ E_γ = 2313 keV	70.48 ± 0.15s (8) 70.588 ± 0.028s (9)	$^{16}O(p, t)^{14}O$	22	—

$$C_X = C_S \frac{A_X^0}{A_S^0} \frac{R_S}{R_X} \quad (1)$$

where C = concentration; A^0 = activity at the end of the irradiation normalized for beam intensity; R = range of the incident particles (g cm^{-2}); and the subscripts X and S refer to the sample and the standard respectively.

This method is known as the "average cross-section" method [10, 11]. Charged particle ranges in the pure elements are tabulated by Williamson et al. [12]. The accuracy of the ranges is given as 10%. The ranges in chemical compounds of n components can be calculated by

$$\frac{1}{R} = \sum_{i=1}^{n} \frac{f_i}{R_i} \quad (2)$$

where R_i = range in the i^{th} component (g cm^{-2}) and f_i = mass fraction of the i^{th} component. The range of 12-MeV protons in nylon 6 is 0.1666 g cm^{-2}.

In practice the situation is not as simple as described. The standard and the samples are placed, during irradiation with 12-MeV protons, behind a 25-μm thick copper flux monitor. The energy of the protons is thus reduced to 11.5 MeV. Moreover, the samples are etched after irradiation, thus reducing further the incident energy to ca. 11 MeV (Fig. 1). Therefore different standards are irradiated, covered with an increasing number of copper foils, so that the energy of the protons incident on the different standards varies from 10.0 to 11.5 MeV; over this range, the activity of the standards as a function of the incident energy of the protons is linear. This can be expected since the cross-section for the $^{14}N(p, n)^{14}O$ reaction is constant between 10.0 and 11.5 MeV, as concluded from the activation curve determined by irradiation of a stack of Kapton polyimide foils (Fig. 2); moreover, the energy loss per unit length is approximately constant in this energy range. This is not quite in agreement with the measurements of Kuan and Risser [7].

The measured activity of the sample (after etching) is A_X^0 to be used in eqn. (1). The exact energy of the protons corresponding to the depth of etching (ca. 11 MeV) is calculated by means of the range-energy data given by Williamson et al. [12]. The activity of a standard (A_S^0) irradiated with protons of this energy is obtained from the plot of the activity of the standard versus the energy of the protons (Fig. 1).

CORRECTION FOR DEAD-TIME AND PULSE PILE-UP IN Ge(Li) SPECTROMETRY

In γ-ray spectrometry, counting losses from dead-time and pulse pile-up may cause systematic errors when the counting rates of the standard and the samples differ. Short-lived nuclides cause a variable counting rate during the measurements and complicate corrections for counting losses.

In the method proposed by Anders [13], pulser signals with known frequency are mixed with the detector signals at the preamplifier. This method

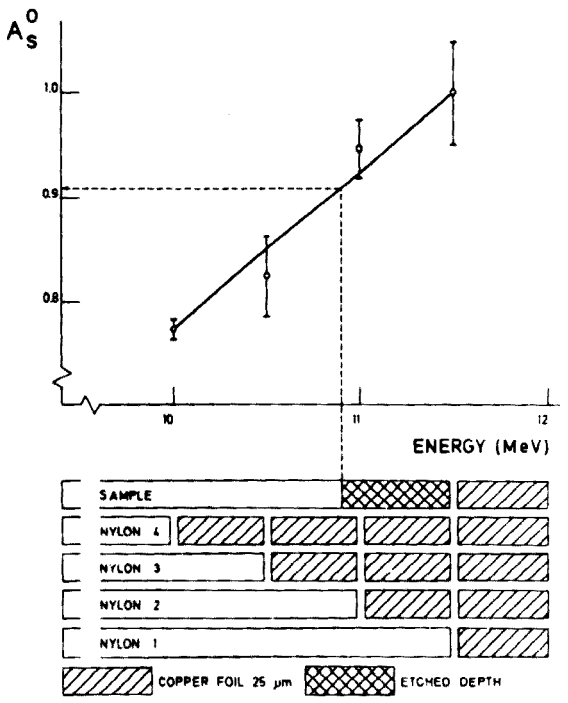

Fig. 1. Plot of the activity of the nylon standard at different incident energies, and linear interpolation of the activity of the standard (A_s^0) for the energy of the protons incident on the sample as measured.

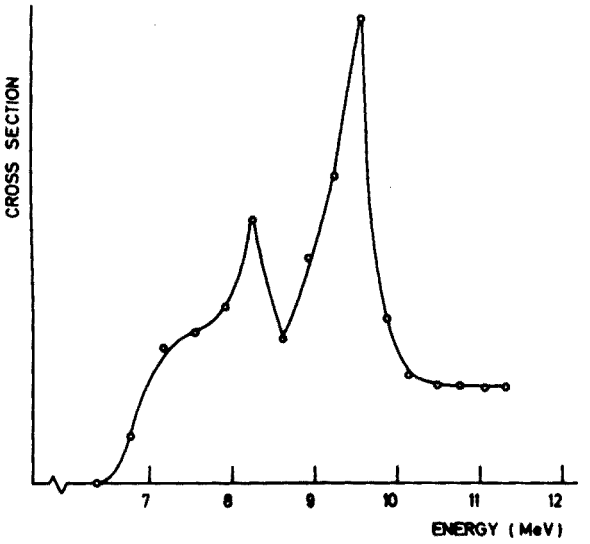

Fig. 2. Activation curve of the $^{14}N(p, n)^{14}O$ reaction, determined by irradiation of a stack of Kapton polyimide foils.

is recommended by Wiernik [14], because the total counting loss can be compensated in this way. There are, at least when a normal (non-random) constant frequency pulser is used, two limitations: (1) the counting rate (the dead-time) must be constant during the measurement; (2) because of the non-random distribution of the signal, there is no counting loss of two pulser signals, so that the pulser frequency must be kept low.

Junod [15] proposed an "actual time" mode of counting. The measurement is carried out in the real time mode (CT = clock time). The period for which the ADC is free is measured by an external scaler (AT = actual time). The corrected number of counts N^* is then given by:

$$N^* = N \times \frac{CT}{AT} \tag{3}$$

where N is the number of counts measured.

This method does not correct for counting losses arising from pulse pile-up. When measuring a short-lived activity, formula (3) yields a negative error. Junod calculated this error for a short-lived nuclide measured alone or in the presence of long-lived activities. For a single short-lived nuclide the error is ca. 2% for a counting time equal to one half-life and for a relative dead-time* of 50%. In the case of a short-lived nuclide in the presence of long-lived activities the error is still less for the same relative dead-time. Junod's method would be sufficiently accurate when counting a mixture of ^{14}O and a long-lived matrix activity at high counting rate during 70 s. Nevertheless, counting losses by pulse pile-up would still cause inaccuracy.

The method used in this paper combines the advantages of both methods. The signals from a precision pulse-height pulser, triggered with the 50-Hz line frequency, are mixed with the detector signal at the preamplifier. The pulse height is set so that the pulser peak is situated above the most energetic photopeak in the spectrum. The low frequency of the pulser gives no additional dead-time. The measurement is done in the real time mode. Junod's calculations for the "actual time" method are applicable to this situation if formula (3) is replaced by:

$$N^* = N \times \frac{CT \times F}{P} \tag{4}$$

where N is the number of counts measured, F is the pulser frequency (50 Hz), and P is the number of counts under the pulser peak.

The negative error caused by this approximation, in counting short-lived activities, is calculated in the same way as in Junod's method. In this method all counting losses are compensated; in Junod's "actual time" method, losses caused by pulse pile-up are not compensated.

The accuracy of this method was checked experimentally. First, measurements were carried out with an ^{88}Y source at a very low dead-time. After-

*The relative dead-time is defined as $RDT = \frac{1}{CT}\int_0^{CT} DT(t)\,dt$ where $DT(t)$ = instant dead-time.

wards, the dead-time was increased by adding other sources with a very large half-life compared with the counting time. The ^{88}Y activity was corrected as described. The results, summarized in Table 2, show that no significant error occured even at a dead-time of 80%. Secondly, the decay of pure sources of ^{28}Al ($T_{1/2}$ = 2.2405 ± 0.0003 [16]) and ^{52}V ($T_{1/2}$ = 3.746 ± 0.007 [17]) was followed at a high initial counting rate, The counting time was one half-life of the measured nuclide. At a relative dead-time of 50% a negative error of 0.5—5.5% occurred.

EXPERIMENTAL

Irradiation

Irradiations were carried out with the external proton beam of the isochronous cyclotron of Louvain-La-Neuve. The sample holder is transferrred to the irradiation position by a pneumatic system. The sample holder can be water-cooled. The irradiations take place in a vacuum of 10^{-4} torr. The irradiation time is commanded by an electronic clock, which removes a Faraday cup that intercepts the beam. The irradiation and measurement conditions are summarized in Tables 3 and 4.

TABLE 2

Error on the pulser correction method: ^{88}Y (1836 keV) measured at increasing dead-time

Dead-time (%)	Error (%)	S.d. (%)
38	−2.26	1.37
55	+4.17	1.58
57	+0.63	1.62
58	−1.87	1.93
80	+1.42	3.30

TABLE 3

Irradiation and measurement conditions (Ge (Li)- detector)
(A counting time of 70 s was used in all cases.)

Target	Intensity (nA)	Irradiation time (s)	Decay time (s)	Dead-time of the counting system (%)
Nylon 6	20—30	4	30—40	15
Ta	3000—4000	60	50—60	10
W[a]	800	60	50—60	80
W[b]	1500	60	50—60	20
Nb	500	60	50—60	30—40
Ti	40	60	50—60	50
Zr	15	60	50—60	70
Ni	30	9	50—60	60
Mo	20	8	50—60	50

[a] Without lead absorber. [b] With a 7-mm lead absorber.

To remove surface contamination, after irradiation a 25-μm surface layer was removed by chemical etching. Table 5 summarizes the etching conditions.

Measurement

Measurements were carried out with an Ortec 8001-0522 Ge(Li) detector with a useful volume of 34.7 cm^3, 5% relative efficiency, and a resolution of 2.2 keV at 1332 keV. The detector was connected to a Canberra 1417 B amplifier, an Intertechnique C 44B ADC (100-kHz oscillator) and an Intertechnique Didac 4000-channel analyzer. An Ortec 419 pulser was used. The samples and standards were measured centered on a plexiglas sample-holder on the detector cap, except for W where a 7-mm thick lead absorber was interposed between the samples and the detector.

The NaI(Tl) detector (7.6 cm × 7.6 cm; Quartz & Silice 76 SF 76) was connected with an Ortec preamplifier and an Ortec amplifier analyzer model 490A. The single-channel output was connected to a scaler-printer unit, commanded by two clocks, permitting cyclic measurements. The amplifier output was connected to a second scaler. To attenuate the low-energy γ-rays of the matrix, a 5-mm lead absorber was interposed between the sample and the detector.

Some details of the counting conditions are summarized in Tables 3 and 4.

TABLE 4

Irradiation and measurement conditions (NaI(Tl)-detector)
(A counting time of 20 s was used in all cases.)

Target	Intensity (nA)	Irradiation time (s)	Decay time (s)	Period of the cyclic measurement (s)
Nylon 6	100	3—6	30—40	20.5
Ti	300—500	15—60	50—60	20.5
Nb	600	10—200	50—60	20.5

TABLE 5

Etching conditions used to remove ca. 25 μm from each side of the sample

Metal	Etching solution[a]		Temperature	Duration of etching (s)
Ta	HF/HNO_3	8/1	boiling	5
W	HF/HNO_3	1/1	boiling	10
Nb	HF/HNO_3	1/1	room temp.	5
Ti	HF/HNO_3	1/1	room temp.	15
Zr	$HF/HNO_3/H_2O$	1/1/8	room temp.	15
Ni	HF/HNO_3	1/1	boiling	5
Mo	HF/HNO_3	1/1	room temp.	15

[a]HF, 50%; HNO_3, 14N.

Flux monitoring

During the irradiation the samples and the standards were placed behind a 19.8 mg cm^{-2} (ca. 25 μm) thick copper foil (Ventron 99.999% purity), used as a flux monitor. Table 6 summarizes some reactions of copper with 12-MeV protons.

The 669.6-keV and 961.9-keV photopeaks of ^{63}Zn were measured by means of the Ge(Li) detector described. Dead-time correction was carried out with the pulser method.

To be able to convert the activity of ^{63}Zn to the beam intensity, a perforated sample holder loaded only with a copper foil was irradiated. The beam intensity during irradiation was measured by means of a Faraday cup, situated behind the sample holder and connected to a digital voltmeter.

RESULTS AND DISCUSSION

The induced activity in the matrix is one of the limiting factors of the instrumental method. The main nuclear reactions are listed in Table 7. The detection limits obtained from the Ge(Li) spectra can be calculated from the formula [20]

$$L_D = 2.71 + 4.65\,(\mu_B)^{\frac{1}{2}}$$

where L_D is the detection limit in counts and μ_B is the background at 2313 keV. These limits, obtained under the conditions given in Tables 3 and 4, are summarized in Table 8. For Mo and Ni, the induced matrix activity is so high that the method becomes useless in view of the nitrogen concentrations commonly found in these materials. For Zr, the ^{90}Nb photopeak at 2319 keV interferes with the 2313-keV photopeak by ^{14}O. For Nb and Ta the detection limits are very low. Figure 3 shows a spectrum of irradiated Nb containing 200 ± 13 $\mu g\ g^{-1}$ nitrogen. For W the detection limit is considerably lowered by inter-

TABLE 6

Reactions of copper with 12-MeV protons

Reaction	Threshold (MeV)	Isotopic abundance (%)	Half-life	γ-energy (keV)
$^{63}Cu(p, n)^{63}Zn$	4.2	69.1	38.4 min [18, 19]	511 (β^+)
			38.38 ± 0.27 min[a]	669.6; 961.9
$^{63}Cu(p, d)^{62}Cu$	8.7	69.1	9.73 min	511 (β^+)
$^{65}Cu(p, n)^{65}Zn$	2.2	30.9	243.8 d	511 (β^+); 1115. 52
$^{65}Cu(p, d)^{64}Cu$	7.8	30.9	12.8 h	511 (β^+)

[a] Average of three decay curve analyses on both 669.6-keV and 961.9-keV photopeaks, measured with three different Ge(Li) measuring systems and the standard deviation on one measurement.

TABLE 7

Main nuclear reactions of 12-MeV protons with the matrices studied

Matrix	Reaction	Half-life	Main γ-energies (keV)
Ta	None	—	—
W	$^{180}W(p, n)^{180}Re$	2.5 min	57.98; 59.32; 67.2; 103.8; 902.4
	$^{182}W(p, n)^{182m}Re$	12.7 h	1121.3; 1189.0; 1221.4
Nb	$^{93}Nb(p, n)^{93m}Mo$	6.95 h	263.23; 684.64; 1477.2
Ti	$^{48}Ti(p, n)^{48}V$	16.1 d	983.5; 1311.6
	$^{47}Ti(p, \alpha)^{44}Sc$	3.92 h	1157.0
Zr	$^{90}Zr(p, n)^{90}Nb$	14.6 h	141.2; 1129.1; 2186.0; 2319.0
	$^{90}Zr(p, n)^{90m}Nb$	18.8 s	122.37
Ni	$^{60}Ni(p, n)^{60}Cu$	23.4 min	826; 1332.5; 1792
Mo	$^{92}Mo(p, n)^{92}Tc$	4.4 min	147.9; 329.3; 773.1; 1509.6
	$^{94}Mo(p, n)^{94m}Tc$	52.0 min	870.9

TABLE 8

Detection limit for the determination of nitrogen ($\mu g\ g^{-1}$) measured with the Ge(Li)-detector

Ta	0.4	Ti	160
W[a]	10	Zr	2000
W[b]	1.6	Ni	3000
Nb	9	Mo	4000

[a,b] See Table 3.

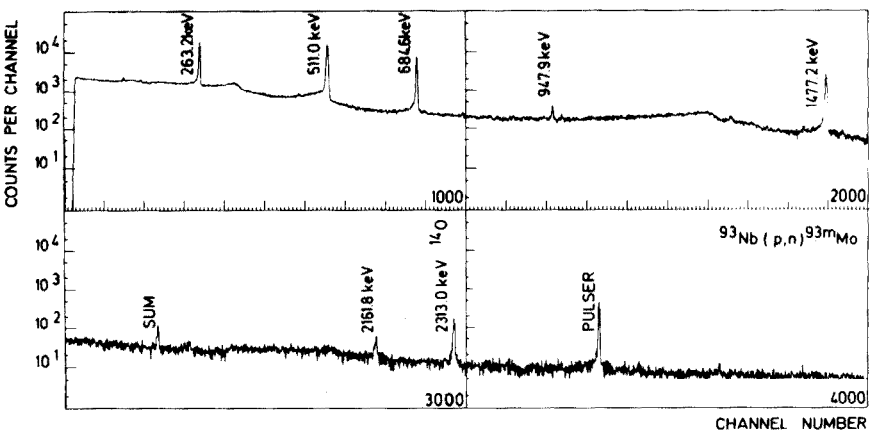

Fig. 3. γ-Ray spectrum of Nb irradiated with 12-MeV protons. Irradiation time, 60 s; beam intensity, 500 nA; decay time 60 s; counting time 70 s.

posing a lead absorber of 7 mm between the sample and the detector, since low energy γ-rays are then absorbed. This results in a lower dead-time at the same beam intensity, so that higher beam intensities can be used (Table 3).

Only Nb and Ta contained nitrogen concentrations above the detection limit of the method. Table 9 summarizes some results of replicate analyses on these materials.

The accuracy of the method was tested by analysis of a stack of Kapton H polyimide film (Dupont de Nemours). Six analyses yielded 7.19 ± 0.60% of nitrogen. This result does not differ significantly from the expected value of 7.65% [21].

With a Ge(Li) detector, connected with a multichannel analyzer in the pulse-height analyzer mode, the detection limit for W and Ti exceeds the nitrogen concentration. When a NaI(Tl) detector connected with a single-channel analyzer is used (with analysis of the decay curve) the detection limit for Ti falls to ca. 30 $\mu g\ g^{-1}$ because (1) the detection efficiency of a NaI(Tl) detector decreases more slowly with energy, which is more favourable for the detection of the 2313-keV ^{14}O γ-ray; (2) counting losses are less important.

The decay curve was analyzed by the CLSQ decay curve program [22], assuming the presence of four components: ^{14}O(70.5 s), ^{47}V(32.0 min), ^{44}Sc (3.92 h) and ^{48}V(16.1 d). As a qualitative criterion for ^{14}O, a best estimate of the half-life was determined. This yielded an average of 62 ± 9 s. Determinations were carried out at different integral counting rates to detect possible errors from counting losses and pulse pile-up. It is clear from Fig. 4 that, in the range of counting rates used, the result does not depend critically on the integral counting rate.

For W, an improvement was not obtained in this way because of the important matrix activity in the vicinity of the 2313-keV peak.

TABLE 9

Nitrogen concentration ($\mu g\ g^{-1}$) in Ta, Nb and Ti

Sample	No. of samples	No. of analyses	$\mu g\ N\ g^{-1}$	S.d.[a]	S.d.[b]
Ge (Li) Detector					
Ta	7	20	9.18	0.99	0.64
Nb	10	17	200	13	10
NaI(Tl) Detector					
Nb	8	8	228	16	—
Ti	7	7	113	8	—

[a] Standard deviation on one measurement.
[b] Standard deviation from counting statistics.

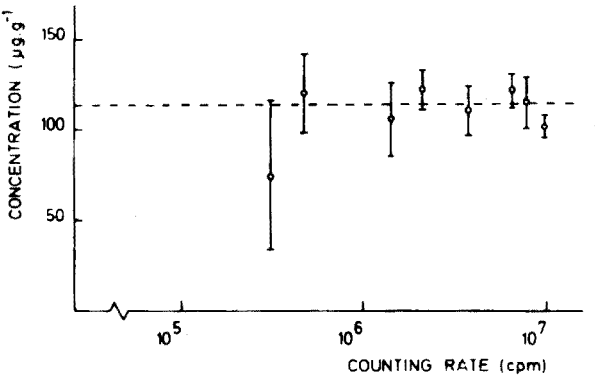

Fig. 4. Plot of the nitrogen concentration found in Ti as a function of the integral counting rate.

Four samples of Nb already analyzed by Ge(Li) gamma-ray spectrometry (Table 9), were also analyzed with the NaI(Tl) detector. The decay curve is composed of the ^{14}O (70.5 s) and the ^{90m}Mo (6.9 h) activities. The results obtained are also given in Table 9. The results for Nb are in good agreement. The results for Ti are also in reasonable agreement with the reported values [23] ranging from 89 to 142 $\mu g\ g^{-1}$ with a mean of 120 $\mu g\ g^{-1}$. These analyses were carried out by reducing fusion, the Kjeldahl method, and photon activation.

Conclusion

The present method permits a sensitive determination of nitrogen in Ta, W, Nb and Ti. Some advantages over other methods are the speed of analysis (ca. 3 min per analysis), no need for chemical separations, and freedom from interferences.

Grateful acknowledgement is made to R. Keiffer for skilful technical assistance, to the "Comité de gestion du Cyclotron" at Louvain-La-Neuve for the use of the cyclotron, and to the I. I. K. W. and the N. F. W. O. for financial support. Thanks are also due to J. Pauwels (CBNM, Geel) for providing the samples.

REFERENCES

1 P. Albert, Le Dosage de l'Azote dans le Métaux Refractaires, son Importance Technologique et Économique (1974). Cahier d'information du bureau Eurisotop, 90 série monographie-34, Eurisotop Brussels.
2 C. Engelmann, Int. J. Appl. Radiat. Isot., 18 (1967) 569.
3 C. Engelmann, J. Radioanal. Chem., 7 (1971) 89.
4 C. Engelmann, J. Radioanal. Chem., 7 (1971) 281.
5 A. Marschal, J. Gosset and C. Engelmann, J. Radioanal. Chem., 8 (1971) 243.
6 C. Engelmann, J. Gosset and C. Grumet, J. Radioanal. Chem., 28 (1975) 185.

7 Hsin-min Kuan and J. R. Risser, Nuclear Physics, 51 (1964) 518.
8 D. E. Alburger, Phys. Rev. C, 5 (1972) 274.
9 G. J. Clark, J. M. Freeman, D. C. Robinson, J. S. Ryder, W. A. Burcham and G. T. A. Squier, Nucl. Phys. A, 215 (1973) 429.
10 E. Ricci and R. Hahn, Anal. Chem., 37 (1965) 742.
11 E. Ricci and R. Hahn, Anal. Chem., 39 (1967) 794.
12 C. F. Williamson, J. Boujot and J. Picard, Tables of range and stopping power of chemical elements for charged particles of energy 0.05 to 500 MeV, Rapport CEA-R 3042 (1966).
13 O. U. Anders, Nucl. Instrum. Methods, 68 (1969) 205.
14 M. Wiernik, Nucl. Instrum. Methods, 95 (1971) 13.
15 E. Junod, J. Radioanal. Chem., 20 (1974) 113.
16 R. Van Schandevijl, R. Van Grieken and J. Hoste, J. Radioanal. Chem., 9 (1971) 55.
17 A. Wyttenbach, J. Radioanal. Chem., 2 (1969) 287.
18 C. Lederer, J. Hollander, I. Perlman, Table of Isotopes, 6th edn., J. Wiley, 1967.
19 G. Erdtmann and W. Soyka, J. Radioanal. Chem., 26 (1975) 375.
20 L. Currie, Anal. Chem., 40 (1968) 587.
21 J. B. Marion and F. C. Young, Nuclear Reaction Analysis, North Holland Publishing Company, Amsterdam, 1968.
22 J. Cumming in G. O'Kelley (Ed.), Applications of Computers to Nuclear and Radiochemistry, NAS-NS 3107, 1963.
23 Meeting of BCR-Group of Specialists, Non-Metals in Refractory Metals, Brussels, 17—18 November 1975, Euratom.

Analytica Chimica Acta, 89 (1977) 267—269

MEASUREMENTS OF OXYGEN, NITROGEN AND CARBON FOR IN VIVO PHOTON ACTIVATION ANALYSIS

D. BRUNE

AB Atomenergi, Studsvik (Sweden)

and

U. LINDH and H. LUNDQVIST

Department of Physical Biology, Gustaf Werner Institute, Uppsala (Sweden)

(Received 21st August 1976)

SUMMARY

When the human body is subjected to Bremsstrahlung radiation at selected maximum energies (13—25 MeV) in a betatron the radionuclides ^{15}O (2.05 min), ^{13}N (10.0 min) and ^{11}C (20.5 min) are formed from oxygen, nitrogen and carbon in the body. In the present study these activities were measured in phantoms consisting of beef tissue weighing about 150 g. In these samples oxygen, nitrogen and carbon could be determined at the following dose levels: oxygen, < 0.5 rad; nitrogen, ~ 5 rad; carbon, < 0.5 rad.

Great interest has been shown in the in vivo activation analysis of man, for the purpose of establishing the elemental composition of the human body in connection with normal and abnormal metabolic processes. Measurements of the total body content of hydrogen, sodium, chlorine, phosphorus, nitrogen and calcium have been accomplished (see e.g. ref. 1). Iodine has been measured in thyroidea [1]. Usually, the analysis is accomplished by a thermal or fast neutron activation technique. The cadmium content of liver of industrial workers has been measured by neutron activation analysis [2].

As an alternative to neutron activation analysis for nitrogen in vivo, a photon activation technique was investigated as a possible analytical tool for the determination of this element as well as for oxygen and carbon. Such studies can suitably be accomplished with a betatron, which is available at most university hospitals. The measurements of the induced activities after irradiation were carried out in this study by the usual method of γ-ray spectrometric analysis, using a 2 × 2-in. NaI(Tl) crystal detector connected to a multichannel analyzer.

Photon activation analysis for the characterization of nitrogen in cereals has been done previously with a betatron [3]. Optimum irradiation conditions, the effect of nuclear interference reactions and the use of internal standards were investigated at that time. In several respects the analytical technique used for the present study was similar to that used previously [3]. Thus, the radionuclide ^{38}K interferes in both cases.

For in vivo measurements it is of the utmost importance to reduce the dose to which the individual is subjected. Consequently, the aim was to accomplish the analysis at doses lower than a few rad. For comparison purposes, it may be mentioned that typical x-ray investigations result in doses of the order of 0.1—10 rad.

EXPERIMENTAL

Betatron

The irradiations were done with the hospital betatron (33 MeV maximum Bremsstrahlung energy) at Akademiska Sjukhuset, Uppsala.

Samples

The samples were composed of beef tissue of about 150-g wet weight.

Activities formed in beef tissues at various maximum Bremsstrahlung energies

Irradiation at 13-MeV maximum Bremsstrahlung energy. At this energy the activities of ^{15}O, ^{30}P and ^{38}K are negligible [3]. However, measurements of ^{13}N were almost impossible at doses lower than 10 rad.

Irradiation at 16-MeV maximum Bremsstrahlung energy. The activity level of ^{13}N is increased by a factor of about 4 compared to irradiations at 13 MeV [3]. The interference from ^{38}K is less than 2%. The measurement of ^{13}N can be done at an estimated dose of about 5 rad (see Fig. 1). The activities of ^{15}O and ^{11}C are still negligible.

Irradiation at 20-MeV maximum Bremsstrahlung energy. In this case irradiation was done at a high dose, i.e. ca. 400 rad (20-min irradiation) in order to check any activities remaining in the tissue after the decay of ^{15}O, ^{13}N and ^{11}C as well as to obtain high activities of all three nuclides. Even at this high dose, no activity could be detected in the sample (ca. 150-g beef) after 1 day. Peaks corresponding to activities exceeding 0.1 pCi could not be measured in a low-level 4 × 4-in. NaI(Tl) detector assembly, except for ^{137}Cs and ^{40}K. For comparison purposes, it should be mentioned that the natural activity of ^{137}Cs and ^{40}K in the body amounts to about 10 pCi in an average man.

The results of resolution of the measured decay curves of the three components, i.e. ^{15}O, ^{13}N and ^{11}C, are presented in Fig. 2. The curves were resolved with a computer based on the program Expamp [4]. The errors quoted were obtained by least square fitting. At this energy oxygen and carbon can be determined at doses lower than 0.5 rad, as deduced from Fig. 2, with short irradiation periods.

APPLICATIONS

The technique of in vivo photon activation analysis for oxygen, nitrogen and carbon with an ordinary hospital betatron may find the following fields of application.

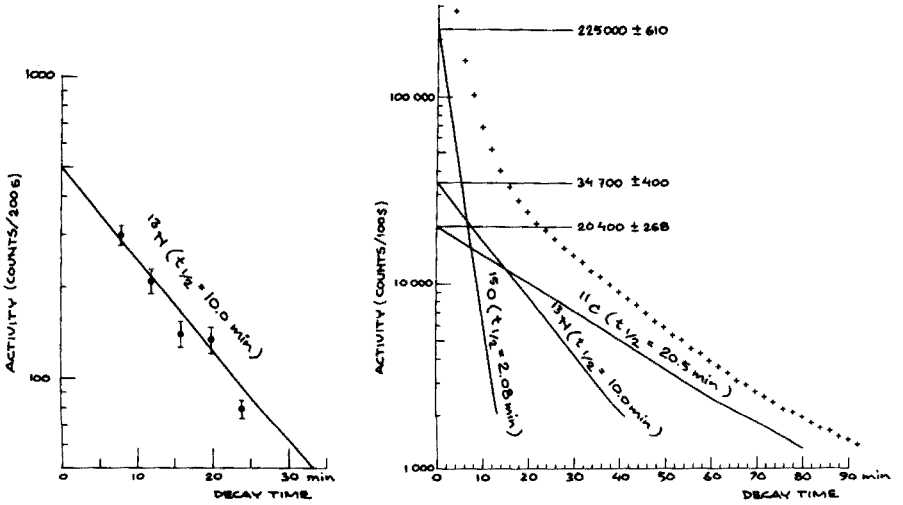

Fig. 1. ^{13}N activity after irradiation at 16-MeV maximum Bremsstrahlung energy. Dose, ca. 5 rad.

Fig. 2. Resolution of the measured decay curves of ^{15}O, ^{13}N and ^{11}C. Irradiation at 20-MeV maximum Bremsstrahlung energy for 20 min. Dose, 20 rad min^{-1}.

Characterization of fluid accumulations (blood or water) in some parts of the body might be possible by means of ^{15}O-measurements. The mean oxygen content of the body is about 65% [5]. The oxygen content of water is 0.89.

Measurements of ^{13}N can be utilized for the estimation of protein distribution in the human body, in connection with studies of the effects of various diseases on protein metabolism.

The technique can also be used for characterization of the protein content in breeding cattle. Further, in quality control of slaughtered cattle, photon activation analysis of nitrogen seems suitable for rapid analysis in routine work [6].

REFERENCES

1 In Vivo Neutron Activation Analysis, Proc. of a Panel, IAEA, Vienna, 17—21 April, 1972.
2 B. J. Thomas, T. C. Harvey, J. S. McLellan, J. H. Fremlin and P. W. Dykes, in R. Höfer (Ed.), Proc. Gasteiner Int. Symp: Radioaktive Isotope in Klinik und Forschung, Verlag H. Egerman, 1976.
3 D. Brune, L. Düring, B. Larsson and H. Lundqvist, Int. J. Appl. Radiat. Isotopes, 24 (1973) 1.
4 B. Tollander, Program developed at AB Atomenergi, Studsvik, Sweden.
5 J. M. A. Lenihan, Conf. Mod. Trends Activation Anal., Gaithersburg, Oct. 7—11, 1968, NBS Special Publication 312, Vol. 1, No. 1.
6 B. Larsson, Gustaf Werner Institute, Uppsala, Sweden, personal communication.

Analytica Chimica Acta, 89 (1977) 271—279

A RAPID CALIBRATION METHOD FOR THE DETERMINATION OF TRACES OF OXYGEN BY 14-MeV NEUTRON ACTIVATION ANALYSIS

WOLFGANG HERZOG and JOCHEN FAHLAND

Staatliches Materialprüfungsamt NW, D-4600 Dortmund 41 (Federal Republic of Germany)

(Received 13th May 1976; in revised form 26th August 1976)

SUMMARY

A dual axis rotation irradiation system has been used in the development of a calibration method for the determination of oxygen in almost any matrix by 14-MeV neutron activation. The method allows the correction of matrix effects which arise from neutron removal and γ-self absorption, thus providing an accuracy of ± 2% for the oxygen analysis. The experimental results are interpreted on the basis of theoretically calculated mass absorption coefficients and neutron removal cross-sections.

The increasing availability of powerful and reliable neutron generators has facilitated the development of neutron activation analysis (n.a.a.) with 14-MeV neutrons as a standard method for the determination of oxygen. However, although this technique has been adopted routinely in some steel plants for process control [1], it has not yet found wider industrial applications. This may be due to the difficulties of standardization, particularly if the sample composition changes frequently. The corrections for matrix effects, which are caused by different neutron absorption and self-absorption of the γ-radiation measured in sample and reference, are very time-consuming. These problems have been discussed in detail by Anders and Briden [2], Nargolwalla et al. [3, 4], Vandecasteele et al. [5] and Adams et al. [6]. Rabbit systems with single axis rotation of the sample [2] and simultaneous double axis rotation of sample and standard [3, 4, 7] as well as irradiation systems with a reference position screened by the sample [5] have been used. More universal approaches for neutron- and γ-absorption corrections have been established by Anders and Briden [2].

For samples with low atomic number Z and low density, they found a linear dependence of the oxygen content on the product of the sample diameter and the total macroscopic cross-section for 14-MeV neutrons. For samples with high Z and densities up to 4.5 g cm^{-3}, they also investigated the self-absorption effect of the high-energy γ-rays of ^{16}N, assuming in a simplified manner that the self-absorption factor is an exponential function of the sample weight.

Nargolwalla et al. [3, 4] have described another method for the measurement of distinct calibration curves with a view to evaluating correction factors for neutron and γ-absorption. These authors observed that the neutron correction factors obtained are related exponentially to the difference of the total neutron removal cross-sections of the standard material and sample. Similarly, the γ-self-absorption corrections are related exponentially to the difference between the calculated mass absorption coefficients for standard and sample. The method [3, 4] is based on a careful selection of substances which have known oxygen contents and the same mass absorption coefficient for the 6-MeV γ-rays; thus the neutron absorption correction factors were first evaluated and then other materials with the same neutron absorption cross-section were used to obtain the γ-self-absorption correction. Besides the selection of suitable substances, Nargolwalla et al. [3, 4] also varied the densities of those substances. Therefore the method seems rather difficult.

In contrast to Anders and Briden [2], who used the total microscopic neutron cross-sections of the elements, Nargolwalla et al. [3, 4] used the semi-empirical neutron removal cross-sections reported by Avery et al. [8]. The advantages of the latter method have been discussed in detail by Adams et al. [6]. The irradiation system developed by Vandecasteele et al. [5] allows the direct determination of the γ- and neutron absorption coefficients with sandwich standard samples.

The aim of the present work was to develop a fast and universal calibration method for an irradiation system with double axis rotation, thus allowing the determination of oxygen in any matrix. Since the fundamental principles of n.a.a. with fast neutrons are well known, a detailed description is not given. Reference may be made to the bibliography of van Grieken and Hoste [9] and the surveys by Wood [7] and Adams et al. [6].

EXPERIMENTAL

Apparatus

A schematic diagram of the irradiation system is shown in Fig. 1. A neutron generator (Brown, Boveri et Cie) with a maximum neutron output of 10^{12} n s^{-1} at 300-kV acceleration and 6-mA beam current was available. For irradiation and transport of the samples, a commercial dual tubing rabbit system (Kaman Nuclear), as described by Wood [7], was used. The irradiation position allows the simultaneous irradiation of sample and reference, both rotating about two axes. Thus the samples are activated uniformly and the influence of beam inhomogeneities is lowered. The samples were of cylindrical shape with dimensions of 8 mm diameter and 38 mm length.

Sample carriers consisted of polyethylene with low oxygen content (ca. 100 p.p.m.) weighing 1.9 g and having the outer shape of a double cone. For samples with oxygen contents less than about 100 p.p.m. another measuring terminal was used. Here the sample carrier was automatically

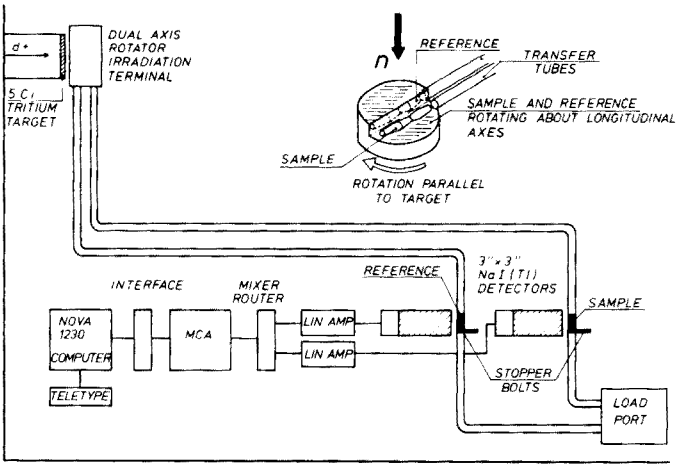

Fig. 1. Schematic diagram of the irradiation system.

stripped off so that the sample could be measured without the interfering ^{16}N activity generated in the polyethylene capsule. Of course, powder samples cannot be handled with this version. The rabbit system runs under nitrogen pressure to avoid interferences caused by ^{16}N recoil atoms. The bombardment time is defined by means of a mechanical beam stopper. After irradiation the sample and the reference material are shot to the measuring positions, stopped by pneumatic stopper bolts and measured simultaneously with two 3 × 3-in standard NaI(Tl) detectors, whose windows are shielded with 4-mm lead, 1-mm cadmium and 1-mm copper against the hard β-rays of ^{16}N. The pulses of both detectors are formed in the conventional way through preamplifiers and linear amplifiers and are then fed via a mixer-router to the memory subgroups of a 4096-channel pulse-height analyzer. A NOVA 1230 computer evaluating the γ-spectra has direct access to the multichannel analyzer. Of the ^{16}N γ-spectrum only the energy range 4.5—7.0 MeV is used for the oxygen determination. However, the main part of the measurements was performed with two timing single-channel analyzers connected to the scalers.

Procedure

In general the samples were measured according to the following time cycle: 15-s irradiation, 3-s transfer time, 15-s measuring. Ten single irradiations were carried out for each oxygen determination. The use of two detector arrangements for measuring standard and sample required that the different counting efficiencies of the systems be taken into account. Therefore two identical Plexiglas (polymethylmethacrylate) standards were irradiated and measured. The resulting counting rate ratio of the sample detector to the standard detector was then used for the normalization of the

counting efficiencies as a so-called "geometry factor". By determination of this geometry factor at regular intervals, the long-term gain-shift of the measuring system can be corrected. The oxygen content of a sample was then obtained via the activation formula as

$$O = \frac{R}{G} \cdot O_S \cdot F - O_B \qquad (1)$$

where O is the oxygen content of the sample; R the ratio of counting rates of sample to standard detector; G the geometry factor as defined above; O_S the oxygen content of standard material (reference); F the total correction factor for neutron removal and γ-self absorption; and O_B the blank value from the oxygen content of the capsule.

For all the measurements a Plexiglas cylinder was used as reference. By comparison with some organic test substances for elemental analysis, it was verified that the oxygen content of this material is in accordance with its stoichiometric composition, and corresponds to the formula $C_5H_8O_2$ (see also Fig. 2). For the determination of blank values, the polyethylene vials were filled with nitrogen, giving results of 100—150 p.p.m. O which corresponds to 0.2—0.3 mg of oxygen.

In addition to the above-mentioned test substances, other compounds of analytical purity, mainly oxides, sulphates and nitrates, were also investigated in order to obtain the calibration curve (see Table 1). These compounds were selected according to increasing density. The powdered substances were pressed into the vials partly by hand, and partly after forming pellets with a hydraulic press to obtain higher density. Thus it was possible to press PbO at 4000 kg cm^{-2} to a density of nearly 9 g cm^{-3} corresponding almost to the density of solid PbO. The formation of pellets has the advantage that no local density variations in the samples are caused by the impacts at the stopper bolts, leading to partial loss of precision.

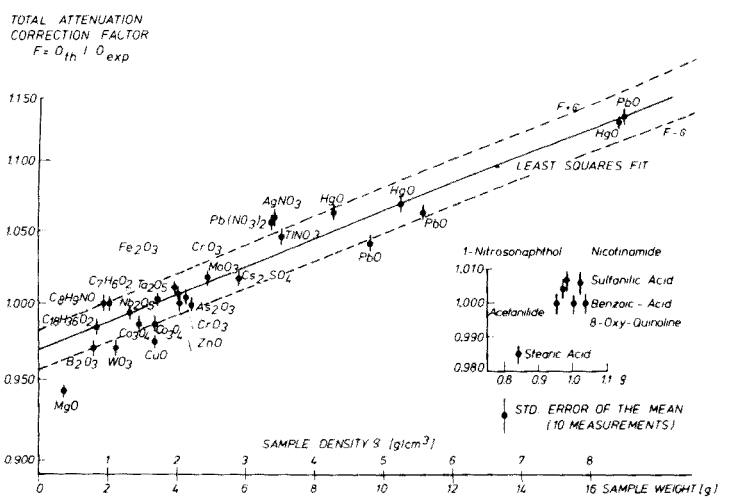

Fig. 2. Experimental calibration curve for neutron and γ-attenuation. The ordinate is logarithmic. Full line: least-squares fit over the values. Dotted lines: 1 σ-limits.

TABLE 1

Chemical compounds used for calibration

Compound	Formula	Purity (%)	Compound	Formula	Purity (%)
Magnesium oxide	MgO	97.0	Tantalum(V) oxide	Ta_2O_5	99.9
Boron trioxide	B_2O_3	99.0	Iron(III) oxide	Fe_2O_3	99.0
Stearic acid	$C_{18}H_{36}O_2$	100[a]	Chromium(VI) oxide	CrO_3	99.0
Acetanilide	C_8H_9NO	100[a]	Zinc oxide	ZnO	99.0
1-Nitroso-2-naphthol	$C_{10}H_7NO_2$	100[a]	Arsenic(III) oxide	As_2O_3	99.5
Nicotinamide	$C_6H_6N_2O$	100[a]	Molybdenum(VI) oxide	MoO_3	99.5
8-Hydroxyquinoline	C_9H_7NO	100[a]	Cesium sulphate	Cs_2SO_4	99.9
Sulfanilic acid	$C_6H_7NO_3S$	100[a]	Lead(II) nitrate	$Pb(NO_3)_2$	99.0
Benzoic acid	$C_7H_6O_2$	100[a]	Silver nitrate	$AgNO_3$	99.8
Tungsten(VI) oxide	WO_3	99.9	Thallium nitrate	$TlNO_3$	99.0
Niobium(V) oxide	Nb_2O_5	99.9	Mercury(II) oxide	HgO	99.0
Cobalt(II, III) oxide	Co_3O_4	96.7	Lead(II) oxide	PbO	99.0
Copper(II) oxide	CuO	98.5			

[a]Reference material according to Merck specifications.

RESULTS AND DISCUSSION

Figure 2 shows in a semi-logarithmic scale the experimental calibration curve resulting from the oxygen determination in high-purity compounds relative to acrylic glass as reference material. The total attenuation correction factor is plotted on the logarithmically divided ordinate. The factor is the ratio of the known stoichiometric oxygen content of each compound to the experimental oxygen content. On the abscissa sample weight and density are plotted. Since the capsules have a volume of 1.91 cm^3, the sample density equals nearly one half of the sample weight. The inset in Fig. 2 shows the area of organic test materials on a larger scale. Here, the small fluctuations of the correction factors from a value of about one prove that Plexiglas is also suitable as a primary standard. The error bars indicate the standard error of the mean of 10 single measurements. The dotted lines represent least-squares fits over the standard deviation. The resulting straight line in the semi-logarithmic plot shows an exponential dependence of the total attenuation correction factor on the sample density. A least-squares fit leads to the following averaged function

$$F = 0.969 \cdot e^{0.0179 \cdot \rho} \qquad (2)$$

where F is the correction factor and ρ the density. The deviations of the averaged curve from the individual values do not exceed 2%, thus lying within the 1σ-limits and being unimportant for routine oxygen determinations at the p.p.m. level. Consequently, it is possible to measure the oxygen content in nearly any matrix by use of an empirical density correction with

an absolute accuracy of ± 2%. This may be important in analyzing materials of unknown or complex composition. Further advantages are the rather short time needed for measuring the calibration curve, and the fact that a mono-standard method is used.

It is interesting to note that elements with high atomic number and large mass absorption coefficients, e.g. tantalum or tungsten, are found in the area around correction factors of unity because of the low densities of their oxides. Evidently the correction factor is determined almost exclusively by the density of the substances. A density correlation of the neutron attenuation has been reported by Anders and Briden [2], and McMahon [10] observed a linear decrease of the induced ^{16}N-activity with increasing bulk density of the irradiated materials. Andersen and Algots [11] found a linear dependence of neutron- and γ-absorption on the density for the 511-keV annihilation radiation of ^{13}N in different nitrogen compounds.

In further work, a more general treatment of the attenuation effects was developed and an attempt was made to calculate the measured attenuation factors from the data given by Nargolwalla et al. [3, 4]. The following assumptions were used.

An exponential absorption law is valid for both neutron- and γ-absorption, leading to the expression

$$I = I_0 \cdot e^{-\mu d} \tag{3}$$

where I_0 and I refer to the intensities before and after passing through a layer with thickness d and μ represents the macroscopic absorption coefficient for neutrons or γ-rays. Considering a homogeneous, mono-directional neutron or γ-flux, Vandecasteele et al. [5] have defined an effective thickness d_{eff} for attenuation in a sample. If $\mu \cdot d \ll 1$, d_{eff} becomes $d/2$, i.e. the average flux in the sample equals the flux in the middle of the sample. This treatment is well known from the self-absorption effect of β-rays where one half of the actual sample thickness is used for d. Taking into account scattering effects and flux gradients in addition to attenuation, Vandecasteele et al. [5] have defined the relationship $\bar{I} = \bar{I}_0 \cdot e^{-\mu d_{eff}}$, where $\bar{I}$ is the average neutron or γ-flux within the sample, and $\bar{I}_0$ is the average neutron or γ-flux in the void volume to be occupied by the sample, and has therefore no attenuation. They measured some effective thicknesses for different metals and γ-energies and found that the values were nearly equal to one half of the actual sample thickness for both neutron and γ-absorption. This is somewhat contradictory to the results of Nargolwalla et al. [3], who found an effective thickness for neutron attenuation which was significantly higher than the actual sample diameter. These authors [3] pointed out that the effective thickness should not need a physical meaning. Nevertheless, we have chosen a d_{eff} = 0.4 cm which equals half the sample diameter for the calculations of neutron and γ-self-shielding, since this choice resulted in the best fit to the experimental data (see Fig. 3). However, this approximation may be restricted to rather thin samples as is the case here.

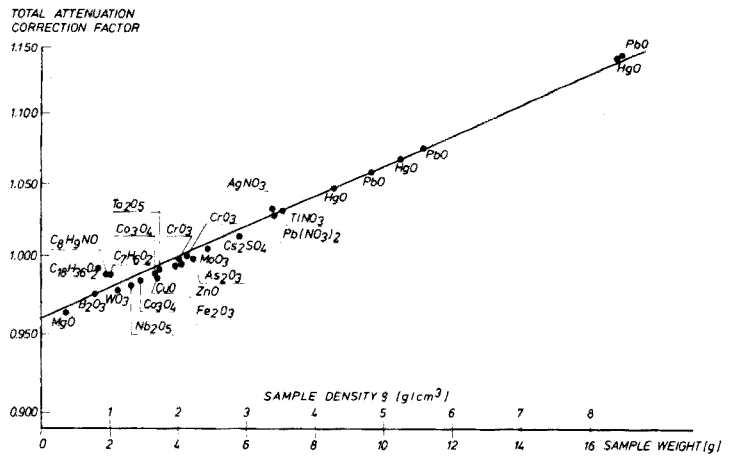

Fig. 3. Theoretical calibration curve for neutron and γ-attenuation. The ordinate is logarithmic. Full line: least-squares fit over the values.

For neutron attenuation calculations, instead of the microscopic 14-MeV neutron cross-sections, the microscopic neutron removal cross-sections are used; the latter have been tabulated [4] for all elements. The reasons for using the neutron removal cross-sections have been discussed in detail by Adams et al. [6] and Vandecasteele et al. [5], as mentioned before. The total macroscopic neutron removal cross-section S_R is then given [3] by

$$S_R = \frac{1}{V} \sum_{i=1}^{n} \frac{\sigma_{R(i)} \cdot W_i \cdot N_L}{A_i} \ [\mathrm{cm}^{-1}] \tag{4}$$

where V is the sample volume given in cm^3; $\sigma_{R(i)}$ is the microscopic neutron removal cross-section of element i given in 10^{-24} cm^2; A_i the atomic weight of element i; N_L is Avogadro's Number; n is the number of elements in the compound; and W_i is the weight of element i.

For calculation of total γ-self-absorption, the mass absorption coefficients for 6 MeV γ-radiation given by Storm et al. [12], which take into account the photo effect, Compton scattering including coherent scattering, and the nucleus and electron components of pair production, were used.

The following expression gives the total γ-attenuation coefficient μ_0

$$\mu_0 = \sum_{i=1}^{n} \left[(\mu/\rho)_i \cdot \frac{W_i}{V} \right] \ [\mathrm{cm}^{-1}] \tag{5}$$

where W_i, V and n are defined as above; $(\mu/\rho)_i$ is the mass absorption coefficient of the element i in the compound considered. Combination of eqns. (3)—(5) leads to a formula for the total correction factor F

$$F = \frac{O_{th}}{O_{ex}} = e^{[S_{R(x)} - S_{R(s)} + \mu_{0(x)} - \mu_{0(s)}] \cdot \frac{d}{2}} \tag{6}$$

where O_{th} is the theoretical oxygen content according to the stoichiometric composition; O_{ex} is the experimental oxygen content; d is the sample diameter; S_R is the total macroscopic neutron removal coefficient; and μ_0 is the mass absorption coefficient. The index x refers to the unknown sample and the index s to the standard.

By means of eqn. (6) the theoretical correction factors of all the calibration compounds used were calculated relative to Plexiglas as reference standard. A semi-logarithmic plot of the results versus the sample density is shown in Fig. 3, together with a least-squares fit leading to a straight line. The corresponding exponential function is given by

$$F = 0.960 \cdot e^{0.01947 \cdot \rho} \tag{7}$$

The agreement with the experimental values shown in Fig. 2 is very good, and this is reflected in the parameters of eqns. (2) and (7). The remaining deviations between the two curves shown in Figs. 2 and 3 are within the experimental 1σ-limits up to a density of about 10. This makes it possible to calculate individual theoretical attenuation correction factors if the chemical composition of the material under investigation is known.

These results agree with the data of Vandecasteele et al. [5], who have tabulated the theoretical total correction factors of some elements with $Z = 13$ to 83 using parameters corresponding to their sample geometry. Plotting these values against the density leads to a straight line similar to the present calculations.

The calibration method described above was applied for the first time to oxygen determinations in copper and titanium, within the framework of a certification analysis of reference materials coordinated by the Eurisotop Office of the European Communities. The results are shown in Table 2. In the case of copper, the total correction factor was taken from the experimental curve in Fig. 2, whereas in the case of titanium this quantity was calculated theoretically as described above. Since then the method has found application to other materials, e.g. steels and compounds of refractory metals.

TABLE 2

Results [13, 14] of the oxygen determination in copper and titanium by 14-MeV n.a.a.

	Mean value (p.p.m.)	Standard deviation (p.p.m.)	No. of analyses	Material
Present work	142	4	36	copper
average of 5 laboratories	140	7	180	
Present work	625	10	48	titanium
average of 5 laboratories	611	18	240	

The authors thank Prof. J. Hoste, University of Ghent, for useful discussions, Miss M. Schiefer and Messrs. G. Bennemann, N. Sauerwald and R. P. Seidel for experimental assistance, and the Bundesministerium für Forschung und Technologie for financial support.

REFERENCES

1 R. Gijbels, J. Hoste and A. Speecke, The Industrialisation of 14-MeV Neutron Activation Analysis for Oxygen in Steel; EUR-4297, Luxembourg, Sept. 1969.
2 O. U. Anders and D. W. Briden, Anal. Chem., 36 (1964) 287.
3 S. S. Nargolwalla, M. R. Crambes and J. R. DeVoe, Anal. Chem., 40 (1968) 666.
4 S. S. Nargolwalla, M. R. Crambes and J. E. Suddueth, Anal. Chim. Acta, 49 (1970) 425.
5 C. Vandecasteele, A. Speecke and J. Hoste, The Determination of Oxygen in Non-Ferrous Metals by 14-MeV Neutron Activation Analysis; Commission of the European Communities, Eurisotop Office Information Booklet No. 68.
6 F. Adams, J. P. Op de Beeck, P. Van den Winkel, R. Gijbels, D. De Soete and J. Hoste, Crit. Rev. Anal. Chem., I, (1971) 499.
7 D. E. Wood, Advances in Activation Analysis, Vol. 2, Academic Press, New York, 1972, p. 265.
8 A. F. Avery, D. E. Bendall, J. Butler and K. T. Spinney, Methods of Calculation for Use in the Design of Shields for Power Reactors, Report AERE-R-3216 (1960).
9 R. van Grieken and J. Hoste, Annotated Bibliography on 14-MeV Neutron Activation Analysis, Commission of the European Communities, Eurisotop Office Information Booklet No. 65, 1972.
10 C. McMahon, Mines Branch Investigation Rep. IR 64-43, Dept. Mines Techn. Survey, Ottawa, Canada, May 1964 cit. in (9).
11 G. H. Andersen and J. M. Algots, J. Radioanal. Chem., 3 (1969) 261.
12 E. Storm, E. Gilbert and H. Israel, Gamma-Ray Absorption Coefficients for Elements 1 through 100, Rep. LA 2237 (1958).
13 G. Kraft and J. Hoste, The Certification of Oxygen in Non-Ferrous Metals, Part S: Oxygen in ETP Copper, ITE-Report No. 86 of the Commission of the European Communities, Eurisotop Office.
14 ITE-Report, Eurisotop Office, CEC, Brussels, to be published.

Analytica Chimica Acta, 89 (1977) 281—286

RADIOCHEMICAL SEPARATION OF SELENIUM FROM HYDROCHLORIC OR HYDROBROMIC ACID INTO TOLUENE

S. LANDSBERGER* and G. G. J. BOSWELL

Department of Chemistry, University of Salford, Salford (Great Britain)

(Received 22nd July 1976)

SUMMARY

A separation of selenium based on the extraction of different concentrations of Se(IV) from 12 M hydrochloric acid or 8 M hydrobromic acid into toluene is described. Recoveries of 92% and 97%, respectively, are achieved in 7 min. Oxidizing agents interfere.

Although several papers have appeared on the extraction of selenium from acids into organic solvents [1—8] with and/or without the use of complexing agents, the solvent extraction of Se(IV) from acid solution into aromatic hydrocarbons, without the use of complexing agents, has received little attention. Se(IV) can be extracted from HBr into benzene containing some phenol [9]; from these results, toluene is obviously an alternative solvent. Tanaka [10] studied the extractibility of Se(IV) into benzene from HBr and from HBr containing HCl, H_2SO_4 or $HClO_4$. Kolesnikova and Iofa reported the extraction of Se(IV) from different concentrations of HCl [11] and HBr [12] into n-octanol, di-n-butyl ether, benzene etc. Toluene was briefly mentioned, but little data were reported.

There is some dubiety in the literature regarding the species formed at equilibrium when Se(IV) is added to HCl, HBr and water, and to the selenium species extracted into organic solvents. Venkateswaran [13] studied the Raman spectra of aqueous Na_2SeO_3 and reported that none of the bands originated from SeO_3^{2-} ions. In contrast, Siebert [14] reported that Raman spectra of aqueous Na_2SeO_3 showed evidence of SeO_3^{2-} ions. Hendra and Jovic [15] reported the existence of complex selenium ions in solutions of HCl and HBr. Kolesnikova and Iofa [11] suggested that selenium may exist in the molecular form $SeCl_4$ in HCl and is probably extracted as a polymer; they also reported that selenium is extracted in the form of $SeBr_4$ and Se_2Br_2 from HBr [12].

---

*Present address: Laboratoire de Physique Nucléaire, Université de Montréal, Case Postale 6128, Montreal H3C 3T4, Québec. This paper is derived from a thesis in partial fulfilment of the requirement for an M.Sc., submitted by S.L. (to whom all enquires should be addressed).

It appeared that further work with the Se(IV)—toluene system might clarify the suggested mechanism by gathering evidence concerning the species of Se(IV) existing at equilibrium in the aqueous phases and determining those species extracted into toluene.

EXPERIMENTAL

Reagents and equipment

Chemical reagents of the highest purity available were used without further purification. Radioactive selenium (^{75}Se, $t_{1/2}$ = 120 d), as Na_2SeO_3, was obtained from the Radiochemical Centre, Amersham, Great Britain.

A Nuclear Enterprises Type 12 A 12 scintillation counter with a well-type NaI(Tl) crystal detector was coupled to an E.M.I. type 9531 photomultiplier. This combination had a deadtime of 1 μs. Counting was done inside a lead castle (5 cm thick). Background radiation was of the order 25—30 counts min^{-1}. The ultraviolet work was done on a Cary 14 ultraviolet spectrometer; the Raman spectrum was obtained with a Cary 82 laser spectrometer.

Preparation of standards

Active and inactive selenium standards were prepared. For the inactive standards, different concentrations of Se(IV) were made up by dissolving appropriate amounts of Na_2SeO_3 in diluted and concentrated acids, (i.e. 12 M HCl, 8 M HBr, and 18 M H_2SO_4). The final selenium concentrations varied between 10^{-2} and 10^{-5} M.

For the active standards, 1 millicurie (mCi) of ^{75}Se was used to determine the percentage of Se(IV) extracted. $Na_2{}^{75}SeO_3$ was dissolved in 100 ml of distilled water to give a Se(IV) concentration of 3.26 μg ml^{-1}. This primary standard was diluted with the appropriate concentrated acid to form a secondary standard containing 0.65^2 μg Se(IV) ml^{-1}; from this secondary standard, a series of calibrating solutions was prepared.

Solvent extraction procedure

Solvent extractions were done rigorously as follows: 9.7 ml of inactive standard Se(IV) solution and 0.3 ml of active tracer solution (0.19^2 μg) were added to 10.0 ml of toluene in a 100-ml separatory funnel and shaken vigorously by hand for 2 min. The phases were separated after 5 min; 2 ml of each phase was taken for counting. Preliminary experiments showed that over 99.5% of the activity was accounted for. Samples were counted for a period of 100 s (more than 10,000 counts). Replicate experiments of the entire separation procedure gave a standard deviation of less than 1%. After subtraction of the background count, the amount (%) of Se(IV) extracted into the toluene phase was calculated.

Effects of experimental variables

Effect of Se(IV) concentrations on the percent extraction into toluene. In this series of experiments, Se(IV) was extracted from concentrated HCl, HBr or H_2SO_4 while the concentration of Se(IV) was varied between 10^{-2} and 10^{-5} M. Figure 1 shows the results. In each case, the minimum extraction occurred at 10^{-2} M and the maximum at 10^{-5} M. The high percentage of Se(IV) extracted at low concentrations was not exhibited by the H_2SO_4—toluene system because sulphuric acid is soluble in toluene. Tanaka [10] reported a 61.1% extraction of Se(IV) from HBr into benzene. The present work gave 58.1% extraction under similar conditions.

Effect of acid concentration on the extractibility of Se(IV) into toluene. The concentration of Se(IV) at which maximum extraction occurred in the previous experiments (10^{-5} M) was used. A plot of the percentage extracted against acid molarity is shown in Fig. 2. The percentage of Se(IV) extracted into toluene increased gradually as the molarity of HCl increased and sharply as the molarity of HBr increased. Similar results with HBr—benzene systems have been obtained [9, 10].

Effect of the addition of oxidizing agents on the extractibility of Se(IV) into toluene under optimum conditions. Oxidizing agents added to the aqueous phases of both HCl and HBr decreased the extractibility of selenium

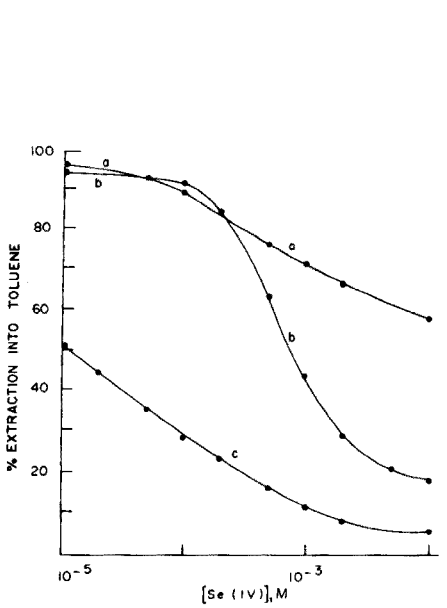

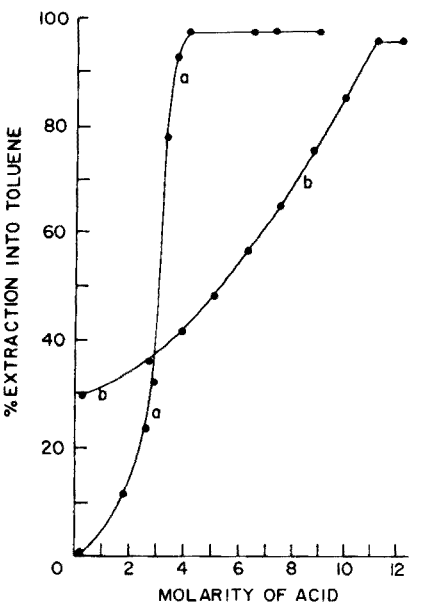

Fig. 1. Influence of the concentration of Se(IV) in the aqueous phase on the percent extraction into toluene. (a) HBr (b) HCl (c) H_2SO_4.

Fig. 2. Extraction of Se(IV) as a function of the concentration of acid. (a) HBr (b) HCl.

into toluene see (Table 1). Increased amounts of oxidizing agents yielded the same results, suggesting that the initial amount was sufficient to complete the oxidation.

Effect of the contact time of the phases on the extractibility of Se(IV) into toluene. When optimum conditions for the extraction of Se(IV) had been determined, i.e., concentrated acid and low (10^{-5} M) Se(IV) concentration, the effect of contact times between the phases was examined for durations of 2—30 min. Time variations were also carried out on the extraction of 10^{-5} M and higher concentrations of Se(IV) from H_2SO_4. The results suggested that contact times greater than 2 min had no influence on the percentage of extraction of Se(IV) into toluene.

RESULTS AND DISCUSSION

Nature of selenium species in solution

To evolve a credible extraction mechanism, a knowledge of the selenium species present in the solution was necessary, hence spectroscopic studies were made.

Ultraviolet spectra of 10^{-4} M sodium selenite in water, 12 M HCl, and 8 M HBr, respectively, were obtained (Fig. 3). Each solution exhibited only one absorption, at 190—192 nm for water, 218—220 nm for HCl, and 325—328 nm for HBr.

A Raman spectrum was obtained for 1.5 M Na_2SeO_3 in 12 M HCl (solutions of lower concentration yielded poor, ill-defined, spectra). The Raman spectrum (Fig. 4) agrees reasonably with that reported by Hendra and Jovic [15] for SeO_2 dissolved in 12 M HCl.

The spectroscopic data appear to be useful in suggesting a mechanism. Thus, sodium selenite in water yields a single absorption at 190 nm; in 12 M HCl and 8 M HBr, this peak does not occur, i.e. the concentration of SeO_3^{2-} (if it is present at all) is too low to show a detectable absorption with the apparatus used, and the considerable change in peak absorption resulting from change of solvent indicates that substitutional-type reactions occur within the concentrated acidic solvents, leading ultimately to highly chlorinated or highly

TABLE 1

Extraction with and without oxidizing agents

Acid	% Se(IV) extracted			
	Without oxidants	With oxidants		
		$KClO_3$ 200 mg	$KMnO_4$ 200 mg	HNO_3 0.5 ml
HCl	95.1	14.7	13.8	13.7
HBr	97.2	49.6	48.0	18.1

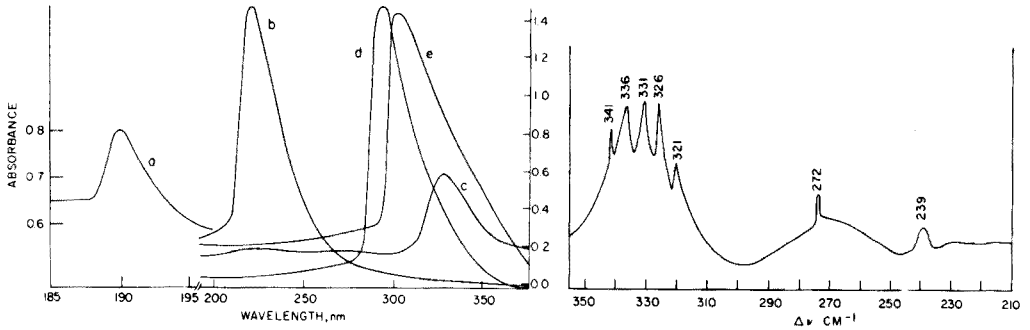

Fig. 3. U.v. spectra of 10^{-4} M Na_2SeO_3 in concentrated acid before and after extraction. (a) H_2O (b) HCl (c) HBr (d) extraction from HCl into toluene (e) extraction from HBr into toluene.

Fig. 4. Raman spectra of 1.5 M Na_2SeO_3 in 12 M HCl.

brominated selenium species. Thus, it would be reasonable to expect the species $SeOCl_4^{2-}$, $SeCl_5^-$, and $SeCl_6^{2-}$ in 12 M HCl, and their direct analogues in 8 M HBr; the ion SeF_5^- has been reported [16].

The Raman spectrum obtained is not inconsistent with this suggestion. Following the analysis of Hendra and Jovic [15], the peak at 272 cm^{-1} in 12 M HCl can be ascribed to the $SeCl_6^{2-}$ ion. However, our spectrum has not yet been completely analyzed, and therefore further conclusions cannot be drawn; the main rationale for depicting the Raman spectrum of sodium selenite in 12 M HCl is that the instrument used resolved the broad band at 340 cm^{-1} reported by Hendra and Jovic [15]. Also, although Na_2SeO_3 in 8 M HBr was not studied, Hendra and Jovic [15] studied the SeO_2—HBr system and obtained peaks that they assigned to the ion $SeBr_6^{2-}$.

Nature of selenium species extracted into toluene

Two further u.v. spectra were obtained, of 10^{-4} M sodium selenite extracted into toluene from 12 M HCl, and from 8 M HBr. These spectra, also shown in Fig. 4, exhibited only one absorption peak, at 290—293 nm and 298—302 nm for the species extracted from concentrated HCl and HBr respectively. Because these peaks, after extraction, show differences from the parent solutions, the u.v. spectra indicate that the selenium species in 12 M HCl or 8 M HBr differ from the species existing in toluene after extraction.

It has been suggested [11] that Se(IV), upon extraction by an alcohol, ketone, or ether, is extracted in the form of a complex, suggested to be of the type $[H_3O(H_2O)_x\ (\text{organic})_x]_2SeCl_6$. A similar type of complex has been suggested [17] to result from the extraction of Te(IV) by ether.

Consequently, the results of this work can be interpreted on the basis of the formation between Se(IV) ions and toluene of complexes of the type: $[H_3O(H_2O)_x\ (C_6H_5CH_3)_x]_2\,Se\ X_6$; $[H_3O(H_2O)_x\ (C_6H_5CH_3)_x]\ Se\ X_5$; and

$[H_3O(H_2O)_x\ (C_6H_5CH_3)_x]_2\ SeO\ X_4$; where X represents either Cl or Br. Aromatic complexes of a similar type have been reported [18]. However, the formation of various complexes in toluene does not explain why a higher percentage of Se(IV) is extracted at lower concentrations. This type of behaviour, (Fig. 1) has been observed previously [11] and attributed to polymerization of the Se(IV) species in aqueous phase. The present results do not suggest a similar type of mechanism, but this does not represent in any way a denigration of the work of Kolesnikova and Iofa [11].

We thank Dr. L. S. Bark, Department of Chemistry, University of Salford, for helpful discussions. One of us (S. L.) is indebted to R. A. Westbury, Department of Chemistry, Concordia University, Sir George Williams Campus, Montreal, for helpful advice.

REFERENCES

1 H. G. Hicks, Atomic Energy Commission, U.S., 2, 481, 795 (1957).
2 N. Jordanov and I. Havesov, Z. Anal. Chem., 248 (1969) 296.
3 K. L. Cheng, Anal. Chem., 28 (1956) 1738.
4 N. Jordanov and L. Futekov, Talanta, 12 (1965) 371.
5 N. Jordanov and L. Futekov, Talanta, 13 (1966) 163.
6 J. H. Watkinson, Anal. Chem., 32 (1960) 981.
7 T. H. Handley and J. A. Dean, Anal. Chem., 34 (1962) 1312.
8 H. Handley, Anal. Chem., 35 (1963) 991.
9 T. McGee, J. Lynch and G. G. J. Boswell, Talanta, 15 (1968) 1435.
10 K. Tanaka, Japan Analyst, 18 (1969) 315.
11 N. M. Kolesnikova and B. Z. Iofa, Russ. J. Inorg. Chem., 11 (1966) 1161.
12 N. Kolesnikova, B. Z. Iofa and A. N. Nesmeyanov, Bulletin of the Institutions of Higher Education, Chemistry and Chemical Technology, 12 (1969) 1023.
13 C. S. Venkateswaran, Proc. Ind. Acad. Sci. 3A, (1936) 533.
14 H. Siebert, Z. Anorg. Chem., 275 (1954) 225.
15 P. J. Hendra and Z. Jovic, J. Chem. Soc. (A), (1968) 600.
16 E. E. Aynsley, R. D. Peacock and P. L. Robinson, J. Chem. Soc. (A), (1952) 1231.
17 S. Kaganovich and L. V. Smiyagin, The Production of Selenium and Tellurium in the Capitalistic Countries (1962).
18 A. P. Bobylev, L. N. Komissarova and V. I. Spitsyn, Zh. Obshch. Khim., 39 (1969) 34.

Analytica Chimica Acta, 89 (1977) 287—296

THE FORMATION OF MIXED COPPER(II) SULFIDE—SILVER(I) SULFIDE MEMBRANES FOR COPPER(II)-SELECTIVE ELECTRODES

G. J. M. HEIJNE, W. E. VAN DER LINDEN and G. DEN BOEF

Laboratory for Analytical Chemistry, University of Amsterdam, Nieuwe Achtergracht 166, Amsterdam (The Netherlands)

(Received 5th October 1976)

SUMMARY

Several methods for the preparation of mixed copper(II) sulfide—silver(I) sulfide precipitates have been investigated. Pellets of these materials have been tested for their suitability as copper(II)-selective membranes. Homogeneous membranes with satisfactory electrochemical properties can be prepared only from precipitates obtained by addition of the metal salts to sodium sulfide. Membrane leakages, limits of detection, calibration curves and titration curves with different types of precipitate are discussed.

Since Ross and Frant [1, 2] introduced the use of metal sulfide membranes for ion-selective electrodes (i.s.e.) as sensors for copper(II), cadmium(II) and lead(II) ions, many authors have published methods for the preparation of copper(II)-selective electrodes (see e.g. references 3—10). Two main aspects of these electrodes have to be distinguished, i.e. the way of preparing the electroactive material and the way in which this material is applied to construct the actual electrode.

For the preparation of the electroactive material by simultaneous precipitation of copper(II) sulfide and silver(I) sulfide, three precipitating agents have been used: sodium sulfide [2, 3, 5, 7, 8], hydrogen sulfide [3, 5] and thioacetamide [5]. Buck [11] recently discussed this subject. He concluded that precipitation with hydrogen sulfide or homogeneous precipitation with thioacetamide in weakly acidic medium has to be preferred over precipitation in sodium sulfide medium; the latter medium is strongly alkaline and coprecipitation of hydroxides is likely to occur. This would result in an electrode with inferior behaviour; especially, unfavourable lower limits of detection may be caused by more soluble species being occluded in the metal sulfide precipitate. As far as copper sulfide is concerned, the literature shows no difference between these precipitants. Mascini and Liberti [3] used sodium sulfide and hydrogen sulfide, while Hansen et al. [5] compared all three precipitants, but no significant difference was reported by these workers.

The electroactive material can be used either as homogeneous or as heterogeneous membranes. In the heterogeneous form a matrix is used to support the

polycrystalline substance. Examination of the literature shows that homogeneous membranes for the copper(II) i.s.e. are made of sodium sulfide precipitates only, except in those cases where a single crystal [9] or a sintering technique [4] has been used. Precipitates obtained with hydrogen sulfide [3, 5] or homogeneous precipitation techniques [5, 6] have always been applied for the preparation of heterogeneous membranes and in the case of the so-called Selectrode. The present study has shown that these precipitates probably cannot be used for homogeneous membranes at all.

If it is assumed that the limit of detection depends only on the solubility of the electrode material, copper(II) sulfide electrodes exhibit a large deviation from theory at low concentrations. A high limit of detection of the electrode is found in the case of ordinary calibration curves as well as in complexiметric titrations [12]. Several explanations have been proposed, for example, based on the existence of a diffusion barrier [13] and on adsorption [14]. Blaedel and Dinwiddie [14] concluded that adsorption is the more important factor in the case of copper(II) sulfide solid-state electrodes.

Prior to a more systematic study of the factors which determine the behaviour of copper(II) sulfide/silver(I) sulfide membranes at such low concentrations, the influence of the preparation of the precipitates and the membranes was investigated. This paper deals with several possible methods for this preparation. To avoid any possible influence of supporting materials only homogeneous membranes are considered.

EXPERIMENTAL

All chemicals used were of analytical-reagent quality. Copper and silver nitrates were used throughout, except where stated otherwise.

Electrode discs were pressed in an evacuated KBr-die (Beckman-RIIC D-01, diameter 13 mm) with a 16-ton hydraulic press (Beckman-RIIC, P-16). Usually 250 mg of the precipitate was sufficient to produce a pellet of about 0.4 mm thickness. This pellet was sealed to a glass tube (external diameter 13 mm) with an α-cyanoacrylate adhesive (Cyanolit). This electrode was used with an internal solution. Measurements were carried out with the following electrochemical cell:

$$\mathrm{Ag} \,\big|\, \mathrm{AgCl,KCl(0.1\ M)} \,\big\|\, \begin{matrix} 10^{-3}\ \mathrm{M\ Cu(NO_3)_2} \\ 10^{-1}\ \mathrm{M\ KNO_3} \\ \text{(internal solution)} \end{matrix} \,\big|\, \mathrm{CuS,Ag_2S} \,\big|\, \begin{matrix} \text{external} \\ \text{solution} \end{matrix} \,\big\|\, \mathrm{KCl(0.1\ M),AgCl} \,\big|\, \mathrm{Ag}$$

In some experiments the internal solution was replaced by a direct silver contact. For comparison a commercial copper(II)—i.s.e. (Orion Research, model 94-29A) was used.

The potentials were measured with a millivoltmeter (Radiometer pHM26) connected to a recorder (Goertz, Servogor RE 511). Because the recorder output of the meter has an offset voltage of about 78 mV, two potentiostats (Knick, S12 and S16) were used to compensate this offset and to select the proper voltage range. Potentials could be read within 0.1 mV.

All experiments were carried out in 10^{-1} M KNO_3, $2 \cdot 10^{-2}$ M acetate buffer pH 4.7. The temperature was kept at 25.0 ± 0.1°C. An air-driven magnetic stirrer was used to avoid electrical noise.

Additions of copper(II) ion for calibration curves and of ligands for titrations were made with a microburette (Metrohm E 457).

RESULTS

Tests for the evaluation of the electrochemical characteristics

Preliminary experiments with discs pressed from precipitates made with thioacetamide showed leakage of the internal solution through the membrane after some time. This was surprising since no indications of leakage have been reported in the literature. Therefore, with all precipitates, discs were tested for leakage by filling the electrode with internal solution and checking daily for the appearance of salt crystals on the outer part of the electrode. If leakage occurred, this could generally be detected within a few days. Precipitates that showed no leakage after two weeks were taken not to be leaking; this was justified by inspection after several months.

When an electrode did not leak after a few days it was tested electrochemically in three ways.

(i) Calibration curves of E vs. pCu were prepared in the concentration range $5 \cdot 10^{-6}$—10^{-2} M by the addition of copper nitrate solution to the buffer solution. The parameters E' and S of the Nernst equation, $E = E' + S \log a_{Cu}$, were determined for the linear part of the curves. These measurements also gave information about the time needed to obtain a stable potential reading. When an electrode started leaking, it was always attended by drifting potentials and a low and continuously decreasing value of S.

(ii) Titrations of 10^{-3} M copper(II) with 10^{-1} M EDTA were carried out with special attention to the electrode behaviour at low copper concentrations in the presence of excess of ligand. Generally, the part of the curve preceding the equivalence point (e.p.) was in accordance with the parameters S and E', but the behaviour around the e.p. and thereafter was different for each precipitate. The magnitude of the potential jump around the e.p. is a significant parameter for the characterization of an electrode. Because of the asymmetric shape of the potentiometric titration curve, it was often difficult to locate the e.p. exactly and to give an unambiguous value for the potential jump. As the titration curves in the neighbourhood of the e.p. were obtained by the addition of equal amounts of about 2.5% of the total equivalent amount of ligand, the potential jump was taken as the largest voltage difference found for two successive additions, i.e. about 5% of the equivalent amount. Theoretically this difference should have a value of 150—180 mV under the chosen conditions.

(iii) The long-term stability was checked by immersing the electrode in 10^{-3} M copper(II). The potential reading was constant within 1 mV for 15 h for all those precipitates that showed a reasonably good response under (i).

Precipitation procedures

Thioacetamide. The procedure described by Hansen et al. [5] was applied because good results were reported by these as well as other authors [12]. However, pellets pressed from this precipitate started leaking after one or several days, although a Selectrode-type electrode prepared from the same material gave a good response. To obtain a more finely divided powder, precipitation was carried out in 1 M solutions instead of 0.1 M [5], but no significant improvement was observed. When the order of addition was reversed and a 1 M metal solution was added to the thioacetamide solution (1 M), the pelleted precipitates showed no leakage, but the response characteristics were still unsatisfactory. The limit of detection of the electrode was rather high, the jump in the e.p. was far too small and the potential stabilized rather slowly (see Table 1). Washing with carbon disulfide to remove any excess of sulfur gave no improvement.

Hydrogen sulfide. Hydrogen sulfide was bubbled at moderate speed through 1 M and 0.1 M metal solutions which were about $3 \cdot 10^{-3}$ M in nitric acid. Each precipitate was washed four times with deionized water, once with 10^{-1} M nitric acid, twice with redistilled water and twice with acetone, and then dried overnight in air at 80° C. In both cases, the pellets showed leakage within a few days. Treatment of the 1 M batch with carbon disulfide had no effect. When the precipitates were washed with 10^{-3} M EDTA the solution was bluish, probably because of the copper—EDTA complex. Since, according to Erdey [15], the presence of more than 1% nitrate interferes with the formation of copper sulfide the precipitation was repeated in 10^{-2} M perchloric acid [3]. Since no positive results were found, metal perchlorates were tried in about 0.9 M perchlorate at pH 2. Although precipitation was completed much faster in this case, leakage of the pellets still occurred, so that electrochemical measurements were not viable.

Sodium sulfide. The procedure used was adapted from that of Czaban and Rechnitz [7], which differs from an analogous method [8] only insofar as the precipitate is not washed with carbon disulfide; excess of sulfide is used in both cases, 10% in [8] and not specified in [7]. The adapted version was as follows: 0.02 mole of copper nitrate and 0.04 mole of silver nitrate were dissolved in 50 ml of redistilled water, and the solution was added dropwise with vigorous stirring to 0.072 mol of sodium sulfide (1 M solution). Both solutions were cooled to about 2° C. The addition took about 3 min. During this period the temperature rose to about 15° C. The solution was gradually heated to 70—75° C in 40 min and kept at that temperature for 30 min, still with vigorous stirring. After settling and decantation of the supernatant liquid (or centrifugation at moderate speed) the precipitate was washed thoroughly: four times with 200 ml of deionized water at 70° C, once with 100 ml of 0.1 M nitric acid and twice with 200 ml of redistilled water at room temperature. Each time the precipitate was stirred for 5 min and the supernatant liquid removed after centrifugation. Finally it was washed with acetone and dried at 80° C in air. Although the precipitate seemed to be dry

after a few hours, it was best dried overnight. The dry precipitate was stored over silica gel.

This procedure yielded reproducible electrodes with reasonable performance characteristics (see Table 1). When the excess of sulfide was reduced to 20%, the resultant electrodes showed less favourable properties. The jump around the equivalence point was smaller, the response was slower, and the potential readings after the e.p. took longer to stabilize and showed larger differences with increasing excess of the ligand. To establish whether the ratio of copper(II) sulfide to silver(I) sulfide has an influence on the characteristics of the membranes, precipitates were prepared with other molar ratios, each in the presence of 20% excess of sulfide. A ratio of 55 : 45 reduced the potential jump to 25—30 mV, whereas for a 70 : 30 mixture there was hardly any response at all and leakage occurred. With ratios of 45 : 55 and 30 : 70 the behaviour did not deviate significantly from that of the equimolar precipitate. These findings do not agree fully with the results of other authors [2, 3, 7]. Thompson and Rechnitz [8] claimed the best results for a 50 : 50 ratio, although variations to both sides were said to be acceptable. In fact, as is found in the present study, the difference is not striking when only the calibration curves are considered, except for the 70 : 30 precipitate. Generally, the response time is slightly worse with ratios deviating from 50 : 50.

The method of preparation given by Frant and Ross [2] with 0.1 M metal concentrations was applied with a molar ratio of 40 : 60 and a 50% or 100% excess of sulfide. In both cases, the results were the same as those obtained with a 50 : 50 ratio and 20% excess of sulfide as described above. Treatment with carbon disulfide seemed to be unfavourable. For pellets containing 66% of copper(II) sulfide, proper sealing appeared to be impossible. The results with the Orion electrode, which was made according to the patent of Frant and Ross [2] are also given in Table 1. This electrode equalled the best precipitate but the signal was noisier. After the e.p., unsteady and slowly drifting potentials occurred. This was also reported by Baumann [16].

Influence of the pressure

The pressure used in the preparation of the discs was varied between 3800 and 9500 kg cm^{-2}. The pressure chosen was applied for 10 min after evacuation for 4—5 min by means of an oil pump. Variations in this procedure were of no importance, which agrees with the results obtained by Czaban and Rechnitz [7]. It was found that, for precipitates which produced leaking membranes, increase of the applied pressure extended the time before leakage could be detected, but did not prevent it. For sodium sulfide precipitates, no leakage occurred in this pressure range, but the electrochemical behaviour and the limit of detection of the electrode were better after pressing at 7600 than at 3800 kg cm^{-2}. No further improvement was observed by increasing the pressure above this value, which is the maximum allowable pressure for the die used.

TABLE 1

Characteristics of several types of simultaneously precipitated copper(II) sulfide—silver(I) sulfide

Type	Precipitation mode	Calibration curves			Titrations		Leakage
		S (mV/pCu)	Linear range[a] (pCu)	Response time (min)	E.p. jump[b] (mV)	Stabilization time after e.p. (min)	
1	Thioacetamide 0.1 M solutions	~ 20	2.0—2.5	5—20	—	—	large
2	Thioacetamide 1 M solutions	⩽ 28	2.0—4.0	5—20	15—25	large	slow
3	As type 2 reversed addition	29—30	2.0—4.5	½—10	40	large	none
4	1 M Na_2S, 80% excess	29—30	2.0—5.0	< 1	85—100	5—10	none
5	1 M Na_2S, 20% excess	29—30	2.0—4.5	½—10	55—80	> 10—15	none
Orion	0.1 M Na_2S, excess unknown	30—31	2.0—4.5	½—2	100—110	5—10[c]	—

[a] Linear ranges were determined in the range $5 \cdot 10^{-6}$—10^{-2} M.
[b] Potential jump at the equivalence point for the addition of 5% of the equivalent amount (see text).
[c] The signal was very noisy.

Detailed examination of type 4 electrodes

Table 1 shows typical values for the more important precipitates. The experiments discussed below were done with electrodes of type 4, except where stated otherwise.

Linear range. Generally calibration curves were measured for the concentration range $5 \cdot 10^{-6}$—10^{-2} M. These curves showed a linear part for $2 \leqslant$ pCu $\leqslant 5$, where pCu = $-\log a_{Cu^{2+}}$. Some extension of this linear part was observed when the calibration was started at $5 \cdot 10^{-8}$ M by the addition of more dilute copper(II) solution. Probably because of the more gradual increase in concentration, the linear range then started at about pCu 5.7. The linear range also depends on the pretreatment of the electrode. Figure 1 shows three typical calibration curves for a type 4 electrode, one directly after preparation, a second immediately after this first calibration curve, and a third after a titration of 10^{-3} M copper(II) with 10^{-1} M EDTA, which was continued until a 100% excess of ligand was present. To obtain the correct copper(II) activities in the upper region of the curve, it is necessary to take into account the changes in $\alpha_{Cu(Ac)}$ [17] and in the activity coefficient [18] caused by the addition of the copper nitrate. For this purpose the following stability constants were used: $\log \beta_{CuAc} = 1.8$, $\log \beta_{CuAc_2} = 3.0$ and $\log \beta_{HAc} = 4.75$.

When 10^{-3}, 10^{-4} and 10^{-5} M copper(II) were titrated, it was found that before the e.p. the response remained linear down to pCu = 7.1.

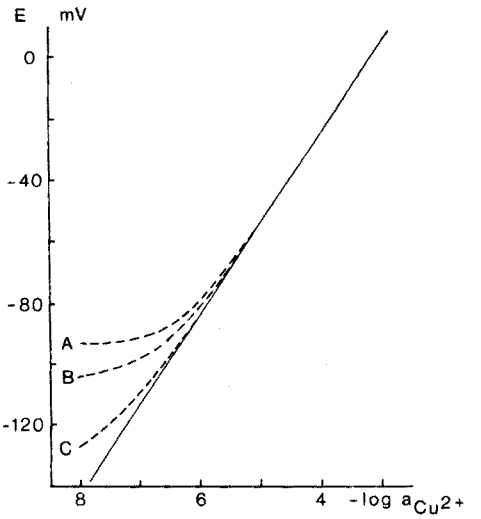

Fig. 1. Calibration curves for an electrode of type 4. Medium: 10^{-1} M KNO_3, $2 \cdot 10^{-2}$ M acetate buffer, pH 4.7. A: Curve for a freshly prepared electrode. B: Curve measured immediately after A. C: Curve measured after a titration of 10^{-3} M copper(II) with 10^{-1} M EDTA and addition of a 100% excess of ligand.

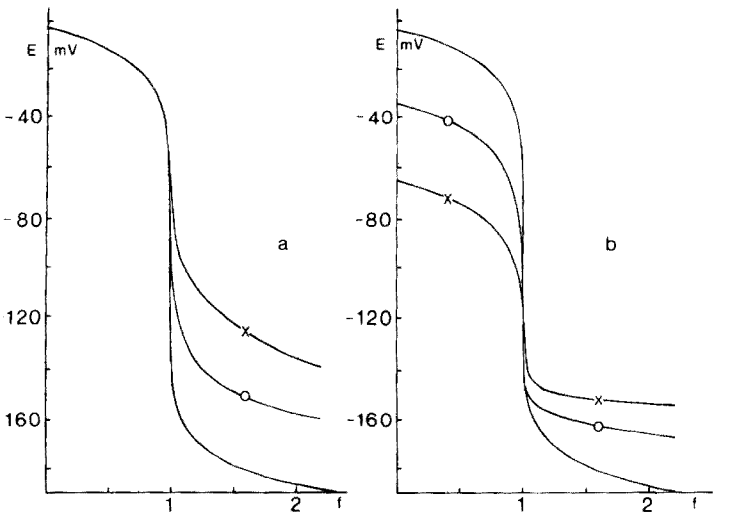

Fig. 2. Titration curves for an electrode of type 4. Medium: 10^{-1} M KNO_3, $2 \cdot 10^{-2}$ M acetate buffer, pH 4.7. a: Titration of 10^{-3} M copper(II) with 10^{-1} M ligand, (——) EDTA, (—x—) Trien and (—o—) Tetren. b: Titration of copper(II), (——) 10^{-3} M, (—o—) 10^{-4} M, (—x—) 10^{-5} M with EDTA, 10^{-1} M, 10^{-2} M and 10^{-3} M, respectively.

Titrations. Titrations of 10^{-3} M copper(II) were done with 10^{-1} M EDTA, Trien and Tetren (Fig. 2a). Plots of the copper concentration vs. the titration parameter f produced straight lines [12]. The same applied to titrations of 10^{-4} and 10^{-5} M copper(II) with 10^{-2} and 10^{-3} M EDTA, respectively (Fig. 2b). As mentioned above, the potentials after the e.p. show a large deviation from theory. Apart from Anfält and Jagner [10], who presented a curve with a jump that is even larger than theory predicts, all other authors [3, 5, 9, 12, 19] also obtained a jump that was too small. Van der Meer et al. [12] obviated this problem by introducing an experimental limit of detection of the electrode in calculating their theoretical titration curves. Only two other authors have paid further attention to this phenomenon. Hulanicki et al. [9], who used a single crystal of copper(I) sulfide as the sensor, found a larger jump when Tetren was used as the titrant instead of EDTA. They explained this by supposing that Tetren forms stronger complexes with copper(I) than does EDTA. Nakagawa et al. [19] suggested that silver ions at the electrode surface, which are not strongly complexed by EDTA, would determine the potential at low concentrations of free copper(II) ions. A small amount of 1,10-phenanthroline indeed extended the jump by about 50 mV, possibly by partly complexing these silver ions.

With the electrodes used in the present study these results could not be obtained. Figure 2a shows that the order of the potential jump for the different ligands is as can be expected from the conditional stability constants ($\log K'_{\mathrm{CuTrien}} \simeq 8.7$; $\log K'_{\mathrm{CuTetren}} \simeq 10.4$; $\log K'_{\mathrm{CuEDTA}} \simeq 11.7$) [20]. If the suggestion of Hulanicki is right then it is clear that copper(I) plays no rôle in the response of the type of electrode used in this investigation. As far as 1,10-phenanthroline was concerned, its presence had some effect. The bend of the curve after the equivalence point was less sharp, resulting in a more negative limit of detection of the electrode, but the potential jump as defined above had the same value in both cases. A similar bending of the curve is presented by Nakagawa et al.

The characteristics of the response to EDTA after the e.p. for the different types of electrodes could roughly be classified into two groups; the potential readings either stabilized rather quickly and showed only a small dependence on the ligand concentration, or they stabilized very slowly and showed a large dependence. Type 4 and the Orion electrode belong to the first group, while all others belong to the latter (cf. Table 1). Therefore it can be concluded that electrodes having a fast response after the e.p. in titrations also have the best calibration curves. Pungor et al. [21] recently reported well defined responses to several complexing agents like citrate and 8-hydroxyquinoline and presented calibration curves of E vs. log [ligand]. For EDTA none of the present electrodes showed a linear relationship between the potential E and the free ligand concentration, [EDTA], or its logarithm, log [EDTA].

DISCUSSION

An effort has been made to find an explanation for the results reported above. In a study of the suitability of many compounds for the preparation of ion-selective sensors, Kahr [22] found that it was difficult to press pellets from copper(II) sulfide, while silver(I) sulfide did not give problems. The same results were found in the present study. Discs of copper sulfide showed leakage quickly and crumbled after some time. In the preparation of the individual sulfides, no difference was observed between the use of either thioacetamide or sodium sulfide as the precipitant. Chemical analysis of the copper sulfide precipitate showed that the relative copper content in the sulfide was too low; the total yield was higher than expected for pure copper(II) sulfide. This could not be attributed to the presence of free sulfur, since prolonged extraction with carbon disulfide gave no loss of weight. Heating to 150° C for 20 h to remove water gave no loss of weight either, so the precipitation of compounds with higher molecular weights must be assumed. For silver sulfide no problems of this kind were encountered. Pellets pressed from mixtures of the separately prepared sulfides showed leakage even when 70% silver sulfide was present. Therefore attention was focused on the simultaneous precipitation of the metal sulfides.

In order to follow the progress of the reaction during the simultaneous precipitation of silver sulfide and copper sulfide with hydrogen sulfide (see procedures), samples were taken at intervals from the supernatant liquid after the precipitate already formed had settled. In the nitrate as well as the perchlorate medium, analysis clearly showed that silver sulfide is formed first while copper ions remain in solution and precipitate at a later stage. Obviously, an inhomogeneous material will result, which consists either of separate silver sulfide and copper sulfide particles or of silver sulfide particles covered by copper sulfide. In the first case, the mechanical properties would be comparable to those of a mixture of the individual sulfides, and in the latter case to those of copper sulfide. Since the appearance of the precipitate is similar to that of copper sulfide, the latter case seems more probable. To avoid this successive precipitation of the two sulfides, it is necessary to create conditions for a really simultaneous precipitation. This can be achieved if an excess of free sulfide ions, with respect to copper and silver, is present in the solution from the beginning. Therefore, the metal ion solution was added to sodium sulfide (Table 1, types 4 and 5). Successive precipitation was then not observed and the resulting pellets showed no leakage except for the 70 : 30 precipitate; this leakage may be explained by the high copper sulfide content leading to predominance of the properties of copper sulfide. A drawback of this mode of precipitation could be the occlusion of other compounds.

The problem of leakage was also encountered when thioacetamide was added to a solution of the metal ions (types 1 and 2). When the metal ions were added to a solution of an excess of thioacetamide, the resulting precipitate (type 3) showed no leakage; the green-blue copper(II) colour disappeared

much faster in this case. Apparently, the formation of sulfide ions from thioacetamide is fast enough to provide a sufficient amount of free sulfide, to ensure simultaneous precipitation to a large extent. However, the electrochemical behaviour of pellets of this precipitate was less satisfactory than that of precipitates prepared with sodium sulfide.

It seems that a balance must be found between a pure precipitate which shows leakage and a precipitate which does not leak, but which may be more contaminated [11]. Contamination with other copper or silver salts may lead to poorer limits of detection. Direct comparison of the detection limits for precipitates formed with sodium sulfide and hydrogen sulfide was impossible because the latter material could not be pelleted properly. To obtain at least some indication of the limits of detection, attempts were made to prepare Selectrode-type electrodes [5, 12] from some precipitates (types 1 and 5, and those prepared with hydrogen sulfide); but the material did not adhere to the teflon—graphite core, except for the precipitates from thioacetamide, which behaved similarly to earlier reports in the literature [12]. These and earlier results [3, 5, 12] indicate that only small differences can be expected between precipitates prepared with sodium sulfide, hydrogen sulfide or thioacetamide. Contamination of the precipitate obtained with sodium sulfide, if any, scarcely affects the limit of detection of the electrode.

REFERENCES

1 J. W. Ross and M. S. Frant, paper presented at Pittsburg Conference on Analytical Chemistry and Applied Spectroscopy, March 1969.
2 M. S. Frant and J. W. Ross, German Offen. 1 942 379 (Cl. G 01 n) 12 Mar 1970.
3 M. Mascini and A. Liberti, Anal. Chim. Acta, 53 (1971) 202.
4 H. Hirata and K. Higashiyama, Talanta, 19 (1972) 391.
5 E. H. Hansen, C. G. Lamm and J. Růžička, Anal. Chim. Acta, 59 (1972) 403.
6 J. Pick, K. Tóth and E. Pungor, Anal. Chim. Acta, 61 (1972) 169.
7 J. D. Czaban and G. A. Rechnitz, Anal. Chem., 45 (1973) 471.
8 H. Thompson and G. A. Rechnitz, Chem. Instrum., 4 (1973) 239.
9 A. Hulanicki, M. Trojanowicz and M. Cichy, Talanta, 23 (1976) 47.
10 T. Anfält and D. Jagner, Anal. Chim. Acta, 55 (1971) 477.
11 R. P. Buck, Anal. Chem., 48 (1976) 23R.
12 J. M. van der Meer, G. den Boef and W. E. van der Linden, Anal. Chim. Acta, 76 (1975) 261.
13 G. P. Bound, B. Fleet, H. von Storp and D. H. Evans, Anal. Chem., 45 (1973) 788.
14 W. J. Blaedel and D. E. Dinwiddie, Anal. Chem., 46 (1974) 873.
15 L. Erdey, Theorie und Praxis der gravimetrischen Analyse, II. Akadémiai Kiadó, Budapest, 1964, pp. 97—111.
16 E. W. Baumann, J. Inorg. Nucl. Chem., 36 (1974) 1827.
17 A. Ringbom, Complexation in Analytical Chemistry, Interscience, New York, 1963.
18 J. Kielland, J. Am. Chem. Soc., 59 (1937) 1675.
19 G. Nakagawa, H. Wada and T. Hayakawa, Bull. Chem. Soc. Jpn., 48 (1975) 424.
20 L. G. Sillén and A. E. Martell, Stability Constants, Spec. Publ. no. 17, The Chemical Society, London, 1964, Supplement no. 1, Spec. Publ. no. 25, 1971.
21 M. Fayez El-Taras, E. Pungor and G. Nagy, Anal. Chim. Acta, 82 (1976) 285.
22 G. Kahr, Diss. ETH Zürich no. 4927, Zürich, 1972.

Analytica Chimica Acta, 89 (1977) 297—302

SIMULTANEOUS POLAROGRAPHIC DETERMINATION OF ADENOSINE-5'-MONOPHOSPHATE AND ADENOSINE-5'-*o*-MONOTHIOPHOSPHATE AT THE NANOGRAM LEVEL

K. WIENHOLD and H. SOHR

Forschungsstelle für chemische Toxikologie der Akademie der Wissenschaften der DDR, Johannisallee 20, 701-Leipzig (German Democratic Republic)

(Received 13th September 1976)

SUMMARY

Surface-active substances, because of adsorption on the mercury electrode, may completely or partially inhibit the deposition of depolarizers. This is true for the d.c. polarographic copper(II) wave in the presence of tri-n-butyl phosphate. Various surfactants capable of forming complexes with copper(II) can cancel such an inhibition within clearly defined ranges of potentials; the result is a new type of catalytic current that may be used for quantitative trace analysis. It is possible to determine AMP/AMP-S simultaneously within certain concentration ranges since the ranges of catalytic activity of these two compounds have a sufficiently large distance between them. With the method described, the two substances can be determined in concentrations between $5 \cdot 10^{-8}$ and 10^{-6} M (for AMP) and between 10^{-8} and $5 \cdot 10^{-7}$ M (for AMP-S). Reliable simultaneous determinations within these ranges are possible when the condition [AMP] $\geq$ 10[AMP-S] is satisfied.

It is well known that surfactants are readily adsorbed on mercury electrodes within certain ranges of potential. The formation of an adsorbed layer may result in electrode processes, e.g. the deposition of depolarizers, being either completely or partially inhibited depending on the potential. Among these surfactants is tri-n-butyl phosphate (TBP) which is capable of inhibiting almost completely a d.c. polarographic copper(II) wave in the range 0—600 mV (vs. SCE).

Even trace concentrations of substances which are surface-active and can also form complexes with copper(II), such as nucleotides [1, 2], sulphur-containing amino acids (cysteine and cystine) [3], or thiourea and its alkyl derivatives [4] are capable of partially cancelling such an inhibition within certain potential ranges. The new catalytic currents detected can therefore be used for the determination of substances meeting the requirements referred to above. If two of these substances are present in the polarographic electrolyte, then simultaneous determination will be possible only when penetration of these compounds into the adsorbed layer is at potentials that are sufficiently separated from each other. The AMP/AMP-S pair of substances provides such a situation. AMP-S has assumed considerable importance in

studies of interactions between enzymes and substrates [5, 6]; consequently, the substance is also of major analytical interest.

Very little information on the determination of these and similar substances is available, apart from the fact that they may be detected by paper chromatography, thin-layer chromatography, electrophoresis, or through the total phosphorus content. The method described here gives a simple technique for determining nucleoside phosphorothioates.

EXPERIMENTAL

A GWP 563 type polarograph (Akademiewerkstätten, Berlin) was used. Polarographic curves were recorded within the 1-V range between 0 and −600 mV, at a scan rate of 100 mV min^{-1}, damping value 7, sensitivity 10 μA, and chart speed 1 cm min^{-1}. For the polarographic curves shown in Figs. 2—4, the 1-V range between 0 and −600 (AMP-S) and between +50 and −250 mV (AMP) was used, with a chart speed of 0.33 cm min^{-1}. A saturated calomel electrode (SCE) was used as reference. The dropping electrode had the following characteristics: outflow velocity m = 0.544 mg s^{-1}, drop time t = 11.2 s; these were determined at a mercury pressure h = 105 cm in 0.25 M Na_2SO_4 with an open circuit.

All the measurements were made in a base electrolyte of the following composition: 0.25 M Na_2SO_4, $3 \cdot 10^{-3}$ M $CuSO_4$, 10^{-3} M KCl, and $4 \cdot 10^{-4}$ M TBP, the pH value of which was adjusted to 5.0 with 0.05 M H_2SO_4. The base electrolyte, after the addition of TBP, was mechanically shaken for 3 h to dissolve the TBP completely. Nucleotides were added to the test solution from graduated 50-μl pipettes.

The Na_2SO_4 used as supporting electrolyte was analytically pure, recrystallized several times from twice-distilled water, and calcined at 500°C. $CuSO_4$ and KCl were of analytical-reagent grade. TBP (n_D^{20} = 1.4240) was prepared in this laboratory [7]. AMP was a commercial product (FERAK Company, West Berlin). AMP-S (made available by Prof. F. Eckstein) was available as the disodium salt containing, as an impurity, 11% of AMP; concentrations are given with due correction for this impurity level. For further experiments, e.g. polarographic curves shown in Figs. 2—4, the AMP-S dilithium salt (Boehringer Mannheim G.m.b.H.) was used.

Comparable conditions for the evaluation of the polarographic waves were achieved by subtracting from the average peak current the i-value of the base electrolyte at the respective peak potential (Δi values).

All measurements were made at 25° ± 0.2°C; high-purity nitrogen was used as a purging gas.

RESULTS

TBP is capable of inhibiting, within a certain range of potentials, the deposition of copper(II) on a mercury electrode. Figure 1 shows the mean polarographic current in the presence of TBP as well as the catalytic current

peak observed after the addition of nucleotide.

Figure 2 shows the catalytic current peaks for a series of AMP concentrations; a concentration of only 10^{-8} M is sufficient to increase the current of the inhibited base electrolyte. The current peak level gradually approaches the value of the limiting diffusion current of the non-inhibited copper(II) wave as the nucleotide concentration increases.

Surprisingly, catalytic action was also observed at a much lower concentration of AMP-S. Of particular interest is the fact that the range of mixed adsorption on the TBP-covered electrode is shifted to more negative potentials. Thus, catalytic activity will appear only in those potential ranges in which AMP has already become ineffective. Corresponding polarographic curves of a series of AMP-S concentrations are shown in Fig. 3. Since the ranges of catalytic activity of the two compounds have a sufficiently large distance between them, the two compounds can be determined simultaneously. This is shown for a number of concentrations in Fig. 4. In addition, the simultaneous determination of the two substances is possible when AMP is present in an equal or higher concentration. In the concentration interval of

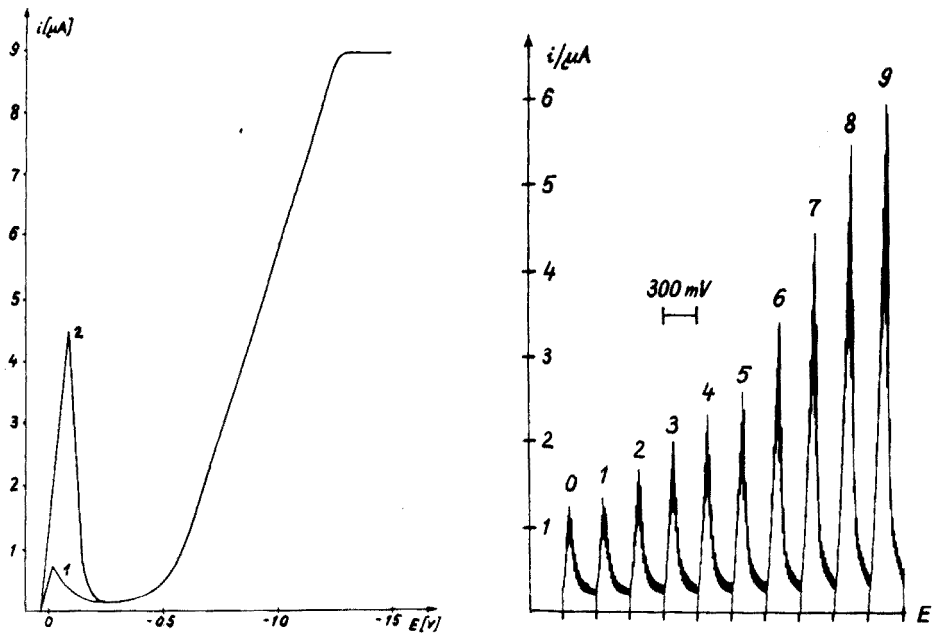

Fig. 1. D.c. Polarograms of a copper(II) wave inhibited by TBP (curve 1), and the same polarogram recorded after the addition of $5 \cdot 10^{-7}$ M adenosine-5'-diphosphate (curve 2).

Fig. 2. Catalytic current peaks for a series of AMP concentrations. (0) Base electrolyte. Base electrolyte plus (M AMP) (1) 10^{-8}, (2) $2.5 \cdot 10^{-8}$, (3) $5 \cdot 10^{-8}$, (4) $7.5 \cdot 10^{-8}$, (5) 10^{-7}, (6) $2.5 \cdot 10^{-7}$, (7) $5 \cdot 10^{-7}$, (8) $7.5 \cdot 10^{-7}$, (9) 10^{-6}.

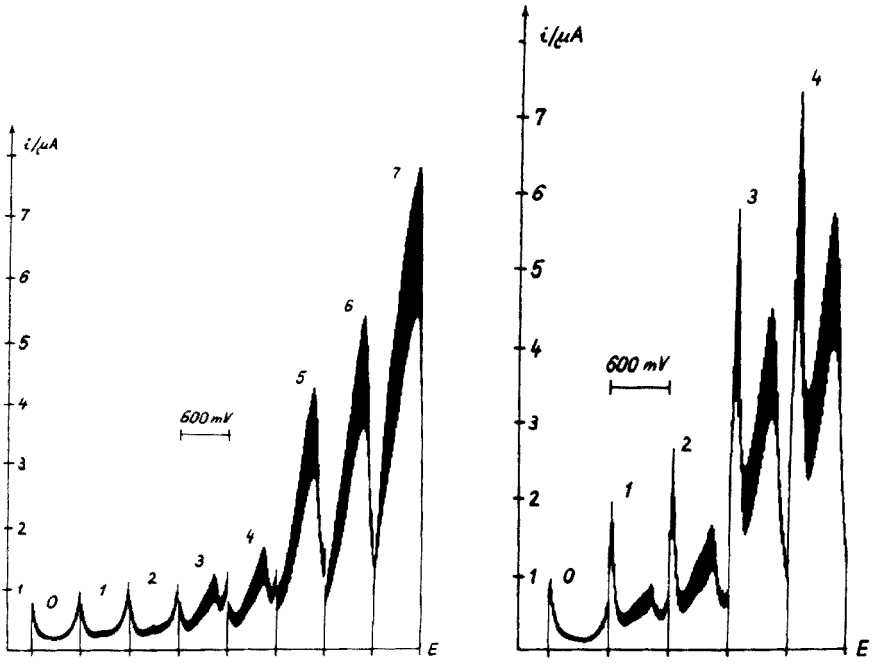

Fig. 3. Catalytic current peaks for a series of AMP-S concentrations. (0) Base electrolyte. Base electrolyte plus (M AMP-S) (1) $5 \cdot 10^{-10}$, (2) 10^{-9}, (3) $5 \cdot 10^{-9}$, (4) 10^{-8}, (5) $5 \cdot 10^{-8}$, (6) 10^{-7}, (7) $5 \cdot 10^{-7}$.

Fig. 4. Polarographic waves of AMP and AMP-S in admixture. (0) Base electrolyte. Base electrolyte plus (1) $5 \cdot 10^{-8}$ M AMP + $5 \cdot 10^{-9}$ M AMP-S, (2) 10^{-7} M AMP + 10^{-8} M AMP-S, (3) $5 \cdot 10^{-7}$ M AMP + $5 \cdot 10^{-8}$ M AMP-S, (4) 10^{-6} M AMP + 10^{-7} M AMP-S.

[AMP-S] > 0.1 [AMP] to [AMP-S] = [AMP], several calibration measurements would be required for simultaneous determinations because of the interactions involved. If, however, the condition [AMP] $\geqslant$ 10 [AMP-S] is satisfied, then a reliable quantitative and simultaneous determination of the two substances is possible over large ranges of concentration.

The sensitivity of detection of the two substances is evident from the Δi vs. log [nucleotide] plot in Fig. 5; obviously, AMP-S and AMP may be determined in concentrations between $5 \cdot 10^{-9}$ and $5 \cdot 10^{-7}$ M and between $5 \cdot 10^{-8}$ and 10^{-6} M, respectively.

The method was used to investigate the stability of freshly prepared aqueous stock solutions which were stored subsequently in a refrigerator. The corresponding Δi values are given in Table 1. The catalytic activity of a 10^{-5} M AMP-S stock solution was 65% and 25% of the original activity after 7 and 15 d, respectively. The actual AMP-S contents were determined graphically from the Δi vs. log [AMP-S] plot.

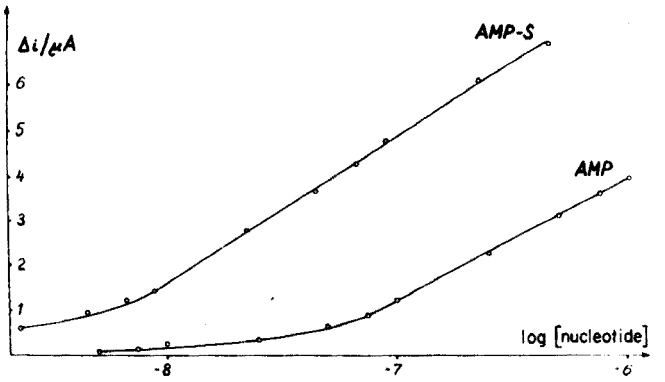

Fig. 5. The Δi vs. log [nucleotide] plot of catalytic currents of AMP and AMP-S.

TABLE 1

Δi values as a measure of catalytic activity

[AMP-S] (mol l^{-1})	Δi_0 (μA)	After 7 d		After 15 d	
		Δi (μA)	Activity (%)	Δi (μA)	Activity (%)
$2.2 \cdot 10^{-9}$	0.60	—	—	—	—
$4.5 \cdot 10^{-9}$	0.95	0.65	60	—	—
$6.7 \cdot 10^{-9}$	1.20	0.90	67	—	—
$8.9 \cdot 10^{-9}$	1.40	1.15	72	—	—
$2.2 \cdot 10^{-8}$	2.25	2.30	66	1.10	25.6
$4.5 \cdot 10^{-8}$	3.65	3.10	66	1.75	26
$6.7 \cdot 10^{-8}$	4.25	3.45	59	2.25	24
$8.9 \cdot 10^{-8}$	4.75	3.55	59	2.65	26

DISCUSSION

The catalytic current peaks arise from a new type of catalytic current. The following processes may be considered to be responsible [8]. The added nucleotides and thio analogs react with the copper(II) in the base electrolyte to form complexes which are surface-active and penetrate into the layer of TBP adsorbed on the mercury electrode and are desorbed only very slowly. There is rapid deposition of copper from the adsorbed complexes; the nucleotide molecules remain adsorbed. A mechanism consisting of an exchange between copper(II) in the solution and co-adsorbed nucleotide particles, as well as a rapid deposition of copper(II) from the adsorbed complex, is suggested.

Unfortunately, the electrode processes, because of the low concentrations of active substances and the relatively complex composition of the base electrolyte, cannot be measured with any degree of accuracy; the mechanism

may therefore be used to explain the presence of catalytic currents only in the form of a model concept which is compatible with the experimental results.

The concentration of TBP in the base electrolyte is chosen so as to obtain full electrode surface coverage (monolayer). If small amounts of a nucleotide are added, $\theta = \theta_{TBP} + \theta_{nucleotide}$ with $\theta_{TBP} \gg \theta_{nucleotide}$ and $\theta \approx \theta_{TBP} \approx 1$, where $\theta = \Gamma/\Gamma_s$ is the degree of electrode surface coverage, with Γ and Γ_s the surface concentrations of a partially and fully covered electrode, respectively. Either AMP or AMP-S will penetrate into the adsorption layer of TBP depending on the potential, thus catalyzing the deposition of copper(II) ions. Studies [9] have shown that, under the conditions chosen, the maximum proportion of nucleotides in the adsorption layer of TBP molecules is 1%. Thus, for example, the proportion of nucleotides in the adsorption layer will be less than 10^{-2}% for a bulk concentration of nucleotide of 10^{-8} M. Inclusion in the adsorption layer of TBP is probably in the form of copper(II) complexes; studies provided evidence for complex formation in the solution. Lowering of the pH value and the addition of complexing cations (e.g. Ce^{3+}) resulted in decreased catalytic currents because of the competition for complex formation sites on the nucleotide. Adverse effects were also observed with ligands capable of forming complexes with the copper(II) ions in solution and surfactants capable of influencing the conditions of adsorption on the mercury electrode.

In conclusion, the method described is a simple and highly sensitive method of determining nucleotides and their thio analogs by d.c. polarography

The authors express their gratitude to Professor F. Eckstein (Max Planck Institut für experimentelle Medizin, Göttingen) for providing AMP-S.

REFERENCES

1 H. Sohr and K. Wienhold, J. Electroanal. Chem. Interfacial Electrochem., 35 (1972) 219.
2 H. Sohr and K. Wienhold, Anal. Chim. Acta, 60 (1972) 413.
3 H. Sohr and U. Waurick, Z. Chem. (Leipzig), 14 (1974) 75.
4 H. Sohr and K. Wienhold, Anal. Chim. Acta, 83 (1976) 415.
5 F. Eckstein, Angew. Chem., 87 (1975) 179.
6 A. W. Murray and M. R. Atkinson, Biochemistry, 7 (1968) 4023.
7 G. R. Dutton and G. R. Noller, in Organic Syntheses, Coll. Vol. 2, J. Wiley, New York, 6th edn., 1950, pp. 109—112.
8 K. Wienhold, Thesis, Karl-Marx-University, Leipzig, 1975.
9 H. Sohr and K. Wienhold, Z. phys. Chem. (Leipzig), 255 (1974) 613.

Analytica Chimica Acta, 89 (1977) 303—314

RAPID POTENTIOMETRIC DETERMINATION OF THE IRON OXIDATION STATE IN SILICATES

E. KISS

Research School of Earth Sciences, Australian National University, P.O. Box 4, Canberra, A.C.T. 2600 (Australia)

(Received 25th October 1976)

SUMMARY

The rapid potentiometric determination of the oxidation state of iron in a wide range of silicates is described. A platinum/platinum—rhodium (20%) bimetallic electrode with a small constant applied current is used for end-point detection. Samples are decomposed in 10—60 min by boiling with hydrofluoric—sulphuric acid in special PTFE decomposition—titration vessels in an atmosphere of nitrogen. Total iron is reduced with mercury-treated zinc or nickel reductors. Sulphides or other constituents do not interfere significantly and the procedures are relatively insensitive to aerial oxidation. The average standard deviation is 0.35% for iron(II) and 0.22% for total iron. The accuracy compares well to the available data for international standard rocks.

The balance between iron(II) and iron(III) in silicates is of prime geochemical interest. Despite the very significant trends and developments toward non-destructive (i.e. solid-state) methods capable of large-volume data acquisition (notably electron microprobe and x-ray fluorescence spectroscopy), the problem of accurately determining iron in its two oxidation states remains to this date an exclusively chemical task.

The abundant literature on the dissolution of silicates and refractory minerals and the subsequent determination of iron(II) and total iron is an indication that this particular analytical problem has not yet been satisfactorily solved. In a comprehensive review Schafer [1] stated that no single method of dissolution can be applied for all silicates; indeed, the choice of methods is governed by the chemical behaviour of the particular mineral. Maxwell [2] summarized important special conditions (such as the presence of sulphides, organic matter and aerial oxidation) which influence the analysis for iron(II). Wilson [3] overcame air oxidation by decomposing the silicate in the presence of excess oxidant and backtitrating. Schafer [1] and Kiss [4] reported the determination of iron(II) by potentiometric titration in an atmosphere of nitrogen; the latter work [4] also dealt with the determination of total iron by compleximetric titration (which was accurate but time-consuming). Although the amount of iron(III) is usually obtained from the difference between total iron and iron(II), Dinsel and Sweet [5]

applied an extractive separation and spectrophotometry for the direct measurement of the two oxidation states. Simultaneous polarographic determination of Fe(II), Fe(III) and total iron was also reported by Beyer et al. [6]. Whitehead and Malik [7] determined iron(II) and total iron by automated colorimetry. On the micro-analytical scale Riley and Williams [8] determined iron(II) using a 5-mg sample; Kiss [9] largely overcame air oxidation of a 1—3 mg sample by decomposing the silicate in the presence of a ferroin reagent.

In special cases, the resolution of metallic iron is also required; Easton and Lovering [10] used mercury(II) chloride and ion-exchange for this purpose, whereas Sant and Prasad [11] reported the extraction of the metallic phase with bromine—ethanol and subsequently determined the other two states separately.

The present work arose from the need, in geochronological application, for a rapid analytical scheme capable of providing a large volume of data on the oxidation state of iron in total rocks. It seems possible that some post-crystallisation oxidation processes may cause redistribution of rubidium and strontium in a total-rock system. The degree of disturbance is likely to be related to the iron oxidation state; thus the least oxidized samples (i.e. highest Fe(II)/Fe(III) ratios) should give the most reliable age results [12].

A previous study [4] dealt in part with the potentiometric titration of iron(II), with a platinum/tungsten bimetallic electrode. But the diminishing and erratic response of the tungsten reference electrode, because of the formation of an oxide film, reduced its general usefulness. As a possible alternative for more accurate end-point detection, the inertness of the platinum/platinum—rhodium (20%) bimetallic electrode as described by Athavale et al. [13] seems well suited. However, the response of this electrode system in zero-current potentiometric mode was found unsatisfactory.

This alternative electrode (Pt/Pt—Rh (20%)) has now been successfully applied for constant-current potentiometric titration of iron(II) in the presence of free hydrofluoric acid. The electrode response was found to be highly reproducible and accurate in this mode. The procedure for iron(II) was also extended to the determination of total iron by the use of mercury-treated metallic reductors. The combined result is rapid and accurate for determination of the iron oxidation state of silicates decomposable by hydrofluoric acid. The scheme described is extremely fast compared with the x-ray fluorescence determination of total iron which involves a fusion, loss-on-ignition and inter-elemental correction [14].

EXPERIMENTAL

Reagents

Potassium dichromate (analytical grade) 0.0139 N (1 ml ≡ 1 mg FeO). Weigh 0.6826 g of the finely ground, dry substance, dissolve and dilute to 1 l. Calibrate for FeO equivalence against the hedenbergite internal laboratory standard after 48 h standing (see below).

Hydrofluoric—sulphuric acid mixture. Mix 1400 ml of water with 1600 ml of 50% sulphuric acid (analytical grade) in a polypropylene container, add 1000 ml of concentrated (48%) hydrofluoric acid (B and A semiconductor grade), and mix thoroughly. This composition gives optimal response for the potentiometric titration.

Gases. Nitrogen (oxygen-free grade), sulphur dioxide, (BDH grade; liquefied) and hydrogen sulphide (Matheson C.P. lecture bottle) were used as received.

Metallic reductors (zinc, cadmium, lead, nickel, tin and copper). Reductors of 30-cm^2 surface area were prepared from the purest available sheet metal, rolled into cylindrical shape, perforated and shaped for easy handling. The surfaces were cleaned by acid etching (appropriate to the individual metal) and treated with various mercury(II) salts (acidified), or mercury and hydrochloric acid, to yield a lustrous surface coating. All reductors were stored in 1% hydrochloric acid except for the Pb—Hg which was immersed in 10% ammonium acetate solution. Pure silver metal sheet (area: 30 cm^2) was cleaned with concentrated hydrochloric acid and stored in dilute hydrochloric acid. Bismuth crystals (Specpure) were cleaned as for silver but treated with mercury(II) chloride.

Apparatus

All titrations were performed with a Metrohm Herisau Potentiograph Type E436 equipped with a synchronized piston burette assembly. The platinum/platinum—rhodium (20%) bimetallic electrode was constructed in a PTFE housing with dimensions identical to the assembly previously described [4]. A Beckman sintered-disc saturated calomel electrode (SCE) in a hydrofluoric acid-resistant bakelite body was used to test the individual electrodes of the bimetallic system (see below). The bimetallic electrode was arranged in the titration stand with a PTFE inlet tube for nitrogen. A set of eight digestion—titration vessels was constructed from PTFE by a moulding technique, to the dimensions as already described [4].

An efficient heating block for eight digestion vessels was machined from solid aluminium; heating was provided with strip contact elements and the temperature was thermostatically controlled. The nitrogen bubbling rate was monitored in transparent FEP—teflon cylinders containing a solution of potassium hydroxide. (Full details of the electrode system, reductors and digestion assembly are available on request.)

Calibration

The weak solution of the standard oxidant, potassium dichromate, showed no deterioration over many months of storage, other than slight increase in concentration (ca. 0.3—0.5%) because of evaporative loss. To ensure uniform accuracy, routine calibration of the dichromate solution was therefore desirable. The usual chemical standard, iron(II) ammonium sulphate, was rejected because its application did not simulate actual silicate matrix

composition. Subsequently, the mineral hedenbergite (ex Rio Marina, Isle of Elba) was selected as an internal laboratory standard for iron oxidation states. A homogeneous batch of approximately 200 g of material was prepared by the usual procedures. Portions of this sample were analyzed for iron(II) and total iron by two independent laboratories; Wilson's method [3], spectrophotometry [8], complexiметric titration [4] and x-ray fluorescence spectroscopy [14] were used. The USGS standard rocks were chosen as monitoring controls. Fifty individual analyses of each iron(II) and total iron were compiled; the average results were as follows: FeO = 20.91 ± 0.079%; $\Sigma Fe(Fe_2O_3)$ = 26.71 ± 0.049%; Fe_2O_3 = 3.48% and Fe(II)/Fe(III) = 6.684.

This analyzed mineral was found to be well suited for the calibration of the standard oxidant; ca. 50 mg of material was required per measurement.

Recommended procedure for determination of iron(II) (Mode A)

Grind the sample under acetone to −200 mesh BSS. After drying, weigh accurately (to contain preferably less than 15 mg Fe), transfer to the PTFE vessel, and wash down the sides with ca. 30 ml of water. For the first set of eight digestions, weigh also ca. 50 mg of the hedenbergite standard (at least in duplicate) and process it as for the samples. Add 25 ml of hydrofluoric–sulphuric acid mixture, mix thoroughly, screw the inlet tube/top assembly in position and attach it to the appropriate outlet of the nitrogen manifold. Connect the side tube to the potassium hydroxide monitor flask and place the vessel into the heating block preheated to 140°C. Start the nitrogen flow to give a steady, moderately fast but uniform flow rate for all decomposition vessels. Turn on the potentiograph. Continue digestion for 15 min (or up to 60 min if garnet, eclogite or similarly resistant silicates are being analyzed). Remove the digestion vessel from the heating block, after first turning off the nitrogen flow at the manifold needle-valve, and disconnecting the side tube and the nitrogen inlet tube in that order. (Failure to observe this sequence could result in loss of some solution by ejection through the nitrogen inlet tube.) Unscrew the inlet tube/top assembly, rinse it thoroughly with unboiled water and further dilute the sample solution by washing all the interior surfaces. Transfer the decomposition vessel to the titration stand and place the bimetallic electrode/nitrogen inlet tube assembly near the bottom of the hot solution. Adjust a steady flow of nitrogen by monitoring on a flow meter, set the potentiograph to function i_{pol}, + 10 μA polarization current, 500 mV range and + 500 mV compensation potential. Set the titration speed to 4 and commence automatic titration. The titration tracings should be noise-free, except in the vicinity of the equivalence point where a drop of the titrant could cause short-term localized excess of the oxidant. Since the delivery of the dichromate is controlled automatically according to the rate of change in the titration curve, it is not possible to over-titrate. An extremely well-defined and sharp peak marks the end-point; the ordinate component of the curve gives directly the volume of the dichromate consumed. The titration results of the standard mineral hedenbergite are used to establish the accurate

FeO equivalency of the dichromate solution. Depending on the length of titration and heating time, 32—40 analyses can be completed in a working day.

The results obtained on standard rocks are presented in Table 1.

Recommended procedure for determination of total iron (Mode B)

Weigh accurately the finely ground silicate into the PTFE digestion vessel; choose the sample weight to contain preferably <15 mg Fe, and proceed as for iron(II) in every detail except for the following; depending on the titanium content (which is roughly known for any particular type of rock), place into the solution after the addition of the acid mixture either (a) a mercury-treated zinc reductor (for samples containing <1% TiO_2) and digest for a minimum of 10 min, or (b) a mercury-treated nickel reductor (for samples containing >1% TiO_2) and digest for a minimum of 40 min. Calibrate the potassium dichromate solution by determining the total iron of the hedenbergite standard, taking ca. 50 mg of sample and using the appropriate reductor for the samples studied. The "FeO equivalence" by this mode should check with the calibration by Mode A. At the end of the digestion time, remove the reductor with a suitably-shaped platinum wire and commence titration, using the identical instrument parameters as for iron(II). The peak values correspond to the total amount of reduced iron present. Calculate total iron expressed as Fe_2O_3. A similar number of rocks can be analyzed in a working day as for Mode A. The results obtained on standard rocks, with various reduction systems, are presented in Table 2.

Existing iron(III) and the oxidation state of iron

"Existing Fe_2O_3" — Fe(III) — and the oxidation state ratio are calculated from the analytical data obtained by modes A and B. Although this is an indirect approach for existing iron(III), the chemical simplicity and identical mode of measurement ensure results free from analytical bias. The relevant data on the standard rocks analyzed are presented in Table 3.

DISCUSSION

The platinum/platinum—rhodium (20%) bimetallic electrode

In an earlier paper [4] potentiometric end-point detection was effected by means of a platinum/tungsten bimetallic electrode. As already mentioned, this system was hampered by erratic response because of the formation of an oxide film on the tungsten reference electrode; this necessitated frequent cleaning in molten sodium nitrite. Bimetallic electrodes constructed of platinum and its rhodium alloy [13] were tested as follows. Initially, the following electrode combinations were used in the zero-current potentiometric mode ($i_{pol} = 0$) for titrating iron(II) ammonium sulphate (1 ml ≡ 1 mg FeO) in hydrofluoric—sulphuric acid medium: (a) Pt/SCE; (b) Pt—Rh (20%)/SCE and (c) Pt/Pt—Rh (20%). The potentiometric curves obtained by the

TABLE 1

Determination of iron(II) oxide

Rock Type	% FeO	s_r (r.s.d.)	Other values
Granite G-2	1.43	0.65	1.45[a], 1.43[b], 1.45[f]
Granodiorite JG-1	1.64	0.34	1.66[a], 1.64[c], 1.63[d], 1.66[f]
Granodiorite GSP-1	2.35	0.51	2.34[a], 2.31[f]
Andesite AGV-1	2.10	0.36	2.02[a], 2.10[b], 2.05[f]
Basalt BCR-1	8.89	0.08	8.97[a], 9.06[b], 8.80[f]
Basalt JB-1	5.96	0.31	6.06[a], 6.02[c], 5.98[d]
Basalt BHVO-1	8.67	0.22	8.5[e]

[a]S. Abbey, Can. Geol. Surv. Pap. No. 72-30 (1972) — "Usable values".
[b]M. E. Beyer, A. M. Bond and R. J. W. McLaughlin, Anal. Chem., 47 (1975) 479.
[c]A. Ando et al., Geochem. J., 8 (1974) 175.
[d]P. H. Beasley, personal communication, 1972.
[e]U.S. Geol. Surv. Bull., in press.
[f]F. J. Flanagan, Geochim. Cosmochim. Acta, 37 (1972) 1189.

electrode systems (a) and (b) were similar to other typical S-shaped redox curves for Fe(II)/Fe(III), but the Pt/Pt—Rh (20%) combination produced rather noisy and ill-defined tracings. This last could be resolved only by applying a constant current to the platinum indicator electrode. The smoothing of zero-current potentiometric titration curves of Fe(II) by polarization of the indicator electrode in the bimetallic system is illustrated in Fig. 1.

It can be seen that the growth of the peak height and its degree of resolution is directly proportional to the magnitude of polarization current employed. Optimal response was obtained when a constant current of $+10\ \mu A$ was maintained on the platinum indicator electrode; the result was nearly full scale deflection of high stability on a 250-mm recording chart. With no inherent errors present in the electrode response, the end-point is precisely read as the maximum displacement of the peak, irrespective of the peak height.

Aerial oxidation

Accidental oxidation during the decomposition step was evaluated by subjecting a number of basalt rock dissolutions to atmospheric oxidation by injection of a fast current of air into the boiling acid solutions. One set of samples was heated under nitrogen for 20 min, then air was bubbled through; the other set was dissolved under air stream alone, followed by flushing with nitrogen. The results in Table 4 show, contrary to other investigations [1, 2], that the hydrofluoric acid—iron system is remarkably insensitive to aerial oxidation. This observation may be explained by the overall stabilizing effect of free hydrofluoric acid on the Fe(II) and Fe(III) species. It has been shown [15] that iron, after liberation from the silicate matrix by hydrofluoric

TABLE 2

Determination of total iron

Rock type	%ΣFe(Fe_2O_3)	s_r	Reductor	Other values‡
Granite G-2	2.66 ± 0.02[g]	—	Zn—Hg	2.67[a], 2.68[b], 2.65[f]
	2.66	0.56	Pb—Hg	
Granodiorite JG-1	2.24 ± 0.0[g]	—	Zn—Hg	2.21[a], 2.17[c], 2.12[d]
	2.18	0.14	Cd—Hg	
	2.13	0.21	Pb—Hg	
Granodiorite GSP-1	4.26 ± 0.026[g]	—	Zn—Hg	4.26[a], 4.27[b], 4.33[f]
	4.30	0.21	Pb—Hg	
Andesite AGV-1	6.79 ± 0.01[g]	—	Zn—Hg	6.73[a], 6.78[b], 6.76[f]
	6.77	0.23	Pb—Hg	
Basalt BCR-1	10.00	—	SO_2	13.40[a], 13.53[b], 13.40[f]
	10.01	0.11	H_2S	
	13.53	0.22	Zn—Hg	
	13.39 ± 0.06[g,h]	—	Cd—Hg	
	13.36	0.11	Ni—Hg	
	13.43	—	Ag	
	13.57[i]	0.30	Zn—Hg	
	13.39[j]	0.35	Zn—Hg	
Basalt JB-1	9.01	0.23	Zn—Hg	9.04[a], 8.96[c], 8.89[d]
	9.00 ± 0.02[g]	—	Cd—Hg	
	8.98	0.13	Pb—Hg	
	8.96	0.19	Ni—Hg	
Basalt BHVO-1	12.38[h]	0.21	Cd—Hg	11.95[e]
	12.49	0.25	Pb—Hg	
	12.32	0.06	Ni—Hg	
	11.79	—	Cu—Hg	
	11.42	—	Ag	
	18.12	5.8	Sn—Hg	
Diabase W-1	11.25	0.39	Zn—Hg	11.09[a], 11.38[b]
	11.22	—	Pb—Hg	

‡Reference key letters (a—f) as for Table 1.
[g]Mean of two results (± total spread).
[h]Corrected for Ti(III) peak.
[i]Average of four runs; after 60 min of reductor contact under nitrogen, air was bubbled through for 0, 1, 2 and 3 min (attempted oxidation of Ti(III)).
[j]As for footnote i, but corrected for Ti(III) peak readings.

TABLE 3

Data for iron oxidation state in silicate rocks

Rock type	FeO	Fe_2O_3	$\Sigma Fe(Fe_2O_3)$	Fe(II)/ Fe(III)	Other Fe_2O_3 values‡
Granite G-2	1.43	1.07	2.66	1.485	1.01[a], 1.08[b], 1.08[f]
Granodiorite JG-1	1.64	0.36	2.18	5.063	0.36[a], 0.38[c], 0.31[d], 0.36[f]
Granodiorite GSP-1	2.35	1.67	4.28	1.564	1.60[a], 1.68[b], 1.77[f]
Andesite AGV-1	2.10	4.45	6.78	0.524	4.39[a], 4.40[b], 4.51[f]
Basalt BCR-1	8.89	3.51	13.39	2.815	3.45[a], 3.45[b], 3.68[f]
Basalt JB-1	5.96	2.36	8.99	2.807	2.30[a], 2.31[c], 2.24[d], 2.30[f]
Basalt BHVO-1	8.67	2.72	12.35	3.542	2.50[e]

‡Reference key letters as for Table 1.

acid attack, forms several complexes in both valency states; it is also co-ordinated with other constituents to form mixed fluoro-complexes. It seems reasonable that the redox potential of iron bound in such a manner could differ sufficiently from that of uncoordinated iron, to exhibit an appreciable degree of resistance to air, a mild oxidant. It should be noted that most analytical methods require masking of hydrofluoric acid before titration.

Performance of various reductors in $HF—H_2SO_4$ medium

Several different reduction systems were tested by reducing existing iron(III) in silicate rock dissolutions and estimation of the total iron by titration. The preconditions for an optimal reduction system were: (a) quantitative removal of any excess reducing agent before titration is commenced; (b) reasonably short reduction time; (c) good selectivity for the reduction of iron(III); and (d) the reaction products should be indifferent to the oxidizing titrant.

Of the very few gaseous reducing agents available, sulphur dioxide and hydrogen sulphide were found to be quite unacceptable; 30 min of digestion in a current of sulphur dioxide, or 20 min of digestion in a current of hydrogen sulphide, followed by flushing with nitrogen, in both cases caused only 3.7% reduction of the available iron(III).

The performance of the following metallic reductors was next examined: mercury-treated zinc, cadmium, lead, tin, copper and nickel, as well as pure silver. Bismuth amalgam was also tested qualitatively; because of its brittleness however, a practical shape could not be fabricated. The silicate samples were heated with the dissolving acid mixture under pure nitrogen flow for various lengths of time in the presence of amalgamated metal reductors. All silicates tested were dissolved in approximately 10 min. As expected, each reductor system required different contact times for quantitative recovery of total iron as follows: Zn—Hg $\leqslant$ 10 min; Cd—Hg $\geqslant$ 20 min; Pb—Hg $>$ 30 min;

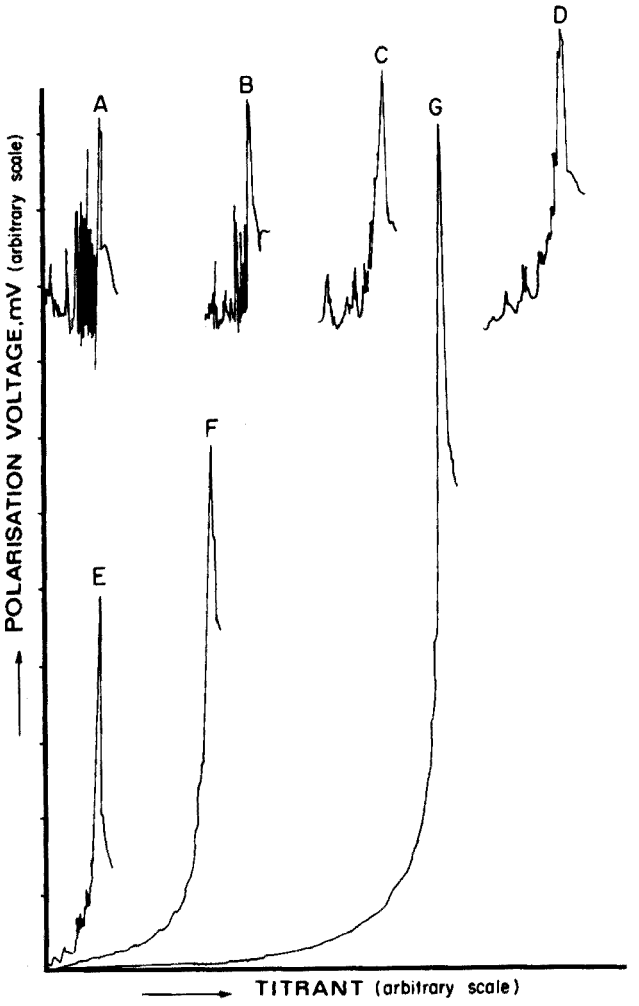

Fig. 1. Change in shape of zero-current potentiometric titration curve of Fe(II) by polarization of the Pt indicator electrode of the Pt/Pt—Rh (20%) bimetallic system. Medium, hydrofluoric—sulphuric acid; titrant, $K_2Cr_2O_7$; concentration, 5.00 mg FeO (added as $FeSO_4(NH_4)_2SO_4.6H_2O$). Polarization current: A, 0 μA; B, 0.1 μA; C, 0.5 μA; D, 1.0 μA; E, 2.5 μA; F, 5.0 μA; G, 10 μA.

Ni—Hg $\leqslant$ 40 min; Cu—Hg $>$ 60 min and Ag $\gg$ 60 min. The Sn—Hg system failed, as the reaction product was the oxidizable Sn(II) giving rise to grossly positive errors (see Table 2). The performance of mercury-treated lead was hampered somewhat by the formation of a sulphate and fluoride film on its surface, although immersion in 10% ammonium acetate solution between determinations resulted in appreciable improvement. If applied too long the powerfully acting surface amalgams (e.g., Zn, Cd and Pb) were capable of

TABLE 4

Aerial oxidation in hydrofluoric—sulphuric acid

Air injection time, min	% FeO(BCR-1)	% Error	Remarks
Nil	8.97	Nil	Samples digested for 20 min under nitrogen; air was then bubbled through for specified time at the boiling point of the acid mixture.
0.5	8.97	Nil	
2	8.85	−1.3	
4	8.86	−1.2	
6	8.77	−2.2	
11	8.55	−4.7	
20	8.28	−7.7	
30	8.08	−9.9	
10	8.63	−3.8	Dissolved directly in air stream for specified times, then degassed with nitrogen and titrated.
20	8.40	−6.2	
30	8.35	−7.0	
40	7.93	−11.6	

reducing Cr(III) and Ti(IV) ions as well as Fe(III). When Zn—Hg, Cd—Hg and Pb—Hg were used as reductors for the determination of total iron in silicate rocks containing $>1\%$ TiO_2, the results showed appreciable positive errors; for all rock types containing $<1\%$ TiO_2 there were no Ti(III) oxidation peaks present, and the results were consistent and accurate. However, the evidence showed that even the most vigorous reductor (e.g. Zn—Hg) is suitable for all silicate rock types if the reduction time is kept to a minimum. Obviously, a digestion apparatus equipped with an externally controllable reductor mechanism would be desirable because the function of reduction could be separated from the digestion time. By injecting air into the hot sample solution which contained a Zn—Hg reductor, the Ti(III) peak value was decreased by two-thirds without affecting iron(II).

Pure silver and mercury-treated nickel and copper showed no evidence of co-reduction of titanium or chromium; in the case of the Cu—Hg reductor, no Cu(I) ions could be detected by the dichromate titration. These systems offer good selectivity towards iron reduction and the Ni—Hg reductor was tested in detail because of conveniently short reduction times. Silver should be used as a powder for maximally reacting surface, but its removal from the solution to be titrated would be troublesome. Thus, the conclusions are as follows: (a) the mercury-treated zinc reductor is suitable for all types of acidic rocks (containing less than 1% TiO_2) and requires about 10 min for reduction and digestion; (b) the mercury-treated nickel reductor is suitable for all decomposable silicates, including high titanium-bearing rocks; there is no evidence for co-reduction of Ti(IV) in the presence of hydrofluoric acid even after 90-min contact.

Interferences

In the determination of iron(II) — Mode A — interferences are seldom encountered in analysis of igneous rocks. Sulphides or free hydrogen sulphide have been found not to interfere and no significant reduction of iron(III) takes place. This presumably is because of the powerful stabilizing effect of hydrofluoric acid on iron(III). By extension, the same is probably valid for organic matter in some types of sediments. In the case of decomposable sulphide minerals, the sulphide-bound iron(II) is also expected to participate in the reaction. In the total iron titration mode, the application of mercury-treated zinc, cadmium and lead reductors could lead to positive errors, because the reducing power is vigorous enough to produce Ti(III) and Cr(II) species under prolonged contact conditions. The existence of Cr(II) ions was not proven unequivocally, but Ti(III) ions were co-titrated with Fe(II) producing sharply defined peaks, all within the first ml of titrant delivered. In most cases acceptable results were obtained when the total volume of dichromate consumed was corrected for the Ti(III) peak values. A possible explanation for the apparent absence of Cr(II) ions may be found in the fact that it is very easily oxidized during the dilution step, with unboiled distilled water. Any dissolved oxygen in the water would also rapidly equilibrate with some of the Ti(III) if present.

However, air injection tests (Table 4) showed only partial success with the oxidation of Ti(III) while the iron(II) was not oxidized to any extent.

Scope and limitations

The proposed method offers a highly reproducible, rapid and simple approach to the determination of bivalent and tervalent iron in all silicates which are decomposable by hydrofluoric—sulphuric acid mixture. Depending on the ease of decomposition and choice of a reductor, the analysis can be completed in as little as 10 min. Therefore, it is highly suitable for rapid data acquisition on a large number of rocks. Since the identical experimental approach is used for both bivalent and total iron in the present scheme, the values for existing iron(III), obtained by difference, show no detectable bias if the recommended procedure is used.

Because the proposed method is limited to the majority of silicates which are decomposable in hydrofluoric acid, the iron content of some minor constituents such as zircon, and of refractory minerals such as chromite, frequently present in ultrabasic rocks, cannot be determined. Some degree of success in total iron determinations of rocks containing chromite can be achieved by using anhydrous hydrofluoric—sulphuric acid mixture ($HF : H_2SO_4 = 1:9$) in a closed PTFE bomb, followed by reduction and titration in the usual way. However, the determination of iron(II) by this approach is not recommended because of the risk of partial oxidation. The general procedures A and B may be scaled down by a factor of ten (by using a weaker solution of potassium dichromate and higher instrument sensitivity) for smaller samples (5—50 mg); but the precision will then be lowered somewhat.

The present scheme was successfully applied in the analytical resolution of co-existing phases containing Fe + FeS + Fe(II) + Fe(III) as illustrated in the analysis of Ijopega meteorite [16], a recent fall. This type of determination involving the distribution of iron in several phases is readily accomplished by the combined application of the bromine—ethanol [11] and mercury(II) chloride [10] extraction techniques in conjunction with potentiometric measurement of the oxidation state.

Precision and accuracy

Iron(II) and total iron concentrations of various standard rocks were reproducible to 0.35% and 0.22% (relative standard deviation), respectively. This degree of precision was attained routinely for a much wider range of silicates, i.e. for those more resistant to acid decomposition, such as garnets and eclogites. Also, the reported precision is independent of the relative amounts of Fe(II) and Fe(III) present. The accuracy of the determination of iron oxidation state compares well with the published data and also with other values compiled from available sources.

The author wishes to thank Dr. J. R. Richards and Mr. P. H. Beasley of the Research School of Earth Sciences for reading the manuscript and for the supply of standard materials, respectively.

REFERENCES

1 H. N. S. Schafer, Analyst (London), 91 (1966) 755.
2 J. A. Maxwell, Rock and Mineral Analysis, Interscience, 1968, pp. 208—210.
3 A. D. Wilson, Bull. Geol. Surv. G. B., 9 (1955) 56.
4 E. Kiss, Anal. Chim. Acta, 39 (1967) 223.
5 D. L. Dinsel and T. R. Sweet, Anal. Chem., 35 (1963) 2077.
6 M. E. Beyer, A. M. Bond and R. J. W. McLaughlin, Anal. Chem., 47 (1975) 479.
7 D. Whitehead and S. A. Malik, Anal. Chem., 47 (1975) 554.
8 J. P. Riley and H. P. Williams, Mikrochim. Acta, 4 (1959) 516.
9 E. Kiss, Anal. Chim. Acta, 72 (1974) 127.
10 A. J. Easton and J. F. Lovering, Geochim. Cosmochim. Acta, 27 (1963) 753.
11 B. R. Sant and T. P. Prasad, Talanta, 15 (1968) 1483.
12 R. W. Page, personal communication, 1976, to be published in Aust. Bur. Min. Res.
13 V. T. Athavale, R. G. Dhaneshwar and D. A. Sarang, Talanta, 14 (1967) 1333.
14 P. H. Beasley, personal communication, 1976.
15 F. J. Langmyhr and P. R. Graff, Publication No. 230, University of Oslo, Chemical Institute A., A. W. Brøggers Boktrykkeri A/S, 1965.
16 A. L. Jaques, P. L. Lowenstein, D. H. Green, E. Kiss, W. B. Nance, S. R. Taylor and N. G. Ware, Meteoritics, 10 (4) (1975) 289.

Analytica Chimica Acta, 89 (1977) 315—320

THE DETERMINATION OF POLYGLYCOLS BY A DERIVATIVE CHRONOPOTENTIOMETRIC METHOD

PER HOLMQVIST

Department of Analytical Chemistry, University of Uppsala, Uppsala (Sweden)

(Received 6th September 1976)

SUMMARY

The potential-dependent adsorption of polyethylene glycols at a mercury electrode has been studied. The potential of desorption is related to the molecular weight of the polyglycol fractions in the range 200—6000. Quantitative analysis is based on the size of the indentation in the dE/dt curve at the potential of desorption.

Polyglycols have molecular weight distributions. Methods for their determination have been based on chromatographic techniques [1, 2], but the hydrophilic character of the compounds makes them difficult to separate. From an electrochemical point of view, polyglycols are neither oxidizable nor reducible within the potential range of the mercury electrode. They can, however, be adsorbed at the electrode. This can be utilized analytically by detection of the amount adsorbed, which can be related to the bulk concentration of polyglycols.

EXPERIMENTAL

The adsorption of the different polyglycol fractions at the dropping mercury electrode (DME) was investigated by a derivative chronopotentiometric method [3]. All measurements were done in a three-electrode cell connected to an instrument [4] for potentiostatic or galvanostatic control. The working electrode was an ordinary DME (Radiometer B400), the counter electrode a platinum wire, and the reference electrode a saturated calomel electrode. The synchronization of the measurement with the working electrode was made by a drop-fall detector [5].

During the first 4.00 s the potential (E) of the working electrode is controlled. The function is then changed and the current through the cell controlled. Simultaneously dE/dt and E are measured and displayed on an oscilloscope (Techtronix, storage oscilloscope 645B). After the measurement the potential of the working electrode attains its initial value and the instrument is ready to indicate a drop fall. The time for every drop is displayed on a digital clock [6].

The potential of the working electrode was measured with a digital voltmeter with high input impedance during potential control (Schneider VN454), and directly on the screen of the oscilloscope during current control. In this investigation the controlled current was 28.4 μA. The iR-drop in the cell can easily be compensated by the instrumentation.

The polyglycol fractions with mean molecular weights from 200 to 6000 (called here PEG 200 ..... PEG 6000; Berol Kemi AB; Stenungsund, Sweden) were used without further purification. Stock solutions were prepared by dissolving the polyglycols in absolute ethanol. Solutions for measurement were prepared by adding the appropriate volume of respective stock solution to the empty cell. After evaporation of the ethanol, the sample was dissolved in a supporting electrolyte of 0.1 M KF + 0.05 M KOH. Before measurements all solutions were deoxygenated with purified nitrogen. The measurements were made at 25 ± 0.5 °C.

RESULTS

In the supporting electrolyte used, the polyglycol fractions were adsorbable at the working electrode if its potential was more positive than −1.55 V vs. SCE during the initial 4.00 s. During a cathodic current pulse, the adsorbed molecules were desorbed at a potential characteristic for each fraction, and an indentation in the dE/dt curve was produced as the structure of the double layer of the electrode changed. The indentation was normalized by taking the ratio between its size and the dE/dt value of the pure supporting electrolyte at the same potential [7]. For identification of the polyglycol fraction, concentrations were chosen to give normalized identations with a value of 0.5 when the potential during the initial 4.00 s was −1.30 V. For these concentrations the change in potential of desorption for each fraction was studied when the starting potential was varied. Figure 1 shows that the potentials of desorption for the lower molecular weight polyglycols are more positive than the corresponding potentials for the higher molecular weight polyglycols.

The amount of adsorbed material in the double layer can be related to a lowering of the differential capacity at potentials where the substance is adsorbed. At a given potential the effect can be normalized by taking the ratio between the lowering and the differential capacity of the pure supporting electrolyte [8]. The effect of change in the starting potential, first on normalized lowering of the differential capacity, and secondly on the normalized size of the indentation of desorption, was studied for PEG 1000. The results from these measurements are shown (Fig. 2) for one of the concentrations investigated.

A change in starting potential also affects the form of the indentation. The effect of small changes (20 mV) in the starting potential on the form, size, and position of the indentation of desorption for PEG 1000 is shown in Fig. 3.

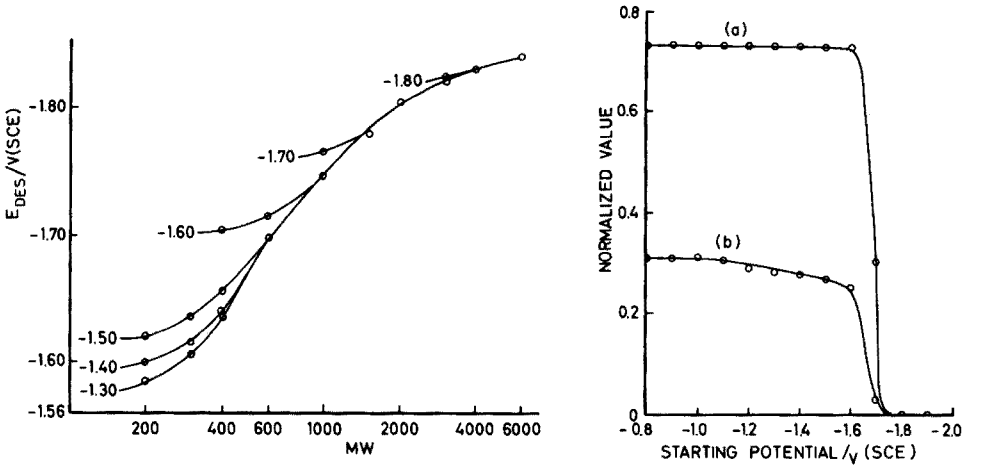

Fig. 1. Shift in the potential of desorption with molecular weight of polyglycol fractions. Potential during the quiescent period is indicated near each curve.

Fig. 2. PEG 1000. Variation of (a) lowering in differential capacity at −1.00 V, and (b) size of indentation of desorption with change in starting potential. Concentration in both cases 5 mg l^{-1}.

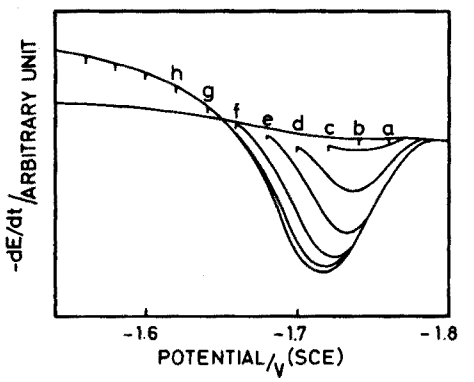

Fig. 3. Part of cathodic dE/dt curves for PEG 1000 (5 mg l^{-1}). Starting potential: (a) −1.76 V, (b) −1.74 V, (c) −1.72 V, (d) −1.70 V, (e) −1.68 V, (f) −1.66 V, (g) −1.64 V, (h) −1.62 V. For more positive starting potentials the same curve as (h) is obtained.

The concentration ranges suitable for analysis by this electrochemical method were investigated for three different polyglycols. The indentation of desorption was measured for PEG 200, PEG 600, PEG 6000, and the normalized sizes were plotted versus concentration. The starting potential used was varied in the range −1.20 V to −1.70 V vs. SCE. Figure 1 shows that PEG 200 is not adsorbed if the starting potential chosen is more negative than −1.55 V; at −1.70 V, PEG 6000 is the only adsorbed fraction of the three polyglycols investigated. An example of curves for the starting potential −1.20 V vs. SCE, where all fractions are adsorbed is shown in Fig. 4.

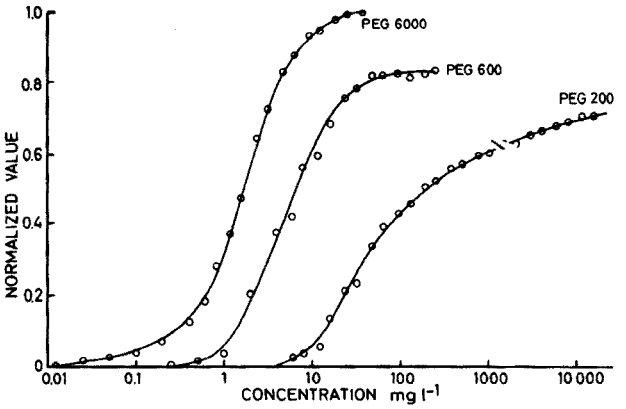

Fig. 4. Variation in size of indentation of desorption with concentration of polyglycol. Starting potential, −1.20 V. Polyglycol fraction indicated near each curve.

DISCUSSION

The potential of desorption for organic molecules usually depends on concentration, with the negative summit potential changing to more negative values with increasing concentration [9]. This effect was also observed for polyglycols [10], and the condition for identification must be specified. In this investigation the size of the normalized indentation was stated to be 0.5, which is fulfilled for concentrations of polyglycols in the range 1 to 10 mg l^{-1}, except for fractions with molecular weights lower than 300.

Investigations of polyglycols by a.c. polarography by Jehring [8] have shown a dependence of the potential of desorption on molecular weight. For qualitative analysis a concentration of 50 mg l^{-1} of polyglycol was recommended. With the proposed method, a lower concentration level can be used, as the material is adsorbed during 4.00 s at a potential where adsorption is facilitated and the total amount is desorbed at the measurement. Furthermore, it is possible to control the adsorption of different polyglycol fractions by choosing a suitable starting potential, which facilitates a correct identification.

Figure 3 shows the change in size of the indentation of desorption for PEG 1000 when the starting potential is varied. If the starting potential chosen is 0.1 V or more positive than the potential of desorption, the size of the indentation is constant; if the starting potential is closer to the potential of desorption, the size of the indentation is considerably diminished. The position of the indentation of desorption depends on the starting potential (Fig. 1). If the adsorption of a fraction takes place close to the potential of desorption the molecules are desorbed at a somewhat more negative potential than if the adsorption is performed at a more positive potential. Even small changes in the starting potential in the neighbourhood

of the potential of desorption have a marked effect (Fig. 3). This phenomenon may be explained by a selective adsorption, the larger molecules of a fraction being adsorbed at a more negative potential than the smaller ones.

Generally the size, form, and position of the indentation of desorption for polyglycols with lower molecular weight are more dependent on the starting potential than for compounds with high molecular weight. The higher fractions give the same size of indentation even if they are adsorbed at potentials close to the potential of the final desorption. The form of the indentation of desorption is broad and shallow for the lower fractions, but narrow and sharp for the higher fractions.

The values of dE/dt are easily transformed to differential capacity [3]. This transformation was performed in the investigation of PEG 1000 at −1.00 V, an arbitrarily chosen potential in the range where molecules are adsorbed. The values obtained for different starting potentials were compared with the corresponding values of the indentation of desorption (Fig. 2). Obviously the two ways of measuring vary in the same manner when the starting potential is changed, but the indentation seems to be a more sensitive measure of the amount of adsorbed material during the initial 4.00 s. Analysis of polyglycol fractions is suitably performed by measuring the indentation of desorption as this also gives information of a qualitative nature and has a higher sensitivity than measurements performed in the potential range where molecules are adsorbed.

When the normalized indentations are plotted versus concentration for PEG 6000, the curves are identical if the starting potential is chosen between −1.20 V and −1.70 V vs. SCE. The useful concentration range for quantitative analysis is between 0.1 and 10 mg l^{-1}. The upper concentration limit is set by the instrumental parameters.

For PEG 600, the plots of the indentation versus concentration are not affected by changes in the starting potential between −1.20 V and −1.40 V. The corresponding indentations, however, are always smaller when −1.50 V vs. SCE is chosen as the starting potential. For this fraction quantitative analysis can be performed in the concentration range 1—40 mg l^{-1}. The upper concentration limit is set in this case by the fact that maximum coverage of the electrode with polyglycol is probably achieved during the initial 4.00 s.

PEG 200 is more sensitive to changes in the starting potential than the other fractions investigated, giving different indentation—concentration plots for every starting potential. The useful concentration range is between 10 mg l^{-1} and 10 g l^{-1}.

For the higher polyglycol fractions investigated, the adsorption process is diffusion-controlled [10]. This is probably not the case for PEG 200 where the amount of adsorbed material may be due either to rate of adsorption or to adsorption equilibrium.

A mixture of two polyglycol fractions is shown as an example in Fig. 5. From the values of the potential of desorption, it is possible from Fig. 1 to

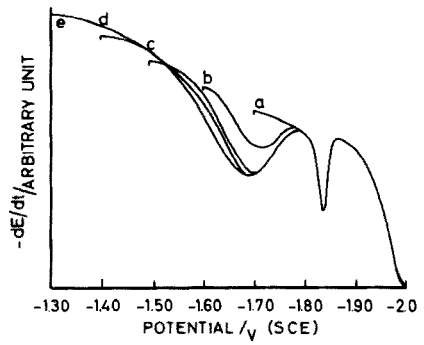

Fig. 5. Part of cathodic dE/dt curves for mixture of PEG 6000 (1.8 mg l^{-1}) and PEG 600 (5.9 mg l^{-1}). Starting potential: (a) −1.70 V, (b) −1.60 V, (c) −1.50 V, (d) −1.40 V. The curve in (e) is obtained for −1.30 V or more positive starting potentials. Indentation at −1.83 V is observed at all starting potentials.

confirm that the mixture contains PEG 6000 and PEG 600. The concentrations, evaluated from plots of the type shown in Fig. 4, are 1.8 and 5.9 mg l^{-1}, respectively.

Generally the fraction with the most negative potential of desorption is determined first. This is done by selective adsorption at a negative potential where competitive adsorption of the other compounds does not take place. The starting potential is then changed to a more positive potential where lower polyglycol fractions are adsorbed.

REFERENCES

1 L. Favretto, L. Favretto Gabrielli and G. Pertoldi Marletta, J. Chromatogr., 66 (1972) 167.
2 J. Törnqvist, Acta Chem. Scand., 21 (1967) 2095.
3 P. Holmqvist, J. Electroanal. Chem. Interfacial Electrochem., 68 (1976) 30.
4 R. Danielsson, Examination Report, Institute of Technology, University of Uppsala, 1969, (in Swedish).
5 R. Danielsson, UUIP Report Oct. 1973, Institute of Chemistry, University of Uppsala.
6 R. Danielsson, UPTEC Report 73 61R, Oct. 1973, Institute of Technology, University of Uppsala.
7 P. Holmqvist, J. Electroanal. Chem. Interfacial Electrochem., 39 (1972) 470.
8 H. Jehring, Elektrosorptionsanalyse mit der Wechselstrompolarographie, Akademie-Verlag, Berlin, 1974.
9 W. Lorenz and F. Möckel, Z. Elektrochem., 60 (1956) 507.
10 T. Yoshida, T. Ohsaka and M. Suzuki, Bull. Chem. Soc. Jpn., 45 (1972) 3245.

Analytica Chimica Acta, 89 (1977) 321—328

RÉACTIONS ACIDE—BASE DANS L'ACÉTAMIDE FONDU À 98° C: ÉTUDE DE L'ACIDITÉ APPARENTE DES IONS Hg(II), Bi(III) ET Cu(II) À L'AIDE D'UNE ÉLECTRODE DE VERRE

M. POURNAGHI*

Laboratoire de Chimie, Institut National des Sciences et Techniques Nucléaires, Saclay (France)

J. DEVYNCK** et B. TRÉMILLON

Laboratoire d'Electrochimie Analytique et Appliquée (associé au C.N.R.S.), Ecole Nationale Supérieure de Chimie de Paris, Université Pierre et Marie Curie, 11 rue Pierre et Marie Curie, 75231 Paris Cedex 05 (France)

(Reçu le 2 septembre 1976)

RÉSUMÉ

Des électrodes de verre de différents types ont été utilisées pour réaliser des titrages acide—base et, en particulier, pour étudier l'acidité des ions métalliques, dans l'acétamide fondu, à 98° C. Les meilleurs résultats sont obtenus avec des électrodes de verre au lithium ("pour milieux alcalins"). L'acidité des ions Hg(II), Bi(III) et Cu(II) a été étudiée à partir de l'analyse des courbes de titrage des ions métalliques par les ions acétamidure; les ions Hg(II) présentent une première acidité forte et une seconde acidité faible, les ions Bi(III) sont diacide fort et manifestent une troisième acidité faible, les ions Cu(II) sont acide faible et forment le complexe acétamidure $Cu(AcNH)_2$ dont la constante de stabilité a été déterminée ($\log \beta_2 = 19.3$).

SUMMARY

Acid—base properties of molten acetamide at 98° C have been studied with different types of glass electrodes. The best results were obtained with lithium glass (for alkaline media). The acidity of metallic ions such as Hg(II), Bi(III) and Cu(II) has been established from titrations with acetamido ions. Hg(II) behaves like a diacid (the first acidity is strong, the second weak); Bi(III) is a triacid (two strong and one weak acidities); Cu(II) is a weak diacid and forms the acetamido complex $Cu(AcNH)_2$ whose stability constant has been determined ($\log \beta_2 = 19.3$).

L'acétamide présente, à l'état fondu (à une température voisine de 100°C) des propriétés de solvant intéressantes, comparables à celles d'autres amides simples, liquides à plus basse température, comme le *N*-méthylformamide ou le *N,N*-diméthylformamide. Certaines de ses caractéristiques en font un solvant comparable à l'eau: sa constante diélectrique ($\epsilon_{AcNH_2} = 59{,}2$ à 100°C) [1, 2] est voisine de celle de l'eau à la même température ($\epsilon_{H_2O} = 55{,}3$); de plus, l'acétamide est, comme l'eau, auto-ionisé. L'équilibre d'auto-ionisation s'écrit: $2\ AcNH_2 \rightleftharpoons AcNH_3^+ + AcNH^-$ ($AcNH_3^+$ représentant le proton solvaté par l'acétamide $AcNH_2$).

*Adresse actuelle: Faculté des Sciences, Université de l'Azarabadeghan, Tabriz (Iran).
**A qui la correspondance doit être adressée.

Le produit ionique a été évalué par Guiot et Trémillon [3] à partir de mesures potentiométriques effectuées avec une électrode à hydrogène: $K_i = [AcNH_3^+][AcNH^-] = 10^{-14}$ à 98°C. Les auteurs ont montré que l'électrode à hydrogène est indicatrice de pH dans tout le domaine d'acidité, depuis les milieux acide fort ($[AcNH_3^+] = 1$ M) jusqu'aux milieux basiques forts ($[AcNH^-] = 1$ M) et ils ont déterminé le pK_A de couples acide—base à partir desquels une échelle d'acidité a été établie.

Si l'utilisation d'une électrode à hydrogène a conduit, dans ce solvant, à des résultats satisfaisants, le pouvoir réducteur de l'hydrogène et les difficultés de mise en oeuvre en limite l'utilisation. En revanche, l'électrode de verre présente, lorsqu'elle fonctionne, une facilité d'emploi bien plus grande.

L'électrode de verre a déjà été envisagée pour la mesure de l'acidité dans d'autres amides: Demange et Badoz [4] ont ainsi montré qu'une électrode de verre à remplissage de DMF est indicatrice de l'activité des ions H^+ dans ce solvant; la "dérive alcaline" ne permet cependant pas les mesures en milieu basique fort. Différents types d'électrodes de verre ont également été étudiées par Juillard [5] dans le même solvant, et Postel [6] a réalisé des mesures de pH dans les mélanges d'amides, *N*-méthylacétamide (NMA) et *N*,*N*-diméthylformamide à l'aide d'électrodes dont le remplissage est réalisé à partir du même mélange d'amides.

Le but de la présente étude est tout d'abord de montrer dans quelles conditions l'électrode de verre peut encore être utilisée dans l'acétamide, à 98°C, pour ensuite mettre en évidence la solvolyse des ions métalliques comme Hg^{2+}, Bi^{3+} et Cu^{2+}. De tels ions ont, en effet, un caractère acide, par suite de réactions du type

$$M^{n+} + m AcNH_2 \rightleftharpoons M(AcNH)_m^{(m-n)^-} + mH^+$$

M^{n+} représentant un ion métallique.

Les résultats de la présente étude seront, par la suite, complétés par ceux d'études voltampérométriques pour analyser le comportement de métaux dans tout le domaine d'acidité accessible, comportement qui sera traduit sous la forme de diagrammes potentiel—pH comparable à celui déjà établi pour l'argent [7].

PARTIE EXPÉRIMENTALE

Solvant

L'acétamide utilisé comme solvant est un produit Prolabo (Paris) "pour usages scientifiques" purifié. Plusieurs méthodes de purification de l'acétamide ont été proposées [2, 3, 8, 9] parmi celles-ci, nous avons choisi la recristallisation dans le dioxanne absolu [9]. L'une des principales impuretés du solvant est l'eau, dont l'importance a été précédemment soulignée [3]. En milieu acide ou basique, le solvant subit, en effet, une hydrolyse qui conduit à la formation d'acétate ou d'acide acétique selon le pH. Cette hydrolyse est gênante lors des études acide—base car les composés formés possèdent des

caractéristiques acido—basiques. En pratique, une grande partie de l'eau éventuellement contenue dans le solvant s'évapore à 98° C et la teneur, mesurée par la méthode de Karl—Fischer, est toujours inférieure à 10^{-3} M. La force ionique des solutions est fixée en ajoutant à l'acétamide du perchlorate de lithium (G. F. Smith) ou du perchlorate de tétraéthylammonium Et_4NClO_4 (Carlo Erba) à la concentration de 1 mol kg^{-1}.

Solutés: acides et bases fortes

Du fait du caractère basique de l'acétamide, de nombreux acides y sont forts. Nous avons utilisé l'acide perchlorique, introduit en solution sous la forme de perchlorate d'acétamide solide, que nous avons préparé selon la méthode de Jander et Winkler [10]. La formule $HClO_4$, 2 $AcNH_2$ a été confirmée par dosage acide—base en solution aqueuse. L'acide chlorhydrique et l'acide nitrique ont également été préparés sous la forme de chlorhydrate (HCl, 2 $AcNH_2$) ou de nitrate (HNO_3, $AcNH_2$) selon la méthode de Strecker [11]. Enfin, l'acide *p*-toluène sulfonique (Carlo Erba) s'est également avéré être un acide fort. Sa forme cristallisée le rend particulièrement intéressant et facile à utiliser.

La base forte est l'ion acétamidure ($AcNH^-$) qui peut être introduit en solution de diverses façons:

(1) sous la forme d'acétamidure de sodium, préparé suivant le mode opératoire de Jander et Winkler [10];

(2) sous la forme de soude. NaOH réagit en effet sur l'acétamide selon la réaction: $OH^- + AcNH_2 \rightleftharpoons AcNH^- + H_2O \uparrow$.
A 98° C, la réaction est fortement déplacée par évaporation d'eau. Ce mode opératoire présente les inconvénients liés à la présence d'eau en solution et à l'hydrolyse de l'acétamide qui s'ensuit. Aussi l'avons-nous peu utilisé.

(3) sous la forme de $AcNH^-$ préparé par électrolyse de l'acétamide. L'étude électrochimique du solvant a montré [3] que la réduction de l'acétamide à une électrode de platine conduit à la formation quantitative d'acétamidure. Il est ainsi possible d'introduire les ions $AcNH^-$ à des concentrations relativement élevées (1 mol kg^{-1}) en réduisant le solvant par coulométrie à intensité constante. Cette méthode a été très utilisée car elle permet d'introduire la base forte en solution sans introduire de solutés gênants ou d'eau.

Electrodes

L'électrode de référence est celle décrite par Guiot et Trémillon [3] et reprise par Petit [12]. Elle utilise le système Ag/AgCl et est constituée d'un fil d'argent plongeant dans un compartiment séparé qui contenait de l'acétamide saturé de chlorure de tétraéthylammonium et de chlorure d'argent. Pour obtenir un dépôt de chlorure d'argent adhérant à l'électrode d'argent, le métal était préalablement oxydé électrochimiquement dans le milieu Et_4NCl.

Divers types d'électrodes de verre, à remplissage aqueux ou à remplissage d'acétamide, ont été utilisées. Les électrodes à remplissage d'acétamide ont

été réalisées à partir d'ébauches Tacussel type TB10 (verre Corning 015) ou TB10HA (verre au lithium, pour utilisation en milieu de haute alcalinité). La solution interne était de l'acétamide saturé de chlorure de tétraéthylammonium de pH fixé par de l'acide perchlorique (0,1 mol kg^{-1}). L'électrode de référence interne utilisait le système de référence précédemment décrit.

Les électrodes à remplissage aqueux étaient des électrodes commerciales Tacussel, spéciales pour utilisation à température élevée, du type TB10HT ou TB10HTA ("haute alcalinité"). Des potentiels assez reproductibles étaient obtenus après trempage dans l'acétamide (+ Et_4NClO_4 1 M) fondu deux heures avant l'utilisation. Notons cependant que les valeurs de potentiel diffèrent sensiblement d'une électrode à l'autre ou d'un jour à l'autre entre deux électrodes du même type; l'évaluation du pH nécessite un étalonnage de l'électrode juste avant son utilisation. Les solutions suivantes ont été utilisées: $HClO_4$ 1 mol kg^{-1}, tampon acétique 0,1 mol kg^{-1}.

Cellule

La cellule utilisée était une cellule Tacussel type RM01 à double paroi, thermorégulée par une circulation d'huile fournie par un thermostat (précision ± 0,1° C). Pour éviter la condensation à l'intérieur du couvercle, l'ensemble était placé sous un épiradiateur.

Les mesures de potentiel étaient effectuées à l'aide d'un millivoltmètre Tacussel S6ER.

RESULTATS EXPÉRIMENTAUX

Etalonnage de l'électrode de verre

Si l'électrode de verre est indicatrice du pH dans l'acétamide, son potentiel varie en fonction de la concentration des ions H^+ selon la loi de: $E = c + 0{,}074 \log [H^+]$ à 98°C et à force ionique constante.

Les courbes de variation du potentiel de diverses électrodes de verre en fonction du pH sont représentées sur la Fig. 1 et les caractéristiques des électrodes regroupées dans le Tableau 1. Ces résultats suggèrent les remarques suivantes.

TABLEAU 1

Caractéristiques de quelques électrodes de verre dans l'acétamide fondu, à 98°C

Verre	Remplissage	Domaine de linéarité (pH)	Pente[a] (mV)
Corning 015	Acétamide	0—3,5	75
Corning 015	Eau	0—3	90
Verre au Li	Acétamide	0—7	90
Verre au Li	Eau	0—8	74

[a] Valeur théorique: 74 mV à 98° C.

(1) Les électrodes à remplissage aqueux sont facilement utilisables malgré la température élevée (98°C).
(2) La nature du solvant de remplissage de l'électrode a peu d'importance sur sa "réponse"; la pente est cependant plus proche de la valeur théorique lorsque l'électrode est à remplissage aqueux. Ceci avait déjà été observé par Juillard [5] lors de l'utilisation d'électrodes de verre dans d'autres amides.
(3) La nature du verre a, par contre, une importance plus grande et les meilleurs résultats sont obtenus avec les verres au lithium qui constituent habituellement les électrodes utilisables en milieu alcalin.
(4) Quelle que soit l'électrode utilisée, il n'est pas possible d'obtenir une réponse correcte en milieu basique (pH > 7 environ, pour un domaine d'acidité s'étendant sur 14 unités). La solvolyse des ions métalliques ne pourra donc être mise en évidence que si elle est suffisamment importante, c'est-à-dire si les ions ont un caractère acide assez prononcé. L'électrode de verre peut cependant être facilement utilisée pour le titrage d'acides relativement forts et pour la détermination de pK_A de couples acide—base; la Fig. 2 illustre ces possibilités d'application à des titrages. L'acide *p*-toluénesulfonique est un acide fort qui peut avantageusement remplacer l'acide perchlorique dont la préparation (sous forme de perchlorate d'acétamide [10]) est assez délicate. L'analyse de la courbe de titrage de l'acide acétique permet de retrouver une valeur de pK_A dans ce solvant (pK_A = 5,6) proche de la valeur obtenue à l'aide de l'électrode à hydrogène (pK_A = 5,8) [3].

Acidités des ions métalliques

Ions mercure(II). Un complexe acétamidure du mercure $Hg(AcNH)_2$ a déjà été mis en évidence [2], mais l'acidité des ions mercure(II) n'avait jamais été étudiée de façon précise. A l'aide de l'électrode de verre, nous avons pu mettre en évidence un caractère mono acide fort de ces ions. La solvolyse des ions Hg^{2+} est donc totale et correspond à la réaction:

$$Hg^{2+} + AcNH_2 \rightarrow Hg(AcNH)^+ + H^+.$$

La courbe de titrage des ions Hg^{2+} par $AcNH^-$ se superpose exactement, dans sa première partie (Fig. 3) à celle du titrage d'un acide fort, un point équivalent étant obtenu par l'addition d'une mole de base forte par mole d'ion Hg^{2+}. Le titrage permet de mettre en évidence le complexe supérieur $Hg(AcNH)_2$ précédemment signalé, mais la mauvaise réponse de l'électrode de verre en milieu basique ne permet pas d'en calculer la constante de stabilité.

Ions bismuth(III). Comme les ions Hg^{2+}, les ions Bi^{3+} (introduits sous forme de nitrate ou par oxydation coulométrique du bismuth métallique en milieu Et_4NClO_4 1 M) provoquent une solvolyse importante que l'on peut mettre en évidence avec une électrode de verre.

L'analyse d'une courbe de titrage des ions Bi^{3+} par les ions acétamidure montre que Bi^{3+} se comporte en diacide fort, selon la réaction

$$Bi^{3+} + 2\ AcNH_2 \rightarrow Bi(AcNH)_2^+ + 2\ H^+$$

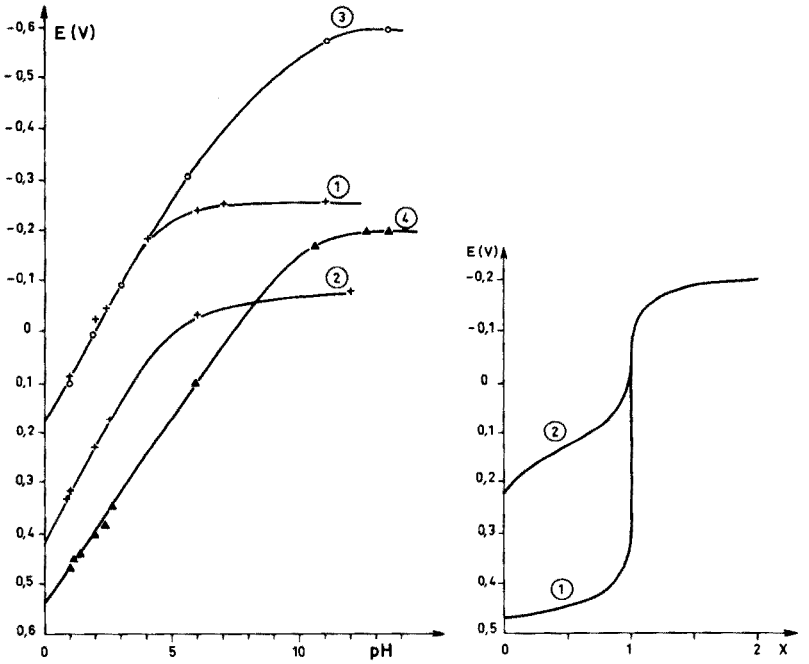

Fig. 1. Variation du potentiel de quelques électrodes de verre dans l'acétamide fondu, à 98° C, en fonction du pH. Verre Corning 015: (1) remplissage, $AcNH_2$; (2) remplissage, eau. Verre au lithium, (3) remplissage, $AcNH_2$; (4) remplissage, eau.

Fig. 2. Variation du potentiel d'une électrode de verre au cours du titrage d'une solution d'acide *p*-toluènesulfonique (1) ou d'acide acétique (2) par les ions acétamidure. Electrode de verre au lithium, remplissage aqueux. x = fraction d'acide titré.

Le titrage permet, par ailleurs, de mettre en évidence la formation de $Bi(AcNH)_3$, composé insoluble qui précipite dès que la quantité d'acétamidure est telle que: $[AcNH^-$ ajouté$] > 2\,[Bi^{3+}]$. Mais, encore une fois, la mauvaise réponse de l'électrode de verre en milieu basique ne permet pas le calcul du produit de solubilité du composé formé.

Ions cuivre(II). Les ions cuivre(II) ne sont pas stables dans l'acétamide fondu; l'addition de chlorure ou de nitrate de cuivre(II) provoque l'apparition d'une couleur verte qui devient progressivement plus foncée. Des études précédentes avaient conduit, à partir de mesures conductimétriques, à la mise en évidence qualitative de deux complexes acétamidure de cuivre [2]. La formation de ces complexes traduit un caractère acide que nous avons également mis en évidence à l'aide d'une électrode de verre. Une courbe de titrage d'une solution de nitrate de cuivre par les ions acétamidure est représentée sur la Fig. 4. L'allure de cette courbe montre que les ions Cu^{2+} sont acide faible et réagissent sur le solvant selon la réaction.

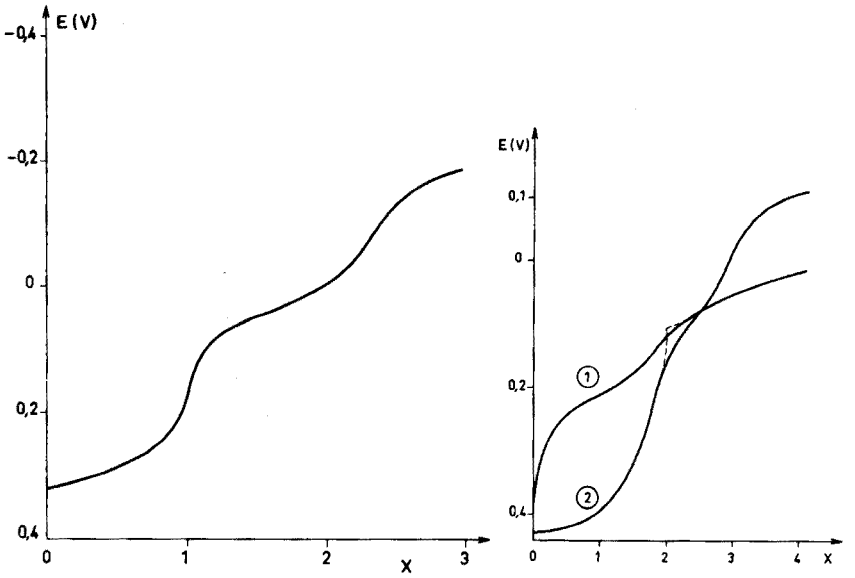

Fig. 3. Variation du potentiel d'une électrode de verre au cours du titrage d'une solution d'ions mercure(II) (10^{-2} mol kg^{-1}) par les ions acétamidure. Electrode de verre Corning 015, remplissage $AcNH_2$. x = (nombre de moles de $AcNH^-$ ajouté)/(nombre de moles de Hg^{2+} initial).

Fig. 4. Variation du potentiel d'une électrode de verre au cours du titrage des ions Bi^{3+} (1) ou Cu^{2+} (2) par les ions acétamidure.

$$Cu^{2+} + 2\ AcNH_2 \rightleftharpoons Cu\ (AcNH)_2 + 2\ H^+$$

avec

$$K_A = [Cu(AcNH)_2]\,[H^+]^2/[Cu^{2+}]$$

La solvolyse n'est pas totale, mais suffisamment importante pour que la valeur de K_A puisse être déduite des mesures effectuées avec l'électrode de verre; le calcul peut être effectué, soit à partir de l'analyse de la courbe de titrage, soit à partir de mesures de pH dans des solutions d'ions Cu^{2+} à diverses concentrations. Cette dernière méthode a conduit à la valeur suivante: pK_A = 9,9 ± 0,5.

La constante de stabilité du complexe $Cu(AcNH)_2$ peut en être déduite facilement: $\log \beta_2 = 2\ pK_i - pK_A$, d'où $\log \beta_2 = 19{,}3 \pm 0{,}4$ $mol^2\ kg^{-2}$.

BIBLIOGRAPHIE

1 K. Schaum et E. Holla, Justus Liebigs Ann. Chem., 542 (1939) 77.
2 G. Jander et G. Winkler, J. Inorg. Nucl. Chem., 9 (1959) 24.
3 S. Guiot et B. Tremillon, J. Electroanal. Chem. Interfacial Electrochem., 18 (1968) 261.

Analytica Chimica Acta, 89 (1977) 329—338

EVALUATION OF MICROMOLAR COMPLEXIMETRIC TITRATIONS FOR THE DETERMINATION OF THE COMPLEXING CAPACITY OF NATURAL WATERS

KENNETH W. HANCK and JAMES W. DILLARD

Department of Chemistry, North Carolina State University, Raleigh, North Carolina 27607 (U.S.A.)

(Received 23rd July 1976)

SUMMARY

The titration of micromolar levels of complexing agents with metal ion titrants, and voltammetric methods to locate the equivalence point, has been evaluated experimentally and theoretically. Both anodic stripping voltammetry and differential pulse polarography give systematically low results if labile metal ions are used as titrants. Low-temperature (0 °C) dual-cell anodic stripping voltammetry greatly minimizes the effects of metal complex lability but the mercury film electrodes deteriorate rapidly because of temperature cycling. A micromolar complexiметric titration with a voltammetric end-point is not a practical method for determining the complexing capacity of natural waters.

The importance of organic matter which forms soluble complexes with metal ions in aquatic environments has become an important topic of discussion. Relatively little work has been conducted in fresh water systems, but extensive work has been conducted in marine systems and in the soil solution to identify the organic functional groups responsible for natural complexation and to test the use of synthetic complexing agents in improving fertility [1–4]. The importance of complexing agents in natural water in solubilizing and transporting a number of trace metals has been studied [5, 6]. The rôle of complexing agents in the toxicity and availability of trace metals to aquatic life has also been investigated [7].

Most of the methods that have been developed for determining complexing agents involve measurement of the amount of metal complex formed on addition of excess of metal or measurement of the remaining free metal directly. Thompson and Duthie [8] proposed a spectrophotometric procedure based on measuring the absorbance of zinc zinconate. Several spectrophotometric procedures for the determination of EDTA at trace levels have been reported [9—13]. Interference from sample turbidity would seem to limit the usefulness of spectrophotometry in determining metal complexes in natural water.

Several trace metals catalyze chemical reactions; complexation reduces their catalytic effect. Several kinetic procedures based on measurement of

the decrease in reaction rate in the presence of sub-micromolar quantities of complexing agents are available [14, 15]. The catalytic effect is inhibited by certain combinations of trace metals and enhanced by others. Since natural water contains a variety of trace metals, application of these procedures may be very unreliable.

Kunkel and Manahan [16] employed the enhanced solubility of copper hydroxide at pH 10 as a monitor of complexing capacity. Atomic absorption was used to monitor the level of soluble copper; the use of a pH 10 medium, however, disrupts the natural equilibria present in the sample.

Various electrochemical techniques have been used to determine trace levels of complexing agents. Cadmium complexes of NTA and EDTA at the millimolar level were determined by d.c. polarography [17]. Indium complexes of NTA at the 0.02-p.p.m. level were determined by linear-sweep voltammetry after preconcentration by anion exchange [18]. Lead and bismuth were used to determine NTA at the 10 $\mu g\, l^{-1}$ level by dual-cell cathode-ray polarography [19]. Ion-selective electrodes have also been employed in determining complexing agents [20—22].

Matson et al. were first to employ anodic stripping voltammetry to estimate complexing capacity [23, 24]. Chau and Chan [7] employed a similar method with copper as titrant and stressed the importance of allowing sufficient time (at least 2 h) for complex equilibrium to be reached before measuring the free metal.

The present paper reports an evaluation of micromolar complexiметric titrations as a method of determining the complexing capacity of natural water. Location of the equivalence point requires an analytical technique capable of distinguishing between complexed and solvated metal ions, and this is often possible by voltammetric methods. Each type of voltammetry obtains the current—voltage curve by a slightly different experimental approach, but the results of all methods can be placed on a common basis through use of a response curve in which i/i_l is plotted vs. potential; i is the current at the plotted potential and i_l is the current under conditions of mass transfer control. The conversion from i/i_l to current (or vice versa) depends on the method used to measure the current; the principles of various voltammetric methods have been reviewed [25—27].

The response curves expected for a system containing $2 \cdot 10^{-6}$ M M^{2+} and 10^{-6} M L are shown in Fig. 1. The curves assume the formation of a single complex, ML^{2+}, and a reversible reduction yielding M^0. The equations derived and discussed by Macovschi [28] were used in calculating the curves. It is obvious from Fig. 1 that the presence of two species (i.e. M^{2+} and ML^{2+}) is not detected until the formation constant of the complex exceeds 10^8. Figure 2 illustrates the changes in the response curves during titration of 10^{-6} M L with a metal titrant. If the response indicative of free metal is plotted vs. the amount of metal added, curves of the type shown in Fig. 3 are expected. Experimentally, the amount of complexing agent in a sample is obtained from the x-intercept of the titration curve. Accuracy is a function

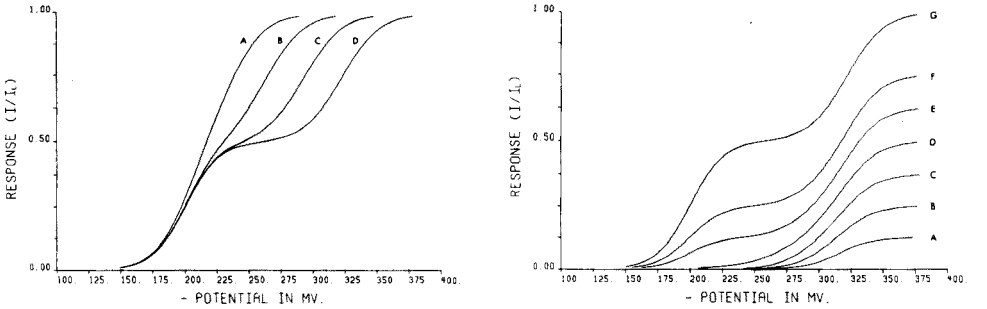

Fig. 1. Effect of formation constant on theoretical response curve. Analytical concentration of $M^{2+} = 2 \cdot 10^{-6}$ M; analytical concentration of $L = 10^{-6}$ M. Formation constant: A, 10^7; B, 10^8; C, 10^9; D, 10^{10}.

Fig. 2. Theoretical response curves during titration of 10^{-6} M L with M^{2+}. Percent titrated: A, 25 %; B, 50 %; C, 75 %; D, 100 %; E, 125 %; F, 150 %; G, 200 %.

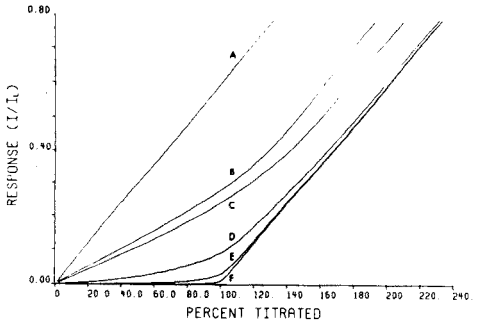

Fig. 3. Theoretical titration curves for the titration of 10^{-6} M L with M^{2+}. Formation constant: A, 10^7; B, $7 \cdot 10^7$; C, 10^8; D, 10^9; E, 10^{10}; F, 10^{11}.

of formation constant (Table 1). To determine the concentration of a 10^{-6} M solution of a ligand with a relative error of 1 % or less, the formation constant of the metal complex formed must exceed 10^{10}.

This paper reports the results of micromolar complexiметric titrations in which the end-point has been located by three voltammetric methods: anodic stripping voltammetry (a.s.v.), differential pulse polarography (d.p.p.) and low-temperature dual-cell anodic stripping voltammetry (l.t.a.s.v.).

TABLE 1

Predicted accuracy of voltammetric methods for different complex formation constants (K_f)

K_f	10^7	$7 \cdot 10^7$	10^8	10^9	10^{10}	10^{11}
Relative error (%)	—[a]	38.6	25.2	6.3	0.8	0.0

[a]No ligand detected.

EXPERIMENTAL

Reagents

The water used was deionized twice, passed through an activated charcoal column and finally filtered through a 0.2-μm membrane filter. The specific resistance was continually monitored and the resulting water was found to be consistently greater than 17 megohm-cm.

The standard solution of ethylenedinitrilotetraacetic acid (EDTA; Fisher Scientific) was prepared from $Na_2H_2Y \cdot 2H_2O$, dissolved in deionized water and standardized by spectrophotometric titration.

Standard solutions of metal ions were prepared at the 10^{-2} M level with deionized water. Copper(II), cadmium(II), lead(II) and indium(III) solutions were prepared by dissolving the appropriate amount of high-purity metal (Alpha Inorganics) in Ultrex nitric acid.

The acetate buffer (pH 5, 0.1 M) was prepared from reagent-grade sodium acetate and glacial acetic acid (Fisher Scientific). A concentrated solution (1.0 M) of the acetate buffer was purified by controlled potential electrolysis at a mercury pool electrode as described by Barendrecht [29] and Mitchell [30]; electrolysis time was generally five days.

All stock and standard solutions were stored in polyethylene containers at 5 °C and at concentrations not lower than 10^{-2} M.

Nitrogen gas (Air Products) used in purging sample solutions was deoxygenated by passage through a Ridox scrubber before use.

Electrodes and cells

A Corning fiber-tipped saturated calomel reference electrode, a platinum auxiliary electrode (3 cm of 26-gauge Pt wire) and a thin mercury film working electrode (GC-A glassy carbon base) were used in the three-electrode cell. The working electrode was made from a 2-cm length of glassy carbon sealed into the end of a 6-mm (o.d.) glass tube with epoxy cement. Electrical contact was made by a mercury junction in the glass tube. The end was polished with moist 500-A silicon carbide paper, followed by 0.3 and 0.1-μm alumina (Fisher Scientific) until a mirror finish was achieved. A 1-μm mercury film was electrodeposited on the electrode at a constant current of 1.0 mA in 0.05 M mercury(I) nitrate in 0.1 M $HClO_4$ before introduction into the electrochemical cell. In the dual-cell configuration, the working electrode was rotated by a Sargent synchronous rotator; the matching "blank" electrode was stationary and separated from the test solution by a medium-porosity glass sealing tube.

For differential pulse polarography, the working electrode was replaced by a standard dropping mercury electrode (DME) (Sargent-Welch S-29417 capillary, m = 3.896 mg Hg s^{-1}) equipped with a PAR 172 drop timer (Princeton Applied Research Corp.).

The cells used were 100-ml Berzelius Pyrex beakers fitted into commercially available polyethylene cell tops (Leeds and Northrup cell cover no. 067513 and ring no. 127182).

Electronic equipment

A PAR Model 174 Polarographic Analyzer (Princeton Applied Research Corp.) was used with a Hewlett-Packard Moseley 7001A X-Y recorder. For dual-cell a.s.v. analysis the PAR Model 174/51 Linear Sweep Module was utilized to subtract blank current from sample current.

Procedures

The a.s.v. electrolysis potential was selected by first obtaining a d.c. polarogram of the metal ion titrant. The potential had to be on the free metal diffusion current plateau, but not so negative that current from the metal—ligand wave was included. A potential $120/n$ mV negative of the polarographic $E_{1/2}$ value was used as an initial guess for the electrolysis potential. Several a.s.v. runs were made on a 10^{-5} M metal ion titrant solution at that potential and compared to additional runs performed at a potential $60/n$ mV more negative. If the average peak current of the two series differed by less than 10 %, the first potential was used as the electrolysis potential; if agreement was not reached the process was repeated until agreement was found. An electrolysis potential was obtained for each metal ion employed as a titrant.

The a.s.v. method involved adding an aliquot of the metal ion titrant to a pH 5 buffered solution containing a known amount of sample. The amount added was in excess of the expected ligand concentration. After solution equilibrium had been reached, at least three anodic stripping voltammograms were run. An additional aliquot of titrant metal was then added to the test solution and another set of voltammograms run. This procedure was continued until at least four additions of titrant metal had been made. The titrant aliquots were normally not more than 50 μl each so that dilution could be ignored. The maximum stripping peak current was plotted as a function of μmoles of titrant added. The x-intercept was a measure of the free metal determined and therefore the amount of complexing capacity of the sample.

RESULTS AND DISCUSSION

Anodic stripping voltammetry

Four supporting electrolytes were evaluated: NaCl, KNO_3, acetate buffer (pH 5) and sodium tartrate. The tartrate ion disturbed the natural complex equilibria. The a.s.v. peak of the Cu(II) titrant was poorly resolved from the large background current in NaCl. In chloride medium, the oxidation of the mercury electrode is moved to more negative potentials, and the resulting current partly overlapped the Cu(II) a.s.v. peak. Potassium nitrate was satisfactory electrochemically but did not permit rigorous pH control. Acetate buffer (pH 5) gave the best results and was adopted as the supporting electrolyte, although it disturbed natural equilibria slightly because of the pH change and the mild complexing power of acetate; this buffer has been used in studies of metal complex formation [7].

Four metal ion titrants were selected for their ability to form strong com-

plexes with organic ligands and for their detectability by electrochemical methods in acetate buffer: Cu(II), Pb(II), Cd(II) and In(III). The electrolysis potential determined for each ion in acetate buffer is shown in Table 2 along with their respective EDTA conditional formation constant. A typical anodic stripping voltammogram for Pb(II) and In(III) in acetate buffer is shown in Fig. 4. Indium(III) was selected as the best titrant because of its strong complexing ability, low detection limit (3-electron process), low natural levels in water and simplicity of electrochemical reduction.

EDTA was chosen among other synthetic ligands because of its high purity, availability and wide commercial use. The complexiметric chemistry of EDTA has been extensively documented and investigated by several earlier workers [9—13, 17]. Representative results of In(III) titrations of EDTA samples (0.16—8.24 μM) are summarized in Table 3. The consistently low results indicate the presence of a systematic error, even though the formation constant of the $InEDTA^-$ complex significantly exceeds the minimum value of 10^{10} needed for accurate determination.

Metal complex lability at the electrode surface is the most likely source of

TABLE 2

A.s.v. electrolysis potentials and metal—EDTA K'_f values

Ion	No. of electrons	E_p [a] (V)	$E_{electrolysis}$ [a] (V)	K'_f
Cu^{2+}	2	−0.075	−0.250	$2.2 \cdot 10^{12}$
Cd^{2+}	2	−0.625	−0.750	$1.0 \cdot 10^{10}$
Pb^{2+}	2	−0.430	−0.600	$3.8 \cdot 10^{11}$
In^{3+}	3	−0.645	−0.675	$3.5 \cdot 10^{18}$

[a]Versus SCE.

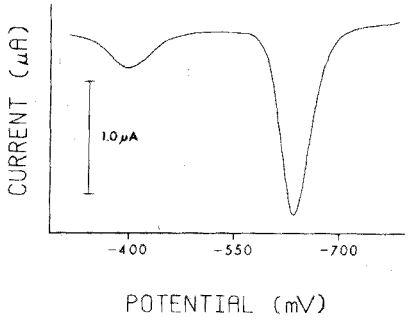

Fig. 4. Anodic stripping voltammogram of $5.0 \cdot 10^{-6}$ M In(III) and $1.2 \cdot 10^{-6}$ M Pb(II) in pH 5 acetate buffer.

TABLE 3

A.s.v. determination of EDTA

EDTA taken (μM)	EDTA found (μM)	Relative error (%)	EDTA taken (μM)	EDTA found (μM)	Relative error (%)
8.24	6.70	−18.7	0.82	0.64	−22
2.19	2.17	−0.91	0.82	0.54	−34
1.73	1.66	−4.05	0.21	0.18	−14
1.59	1.52	−4.40	0.21	0.15	−29
1.04	1.05	+0.96	0.16	0.13	−19

the low results. Since a small fraction of metal (approximately 1 % for a 2-min electrolysis) is removed from solution while monitoring the uncomplexed fraction of metal ion titrant, the concentration of free metal ion is decreased slightly in the bulk of solution but drops very close to zero at the electrode surface. This loss of free metal ion from solution and establishment of a concentration gradient near the electrode surface, drives the metal-ion/metal-complex equilibrium towards dissociation. The released metal ion is then measured as free metal and the amount of complexing agent determined is therefore smaller than expected. Using a.s.v. with a hanging mercury drop electrode to locate the equivalence point, Shuman and Woodward [31] found significant dissociation of the metal complex during the deposition step while titrating $4.45 \cdot 10^{-5}$ M EDTA with Cd(II) solution. This concentration is over ten times the expected ligand levels of natural water.

Whether a metal complex is labile or inert is predominantly a function of the metal ion in the complex. Unfortunately, the electronic structures of all the metal ions tested by the a.s.v. procedure were such that labile complexes would be formed with the ligands present in the sample. Metals which form inert EDTA complexes such as Co(III), Cr(III), Fe(III), Rh(III), and Ru(II), form the complexes very slowly and exhibit Nernstian electrochemistry only in electrolytes which would disrupt natural complex equilibria.

Low-temperature a.s.v.

The effect of chemical reactions before electron transfer can be minimized by shortening the time of measurement and by lowering the solution temperature. Because of the reduced current associated with shorter deposition times, a dual-electrode a.s.v. procedure was devised in order to increase the a.s.v. peak signal-to-background ratio. By electronically subtracting the background current common to both electrodes, the dual procedure permitted a.s.v. measurements after only 10 s of electrolysis. Details of the operation of the dual-cell device are available [32]. The results obtained when dual-electrode a.s.v. was used to determine the complexing capacity of nine samples each containing $96.2 \cdot 10^{-9}$ M of EDTA are summarized in Table 4. An analysis of variance of these data at the 95 % level of confidence indicated that electrolysis time significantly affected the results.

TABLE 4

Effect of electrolysis time on a.s.v. results for $96.2 \cdot 10^{-9}$ M of EDTA

Electrolysis time (s)	EDTA found ($\cdot 10^{-9}$ M)				
	Sample 1	Sample 2	Sample 3	Av.	s^a
10	126.3	91.9	106.5	108.2	17.3
20	110.7	101.3	56.4	89.5	29.0
50	70.9	10.4	28.2	36.5	31.1

[a]Standard deviation.

Lowering the sample temperature to 0 °C was effective in decreasing the lability of metal complexes. However, the lowered temperature also slowed the rate of complex formation, necessitating the addition of metal titrant to a sample at 25 °C, allowing equilibrium to be established, and then cooling the sample to 0 °C for monitoring the free metal-ion concentration. Time-consuming recycling was necessary for each addition of metal-ion titrant. The results obtained when 103.7 nmol of EDTA was titrated showed a mean value of 99.8 nmol with a standard deviation of 13.8 (8 determinations). Temperature also affected the stripping current of the metal ion titrant; the In(III) a.s.v. peaks at 0 °C were approximately one third that at 25 °C. Moreover, cycling the mercury film electrodes over such a large temperature range, greatly reduced their already short lifetime. The thin film mercury electrodes are difficult to prepare reproducibly and the dual-cell temperature variation procedure demands that the two electrodes be exactly matched, otherwise the PAR 174/51 cannot balance the blank signals correctly. The use of a hanging mercury drop electrode (HMDE) would aid in the balancing problem, but because of the lower area:volume ratio of a drop compared to a film, the peak currents are much smaller. Location of baseline current from either thin film or HMDE anodic stripping voltammograms is somewhat arbitrary, making a.s.v. measurements difficult to automate conveniently.

Although lowering the temperature minimized the lability effects, the increased length of analysis, the shorter lifetime of electrodes and the reduced sensitivity of the method led to the conclusion that a.s.v. is neither practical nor satisfactory for measuring the complexing capacity of natural water.

Differential pulse polarography

D.p.p. with a dropping mercury electrode was used to locate the end-point of the titration of 10^{-5} M EDTA with Cu(II) solution in pH 5 acetate buffer. The same titration procedure used for a.s.v. measurements was also followed for the d.p.p. measurements.

In the pH 5 buffer, two reduction peaks for the titration of EDTA with Cu(II) were observed: the free metal at +0.035 V (vs. SCE) and the metal

complex at −0.100 V. As the titration proceeds, both peak currents change; initially only the metal complex peak increases with added metal titrant, then after the equivalence point the free metal peak appears and increases while the metal complex peak current levels to a constant value. A third peak is also present initially at +0.08 V which is due to the oxidation of Hg to $HgEDTA^{2-}$; its peak current decreases as EDTA is consumed during the titration. This mercury ligand peak is not reliably present in natural water samples.

As is shown in Fig. 5, the free copper line when extrapolated to zero current, resulted in a low determination. The curve associated with the $CuEDTA^{2-}$ peak current theoretically should have reached a plateau at the 100 % titrated point, but experimentally continued to increase significantly beyond the equivalence point. Therefore, as observed earlier with a.s.v., differential pulse polarography is also subject to kinetic effects. During d.p.p. reductions, the potential of the DME is slowly scanned to negative potentials; the electrode is polarized for most of drop life, typically 0.5—5.0 s. Depletion of the free-metal concentration at the electrode surface during the polarization period provides the driving force for dissociation of the metal complex; the drop time is apparently long enough for significant dissociation to occur. The effects of metal complex lability on differential pulse polarograms have been studied by digital simulation [33]; the results are in qualitative agreement with the present observations.

A procedure for determining complexing capacity which utilizes an inert metal ion is currently under development in this laboratory.

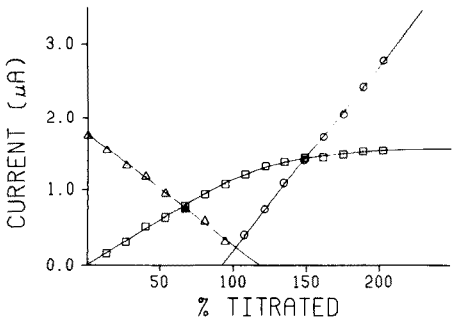

Fig. 5. Differential pulse polarographic titration of $1.64 \cdot 10^{-5}$ M EDTA with Cu(II) in pH 5 acetate buffer. Free copper (○); $CuEDTA^{2-}$ (□); $HgEDTA^{2-}$ (△).

A grant from the Water Resources Research Institute of the University of North Carolina (A-052-NC) partially supported this work.

REFERENCES

1 J. Shapiro, J. Am. Water Works Assoc., 56 (1964) 1062.
2 R. T. Barber, R. C. Dugdale, J. J. Mac Isaac and R. L. Smith, Invest. Pesq., 35 (1971) 171.
3 M. Schnitzer, Metal—Organic Matter Interactions in Soils and Waters, in S. D. Faust and J. V. Hunter (Eds.), Organic Compounds in Aquatic Environments, M. Dekker, New York, 1971, pp. 297—315.
4 A. Siegel, Metal—Organic Interactions in the Marine Environment, in S. D. Faust and J. V. Hunter (Eds.), Organic Compounds in Aquatic Environments, M. Dekker, New York, 1971, pp. 265—295.
5 C. G. Gregor, Environ. Sci. Technol., 6 (1972) 278.
6 R. D. Guy, C. L. Chakrabarti and L. L. Schramm, Can. J. Chem., 53 (1975) 661.
7 Y. K. Chau and K. Lum-Shue-Chan, Water Res., 8 (1974) 383.
8 J. E. Thompson and J. R. Duthie, J. Water Pollut. Control Fed., 40 (1968) 306.
9 O. Menis, H. P. House and I. B. Rubin, Anal. Chem., 28 (1965) 1439.
10 W. S. Knight and R. A. Osteryoung, Anal. Chim. Acta, 20 (1958) 481.
11 D. Roubalova and J. Dolezal, Chemist—Analyst, 49 (1960) 76.
12 B. Kratochvil and M. White, Anal. Chem., 37 (1965) 111.
13 C. O. Huber and D. R. Tallant, J. Electroanal. Chem. Interfacial Electrochem., 18 (1968) 421.
14 H. A. Mottola, M. S. Haro and H. Freiser, Anal. Chem., 40 (1968) 1263.
15 H. A. Mottola, Anal. Chem., 42 (1970) 630.
16 R. Kunkel and S. E. Manahan, Anal. Chem., 45 (1973) 1465.
17 R. B. Le Blanc, Anal. Chem., 31 (1959) 1840.
18 J. P. Haberman, Anal. Chem., 43 (1971) 63.
19 B. K. Afghan and P. D. Goulden, Environ. Sci. Technol., 5 (1971) 601.
20 G. A. Rechnitz and N. C. Kenny, Anal. Lett., 3 (1970) 509.
21 J. A. Blay and J. H. Ryland, Anal. Lett., 4 (1971) 653.
22 B. van't Riet and J. E. Wynn, Anal. Chem., 41 (1969) 158.
23 H. E. Allen, W. R. Matson and K. H. Mancy, J. Water Pollut. Control Fed., 42 (1970) 573.
24 M. E. Bender, W. R. Matson and R. A. Jordan, Environ. Sci. Technol., 4 (1970) 520.
25 J. G. Osteryoung and R. A. Osteryoung, Am. Lab., 4 (1972) 8.
26 J. B. Flato, Anal. Chem., 44 (1972) 75A.
27 P. E. Sturrock and R. J. Carter, Crit. Rev. Anal. Chem., 5 (1975) 201.
28 M. E. Macovschi, J. Electroanal. Chem. Interfacial Electrochem., 16 (1968) 457.
29 E. Barendrecht, Stripping Voltammetry, in A. J. Bard (Ed.), Electroanalytical Chemistry, Vol. II, M. Dekker, New York, 1967, pp. 53—109.
30 J. W. Mitchell, Anal. Chem., 45 (1973) 492A.
31 M. S. Shuman and G. P. Woodward, Anal. Chem., 45 (1973) 2032.
32 Instrument Manual for Model 174/51 Linear Sweep Module, P.A.R. Corp., Princeton, N.J., 1971.
33 J. W. Dillard, Ph.D. Thesis, N.C. State University, 1976.

Analytica Chimica Acta, 89 (1977) 339—345

ANALYTICAL STUDIES OF THE CYCLOPOLYMETHYLENETETRAZOLES AND THEIR MIXTURES BY GAS CHROMATOGRAPHY

ROBERT G. BAUM, DAVID W. DeBROSSE, and ALEXANDER I. POPOV
Department of Chemistry, Michigan State University, East Lansing, Michigan 48824 (U.S.A.)
(Received 24th March 1976)

SUMMARY

Gas chromatography is shown to be useful in analyses for cyclopolymethylenetetrazoles. The relative retention times are very nearly the same for trimethylenetetrazole, tetramethylenetetrazole, and pentamethylenetetrazole, but vary considerably as the number of methylene groups is increased. Working curves obtained for the cyclopolymethylenetetrazoles are linear over the 10^{-3}—10^{-1} M range but become curved at higher concentrations. These compounds can be determined routinely at the 50—100 p.p.m. level; concentrations of less than 10 p.p.m. can be estimated.

The cyclopolymethylenetetrazoles (I) and their derivatives can cause epileptic convulsions. The convulsant activity

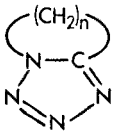

(I)

varies with the number of methylenes in the hydrocarbon chain as well as with the nature and position of substituent groups [1]. A number of cyclopolymethylenetetrazoles has been reported in the literature but only pentamethylenetetrazole (PMT) has been used in chemotherapy as a respiratory and cardiac stimulant and, in higher doses, as an analeptic in barbiturate overdoses. Pentamethylenetetrazole has also been employed for screening anticonvulsant drugs and, in veterinary medicine, in hastening the recovery of animals from anesthesia [2]. Because of its use in chemotherapy, the chemistry of PMT has been studied in some detail. However, the analytical chemistry of PMT and the other cyclopolymethylenetetrazoles has not been thoroughly investigated.

Many studies have been devoted to the investigation of several PMT—transition metal complexes [3, 4]. In gravimetry, complexes such as CuCl · PMT [5], $HgCl_2$ · PMT [6], and $CdCl_2$ · PMT [7] have been

recommended as weighing forms for the drug. The precipitates, however, are not strictly stoichiometric and the reaction conditions must be rigorously controlled to obtain precipitates of the same composition.

Pentamethylenetetrazole and substituted pentamethylenetetrazoles have been determined by nonaqueous potentiometric titrations [8, 9], but the elaborate procedure required does not make this method practical for routine analysis.

The most sensitive methods developed for the determination of PMT are based on gas chromatography; one of the first studies was reported by Kawamoto [10], who used a phenylmethylsilicone column with a thermal conductivity detector. The lowest concentrations of PMT detected were of the order of 1000 p.p.m. More recent investigations have utilized flame ionization detection systems [11—13]. Marcucci et al. [11] reported a method for determining brain levels of PMT which could detect as little as 50 ng of this drug. Stewart and Story [12] described a method for the determination of PMT in biological fluids; when a column packed with 5 % polyethylene glycol 20,000 on 80/100 mesh diatomaceous earth was used as little as 1 p.p.m. of PMT could be detected.

Although this technique has proved to be successful for PMT, there have been no reports on the determination of the other cyclopolymethylenetetrazoles. To study possible correlations between the physicochemical properties and convulsant activities of these tetrazoles, it is necessary to have a method for their analysis. Thus, the purpose of this investigation was to determine the chromatographic characteristics of several cyclopolymethylenetetrazoles and to determine the conditions for their routine determination by gas chromatography.

EXPERIMENTAL

Reagents

Carbon tetrachloride (Fisher) was shaken with alcoholic sodium hydroxide, washed several times with water, dried over calcium chloride, and fractionally distilled. Water was doubly distilled in an all-glass apparatus, once with potassium permanganate present in the charge to remove all oxidizable organic impurities. Chloroform (Fisher, Certified A.C.S.) was used without further purification.

Pentamethylenetetrazole (Aldrich) was recrystallized from diethyl ether and dried in vacuo. Trimethylenetetrazole (Aldrich) was purified by recrystallizing about 10 g of the tetrazole from a mixture of 50 ml of carbon tetrachloride and 10 ml of ethanol.

The other cyclopolymethylenetetrazoles were prepared and purified as described previously [14, 15].

Gas chromatographic measurements

Gas chromatography measurements were carried out on a Varian 1440-10 gas chromatograph equipped with a flame ionization detector. The column was constructed of 6 ft. × 1/8 in. stainless steel tubing and packed with 3 % Hi-Eff 8-BP (Applied Science Laboratories, Inc.) on 100/120 mesh Gas-Chrom Q (Applied Science Laboratories, Inc.). The 8-BP liquid phase is a polyester, produced from cyclohexanedimethanol succinate, which can tolerate a maximum operating temperature of 250 °C. Gas-Chrom Q is a high quality silane-treated support used for separations of steroids, pesticides, alkaloids, pharmaceuticals and other compounds that require very inert supports. Helium was used as the carrier gas, and the flow rate was monitored daily with a 10-ml soap film flowmeter and stop watch. The flow rates of hydrogen and compressed air to the flame unit were monitored in the same manner. The readout was a Houston Instruments Model 5113-4 single pen recorder with a sensitivity of 1 mV full scale.

For most measurements the operating conditions were: injector temperature, 220 °C; column temperature, 210 °C; detector temperature, 300 °C; He flow, 55—65 ml min^{-1}; H_2 flow 20—25 ml min^{-1}; air flow, 300—350 ml min^{-1}. All determinations were made at least in triplicate.

Analytical studies

Working curves were obtained for each cyclopolymethylenetetrazole by analyzing a series of solutions prepared by the appropriate dilution of a stock solution.

The average detector response was determined in units of peak height and peak area. In the case of peak height, the response was determined from the product of the chart deflection and the attenuation factor. When peak area was used, the detector response was determined from the products of the chart deflection, the attenuation factor, and the peak width at half-height.

The retention times were measured with a stop watch as the period (in s) from the appearance of the leading edge of the solvent peak to the appearance of the peak maximum of the sample.

RESULTS AND DISCUSSION

Retention times and sensitivities

In these studies PMT was chosen as the standard, and all the retention times reported are relative to it. The retention time of PMT is 210 s at a carrier gas flow rate of 60 ml min^{-1} and an oven temperature of 210 °C. The relative retention times were determined for single component solutions of the cyclopolymethylenetetrazoles and some cyclopolymethylenetetrazole derivatives in chloroform. The values obtained are listed in Table 1. A plot of the relative retention times versus molecular weight of the compounds studied is shown in Fig. 1. Relative retention time increases exponentially with an increase in the length of the hydrocarbon chain, as has frequently been observed for members of other homologous series [16].

TABLE 1

Relative retention times and sensitivities for the cyclopolymethylenetetrazoles

Tetrazole	Relative retention time	Relative sensitivities	
		Peak height	Peak area
Trimethylenetetrazole	0.99	0.16	0.16
Tetramethylenetetrazole	1.03	0.71	0.78
Pentamethylenetetrazole	1.00	1.00	1.00
Hexamethylenetetrazole	1.20	1.05	1.28
Heptamethylenetetrazole	1.59	0.93	1.41
Octamethylenetetrazole	1.96	0.92	1.71
Nonamethylenetetrazole	2.41	0.93	1.91
Undecamethylenetetrazole	4.95	0.50	2.13
8-Tert-butylpentamethylenetetrazole	2.77	0.73	1.80
8-Sec-butylpentamethylenetetrazole	3.09	0.66	1.75

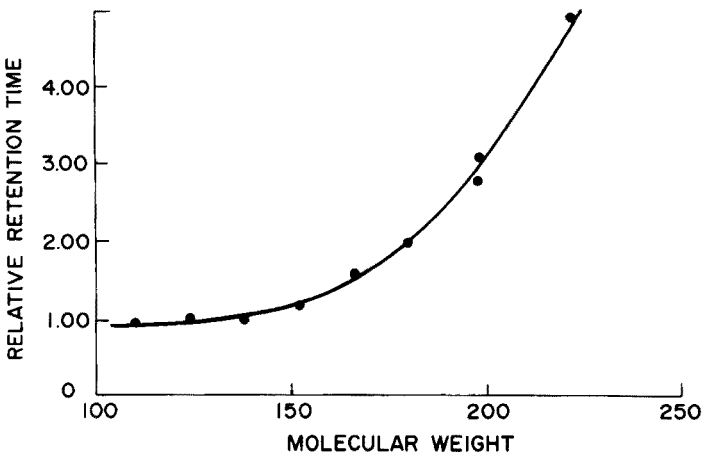

Fig. 1. Plot of the relative retention times vs. the molecular weight of the cyclopolymethyltetrazoles.

The chromatographic sensitivities of the cyclopolymethyltetrazoles were measured for single component solutions in chloroform. The values, listed in Table 1, were obtained by dividing the average detector response by the number of nanomoles of tetrazole in the sample. Since changes in the instrumental parameters can greatly affect the detector response, the sensitivities are also reported relative to that of PMT. However, the relative detector response can be measured either in terms of peak height or peak area. Since the concentration of the sample is proportional to the peak area, the values determined on this basis may be more significant. On examining the relative sensitivities based on peak area in Table 1, a near linear increase is observed as methylene groups are added to the hydrocarbon chain. The glaring exception is trimethylenetetrazole, which has a very low value (0.16). This

compound was investigated in more detail, and it was found to undergo thermal decomposition at 210 °C. By lowering the injection port temperature to 175 °C decomposition was reduced but not completely eliminated.

Resolution of a mixture of tetrazoles

The resolution of a mixture of cyclopolymethylenetetrazoles was tested with a solution containing 0.0138 g of C_3, C_4, C_5, C_6, C_7, C_8, C_9 and C_{11} derivatives in 10 ml of chloroform. As can be seen in Fig. 2, baseline resolution is achieved in most cases, and the only problem encountered is that of trimethylenetetrazole, tetramethylenetetrazole, and pentamethylenetetrazole are all eluted at the same time; the relative retention times of these compounds are very similar. Thus to separate these three tetrazoles, either a different column packing must be used or the column temperature must be reduced.

The other cyclopolymethylenetetrazoles are quite well resolved, however, and the relative retention times of the components in the mixture are identical to those measured for the single component solutions. Thus, the

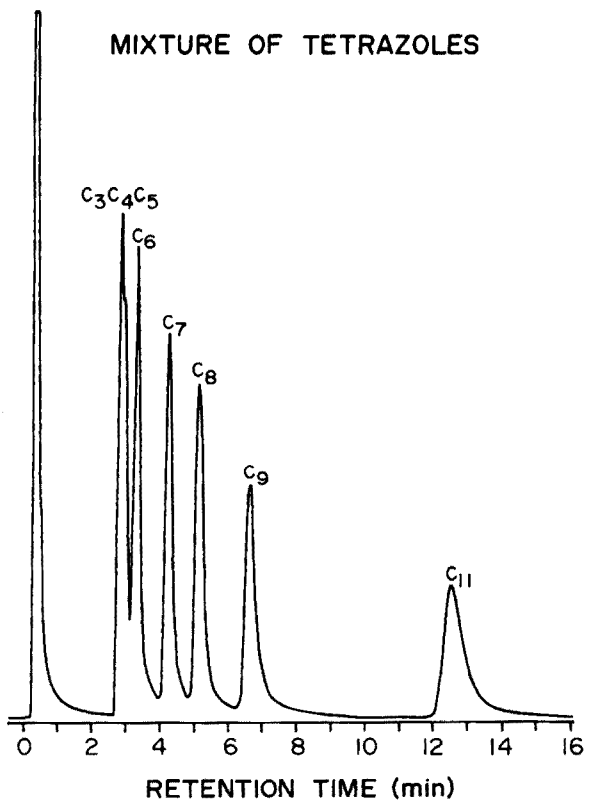

Fig. 2. Chromatogram of a mixture of cyclopolymethylenetetrazoles. Sample: 2.0 μl of C_3—C_{11} tetrazoles, each present at a concentration of 0.0138 g/10 ml of chloroform. Injector, 220 °C; column, 210 °C; detector, 300 °C; He, 60 ml min^{-1}; sensitivity, $128 \cdot 10^{-11}$ a.f.s.

retention times are not influenced by the presence of other species in solution and can be used to identify these cyclopolymethylenetetrazoles.

Working curves

To determine the cyclopolymethylenetetrazoles, it was necessary to construct working curves for each compound. For tetrazole solutions up to a concentration of 0.1 M, the peak shape was symmetric and reproducible, with no broadening at the higher concentrations. Thus, the calibration curves were prepared by plotting the average detector response (in units of peak height) versus the concentration of the tetrazole. An example is given in Fig. 3. The average detector response was monitored as a function of PMT concentration which ranged from 10^{-3} to 10^{-1} M; linear plots were obtained over this concentration range. Similar working curves were obtained for the other cyclopolymethylenetetrazoles in this range.

At concentrations greater than 0.1 M, however, the curves begin to deviate from linearity. This behaviour is illustrated for heptamethylenetetrazole (Fig. 4); as can be seen, at the higher concentrations the curve bends towards the concentration axis above about 0.2 M. Despite this deviation from linearity, these calibration plots are still useful for the determination of tetrazoles at these higher concentrations.

As a result of this investigation, a gas chromatographic method for the routine determination of cyclopolymethylenetetrazole at the 50—100 p.p.m. level was developed; concentrations of less than 10 p.p.m. can also be determined.

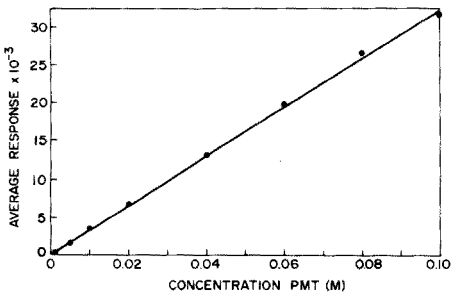

Fig. 3. Plot of average detector response vs. concentration pentamethylenetetrazole in aqueous solution.

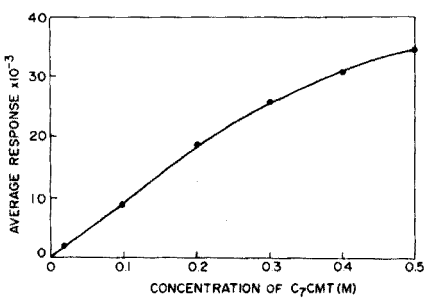

Fig. 4. Average detector response vs. concentration heptamethylenetetrazole in carbon tetrachloride solution.

REFERENCES

1 W. E. Stone, Pharmacology, 3 (1970) 367.
2 Merck Index, 8th edn., Rahway, New Jersey, 1968, p. 796.

3 A. Dister, J. Pharm. Belg., 3 (1948) 190.
4 A. I. Popov, Coord. Chem. Rev., 4 (1969) 463.
5 L. K. Sharp, J. Pharm. Pharmacol., 4 (1952) 52.
6 T. E. V. Horsley, Analyst (London), 71 (1946) 308.
7 E. Anderson, M. Fors and J. Lindgren, Acta Chem. Scand., 14 (1960) 1957.
8 A. I. Popov and J. C. Marshall, J. Inorg. Nucl. Chem., 19 (1961) 340.
9 A. I. Popov and J. C. Marshall, J. Inorg. Nucl. Chem., 24 (1962) 1667.
10 H. Kawamoto, Kumamoto Med. J., 16 (1962) 69.
11 F. Marcucci, M. L. Airdoli, E. Mussini, and S. Garattini, Eur. J. Pharmacol., 16 (1971) 219.
12 J. T. Stewart and J. L. Story, J. Pharm. Sci., 61 (1972) 1651.
13 C. Cardini, G. Cavazzutti, and V. Quercia, Boll. Chim. Farm., 109 (1970) 333.
14 F. M. D'Itri, Ph.D. Thesis, Michigan State University, East Lansing, Michigan, 1968.
15 R. G. Baum, Ph.D. Thesis, Michigan State University, East Lansing, Michigan, 1976.
16 H. M. McNair and E. J. Bonelli, Basic Gas Chromatography, Varian-Aerograph, Walnut Creek, Calif., 1969, p. 127.

Analytica Chimica Acta, 89 (1977) 347—354

CHLORINATION AND GAS-CHROMATOGRAPHIC DETERMINATION OF ANTIMONY IN OXIDES, SULFIDES, ORES AND ALLOYS

B. IATRIDIS and G. PARISSAKIS

Inorganic and Analytical Chemistry Department, National Technical University of Athens, Athens (Greece)

(Received 12th October 1976)

SUMMARY

The conditions for quantitative chlorination of antimony and subsequent determination of the volatile products by g.l.c. are described. The chlorinating agent, CCl_4, and the antimony-bearing compound are encapsulated in a small glass ampoule, and reaction takes place at 575°C in ca. 6 min. A crushing device is used to introduce the volatile chlorination products into the g.l.c. system; the $SbCl_5$ produced by chlorination is converted quantitatively to $SbCl_3$, which does not react with the column packing materials. The proposed method is rapid, simple, precise (relative error ±0.5%), selective and sensitive. Antimony, arsenic and tin can be determined simultaneously in some alloys.

The extensive use of antimony in a wide range of percentages in alloys greatly influences their hardness and mechanical properties. The highly purified metal finds application in the technology of semi-conductors, and its compounds are widely used.

This paper presents a method for the determination of antimony which involves simple manipulations, gives results within 10—40 min over a wide range of concentrations and does not depend on the character or amount of the antimony compound. The presence of other elements in the sample does not interfere.

This is achieved by a combination of chlorination reactions and a g.l.c. technique. Some quantitative information on the chlorination with CCl_4 of antimony oxides and sulfides — carried out in an open system — has been reported [1, 2].

Carbon tetrachloride was chosen as a chlorinating agent because good results have been obtained [3—5] and because it acts on oxygen- and sulfur-containing compounds, as well as on alloys. The chlorination reactions take place at elevated temperatures in a small glass capsule. Optimal conditions for the quantitative conversion of the antimony to antimony chlorides were deduced after a thorough study of the chlorination reaction as a function of temperature and time.

The volatile products are introduced into the g.l.c. system; the quantitative determination of antimony is based on the $SbCl_3$ peak, which is the only volatile antimony compound appearing in the chromatogram.

Chlorination of antimony compounds with CCl_4 gives a mixture of $SbCl_5$ and $SbCl_3$ in amounts according to the equilibrium $SbCl_5 \rightleftarrows SbCl_3 + Cl_2$ and the applied conditions [6]. The formation of $SbCl_3$ is greatly favoured at 140°C because of the thermal instability of antimony pentachloride.

Previous attempts [7, 8] to determine antimony by g.l.c. gave non-reproducible results because of the uncontrolled decomposition of $SbCl_5$ at the time of injection by syringe. This results in distortion of the $SbCl_3$ peak, and in the appearance of a number of peaks which arise from reaction between the $SbCl_5$ and the column-packing material.

By using a crushing device attached to the injection port of the gas chromatograph, contact of the antimony chlorides with the column packing material is delayed; quantitative conversion of $SbCl_5$ to $SbCl_3$ and Cl_2, which is greatly promoted by the temperature of the crushing chamber (250°C) results.

With the proposed procedure and the suggested chromatographic conditions, the determination of antimony in oxides, sulfides, ores, concentrates and alloys is successfully carried out. With appropriate column packing materials it is possible to achieve very rapid analysis (ca. 10 min) for antimony only, or the co-determination of antimony and arsenic, antimony, tin and arsenic, by increasing the analysis time to ca. 40 min. Under selected chromatographic conditions, the excess of CCl_4 and the by-products formed during the chlorination process e.g. $COCl_2$ and Cl_2 (which act as chlorinating agents) and the thermal decomposition products of CCl_4 do not interfere.

EXPERIMENTAL

Reagents and materials

Antimony pentachloride, obtained from commercial sources, was purified by isothermal distillation and kept under anhydrous conditions. Antimony trioxide and antimony trisulphide (Alpha Ventron; Beverly, U.S.A.) were of A.R.-grade.

Chemical analysis and x-ray diffraction measurements of an antimony concentrate, containing Sb_2S_3, As_2S_3, Sb_2O_3, As_2O_3, $AsSbS_3$, $Cu_3(SbAs)S_4$, $PbSb_2S_4$, FeAsS, $CuSbS_2$ etc. gave the following results: Sb = 60.50 ± 0.03%, As = 0.89 ± 0.01%, SiO_2 = 9.80 ± 0.05%, Fe = 1.16 ± 0.06%, Cu = 0.21 ± 0.04%, Pb = 0.03 ± 0.01%, Al = 1.06 ± 0.04%.

The alloys used had the following composition:

(1) Babbit alloy: Sb = 15.00 ± 0.03%, As = 1.00 ± 0.01%, Sn = 1.00 ± 0.05%, Cu = 0.50 ± 0.04%, Pb = Balance.

(2) Shot alloy: Sb = 3.32 ± 0.03%, As = 0.77 ± 0.01%, Pb = Balance.

(3) Antimony alloy: Sn = 83.50 ± 0.01%, Sb = 11.27 ± 0.03%, Pb = 5.23 ± 0.05%.

Sample preparation, chlorination technique and gas chromatographic determination

A borosilicate tube (4 cm long, 6 mm o.d., 4 mm i.d.) cleaned and dried at 130°C is used as a reaction tube. A weighed amount (see Tables 2, 3) of the sample in small pieces or in powdered form (400-600 mesh) dried at 140°C is introduced. The open end of the tube is closed with adhesive tape in an atmosphere of dry N_2. The lower part of the tube, which is held vertically, is placed in a container of dry ice and the CCl_4 (Table 1) is added. The tape is removed, the open end is sealed, and the capsule is placed in an oven at 575°C for the time (Table 1) necessary for quantitative chlorination of the sample. The capsule is then transferred to a crushing device [3] and the volatile compounds are swept into the g.c. system by the carrier gas.

Before any quantitative measurements, it is necessary to saturate the column with the compound or compounds to be determined, by injecting 10—15 μl of the compound into the g.c. system.

Calibration graphs can be obtained by two different techniques.

(a) Injection by syringe. Appropriate amounts of the substance to be analysed are injected into the g.c. system. Care must be taken to avoid deposition of hydrolysed material. It is essential for the syringe to be washed carefully after each use by immersing the lower part of the needle in acetone and dropping acetone simultaneously on the entrance of the plunger. The syringe is then washed with ether and dried under vacuum. One syringe treated thus, can be used for a large number of injections.

(b) By glass capsule. Different amounts of elemental antimony , introduced into capsules of the size and form used for the determinations, are treated with the appropriate amount of CCl_4, and then submitted to g.c. as described above.

TABLE 1

Chlorination and gas chromatographic conditions for various antimony samples

Sample	CCl_4 added (μl/mg of sample)	Chlorination time at 575°C (min)	Chromatographic conditions				Flow-rate carrier gas (ml min^{-1})
			Temperature (°C)				
			Crushing device	Inj. port	Column	Detector	
Sb_2O_3	1.0	6	250	230	150	200	10
Sb_2S_3	1.0	6	250	230	150	200	30
Antimony concentrate	1.0	15	250	230	150	200	30
Babbit alloy	0.5	6	250	230	150	200	30
Shot alloy	0.5	6	250	230	150	200	30
Antimony alloy	0.5	6	250	230	150	200	30

Crushing device

The crushing device [3] accepts capsules of various types and sizes, and can be used for gases, liquids, solids, and heterogeneous sample systems. It can also serve as a microreactor.

Apparatus

Silicone Gum Rubber UCC-W 982 10% (w/w) on Chromosorb [9] — for a fast analysis — and Silicone Oil DC 550 20% (w/w) on Celite 545 were used because of their inertness towards $SbCl_3$ and the very good resolution given for a number of chlorides [10].

A Hewlett-Packard 700 gas chromatograph equipped with TCD (Gow-Mac 4 tungsten filaments) was modified to keep the oven temperature constant within ±0.1 °C. Nitrogen, used as the carrier gas, was dried by passing through an activated molecular sieve and a P_2O_5 trap at 10—100 ml min^{-1}. The detector showed a satisfactory response toward $SbCl_3$, $SnCl_4$, $AsCl_3$, etc. From time to time, the detector was washed with acetone—hydrochloric acid solution to prevent alterations of response arising from the deposition on the filaments of hydrolysis or reaction products. To avoid reaction with highly corrosive chlorides, glass columns (4 mm i.d., 6 mm o.d., 183 cm long) were used.

These columns were packed under anhydrous conditions by inserting glass wool at one end of the column, applying vacuum to that end and adding the packing material from the other end. The column was vibrated under vacuum until the packing material did not settle any further.

Columns were conditioned overnight at the maximum permitted temperature. The effluent end of the column was not connected to the detector during the conditioning period. Column oven temperatures were kept at 30 °C below the maximum recommended temperature limit for the liquid phase. The chlorinating and chromatographic conditions are shown in Table 1.

RESULTS AND DISCUSSION

Figure 1 shows the results obtained when the antimony-bearing compound is an oxide. Two peaks are present. The first is the sum of chlorine, carbon dioxide, phosgene, and carbon tetrachloride. Chlorine results from the conversion of $SbCl_5$ to $SbCl_3$, which is completed within the crushing device and the injection port. The chromatogram, obtained with Silicone Gum Rubber UCC-W 982 10% (w/w) on Chromosorb, indicates the appearance of an antimony peak with a short retention time. Arsenic and antimony (or tin, arsenic, and antimony) cannot be therefore co-determined (cf. Figs. 3, 4); this constitutes a limitation of the method.

Figure 2 depicts the peaks obtained after the chlorination of antimony sulfide with carbon tetrachloride. A characteristic product is carbon disulfide. The third peak arises from an excess of the chlorinating agent.

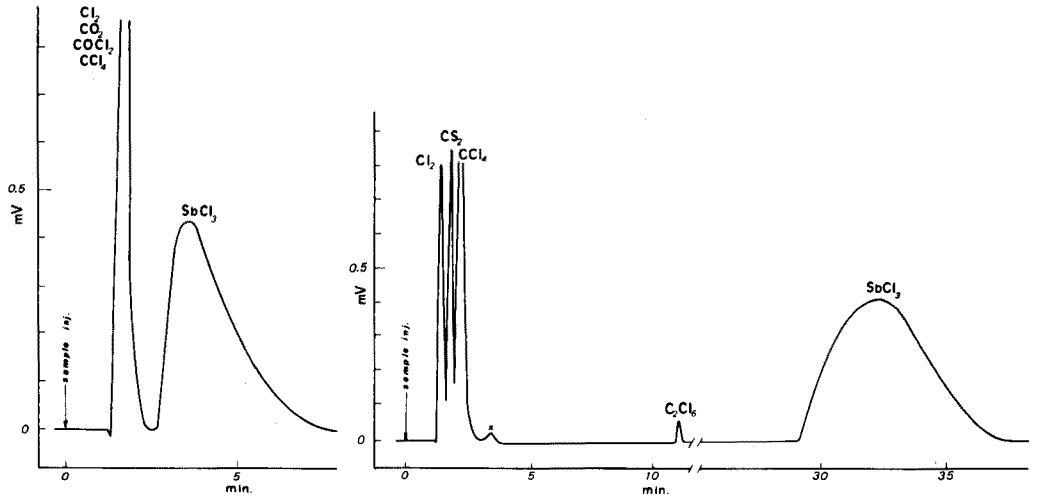

Fig. 1. Chromatogram of the reaction products given by antimony oxide with CCl_4 in a sealed glass capsule. Chromatographic conditions: glass column 183 cm long, 5 mm o.d., 4 mm i.d.; Silicone Gum Rubber UCC-W 982 15% (w/w) on Chromosorb; carrier gas flow rate, 10 ml N_2 min^{-1}; TCD (Gow-Mac 4 Tungsten filaments); bridge current 150 mA. Temperatures: capsule chamber 250°C; inj. port 230°C; column 150°C; detector 200°C.

Fig. 2. Chromatogram of the reaction products given by antimony sulfide with CCl_4 in a sealed glass capsule. Chromatographic conditions: column as for Fig. 1, packed with Silicone Oil DC 550 20% (w/w) on Celite 545. Carrier gas flow rate 30 ml N_2 min^{-1}. Detector and temperatures as in Fig. 1.

Under increased detector sensitivity a small fourth peak (unidentified) appears. The fifth peak arises from hexachloroethane, a thermal decomposition product of CCl_4. Because of the long retention time of $SbBl_3$ (the final peak), other more volatile chlorides with shorter retention times, e.g. tin and arsenic, may appear earlier. Some quantitative results for antimony(III) oxide and sulfide are given in Table 2.

TABLE 2

Determination of antimony(III) oxide and sulfide

Antimony(III) oxide				Antimony(III) sulfide			
Taken (mg)	Found (mg)	Error	% Error	Taken (mg)	Found (mg)	Error	% Error
4.09	4.15	+0.06	+1.46	10.18	10.10	−0.08	−0.80
3.83	3.76	−0.07	−1.83	10.04	10.06	+0.02	+0.20
5.20	5.26	+0.06	+1.14	9.88	9.75	−0.13	−1.32
2.88	2.91	+0.03	+1.04	10.98	10.89	−0.09	−0.80
4.41	4.40	−0.01	−0.20	12.04	12.15	+0.11	+0.91
5.86	5.78	−0.08	+1.36	11.42	11.27	−0.15	−1.31
		Av:	1.08			Av:	0.52
		s_r:	1.30			s_r:	0.88

Figure 3 shows the reaction products of antimony concentrate with CCl_4. In this sample oxygen- and sulfur-containing compounds, and arsenic are present. The possibility of determining the arsenic trichloride peak is an advantage of the method.

The possibility of a simultaneous determination of tin is shown in Fig. 4, obtained for the volatile products of the chlorination of Babbit alloy with

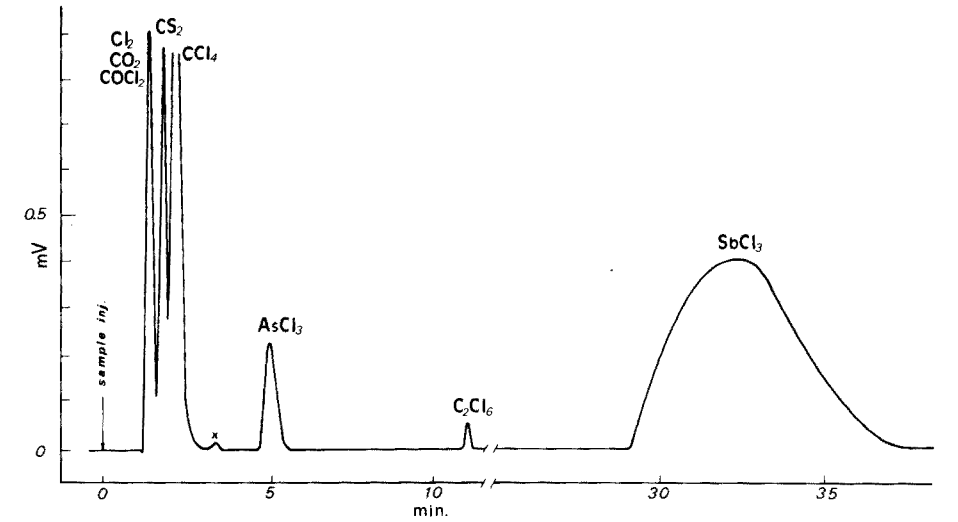

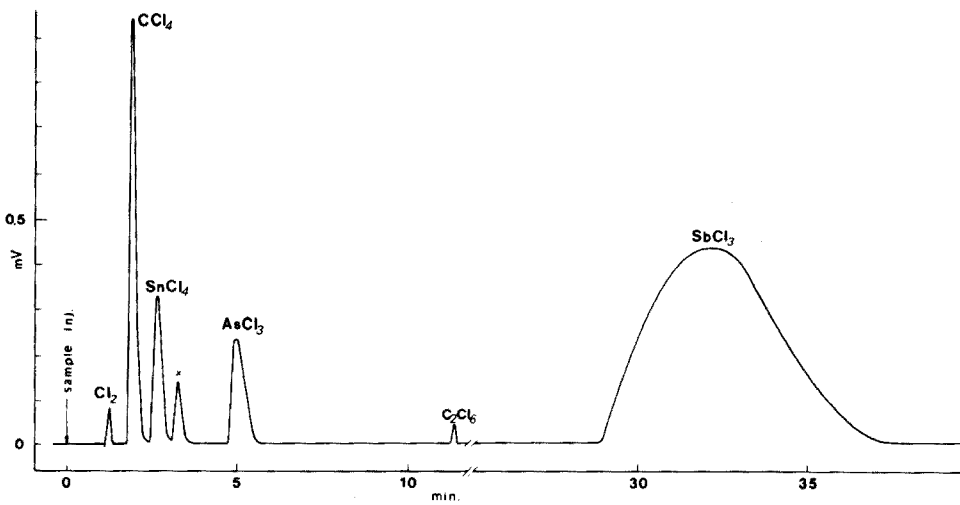

Fig. 3. Chromatogram of the reaction products of antimony concentrate with CCl_4 in a sealed glass capsule. Chromatographic conditions: identical to Fig. 2.

Fig. 4. Chromatogram of the reaction products of antimony-bearing alloys with CCl_4 in a sealed glass capsule. Chromatographic conditions identical to Fig. 2.

carbon tetrachloride. Chlorine and carbon are the main by-products of the reaction of alloys with CCl_4. The by-products from thermal decompositions of CCl_4 are produced in minute quantities, only hexachloroethane gives a small peak under increased sensitivity.

The chromatogram for shot alloy was the same as that in Fig. 4, but without the $SnCl_4$ peak. That for antimony alloy was also the same as Fig. 4 (without the $AsCl_3$ peak). Because of the large amount of tin present, and the chromatographic conditions applied, a quantitative separation between the CCl_4 and $SnCl_4$ peaks was not always possible.

In all these chromatograms, carbon dioxide, phosgene and chlorine were identified by infrared spectra for fractions collected at the chromatographic outlet. CCl_4, CS_2, $SnCl_4$ and $AsCl_3$ were identified by a comparison of their retention times with those of authentic samples. The $SbCl_3$ peak was identified by dissolving $SbCl_3$ in CCl_4 and taking a chromatogram of the mixture.

Table 3 shows the results obtained for antimony (and arsenic and tin, where appropriate) in antimony concentrate and several alloys.

The use of a TCD detector, although there are more selective detectors for chlorides, is adequate even for the relatively small samples used; good sensitivity and resistance over long periods towards these very corrosive chloride compounds are shown. Throughout all determinations the detector sensitivity was 250—1500 mV ml mg^{-1}; the calibration graphs were linear within the range 1.0—20 mg of antimony. The baseline drift was about 0.01 mV for 1-mV full scale deflection of the recorder over a great number of determinations.

The proposed method has several advantages over wet chemical methods of analysis. It is much faster; at least several samples per hour can be analysed. As only two simple steps — chlorination in the capsule and subsequent g.c. determination — are involved, the method is simple. Moreover, the method is not concentration-dependent; it gives quantitative results over the range

TABLE 3

Determination of antimony, arsenic and tin in ores and alloys

Sample	Weight (mg)	No. of detns.	Element	%, w/w			Error
				Present	Found	s	
Antimony concentrate	13.0—30.0	6	Sb	60.50	60.72	±1.01	+0.20
			As	0.89	0.88	±0.05	—0.01
Babbit alloy	10.0—20.0	7	Sb	15.00	14.90	±0.80	—0.10
			As	1.00	0.98	±0.02	—0.02
			Sn	1.00	0.99	±0.06	—0.01
Shot alloy	15.0—20.0	8	Sb	3.45	3.50	±0.70	+0.50
			As	0.77	0.74	±0.03	—0.03
Antimony alloy	20.0—35.0	8	Sb	83.50	83.80	±0.90	+0.30

1—99% of antimony. As little as 0.03% of antimony can be detected in the amount of sample used.

The presence of other elements, e.g. cobalt, nickel, iron, lead, tin, and arsenic, in the antimony-bearing compounds affects the accuracy of the method less than is the case with other methods. The elimination of the analytical uncertainties which result from extensive sample preparation is an additional advantage, and the variety of elements detected make this method attractive for multi-element analysis.

The authors thank the General Cement Company (A.G.E.T.) Athens, for a research grant. They also are indebted to the metallurgical companies which kindly supplied samples.

REFERENCES

1 P. Camboulives, C.R. Acad. Sci., Paris, 150 (1910) 175.
2 M. H. Khundkar, S. S. M. A. Khorasani and K. R. Ahmad, Pak. J. Sci. Ind. Res., 10 (1967) 155.
3 G. Parissakis and B. Iatridis, J. Chromatogr. Sci., 12 (1974) 734.
4 B. Iatridis, Doctoral dissertation, National Technical University of Athens, 1974.
5 B. Iatridis and G. Parissakis, J. Chromatogr., 122 (1976) 505.
6 Von. H. Oppermann, Z. Anorg. Allg. Chem., 356 (1967) 1.
7 S. I. Sie, J. P. A. Bleumer and G. W. A. Rijnders, Sep. Sci., 2 (1967) 645.
8 G. Parissakis, D. Vranti-Piscou and J. Kontoyannakos, J. Chromatogr., 52 (1970) 461.
9 Ch. Markantonatou, Internal report NTU No. 65 (1976).
10 G. Parissakis, D. Vtanti-Piscou and J. Kontoyannakos, Chromatographia, 3 (1970) 541.

Analytica Chimica Acta, 89 (1977) 355—361

SPECTROPHOTOMETRIC STUDY OF COVERAGE AND ACID—BASE EQUILIBRIUM OF A CHEMICALLY BONDED BASE

L. T. MIMMS, M. A. McKNIGHT and ROYCE W. MURRAY

Kenan Laboratories of Chemistry, University of North Carolina, Chapel Hill, North Carolina 27514 (U.S.A.)

(Received 17th August 1976)

SUMMARY

An aniline azo dye is immobilized on glass slides by reacting an organosilane reagent with the glass surface. The immobilized dye absorption spectral characteristics closely resemble those of the analogous solution form of the dye. The coverage of the immobilized dye, $1.1 \cdot 10^{-10}$ mol cm^{-2}, is consistent with simple monolayer coverage. The immobilized dye is a weaker base than the soluble form by an equilibrium constant factor of about 10, consistent with an electrostatic effect.

The commercially available organosilane, γ-aminopropyltriethoxysilane, reacts with silica, binding the propylamine moiety to the glass surface [1, 2]:

$$\text{Si} \dashv \text{OH} + (\text{EtO})_3\text{Si}(\text{CH}_2)_3\text{NH}_2 \rightarrow \text{Si} \dashv \text{O}\underset{|}{\text{Si}}(\text{CH}_2)_3\text{NH}_2 \qquad (1)$$

Such a chemically modified surface can be further derivatized, through the amine function, to synthesize surfaces bearing a variety of analytically-useful immobilized reagents. Weetall has recently reviewed the applications of reaction (1) to Controlled Pore Glass in preparing immobilized enzymes [3] and column materials for affinity chromatography [4]. Metal scavenging based on immobilized 8-hydroxyquinoline (on Controlled Pore Glass [5]) and dithiocarbamate (on silica gel [6] and glass wool [7]) ligands has been described. Other amine-functionalized organosilanes are also available for use in the surface modification reaction (1).

In derivatization reactions on immobilized propylamine, and in metal coordination studies with the mentioned ligands, the chemical reactivity of the immobilized reagents has thus far been reported as being normal qualitatively. A more detailed, quantitative scrutiny of the chemistry of the reagent on surfaces is desirable. No studies appear to have been conducted on organosilane-modified silica surfaces (or on any other form of chemically modified surface materials) which quantitatively portray, for example, dissociative equilibrium properties of an immobilized chemical.

The purpose of the present investigation was to demonstrate that optical absorption spectrophotometry can be employed to characterize quantitatively acid—base equilibria between contacting solution and immobilized reagents on silica surfaces. The necessary ingredients for the study were (i) use of flat surfaces, rather than powder or beads, to avoid optical scattering,

(ii) functionalization of the surface so that an immobilized reagent base site interacts with a strong chromophore group, and (iii) that a solution of the surface reagent could be prepared for comparative study.

A convenient chemical system for this purpose was described by Harper [8]; starting with reaction (1) he immobilized a variety of pH indicator reagents on porous glass materials. The surface synthesis of the selected indicator is

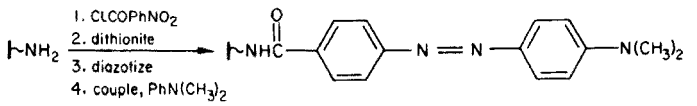

(2)

The surface acid—base equilibrium of the immobilized indicator dye (ID) is

$$\underset{\text{(red)}}{HID^+} \overset{K_a^s}{\rightleftharpoons} H^+ + \underset{\text{(orange)}}{ID} \qquad (3)$$

and the site of protonation is presumed to be the aniline function. The corresponding free indicator dye (FD) is synthesized starting with n-propylamine as substrate in reaction (2).

An additional feature of the optical spectrophotometric comparison of ID and FD is estimation of the absolute surface population (mol cm^{-2}) of the immobilized reagent ID.

EXPERIMENTAL

Preparation of free indicator dye

After the exothermic reaction of 20 ml of n-propylamine with 3 g of *p*-nitrobenzoyl chloride subsides, warm the mixture for a few min and pour into cold water; collect the waxy white benzamide and wash. Reduction is accomplished by addition to 2 g of sodium dithionite in 100 ml of cold (slightly basic) water. After warming for 45 min, extract successively with chloroform and ether in the presence of Na_2CO_3. Dry the combined organic extracts with $MgSO_4$, evaporate to several ml of yellow oil, acidify with HCl, and add to cold acetone. Collect the white precipitate, and form the diazonium salt in 50 ml of ice water containing 0.1 g $NaNO_2$ to which 5 ml of 5 M HCl is added dropwise. Add 5 ml of *N,N*-dimethylaniline and 2 ml of acetic acid, and after 10 min adjust the pH to ca. 9; collect the orange precipitate and wash thoroughly with water. Recrystallize from hot 2 M HCl or 1 : 1 : 1 hexane/chloroform/benzene; the latter is more satisfactory. Found: 69.4%C, 6.9%H, 17.8%N; calcd: 69.7%C, 7.0%H, 18.0%N.

Preparation of immobilized indicator dye

The procedure differed slightly from that of Weetall [1, 2] and Harper [8]. Glass (2.5 × 1 cm) rectangles, cut from Gold Seal microscope slides, were degreased in boiling heptane overnight, rinsed with acetone, and oven-dried

at 350°C. Reaction (1) was conducted by covering the glass strips with silane in a sealed tube at 90°C overnight. After opening the tube, the slides were washed thoroughly with benzene, ethanol, and water. Amidization was achieved with 0.5 g *p*-nitrobenzoyl chloride in hot 5% triethylamine/chloroform, and after thorough washing, reduction was carried out in 3.0 g of sodium dithionite in 100 ml of water (first cold, then heated gently for 45 min). X-ray photoelectron spectroscopy examination after amidization revealed nitro and amide N 1s bands of equal intensity, separated by ca. 7 eV; the nitro band disappeared after reduction. The strips were placed in 25 ml of ice-cold 2 M HCl containing 0.2 g of $NaNO_2$ for 30 min, washed with cold water, and placed immediately in *N,N*-dimethylaniline for 30 min. The colored slides were washed thoroughly with benzene, ethanol, and water. The glass was visibly (very faintly) orange in basic and neutral solution, and red in acid.

Reactions were also conducted on microscope glass frosted by exposure to HF gas, on glass microbeads, on SnO_2 powder, and on thin films of SnO_2 on glass; visually, the products were identical in color.

Spectrophotometry of immobilized indicator dye

The optical (transmission) absorbance of one glass slide is quite small, but acceptable levels of absorbance for a Unicam SP1800 spectrometer were obtained with a stack of seven (7) strips (14 surfaces bearing the immobilized dye). The seven strips in a 1-cm cuvette were covered with solvent or solution of interest, great care being taken to see that each side was bathed thoroughly with solvent and that a thin solution film existed between adjacent strips. The spectrophotometer reference beam was balanced with seven blank strips to produce an acceptable baseline above about 375 nm.

Spectra of immobilized dye in limiting base and acid forms were obtained (by addition of an excess of strong acid and base) in DMSO solvent, in aqueous CH_3CN, and in water. In the latter solvents, spectra were also taken at a series of pH values of the bathing solution.

Spectra of standard solutions of free indicator dye in acid and base forms were obtained in DMSO and in aqueous CH_3CN, and pH profiles were obtained in the latter. A satisfactory pH profile of FD spectra could not be taken in water because the solubility of the free FD base form is low.

RESULTS AND DISCUSSION

Spectral comparison of ID and FD

Spectral parameters for limiting acidic and basic forms of free (FD) and immobilized (ID) dye in various solvents are summarized in Table 1. The absorbance spectra of ID and FD are quite similar. The band maximum for the acidic immobilized form (HID^+) is shifted by about 15 nm to higher energy but with an essentially unchanged spectral shape. For the base form λ_{base}^{max} appears to be the same for ID and FD. Careful comparison of band shapes for the base form was not possible because the reproducibility of

TABLE 1

Spectral characteristics of free and immobilized dye

Sample	Solvent	λ^{max}_{acid} nm	λ^{max}_{base} nm	λ_{Isosb}	ϵ_A/ϵ_B	ϵ_A ($\cdot 10^4$ l mol^{-1} cm^{-1})	pK_a
FD	DMSO	524	430	—	1.18 ± 0.03	3.18 ± 0.12	—
ID	DMSO	505—510	425—435	470	1.37 ± 0.14	—	—
FD	H_2O	514	—[a]	—	—	2.76 ± 0.09	—
ID[b]	H_2O	499	425	455	1.59 ± 0.23	—	1.1—1.2
FD[b]	H_2O/CH_3CN(1 : 1.4)	508	448	465	1.62	3.15	2.27
FD	H_2O/CH_3CN(1 : 2.7)	508	430	462	1.69	2.26	1.65
FD	H_2O/CH_3CN(1 : 4)	510	425	460	—	—	1.70
ID	H_2O/CH_3CN(1 : 1)	∿500	435	∿455	—[c]	—	1.1—1.2

[a] FD base form insoluble. [b] Data of Fig. 1. [c] Not calculated since background spectrum not taken. [d] After specimens washed with solvent for ∿1 week.

the spectral (glass/glass) background was poor below 400 nm. Comparison of molar absorptivities (ϵ) of ID and FD is also not possible, since the surface population of ID is not known a priori. Relative absorptivities of acidic and basic forms (ϵ_A/ϵ_B) are obtained, however. Table 1 shows that, in a given solvent, the values for ϵ_A/ϵ_B for ID and FD (compare DMSO(ID)—DMSO(FD) data, and H_2O(ID)—H_2O/CH_3CN(FD) data) are the same within 15%.

The spectral similarity of the immobilized reagent dye to that of a known solution molecule supports the notion that reaction sequence (2) proceeds as indicated, i.e. the predominant chromophore on the glass surface is identical to the conventionally synthesized free dye FD. (The spectral observations do not, of course, rule out the possibility of surface synthesis side-reactions leading to non-colored surface residues.)

Determination of surface coverage of ID

The results in Table 1 make it reasonable to assume that the absolute values of the molar absorptivity of ID and FD are equal. This permits an evaluation of the surface coverage of the immobilized dye ID by means of the surface form of Beer's Law, $A = 10^3\,\epsilon\Gamma$, where Γ is the coverage in mol cm^{-2}. Table 2 gives the data for eight different preparations of ID specimens. Over all eight samples (56 strips) the average coverage is 1.12 (±0.14) $\cdot 10^{-10}$ mol cm^{-2}.

Considering the fact that the ID specimens were prepared in different experiments spanning several weeks, and result from a five reaction step surface synthesis, the observed consistency in surface coverage Γ by ID on the flat glass is somewhat remarkable. Careful pretreatment of the glass substrate is certainly important; glass specimens that are not degreased or thermally activated are unreactive. More importantly, the results indicate that extensive siloxane polymer formation or deposition in reaction (1) has been

avoided. The incorporation of additional amine functions via polymerization would lead both to varying Γ and much higher observed chromophoric coverages. Numerous surface silanization procedures (for glass and chromatographic substrates) employ reaction conditions under which water is not excluded rigorously, or may even be used as reaction solvent. Such procedures are conducive to hydrolysis of the organosilane reagent and the formation of either precipitated or surface-bonded polymer phase formation as opposed to the formation of a monolayer of bonded molecules. This laboratory's experience [9, 10] in chemical modifications of electrodes made of SnO_2, which is a more reactive substrate than glass, and ESCA observations, have given convincing evidence that polymer formation can be avoided, or at least minimized, by the rigorous exclusion of water from the reaction mixture (and through the stage where specimens have been thoroughly rinsed of excess organosilane reagent). This strategy was used in the present study on glass.

A molecular model of the immobilized dye molecule was examined to estimate its geometrical surface area requirements. Extension of the chain normal to the surface leads to a molecular area of approximately 50 $Å^2$, which translates to a limiting monolayer coverage of $3.3 \cdot 10^{-10}$ mol cm^{-2}. Folding of the molecule so that the azobenzene system lies parallel to the surface increases the area requirement to about 120 $Å^2$, or $1.4 \cdot 10^{-10}$ mol cm^{-2}. These estimates, entirely consistent with the view that surface polymer structures are absent, also suggest, since both are higher than $\Gamma_{measured}$, that some steric disorder is possible in the bonded monolayer (e.g., the molecules are not close-packed). A disordered, as opposed to structured close-packed, layer is consistent with the observed overall spectral similarities to the FD form.

Room temperature washing or soaking of ID samples in water, benzene, ethanol, or DMSO for a few hours has no effect on the measured ID absorbance. Exposure to boiling benzene reduces the observed absorbance (Table 2); exposure overnight leads to complete loss of color. This is interpreted as reflecting a thermal instability of the azo dye assembly. Exposure of ID samples to strong base leads to immediate discoloration.

pK_a of FD and ID

The spectral similarities of ID and FD, and their presumed structural similarity, enable a meaningful direct comparison of the acid dissociation constants of HFD^+ and HID^+ to be made. Figure 1 shows spectra of ID at various bathing aqueous solution pH values, and the profile of absorbance vs. pH obtained from measurements on the acid and base bands. A clean isosbestic point is observed. The value of pK_a^s (eqn. 3), taken at the midpoint of the absorbance—pH inflection, is 1.1. This value was reproduced, in a second spectral series, for samples soaked previously with the aqueous CH_3CN solvent for 1 week (Table 1). This small value of pK indicates that the immobilized dimethylaniline function is a very weak base.

A direct determination of the pK_a for HFD^+ in water as solvent proved to be impossible because of the low solubility of the base form. Admixture

TABLE 2

Surface coverage of immobilized dye

Sample[a]	Solvent	Abs. acid	Abs. base	Av. Γ^d ($\cdot 10^{-10}$ mol cm
1	DMSO	0.044, 0.303[b]	0.034, 0.030[b]	0.95, 0.74[b]
2		0.058, 0.039[b], 0.022[c]	0.037, 0.030[b], 0.020[c]	1.16, 0.84[b], 0.
3		0.050	0.034	1.01
4		0.044	0.044	1.03
5		0.066	0.042	1.30
6		0.051	0.043	1.14
7	H_2O	0.062	0.034	1.50
8		0.030	0.022	0.84

[a]Each sample represents a different set of seven glass strips bearing ID. [b]Samples boiled in benzene for 15 min. [c]Samples boiled in benzene for 1 h. [d]In DMSO, $A = 10^3 \epsilon \Gamma$ where $\epsilon_A = 3.18 \cdot 10^4$, $\epsilon_B = 2.69 \cdot 10^4$. In H_2O, $A = 10^3 \epsilon \Gamma$ where $\epsilon_A = 2.76 \cdot 10^4$, $\epsilon_B = 1.70 \cdot 10^4$.

of acetonitrile allowed the collection of conventional pH—absorbance profiles (an example is given in Fig. 1); the pK_a increases with decreasing proportion of acetonitrile. At the lowest usable proportion of acetonitrile, the pK_a of HFD^+ exceeds that (pK_a^s) of HID^+ by ca. 1.1 unit.

That the immobilized dye should be a weaker base than its solution analog is expected qualitatively. Complete protonation of the ensemble of surface aniline functions involves considerable repulsive effects as the cationic surface charge rises. In ionizable polyelectrolytes in solution, the effects of charge density in the polymer chain volume produce [11] significant alterations in the pK of functional groups (from their normal monomer values). These alterations are mediated by the counter-ion (or salt) concentration in the polyelectrolyte solution.

The estimated length of the immobilized dye molecule in its fully extended form, and thus the thickness of the bonded monolayer, is about 30 Å.

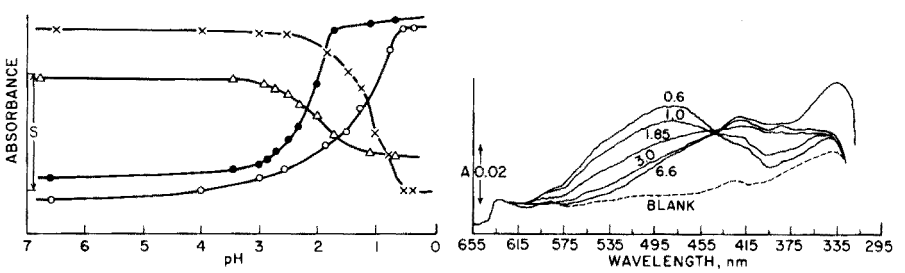

Fig. 1. Right: Spectra of immobilized indicator dye as a function of pH in water. Left: Absorbance as a function of pH for immobilized indicator dye in water (sensitivity $S = 0.01$ absorbance units, —○— at 490 nm, —×— at 425 nm) and free indicator dye in 1 : 1.4 water/CH_3CN ($S = 0.2$, —●— at 510 nm, —△— at 440 nm).

Combining this dimension with the coverage value of Table 2 yields a surface "concentration" of about 0.4 M. In the fully protonated HID^+ form, this charge concentration probably promotes a chain orientation or ordering which minimizes neighboring repulsive interactions, similar to the shape change in a polyelectrolyte coil which is thought to occur on ionization of chain groups [11]. Were it not for the fact that the bathing solution "salt" population is high at the low pH values involved in forming HID^+ ($> 10^{-2}$ M concentrations of strong acid, HCl), with the consequent mediating effect on ΔpK, an even larger difference in acidity constant from FD might have resulted.

Alterations in pK caused by electrostatic-repulsive effects also, in principle, cause elongation of the pH range over which protonation occurs [11]. The data for the absorbance—pH profile shape of Fig. 1 are thought to be insufficiently precise to assess this factor, however.

This study has shown that surface-bonded monolayers of reasonably strong chromophores can be examined from a coverage and equilibrium viewpoint with relatively unsophisticated spectrophotometric equipment. Two additional consequences of the coverage results should also be mentioned. To the extent that Γ is optically determinable, calibrated monolayer standards for absolute intensity ESCA measurements become available. These standards, being monolayers, do not in principle involve an escape depth parameter, which is a useful circumstance. Secondly, the disorder possibilities suggested by the comparisons between Γ_{models} and $\Gamma_{measured}$ indicate that steric constraints on the utility of organosilane linkages [9] between redox functions and electrodes may not be severe.

This research has been facilitated by National Science Foundation Grants MPS-73-08758 and MPS-75-07863. L.T.M. was an N.S.F. Undergraduate Research Participant at U.N.C., Summer 1975.

REFERENCES

1 H. H. Weetall, Biochim. Biophys. Acta, 212 (1970) 7.
2 H. H. Weetall, Res. Develop., 22 (12) (1971) 18.
3 H. H. Weetall, Enzymes Immobilized on Inorganic Supports, in Immobilized Biochemicals and Affinity Chromatography, R. B. Dunlap, [Ed.], Plenum.
4 H. H. Weetall, Affinity Chromatography, in Sep. Purif. Methods, 2 (1973) 199.
5 K. F. Sugawara, H. H. Weetall and G. D. Schucker, Anal. Chem., 46 (1974) 489.
6 D. E. Leyden and G. H. Luttrell, Anal. Chem., 47 (1975) 1612.
7 D. M. Hercules, L. E. Cox, S. Onisick, G. D. Nichols and J. C. Carver, Anal. Chem., 45 (1973) 1973.
8 G. B. Harper, Anal. Chem., 47 (1975) 348.
9 P. R. Moses, L. Wier and R. W. Murray, Anal. Chem., 47 (1975) 1882.
10 P. R. Moses and L. Wier, Univ. North Carolina, 1975, unpublished results.
11 F. Oosawa, Polyelectrolytes, M. Dekker, N.Y., 1971, p. 73.

Analytica Chimica Acta, 89 (1977) 363—368

IMPROVED SENSITIVITY FOR BORON AND SILICON IN FLAME SPECTROMETRY BY A FLUORIDE EVOLUTION TECHNIQUE

J. F. CHAPMAN and L. S. DALE

Chemical Technology Division, Australian Atomic Energy Commission, Research Establishment, Lucas Heights, New South Wales, 2232 (Australia)

(Received 16th September, 1976)

SUMMARY

Improved sensitivity can be achieved for boron and silicon by the introduction of their volatile fluorides into chemical combustion flames. The fluorides are produced by reaction with copper hydroxyfluoride. The apparatus consists of a graphite crucible, a resistance furnace and a water jet pump modified to operate with air. The feasibility of this technique for the determination of boron by flame emission, and silicon by atomic absorption, has been demonstrated for solutions and solids.

Boron and silicon form refractory oxides in chemical combustion flames. This reduces the sensitivity of their resonance lines in flame spectrometry by restricting the free atom population. High-temperature sources such as the direct-current plasma jet [1], the high-frequency induction-coupled plasma [2] or the nitrous oxide—acetylene flame [3] are required to produce useful analytical signals for these elements.

In flame spectrometry, improved detection limits for many elements may be achieved by using concentration procedures such as solvent extraction [4]. Another way is to isolate a volatile compound of the element to be analyzed from a volume of sample. An example of this is the well known hydride evolution technique for the determination of arsenic, selenium and other hydride-forming elements by atomic absorption spectrometry [5]. The application of an evolution technique to boron has been investigated by Belcher et al. [6] who produced the volatile methyl borate by distillation from a mixture of methanol and sulphuric acid. Molecular emission cavity analysis (MECA) was used to obtain emission signals from the BO_2 band system in a nitrogen—hydrogen flame. The methyl borate was carried into the flame in the nitrogen stream.

The BO_2 band emission in chemical combustion flames gives high sensitivity as indicated in the above work. However, similar procedures are apparently not applicable to silicon because of the low intensities of SiO bands in the region 241.4—258.7 nm.

A possible evolution technique applicable to boron and silicon is the production of their volatile fluorides. Previous work [7] has shown that boron and silicon can be converted to their fluorides by reaction with copper

hydroxyfluoride (CuOHF). The evolution of the volatile fluorides from solids or dried solutions mixed with the compound is very rapid when the temperature reaches 345° C, which is the decomposition temperature of copper hydroxyfluoride.

Introduction of the volatile reaction products into flames was accomplished with an apparatus based on a water jet pump which was modified to operate with air. The feasibility of this technique for the determination of boron and silicon was investigated by flame emission and atomic absorption spectrometry.

EXPERIMENTAL

The apparatus is shown schematically in Fig. 1. By reducing the nozzle diameter of the water jet pump (Edwards demountable type) to 0.8 mm, a suitable flow of air was maintained through the holes in the crucible, allowing the evolved gases to be drawn through the line to the flame. The crucibles (Fig. 2) were manufactured from Ringsdorff RWIV spectroscopic grade graphite. A small furnace was made by winding 27 gauge Kanthal A resistance wire (15.4 Ω m^{-1}) around a quartz tube and coating with asbestos. The centre core was machined from graphite and contained a "well" into which the crucibles fitted. The furnace was operated at 800° C and the crucibles were heated for 30 s during which time the peak was recorded.

Quantities of copper hydroxyfluoride (50—100 mg) were weighed into the crucibles and solutions were pipetted on top of the powder; the contents of the crucibles were then oven-dried at 105° C. Solid samples were mixed with the compound (usually 20%) and weighed into the crucibles. For standardization, it was found convenient to take various weights of a master standard of 200 $\mu g\ g^{-1}$ each of boron and silicon in copper hydroxyfluoride. This was prepared by evaporating appropriate volumes of boron and silicon standard solutions onto a bed of copper hydroxyfluoride and homogenizing the mixture on a mechanical mixer. The copper hydroxyfluoride was obtained from Spex Industries Inc., N.J., U.S.A. Solutions of boron and silicon were prepared, respectively, from A.R.-grade boric acid and sodium silicate.

Flame emission measurements were made with a 0.5-m Ebert plane grating monochromator (Jarrell-Ash Co., U.S.A.) fitted with an EMI 6256B photomultiplier and Keithley 414S picoammeter. The burner from a Unicam SP900 flame spectrophotometer was used. The stoichiometry and height of observation for the air—acetylene flame were adjusted to give maximum intensity of the BO_2 emission at 547.6 nm. The apparatus used for producing the fluorides was connected to the air line of the burner.

For the atomic absorption measurements, a Varian-Techtron Model AA5 atomic absorption spectrometer was used. A nitrous oxide—acetylene flame was supported on a 5-cm high-temperature slot burner. Since the apparatus was connected to the auxiliary air line of the spray chamber, the absorption source was, therefore, an air-diluted nitrous oxide—acetylene flame. Emission and absorption signals were recorded on a 0—10 mV strip chart recorder with a chart speed of 15 mm min^{-1}.

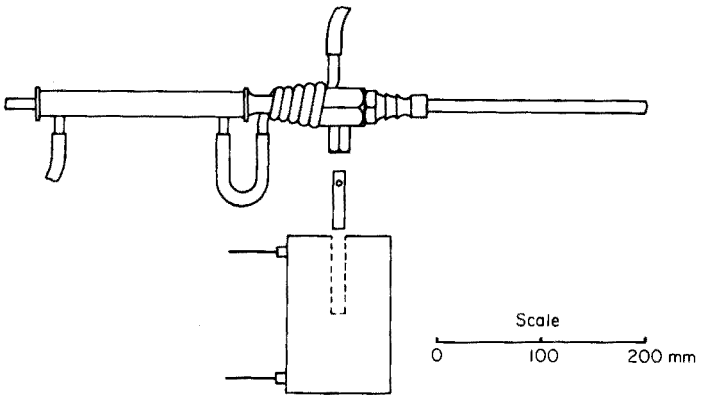

Fig. 1. Schematic diagram of apparatus for production of fluorides.

RESULTS

Flame emission

When concentrated solutions of boron and silicon were sprayed into both air—acetylene and nitrous oxide—acetylene flames, the only emissions of useful analytical sensitivity were those obtained from the BO_2 band system. Boron and silicon atomic lines at 249.8 nm and 251.6 nm could not be detected. Band emission from SiO in the region 241.4—258.7 nm also could not be detected. Band spectra from BO_2 with maxima at 518, 548, 579 and 603 nm were measured in both flames, and the emission at 548 nm in the air—acetylene flame was found to be the most sensitive. The maximum intensity occurred 2 cm above the blue cones. All results for boron were obtained under these conditions.

Figure 3 shows a typical calibration for boron in the range 0—25 μg obtained with various weights of the master CuOHF standard. The curvature is probably due to the response characteristics of the system. Figure 4 shows the reproducibility obtained with replicate runs of a 1-μg boron standard. The relative standard deviation was 3.9% and the absolute sensitivity (based on twice the standard deviation of the background noise level) was calculated

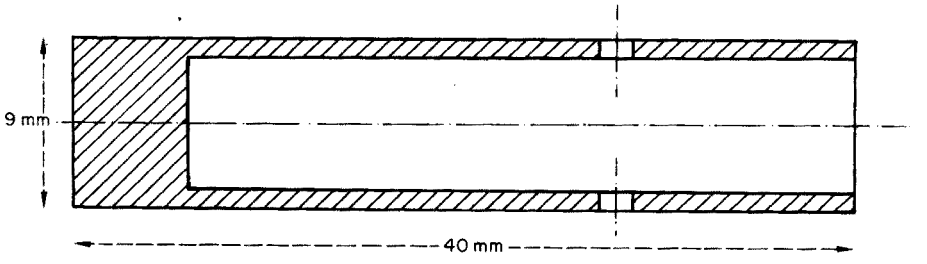

Fig. 2. Details of crucible.

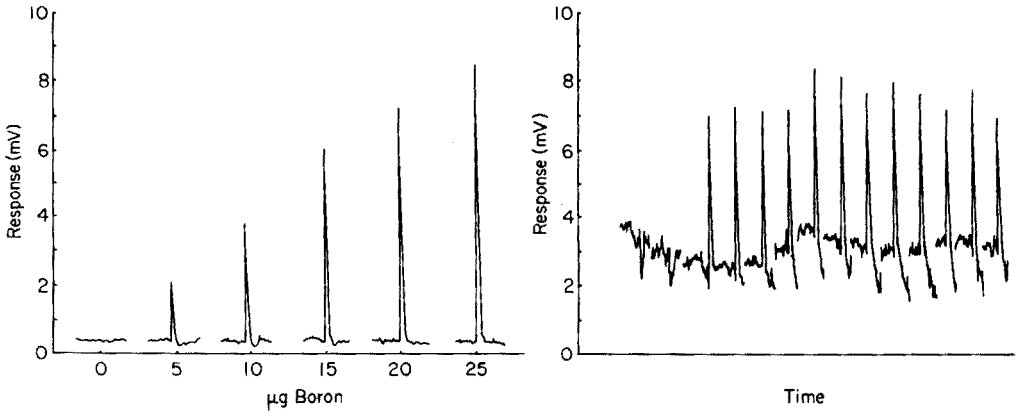

Fig. 3. Typical calibration for 0—25 μg of boron.

Fig. 4. Reproducibility for 1-μg boron standards.

to be 0.02 μg B. The rapid evolution of the volatile fluorides is evident from the sharp peaks which allow peak height measurements to be used for quantitative work.

Atomic absorption

The experimental arrangement gave good results for silicon with the air-diluted nitrous oxide—acetylene flame. Figure 5 shows a calibration for silicon which is only slightly curved in the range 0—25 μg. The relative standard deviation of replicate runs at the 5-μg level (Fig. 6) was 4.6% and the sensitivity (based on 1% light absorption) was 0.25 μg Si. Poor sensitivity was found for boron and no useful data could be obtained for this element.

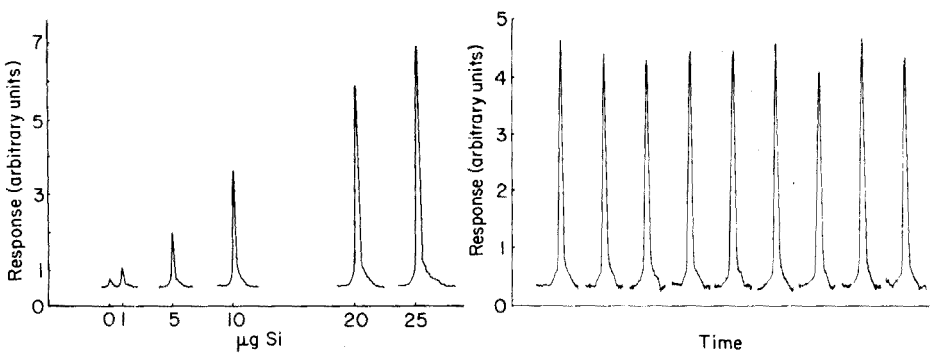

Fig. 5. Typical calibration for 0—25 μg of silicon.

Fig. 6. Reproducibility for 5-μg silicon standards.

DISCUSSION

After a short operating period, the intensity of signals gradually weakened and became erratic as the temperature of the pump increased. This was apparently due to reaction of the evolved fluorides with the interior metal surfaces of the pump. Good repetitive signals were obtained when the pump was allowed to cool between runs, so a water jacket and cooling coils were added to the assembly. An alternative solution may be to nickel-plate the interior of the pump to render it unreactive to fluoride attack.

The technique was found suitable for the analysis of powders. This is shown in Table 1. When Spex G standards and spiked samples of graphite were mixed with 20% CuOHF, evolution of the fluorides gave similar peaks to the standards prepared by solution evaporation. A single determination gave a variation of about ±10—20% from the expected values for both boron and silicon. The fluoride evolution technique had been used in emission spectrographic analysis [7] where it was found that a wide range of materials was amenable to analysis for boron and silicon. The ability to determine these elements in solid samples by flame techniques provides a significant improvement in sensitivity over conventional spray-in-flame techniques.

Although chemical combustion flames provide good sensitivity, carbon furnaces and high temperature sources such as the plasma jet could possibly be used as alternative methods of analysis. Preliminary experiments with a carbon furnace indicated that open-ended cups were unsuitable because of low-temperature formation of the volatile fluorides. It appeared that the fluorides volatilized rapidly from the cup before the temperature was high enough to cause dissociation into free atoms. Closed systems [8, 9] may be more successful. The use of a plasma jet [1] to determine boron and silicon in the evolved vapours was investigated and high sensitivities were observed for their atomic emission lines at 249.8 nm and 251.6 nm, respectively. How-

TABLE 1

Boron and silicon results on graphite standards and spiked graphite by the fluoride evolution technique

Element	Sample type	μg Expected	μg Found
B	Spex G-1[a]	8.1	7.3
	Spex G-2	5.5	6.2
	Spiked graphite No. 1	2.2	2.5
	Spiked graphite No. 2	5.0	6.0
	Spiked graphite No. 3	10.5	9.3
Si	Spiked graphite No. 4	1.0	1.4
	Spiked graphite No. 5	5.0	5.0
	Spiked graphite No. 6	10.0	10.8

[a] Diluted 1 : 1 with graphite.

ever, instability of the discharge caused by high carrier gas flows indicates the need for further investigation of this technique.

CONCLUSION

It has been demonstrated that boron and silicon can be detected with high sensitivity in flame emission and atomic absorption, respectively, by introduction of their volatile fluorides into chemical combustion flames. The apparatus needed to produce the fluorides is simple to construct and convenient to operate.

The procedure provides a means for determining these elements in solution residues, or in solids. It may also be applicable to the analysis of other elements which yield volatile fluorides under similar conditions.

REFERENCES

1 J. F. Chapman, L. S. Dale and R. N. Whittem, Analyst (London), 98 (1973) 529.
2 V. A. Fassel and R. N. Kniseley, Anal. Chem., 46 (1974) 1110A.
3 M. D. Amos and J. B. Willis, Spectrochim. Acta, 22 (1966) 1325.
4 E. Brown, M. W. Skougstad and M. J. Fishman, Methods for Collection and Analysis of Water Samples for Dissolved Minerals and Gases, U.S. Govt. Printing Office, Washington, 1970.
5 E. N. Pollock and S. J. West, At. Absorpt. Newsl., 12 (1973) 6.
6 R. Belcher, S. A. Ghonaim and A. Townshend, Anal. Chim. Acta, 71 (1974) 255.
7 L. S. Dale, Proc. 6th Aust. Spect. Conf. Brisbane, Australia, 1967.
8 G. Lundgren and G. Johansson, Talanta, 21 (1974) 257.
9 J. W. Robinson and D. K. Wolcott, Anal. Chim. Acta, 7 (1975) 43.

Analytica Chimica Acta, 89 (1977) 369—376

VAPORIZATION OF ATOMS AND MOLECULES DURING HEATING OF CADMIUM, LEAD AND ZINC SALTS IN A CARBON TUBE ATOMIZER

SEIJI YASUDA and HITOO KAKIYAMA

National Industrial Research Institute of Kyushu, Tosu, Saga 841 (Japan)

(Received 4th August 1976)

SUMMARY

Vaporization characteristics of atoms and molecules produced during heating of aqueous solutions of Cd, Pb and Zn salts in the carbon tube atomizer are described. Sulfates, nitrates and fluorides are decomposed completely to free atoms without losses. When concentrated halide solutions are employed, gaseous metal chlorides, bromides and iodides are removed partly from the atomizer in the initial atomization phase, and the atomic absorption response is decreased. This loss can be suppressed effectively by adding nitric or sulfuric acid to the halide solutions.

In flameless atomic absorption techniques with electrically heated atomizers, an understanding of the formation and vaporization of undissociated molecules is important since it will provide information about background absorption, chemical interference mechanisms and atomization processes. Background absorption is one of the primary interferences encountered in analyses for trace elements in heavy matrices. The nature of this absorption has been investigated for some inorganic salts by measuring their absorption spectra [1—5]. Vaporization losses of analyte elements as volatile molecules have been suggested in chemical interference studies [6—9], but few of the molecules have been characterized. Atomization processes in flameless atomizers have been studied by applying thermodynamic and kinetic theories to the dissociation of metal oxides to free atoms [10—13]. This approach is based on the assumption that the elements remain as their oxides in the initial atomization phase.

In previous papers [4, 5], the vaporization of gaseous alkali and transition metal halides in the carbon tube atomizer has been discussed with regard to their absorption spectra. The present paper describes the vaporization characteristics of atoms and molecules produced when aqueous solutions of cadmium, lead and zinc halides, sulfates and nitrates, are heated in the carbon tube atomizer. The suppressing effects of acids on the vaporization of halide molecules are reported.

EXPERIMENTAL

Apparatus and reagents

Atomic and molecular absorptions were measured with a Shimazu MAF-1 atomic absorption spectrometer combined with a Nippon Jarrell-Ash FLA-1

carbon tube atomizer of the mini-Massmann type [14]. A deuterium lamp (Hamamatsu TV, L233-1DQ) was used as a continuous light source and single-element lamps of cadmium, lead and zinc (Hamamatsu TV, L233 type) were also used for atomic absorption measurements. Eppendorf micropipettes were used to place test solutions in the atomizer. Tube temperatures were measured with a calibrated chromel—alumel thermocouple or an optical pyrometer.

Aqueous solutions of halides, sulfates and nitrates of cadmium, lead (except $PbSO_4$) and zinc were prepared by dissolving reagent-grade chemicals (as received) in distilled water. All other solutions were made from reagent-grade materials.

General procedures

The test solution (20 μl) was placed in the atomizer, dried for 10 s at 1.0V—20A (below 150° C) and ashed for 10 s at 1.5V—40A (below 250° C). The voltage was then increased rapidly to a higher value for 5 s to give a temperature high enough to obtain the most intense absorption of atoms or molecules. The optimal voltage settings and temperatures for atomic and molecular absorption measurements are described in the appropriate place in the text. Argon gas was employed as the inert sheath gas at a flow rate of 2.0 l min^{-1}.

RESULTS AND DISCUSSION

Absorption spectra of vaporized molecules

Absorption spectra (200—450 nm) for halides, sulfates (except $PbSO_4$) and nitrates of cadmium, lead and zinc were measured as described previously [5] with a deuterium lamp. Experimental conditions for the spectral measurement are summarized in Table 1 together with the minimum temperatures at which an absorption signal could be detected.

When any of the fluoride solutions was heated to 300—2600° C, no molecular absorption was observed in the wavelength region studied, whereas other halides gave characteristic band spectra. The spectra observed for cadmium halides are shown in Fig. 1 and those for zinc halides in Fig. 2. Chlorides and bromides gave almost similar spectra below 280 nm, which extended into the far u.v. region and exhibited no significant absorption maxima in the wavelength region of interest. U.v. spectroscopic studies of cadmium and zinc halide vapors have been reported by Oeser [15] who noted that the absorption maxima of CdX_2 and ZnX_2 (X = Cl, Br) vapors are located below 200 nm. In addition, vaporization of these molecules under the present experimental conditions would be expected from data on the vapor pressure [16, 17] and mass spectrometry [17]. Consequently, it seems reasonable to consider that the spectra observed can be attributed to the vaporization of $CdCl_2$, $CdBr_2$, $ZnCl_2$ and $ZnBr_2$, respectively. The spectrum for cadmium iodide had two absorption maxima near 222 and 262 nm, while zinc iodide

TABLE 1

Experimental conditions for the measurements of absorption spectra

Reagent	Conc. of metal ($\mu g\ ml^{-1}$)	Power setting (V—A)	Temp. after 5 s (°C)	Minimum temp. (°C)
$CdSO_4 \cdot 4H_2O$	1000	4.0—180	1400	450
$CdCl_2 \cdot 5/2H_2O$	1000	4.0—180	1400	430
$CdBr_2 \cdot 4H_2O$	500	3.5—160	1100	350
CdI_2	300	3.0—140	800	300
$PbCl_2$	1000	4.0—180	1400	450
$PbBr_2$	500	3.5—160	1100	370
PbI_2	300	3.5—160	1100	320
$ZnSO_4 \cdot 7H_2O$	1000	4.0—180	1400	420
$ZnCl_2$	1000	3.5—160	1100	350
$ZnBr_2$	500	3.0—140	800	300
ZnI_2	300	3.0—140	800	300
Fluorides	1000	8.0—260	2600	—
Nitrates	1000	1.5— 40	200	100—150

gave a maximum near 238 nm. These bands agree closely with those of CdI_2 and ZnI_2 vapors [15, 17, 18]. As shown in Fig. 3, three absorption bands were observed for lead chloride near 270, 325 and 365 nm, for lead bromide near 245, 310 and 415 nm and for lead iodide near 235, 285 and 400 nm. These bands observed were almost identical with those of the respective $PbCl_2$, $PbBr_2$ and PbI_2 vapors [19—21].

When halide solutions were heated above 400—500 °C, atomic absorption signals of the constituent metals were observed at their resonance lines together with halide signals, since these lines lie in the same spectral region as that of halide bands. Figure 4 shows the recorder traces of the signals

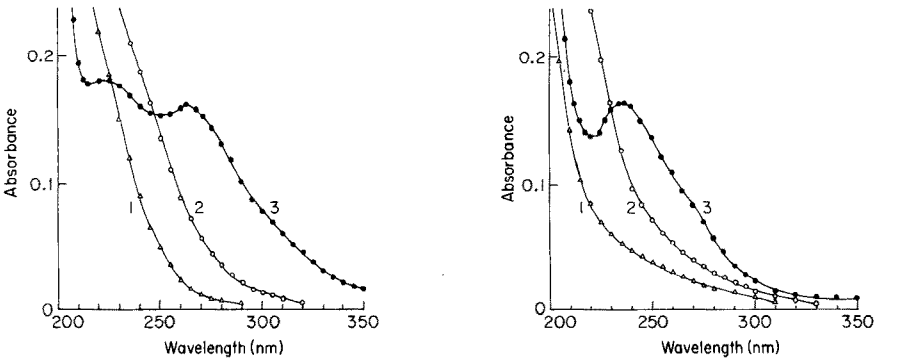

Fig. 1. Absorption spectra for cadmium halides. (1) $CdCl_2 \cdot 5/2H_2O$; (2) $CdBr_2 \cdot 4H_2O$; (3) CdI_2.

Fig. 2. Absorption spectra for zinc halides. (1) $ZnCl_2$; (2) $ZnBr_2$; (3) ZnI_2.

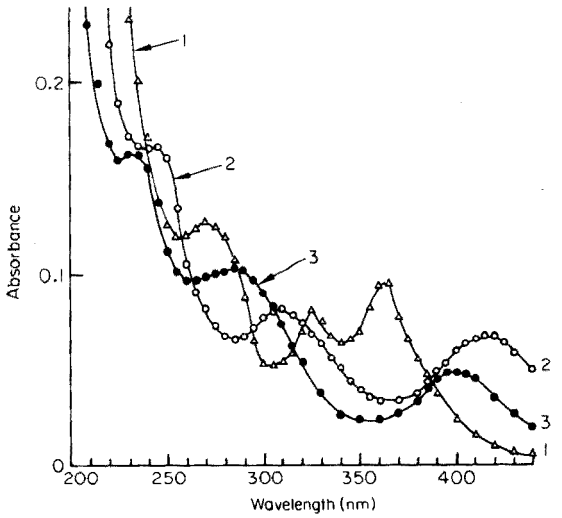

Fig. 3. Absorption spectra for lead halides. (1) $PbCl_2$; (2) $PbBr_2$; (3) PbI_2.

measured with a deuterium lamp at 228.8 nm for cadmium halides (500 μg Cd ml^{-1}), at 217.0 nm for lead halides (200 μg Pb ml^{-1}) and at 213.8 nm for zinc halides (500 μg Zn ml^{-1}). Halides were atomized for 20 s at relatively low voltages (3—4V), so that resolution between atomic and molecular signals was obtained. Fluorides gave only an atomic signal and are therefore not shown here. Except for cadmium chloride, the first peak could be attributed to the vaporization of halide molecules, whereas the second peak arose from atomization of the constituent metals. Cadmium chloride gave an unseparated peak caused by absorption overlapping of cadmium atoms with $CdCl_2$ because of their similar volatilities. The above assignments are based on the fact that the first peak gives the same wavelength dependence as that of halide bands.

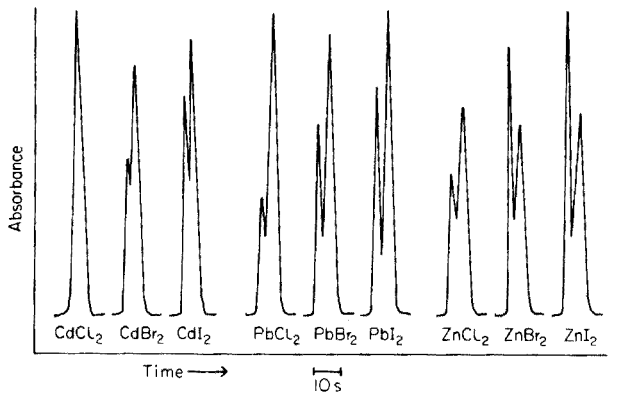

Fig. 4. Recorder traces of absorption signals at 228.8 nm for cadmium halides, at 217.0 nm for lead halides and at 213.8 nm for zinc halides.

Throughout the experiments, no appreciable memory effects were encountered. Further increase of voltage setting reduced the peak separation and finally overlapping occurred. However, there were no differences in the halide spectra obtained at any higher voltages up to 8V (about 2600° C). The results suggest that gaseous metal dihalides (MX_2) are removed partly from the atomizer in the initial atomization phase at temperatures beyond 300—450° C.

When cadmium and zinc sulfates were heated above 400—450° C, the spectrum of sulfur dioxide was found below 250 nm and at 270—310 nm. Nitric oxide (NO) gamma bands near 204.6, 214.6 and 226.0 nm were observed for all nitrates during ashing about 150—250° C. In both cases, no absorption by other molecules was observed at any higher temperatures. This indicates that these salts are decomposed to oxides after evolution of SO_2 and NO. However, when mixtures of metal nitrate (1.0 mg ml^{-1} metal) and ammonium halide (1.0 mg ml^{-1} halide ion) were heated above 300—450° C, the same spectra as those of the corresponding metal halides were obtained. Furthermore, $CdCl_2$ and $ZnCl_2$ spectra were observed for 1 M hydrochloric acid solutions of these metals (1.0 mg ml^{-1} metal). These results suggest that metal halides are vaporized during heating of metal solutions containing large amounts of halide ions.

Atomic absorption response of various salts

Campbell and Ottaway [10] have suggested that standard metal solutions of oxy-anion salts should be preferred for flameless atomizers rather than halides which decrease the degree of atomization because of molecular vaporization. To investigate this further, the atomic absorption responses of halide, sulfate and nitrate standards of each metal at the 100 μg ml^{-1} level or less were compared by measuring absorbances at appropriate resonance lines with a deuterium or metal lamp. The instrumental settings and metal concentration of the standards are summarized in Table 2. Nitrate was used to determine the optimal atomization conditions listed and was employed as a reference for comparison of the responses of the standards.

When concentrated standards were atomized, the chlorides, bromides and iodides of the metals gave lower responses than the fluorides, sulfates and nitrates, which showed almost comparable responses (Table 3). In general, an increase in applied voltage produces a faster rate of rise of atomizer temperature and results in an increase in the degree of atomization [22, 23]. In the present studies, however, little improvement in the responses of chlorides, bromides and iodides was obtained by increasing the applied voltage. In certain cases in which the highest voltage (8 V) obtained with our apparatus was employed, these halides gave lower responses (about 40—60%) than those of other standards. The poor responses indicate that vaporization losses of metal halides can occur in the initial atomization phase at temperatures beyond the minima listed in Table 1, even when a higher heating rate is used. The similar responses obtained for fluorides, sulfates and nitrates at various voltages suggest that the same mechanisms are involved in their atomization

TABLE 2

Instrumental settings and metal concentrations for the comparison of atomic absorption responses of various salts

Metal	Atomization	Conc. of metal (μg ml^{-1})	Wavelength (nm)	Lamp
Cd	4V—180A	100	228.8	D_2
		1	326.1	Cd
		0.01	228.8	Cd
Pb	5V—220A	100	283.3	D_2
		0.1	283.3	Pb
Zn	5V—220A	100	213.8	D_2
		1	305.7	Zn
		0.01	213.8	Zn

processes. These salts are probably decomposed on heating to an intermediate metal oxide and then dissociated to free atoms. However, all standards at 1 μg ml^{-1} metal or less gave similar responses within experimental error; this shows that no losses of analyte metal occur when halides are used to prepare standards at low concentrations employed under the most sensitive conditions for the determinations of these metals. Similar results have been found when zinc chloride, nitrate, sulfate and acetate are atomized with a carbon filament atomizer [24]. When only small amounts of metal and halide ions are present, the halides are probably decomposed completely to free atoms without losses.

Further experiments were done to investigate the effects of halide ions on the responses of cadmium nitrate standards at 100, 1 and 0.01 μg Cd ml^{-1}. Halide ions (1—1000 μg ml^{-1}) were added as ammonium halides. Figure 5 shows the relative absorbance of cadmium nitrate standards with and without halide ions. In most cases, fluoride ion had no significant effect on cadmium response. For 0.01 μg Cd ml^{-1}, chloride, bromide or iodide did not affect

TABLE 3

Comparison of atomic absorption responses of metal solutions (100 μg ml^{-1}) prepared from various salts

Salt	Cadmium	Lead	Zinc
Nitrate	100	100	100
Sulfate	100	—	100
Fluoride	100	100	100
Chloride	54	52	49
Bromide	36	41	35
Iodide	38	47	37

cadmium responses even when present in 1000-fold amounts, but the response for 1 μg Cd ml^{-1} was reduced slightly by this amount of chloride, bromide or iodide. The most severe effects were observed for 100 μg Cd ml^{-1} standards. For example, chloride, bromide and iodide ions in 10-fold amounts (1000 μg ml^{-1}) gave reduced responses of about 38, 74 and 55%, respectively. This is probably due to the vaporization losses of cadmium halides as described above.

Suppression of halide vaporization

The effects of sulfuric and nitric acids on the vaporization of the metal halides were investigated by adding the acids to chloride, bromide and iodide solutions of each metal at 400 μg ml^{-1}. This concentration of metal made it possible to measure both atomic and molecular absorptions for the same solutions at metal resonance lines and halide bands with a deuterium lamp source. The degree of suppression of halide vaporization was estimated by comparison of molecular absorption intensities for halide solutions with and without the acid, while the degree of atomization for the same solution was determined by use of the calibration curves obtained from nitrate standards. The experimental conditions for both measurements were the same as those used in the preceding sections.

In all cases, molecular absorption decreased with increasing acid concentration in the halide solutions, whereas the atomic absorption of the constituent metal increased with it. Sulfuric acid was not available for lead halides since lead sulfate precipitated rapidly from the test solutions. Figure 6 shows the effects of both acids on the vaporization and atomization of cadmium halides. For lead and zinc halides, the effects of the acids were very similar to those for cadmium halides and are therefore not shown. Except for chlorides in nitric acid, all halides gave almost complete atomization in the presence of more than 0.01 M sulfuric acid or 0.5 M nitric acid. In addition, these solutions gave no significant molecular absorptions, indicating no halide vaporization. These results indicate that less volatile sulfates and nitrates are formed during the pre-heating of halide—acid solutions. For all chlorides in 1 M nitric acid, which showed a degree of atomization of about 80—90%, it is probably difficult to convert chlorides completely to nitrates during pre-heating. The effects of other acids on the halide vaporization are under investigation.

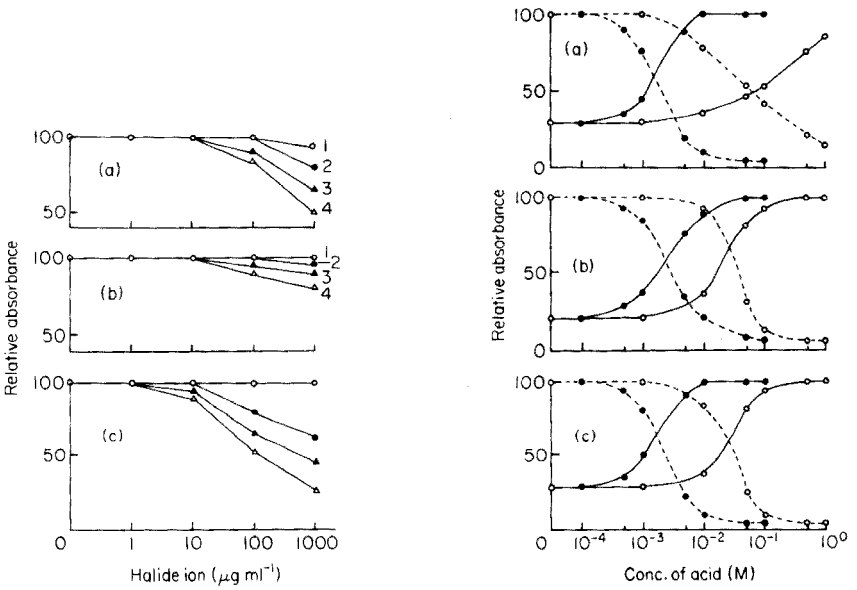

Fig. 5. Effects of halide ions on cadmium absorbances at (a) 0.01, (b) 1 and (c) 100 μg Cd ml^{-1} (1) F^-; (2) Cl^-; (3) Br^-; (4) I^-.

Fig. 6. Effects of nitric and sulfuric acids on the vaporization (dotted curves) and atomization (solid curves) of (a) $CdCl_2$, (b) $CdBr_2$ and (c) CdI_2. (○) HNO_3; (●) H_2SO_4.

REFERENCES

1 B. R. Culver and T. Surles, Anal. Chem., 47 (1975) 920.
2 M. J. Adams, G. F. Kirkbright and P. Rienvatana, At. Absorpt. Newsl., 14 (1975) 105.
3 M. W. Pritchard and R. D. Reeves, Anal. Chim. Acta, 82 (1976) 103.
4 S. Yasuda and H. Kakiyama, Bunseki Kagaku, 24 (1975) 377.
5 S. Yasuda and H. Kakiyama, Anal. Chim. Acta, 84 (1976) 291.
6 C. W. Fuller, Anal. Chim. Acta, 62 (1972) 442.
7 T. Kantor, S. A. Clyburn and C. Veillon, Anal. Chem., 46 (1974) 2205.
8 W. Frech and A. Cedergren, Anal. Chim. Acta, 82 (1976) 83.
9 F. Shaw and J. M. Ottaway, Analyst (London), 99 (1974) 184.
10 W. C. Campbell and J. M. Ottaway, Talanta, 21 (1974) 837.
11 F. J. M. J. Maessen and F. D. Posma, Anal. Chem., 46 (1974) 1439.
12 C. W. Fuller, Analyst (London), 99 (1974) 739.
13 J. Aggett and A. J. Sprott, Anal. Chim. Acta, 72 (1974) 49.
14 S. Yasuda and H. Kakiyama, Bunseki Kagaku, 23 (1974) 406.
15 E. Oeser, Z. Phys., 95 (1935) 699.
16 D. R. Stull, Ind. Eng. Chem., 39 (1947) 540.
17 F. J. Keneshea and D. Cubicciotti, J. Chem. Phys., 40 (1964) 191.
18 K. Butkow, Z. Phys., 71 (1931) 678.
19 K. Butkow, Phys. Z. Sowjetunion, 4 (1933) 577.
20 J. M. Hastie, R. H. Hauge and J. L. Margrave, J. Mol. Spectrosc., 29 (1969) 152.
21 I. G. Murgulescu and E. Ivana, Rev. Roum. Chim., 18 (1973) 1667.
22 G. Torsi and G. Tessari, Anal. Chem., 45 (1973) 1812.
23 R. E. Sturgen, C. L. Chakrabarti, I. S. Maines and P. C. Bertels, Anal. Chem., 47 (1975 1240.
24 D. J. Johnson, B. L. Sharp and T. S. West, Anal. Chem., 47 (1975) 1234.

Analytica Chimica Acta, 89 (1977) 377—382

FLUORESCENCE CHARACTERIZATION AND IDENTIFICATION OF POLYNUCLEAR AROMATIC HYDROCARBONS IN SHALE OIL*

R. J. HURTUBISE**, J. F. SCHABRON, J. D. FEASTER and D. H. THERKILDSEN

Department of Chemistry, University of Wyoming, Laramie, Wyo. 82071 (U.S.A.)

R. E. POULSON

Laramie Energy Research Center, United States Energy Research and Development Administration, Laramie, Wyo. 82070 (U.S.A.)

(Received 14th July 1976)

SUMMARY

Fluorescence spectrometry, dry-column chromatography, and thin-layer chromatography are combined to separate, characterize and identify rapidly polynuclear aromatic hydrocarbons in shale oil. The fluorescence profile of separated fluorescent components is obtained directly on a chromatoplate and a semi-quantitative determination of polynuclear aromatic hydrocarbons in shale oil is discussed. Pyrene and benzo-[*a*]-pyrene can be identified by order of elution on a dry column, R_F value on a chromatoplate, color of fluorescence, and fluorescence excitation and emission spectra.

Polynuclear aromatic hydrocarbons (PAH) have been investigated extensively in recent years because of their occurrence in sources such as automobile exhaust, coal tars, processed foods, and high-boiling petroleum. It has been established that many PAH are carcinogenic to animals and probably to man [1]. Much effort has gone into developing separation methods, characterization methods, and identification methods for PAH in complex samples [2—7]. Because of the complexity of these samples, no one set of separation procedures or no one way of characterizing the samples will give the analyst all the information he needs. Because of the world-wide interest in energy, particularly fossil-fuel energy, there is an even greater need for reliable methods for separation, characterization, and identification of PAH in complex samples. This paper reports on relatively inexpensive, rapid, and sensitive methods for separating, characterizing, and identifying PAH in shale oil samples.

EXPERIMENTAL

Apparatus and reagents

All fluorimetric measurements were made with a Schoeffel SD3000 spectrodensitometer in the reflection mode. The fluorescence emission spectra were

*Presented in part at the Symposium on Management of Residuals from Synthetic Fuels Production, Denver, Colo., May 1976.

**To whom correspondence should be sent.

obtained with a Schoeffel scanning grating monochromator. The excitation monochromator was a Schoeffel QPM30 miniature quartz prism.

PAH were obtained from commercial sources and were recrystallized when needed. The shale-oil samples were obtained from the Laramie Energy Research Center, Laramie, Wyo. (U.S.A.).

The silica gel thin-layer chromatoplates were Brinkmann pre-coated Sil G-25 plates. The 30 % acetylated cellulose thin-layer chromatoplates were Brinkmann pre-coated Cel 200 AC-30 plates. The adsorbent for dry-column chromatography was ICN Pharmaceuticals aluminum oxide, (activity II—III according to Brockmann). The nylon film tubing was ICN 30 mm for dry-column chromatography.

General characterization procedure

An approximate 250-mg sample of shale oil was weighed accurately, dissolved and diluted to 25 ml with n-hexane. A 10-μl sample was spotted on a silica gel plate, and the plate was developed with n-hexane/ether (19 : 1). The developed plate was air-dried for 15 min and then positioned on the stage of the spectrodensitometer. The excitation monochromator was set at 310 nm. There was no monochromator in the emission mode; thus total fluorescence from the plate was measured. The stage of the spectrodensitometer was started and the fluorescence of the components distributed on the plate recorded.

Separation of PAH from shale oil

A 0.1-g sample of shale oil dissolved in n-hexane was poured evenly onto the top of the aluminum oxide packed into a 50-cm nylon tube. After the n-hexane had evaporated (15—30 min), the elution was begun with n-hexane/ether (19 : 1). The fluorescent components were located by viewing the column with an ultraviolet handlamp. When the leading edge of the fluorescence reached a point about 15 cm from the bottom of the column, no more eluant was added to the column. This prevented the fluorescent components from leaving the bottom of the column. The fluorescent edge stopped about 5—10 cm from the bottom of the column. A small pin hole was punched at the bottom of the column before elution began. This allowed the eluant to come out the bottom of the column and the fluorescent components to advance almost to the bottom of the column.

After development, the nylon tube was placed on a bench top and viewed under ultraviolet radiation with the ultraviolet handlamp. Several distinct fluorescent fractions were observed. The fraction of interest was cut out with a razor blade, the adsorbent was transferred to a 100-ml beaker, and 25 ml of reagent-grade 1,2-dichloroethane was added [5]. The contents were stirred for 30 min and then filtered with rinsing into an Erlenmeyer flask. The filtrate was evaporated to dryness under vacuum, and the residue was dissolved in 200 μl of n-hexane.

Aliquots of this n-hexane solution were spotted on 30 % acetylated cellulose chromatoplates. The amount spotted depended on the sample; 2 μl was used for pyrene and 50 μl was used for benzo-[*a*]-pyrene. For the separation of pyrene and other components, the solvent system n-propanol/acetone/water (2 : 1 : 1) was used as eluant. Benzo-[*a*]-pyrene was separated with ethanol/n-hexane/acetone (2 : 1 : 1).

The fluorescence emission spectra were obtained directly from the chromatoplate with the spectrodensitometer by setting the appropriate excitation wavelength and scanning with the grating emission monochromator. Pyrene samples on the chromatoplate were excited at 315 nm, and benzo-[*a*]-pyrene samples at 300 nm.

RESULTS AND DISCUSSION

General characterization

Figure 1 shows the general fluorescence characterizations of four different shale oil samples. Each shale oil has a different fluorescence profile; this information should be useful in process control work and possibly in oil spill identification. Just as the shale oil samples have a different profile, so should oil spill samples from different sources. The peak relative fluorescence intensities are different for each sample. This fact and the fact that each sample has a unique fluorescence profile indicate that the aromatic character is different for each sample. The most important conclusion relates to the PAH content of the samples. The R_F values of benzo-[*a*]-pyrene, fluoranthene, pyrene, and anthracene on silica gel with the same eluant as for the shale oil samples are 0.62, 0.74, 0.75, and 0.77, respectively. This indicates that generally small PAH will migrate farther on the plate than large ring systems. Other carcinogens such as benzo-[*b*]-fluoranthene and benzo-[*j*]-fluoranthene, each with five rings, should have R_F values similar to benzo-[*a*]-pyrene. With the chromatographic system used, polar molecules and larger PAH with more than five rings, should have R_F values less than about 0.62. Thus the first shale oil sample (Fig. 1a) appears to have a greater PAH content with five or fewer ring systems than the remaining three samples. This conclusion and the following conclusions are based on the shapes of the fluorescence profile at greater than R_F 0.62 and the relative fluorescence intensities of the samples. Sample 2 (Fig. 1b) has less PAH with five or fewer rings than sample 1. Sample 3 (Fig. 1c) has even fewer PAH with five rings or less, than samples 1 and 2. Sample 4 (Fig. 1d) appears to have more PAH with five or fewer rings than sample 3, but less than samples 1 and 2.

Sample 4 is unique among the samples, having sharp peaks at R_F values of 0.05, 0.29, and 0.34. Sample 3 has peaks at identical R_F values, but they are not as sharp, possibly because other components are present.

The areas under the curves for R_F values from 0.62 to 1.0 for each sample were determined by cutting out the appropriate area of chart paper and then weighing it. The area per microgram of sample was calculated on a relative

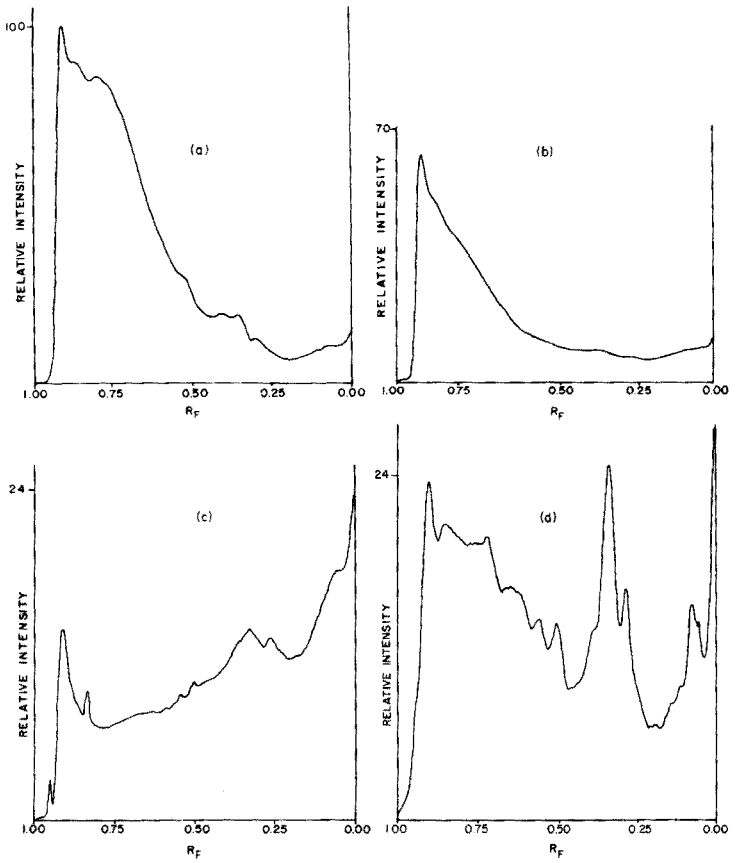

Fig. 1. Fluorescence characterization of four different shale oil samples.

basis, and the values obtained for samples 1—4 were, respectively, 1.0, 0.76, 0.14 and 0.39. These results show that a quick semi-quantitative measure of PAH content with five rings and less in the shale oil samples can be obtained readily. Sample 1 contains the greatest amount of PAH and sample 3 the least.

This general characterization approach is a very rapid and simple way of deciding qualitatively about the PAH content of shale oil samples. It should be useful not only in process control testing but to toxicologists who need rapid, general information on the PAH content of shale oil samples.

Isolation of PAH

Several column-t.l.c. chromatographic systems were tested. The Al_2O_3 dry-column—30 % acetylated cellulose t.l.c. combination was found to give excellent separation, and was rapid, inexpensive and simple. The initial dry-columr separation of shale-oil samples consistently gave five major distinct fluorescen

bands, each approximately 5 cm in length when viewed under ultraviolet radiation. The color of each band from the top of the column to bottom were bright blue, blue, violet, bluish-green and violet. Experiments with known PAH standards applied to Al_2O_3 dry-columns or Al_2O_3 chromatoplates with n-hexane/ether (19 : 1) as eluant, and 30 % acetylated cellulose chromatoplates with n-propanol/acetone/water (2 : 1 : 1) as eluant indicated that PAH separated according to ring size on the dry column. For example, anthracene and dimethylnaphthalenes would appear at the bottom of the column, fluoranthene and pyrene in the next fluorescent band up the column, and benzo-[*a*]-pyrene in the fluorescent band above fluoranthene and pyrene. Pierce and Katz [5] separated isomeric PAH in ambient particulate matter by thin-layer chromatography. They first carried out a group separation of isomeric PAH with aluminum oxide chromatoplates and hexane/ether (19 : 1). In this work a similar approach was used but the dry-column technique was employed as described above. Pierce and Katz then used acetylated cellulose and n-propanol/acetone/water (2 : 1 : 1) for the resolution of individual members of each isomeric group. Twelve PAH — five pentacyclics and seven hexacyclics — were resolved with this chromatographic system. In this work, after dry-column separation, individual fractions were treated as described in "Experimental" and the individual fractions separated on 30 % acetylated cellulose with n-propanol/acetone/water (2 : 1 : 1). Numerous brightly colored fluorescent spots were observed under ultraviolet radiation. In order to identify the isolated PAH, fluorescence excitation and emission spectra were obtained directly from the chromatoplate. Figure 2 shows the similarity of the fluorescence emission spectra of a suspected pyrene spot and a standard pyrene spot separated with the same chromatographic system. The excitation spectra of

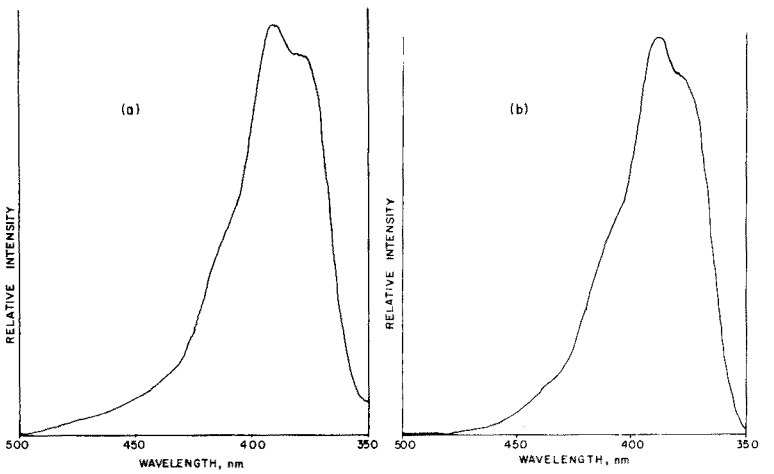

Fig. 2. Fluorescence emission spectrum of pyrene spots. (a) Suspected pyrene spot; (b) standard pyrene spot.

the suspect spot and the standard spot were essentially identical. Several pieces of information taken together confirmed that pyrene was present. For example, the dry-column chromatographic system separated PAH according to ring size, the R_F values and the fluorescence colors of the suspected pyrene and standard pyrene were on the chromatoplate and the fluorescence excitation and emission spectra of the suspected pyrene and standard pyrene were the same. All this evidence confirms the presence of pyrene.

A different eluting system had to be used to separate benzo-[*a*]-pyrene on 30 % acetylated cellulose because of fluorescent interferences. Ethanol/n-hexane/acetone (2 : 1 : 1) was satisfactory. Figure 3 shows the similarity of the fluorescence emission spectra of a suspected spot and a standard benzo-[*a*]-pyrene spot separated on 30 % acetylated cellulose. The excitation spectra from these two spots were identical. The excitation and emission spectra alone with the same type of additional information obtained for pyrene verified that benzo-[*a*]-pyrene was present. Work is continuing to identify other PAH in shale oil. Because of the numerous fluorescent components observed on the chromatoplates, other types of molecules such as nitrogen heterocycles should be identifiable by the approaches described.

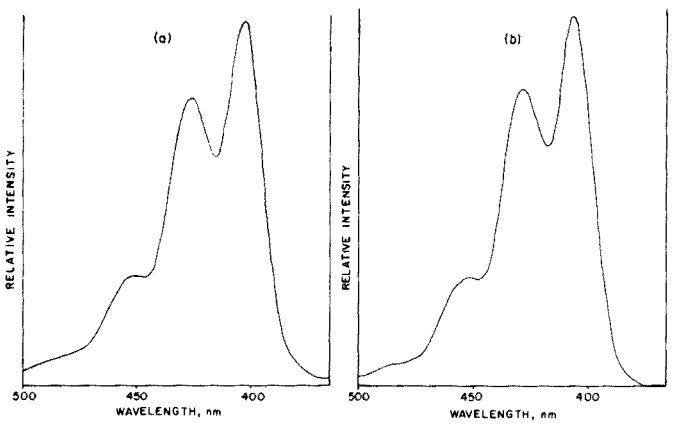

Fig. 3. Fluorescence emission spectrum of benzo-[*a*]-pyrene spots. (a) Suspected benzo-[*a*]-pyrene spot; (b) standard benzo-[*a*]-pyrene spot.

REFERENCES

1 J. B. Andelman and J. E. Snodgrass, CRC Critical Reviews in Environmental Control, 4 (1974) 69.
2 G. F. Kirkbright and C. G. de Lima, Analyst (London), 99 (1974) 338.
3 W. Giger and M. Blumer, Anal. Chem., 46 (1974) 1663.
4 G. M. Janini, K. Johnston and W. L. Zielinki, Anal. Chem., 47 (1975) 670.
5 R. C. Pierce and M. Katz, Anal. Chem., 47 (1975) 1743.
6 K. Potthast and G. Eigner, J. Chromatogr., 103 (1975) 173.
7 M. L. Lee, M. Novotny and K. D. Bartle, Anal. Chem., 48 (1976) 405.

Analytica Chimica Acta, 89 (1977) 383—389

A TURBIDIMETRIC METHOD FOR COLLOID TITRATIONS

KYOJI TÔEI and MIHO SAWADA

Department of Chemistry, Faculty of Science, Okayama University, 3-1-1, Tsushima-naka, Okayama-shi 700 (Japan)

(Received 3rd September 1976)

SUMMARY

Positive colloid solutions can be titrated with the polyanion potassium polyvinylsulfate with toluidine blue as indicator, but negative colloid solutions must be treated with an excess of the polycation polydiallyldimethylammonium chloride which is back-titrated with potassium polyvinylsulfate. By turbidimetry however, positive or negative colloid solutions can be directly titrated with, respectively, the polyanionic or polycationic titrant. Two methods, the construction and differential methods, can be used. The latter method is particularly useful when a flocculent precipitate appears during the titration.

Colloid titration is widely used for the determination of polyelectrolytes. Recently, PVSK (potassium polyvinylsulfate) and Cat-Floc (polydiallyldimethylammonium chloride) were used as polyanionic and polycationic titrants, respectively [1]. The color change of toluidine blue could be used for the direct titration of positive colloid solutions by PVSK, but negative colloid solutions could not be titrated directly by Cat-Floc, because no indicator was available. A negative colloid solution must be treated with an excess of Cat-Floc, which is back-titrated with PVSK with toluidine blue as indicator.

The conductimetric method is useful; negative and positive colloid solutions can be titrated directly with Cat-Floc and PVSK, respectively [2]. In the work described here, the turbidimetric method has been used to indicate the end-point in the direct titration of positive and negative colloid solutions by PVSK and Cat-Floc, respectively.

EXPERIMENTAL

Apparatus

Turbidity was measured by a Metrohm Spectrocolorimeter E1009 at 420 nm. Turbidimetric titration curves were recorded by a Metrohm Potentiograph E336 with a Metrohm E436E Titrator. A Hitachi-Horiba F5ss pH meter was used.

Reagents

PVSK solution and Cat-Floc solution were used as the anionic and cationic titrants, respectively. The PVSK solution (0.00125 M or 0.0025 M) was standardized by 0.00125 M cetylpyridinium chloride monohydrate solution with toluidine blue as indicator, and the Cat-Floc solution (0.00125 M or 0.0025 M) was evaluated with the PVSK solution.

The turbidimetric standardization of PVSK by cetylpyridinium chloride monohydrate was not successful; the end-point appeared before the equivalence point during automatic titration.

Sample solutions

Glycolchitosan, methylglycolchitosan, polyethyleneimine, sodium chondroitin sulfate, sodium alginate, ammonium alginate, carrageenan, and sodium lignin sulfonate were dried in vacuo below 50°C, weighed accurately, and the solutions diluted to a constant volume. The concentration was adjusted to about 0.00125 M.

Titration procedures

Indicator method. Toluidine blue was used as indicator as described previously [2]. As the titration proceeded, the solution became turbid; close to the end-point the cloudy solution coagulated suddenly, and the color changed from blue to red-violet.

Turbidimetric method. Positive and negative colloid solutions were titrated directly with PVSK or Cat-Floc, respectively. The transmittance at 420 nm was measured with the Spectrocolorimeter, and the titration curve was recorded automatically. The sample solution (10 ml) was diluted to 40 ml with distilled water, and titrated in a 100-ml cylinder with mechanical stirring.

RESULTS

Turbidimetric titration curves

Cat-Floc solution (10 ml, 0.00125 M) was diluted to 40 ml with distilled water and titrated with 0.00125 M PVSK turbidimetrically. The titration curve is shown in Fig. 1. Conversely, when 40 ml of PVSK was titrated with Cat-Floc solution, almost the same curve was obtained. In both cases, as the titration proceeded, the turbidity increased. Near the end-point, the transmittance decreased abruptly. The inflection point of the titration curve was determined either by the construction method or by the differential method by setting to "Diff" on the E336, as shown in Fig. 1.

The molarity found for the Cat-Floc solution by the indicator and turbidimetric methods is shown in Table 1, in which a, b, and c correspond to a, b and c in Fig. 1, respectively; point b indicates the end-point and the value is coincident with that of the indicator method within experimental error.

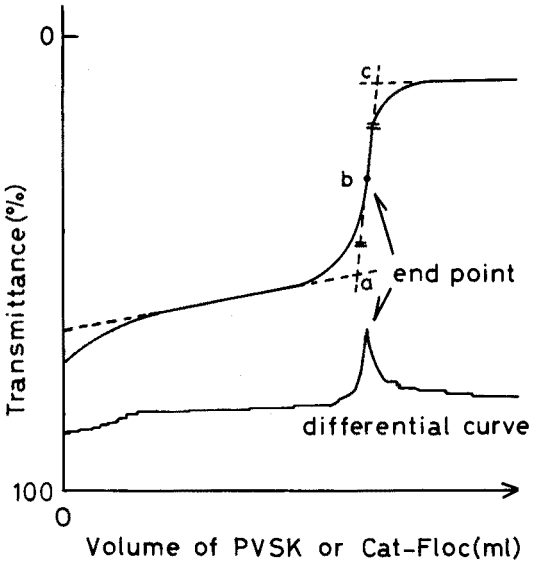

Fig. 1. Turbidimetric titration curve.

TABLE 1

Molarity of Cat-Floc determined by the indicator and turbidimetric methods. The PVSK solution was $2.30 \cdot 10^{-3}$ M

Method	Cat-Floc taken (ml)	PVSK taken (ml)	PVSK titrated (ml)	Cat-Floc titrated (ml)	Cat-Floc concn. ($\cdot 10^{-3}$ M)
Indicator	10.00	—	9.62		2.21
Turbidimetric	10.00	—	a9.49		2.18
	—	—	b9.55		2.20
	—	—	c9.60		2.21
	—	10.00	—	a10.38	2.22
				b10.43	2.21
				c10.47	2.20

The end-point obtained by the construction method was compared with that given by the differential method by changing the titration speed. Good agreement between the methods was obtained at 0.33 ml min^{-1} when 10.00 ml of Cat-Floc or PVSK solution was used (Table 2).

Standard solutions of the same molarity of PVSK and Cat-Floc ranging from 0.0025 M—10^{-4} M were prepared; 10 ml of each solution was diluted to 40 ml with distilled water and titrated turbidimetrically with the titrant of the same strength. As a standard, $2.30 \cdot 10^{-3}$ M PVSK was diluted 2, 3, 5 and 25 times, and the standard Cat-Floc solution (0.00125 M) was diluted in the same way. The molarity of the standard Cat-Floc solution, calculated

TABLE 2

Effect of titration speed on the construction and differential methods

Titration of Cat-Floc with PVSK			Titration of PVSK with Cat-Floc		
Speed (ml min^{-1})	PVSK required (ml)		Speed (ml min^{-1})	Cat-Floc required (ml)	
	Constr.	Diff.		Constr.	Diff.
0.70	10.63	10.81	0.70	9.48	9.52
0.58	10.63	10.75	0.58	9.39	9.57
0.58, 0.33[a]	10.65	10.66	0.58, 0.33[a]	9.46	9.49
0.33	10.64	10.66	0.33	9.44	9.44

[a]0—8 ml: 0.58 ml min^{-1}, 8—10 ml: 0.33 ml min^{-1}, PVSK: $1.17 \cdot 10^{-3}$ M.

from the various concentrations of Cat-Floc and PVSK obtained by turbidimetric titration, was constant at $2.20 \pm 0.01 \cdot 10^{-3}$ M.

The titration curve for 0.0025 M PVSK or Cat-Floc is distorted initially, but the correct end-point can be obtained. In the titration of 10^{-4} M solution, the turbidity can hardly be seen and the decrease in transmittance at the end-point is very small, although the end-point is detectable. Accordingly, the standard 0.00125 M solution of PVSK or Cat-Floc can be used conveniently.

Examples of colloid titration

Glycolchitosan. Dried glycolchitosan (0.1269 g) was dissolved in a 500-ml measuring flask. The solution (10 ml) was diluted to 40 ml with distilled water and titrated with $1.13 \cdot 10^{-3}$ M PVSK by the indicator and turbidimetric methods. The results are shown in Fig. 2. Below pH 5, the values of meq g^{-1} from the turbidimetric method are constant (3.47 meq g^{-1}) and values given by the indicator method are 1.7% higher. In this pH range, the amino groups in glycolchitosan are in the ammonium form. As the color change of toluidine blue is not instantaneous above pH 6.5, the end-point is indistinct; in the turbidimetric method, the decrease in transmittance is not sharp and the end-point is indistinguishable.

Methylglycolchitosan. Dried methylglycolchitosan (0.2363 g) was dissolved in a 500-ml measuring flask. The solution (10 ml) was titrated with $1.13 \cdot 10^{-3}$ M PVSK. The results are shown in Fig. 3. Below pH 6 a constant value was obtained by the indicator and turbidimetric methods. At about pH 10, the value is 6% lower than that of an acidic solution.

Polyethyleneimine. Commercial polyethyleneimine solution is pale yellow and contains 30% polyethyleneimine. The solution (0.1 ml) was dissolved and diluted to 1 l and 10 ml of this solution was titrated with $1.22 \cdot 10^{-3}$ M PVSK. The results are shown in Fig. 4. The titration values by the construction method agree with those of the differential method. Above pH 7, the values given by the indicator method are scattered, because the color change

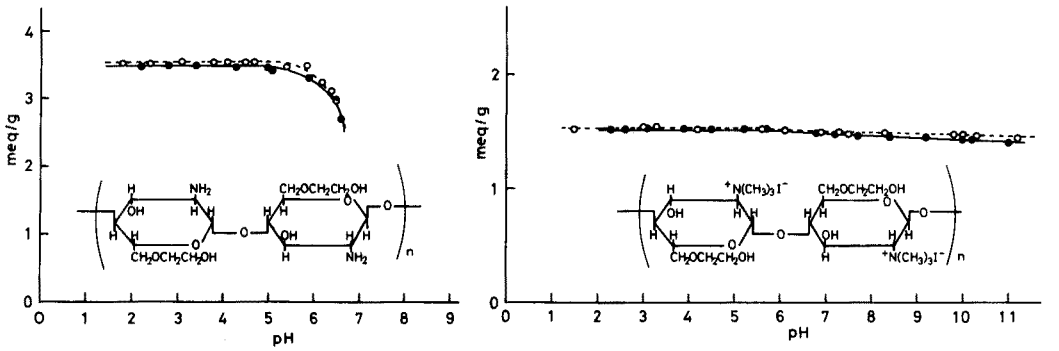

Fig. 2. Colloid titration results of glycolchitosan. ○ Indicator titration. ● Turbidimetric titration.

Fig. 3. Colloid titration results of methylglycolchitosan. ○ Indicator titration. ● Turbidimetric titration.

is not instantaneous at the end-point and coagulation of the complex at the end-point may not occur. A constant value (meq l^{-1}) could not be obtained. This implies that polyethyleneimine has hydrogen-bonded imino groups.

Sodium chondroitin sulfate. The solution (0.2586 g l^{-1}) was titrated with $1.02 \cdot 10^{-3}$ M Cat-Floc turbidimetrically, and also indirectly by the indicator method. The results are shown in Fig. 5. The value by the turbidimetric method (3.53 meq g^{-1}) is 89% of the calculated value.

Sodium alginate. The solution (0.2252 g l^{-1}) was titrated with $1.22 \cdot 10^{-3}$ M Cat-Floc turbidimetrically. The solution (10 ml) was also titrated by the indicator method with $1.22 \cdot 10^{-3}$ M Cat-Floc and $1.17 \cdot 10^{-3}$ M PVSK.

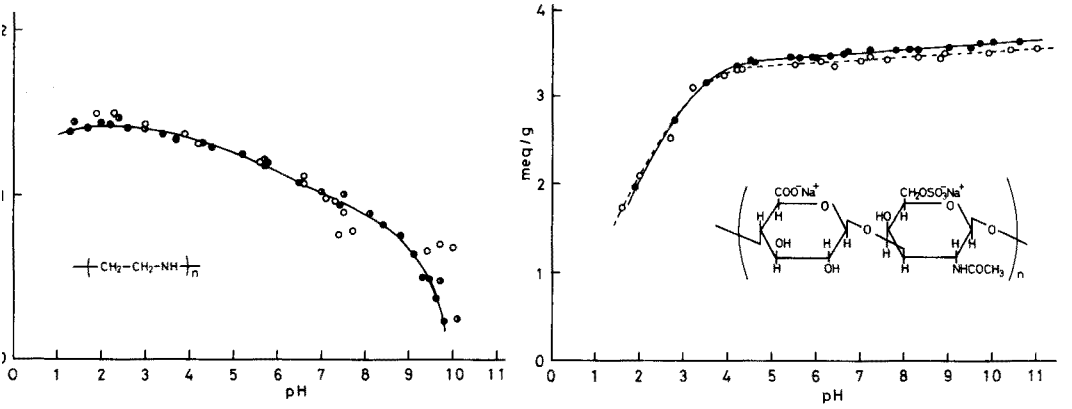

Fig. 4. Colloid titration results of polyethyleneimine. ○ Indicator titration. ● Turbidimetric titration (construction method). ◑ Turbidimetric titration (differential method).

Fig. 5. Colloid titration results of sodium chondroitin sulfate. ○ Turbidimetric titration. ● Indicator titration.

The results are shown in Fig. 6. In the turbidimetric method, the construction method cannot be used below pH 3 because a sol is formed near the end-point. Above pH 5, a constant value (4.62 meq g^{-1}) was obtained; this corresponds to 92% of the calculated value.

Ammonium alginate. The solution (0.1348 g l^{-1}) was titrated by the turbidimetric and indicator methods (Fig. 7). The value (5.08 meq g^{-1}) at pH 11 and above is equivalent to 98% of the calculated value. In the titration of the copolymer of sodium maleate and methylvinyl ether, the values (meq g^{-1}) given by sodium hydroxide are lower than those given by tetrabutylammonium hydroxide solutions at the same pH [3], but there was no difference in the titration of the alginate.

Carrageenan. The solution (0.4166 g l^{-1}) was titrated with $1.21 \cdot 10^{-3}$ M Cat-Floc. The construction method could not be used, because a flocculent precipitate was formed, and the end-point was found from the peak of the differential curve. The results are shown in Fig. 8. Carrageenan is a mixture of different forms, depending on its origin.

Sodium lignin sulfonate. A brown commercial sample of sodium lignin sulfonate (0.3550 g) was dissolved in 1 l of water. When the concentration is higher than this (ca. 0.0006 M) the end-point cannot be detected by the indicator and turbidimetric methods because of the color of the solution. The results are shown in Fig. 9. Between pH 2 and 6.5, the values given by the indicator and turbidimetric methods are almost the same; above pH 6.5 the indicator method gives higher values than the turbidimetric method. Above pH 6.5, the color of the solution deepened; phenolic hydroxyl, enol or ammonium groups etc. would be dissociated or decomposed by air. Hydrolysis of the ester content of the sample may occur and would be accelerated by the presence of Cat-Floc in the indicator method [4]; direct titration by turbidimetry would therefore be preferable to the indicator method.

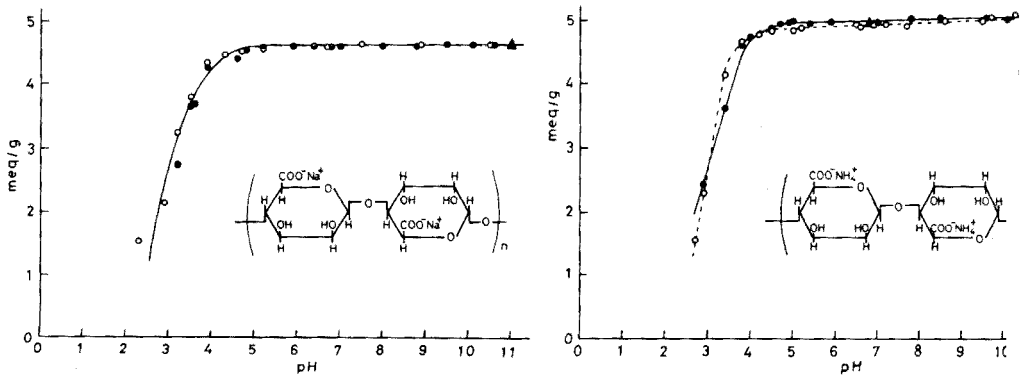

Fig. 6. Colloid titration results of sodium alginate. • Turbidimetric titration (NaOH). ▲ (Bu_4NOH). ○ Indicator titration.

Fig. 7. Colloid titration results of ammonium alginate. ○ Indicator titration. • Turbidimetric titration (NaOH). ▲ (Bu_4NOH).

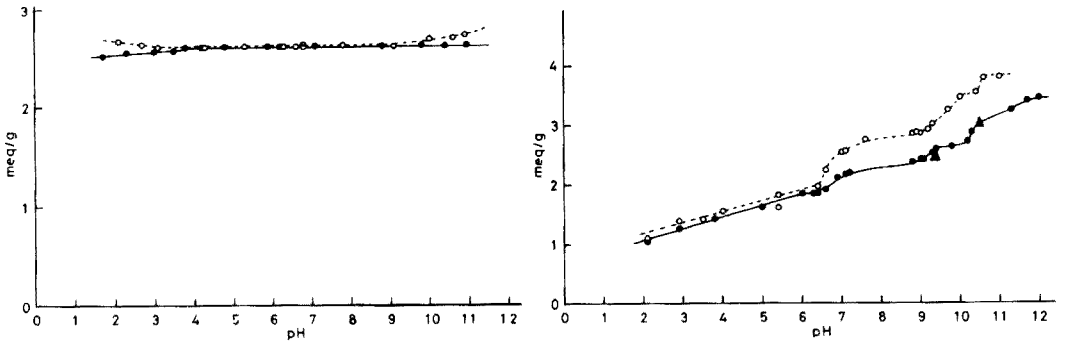

Fig. 8. Colloid titration results of carrageenan. ○ Indicator titration. ● Turbidimetric titration.

Fig. 9. Colloid titration results of lignin sulfonic acid, sodium salt. ○ Indicator titration. ● Turbidimetric titration (NaOH). ▲ (Bu_4NOH).

CONCLUSIONS

The indicator method is useful for cationic polymers such as glycolchitosan, methylglycolchitosan and polyethyleneimine; the values obtained agree with those from the turbidimetric method within experimental error.

Anionic polymers with sulfate groups combine strongly with Cat-Floc and the turbidimetric titration values agree with those obtained by titrating the excess of Cat-Floc with PVSK by the indicator method.

Anionic polymers with carboxyl groups can be titrated directly with Cat-Floc turbidimetrically. The titration values agree fairly well with those from the indicator method. An intricate anionic polymer such as sodium lignin sulfonate should be titrated directly by the turbidimetric method; higher values would be given by the indicator method because of a secondary reaction in the presence of Cat-Floc at higher pH.

REFERENCES

1 K. Tôei and K. Kawada, Japan Analyst, 21 (1972) 1510.
2 K. Tôei and T. Kohara, Anal. Chim. Acta, 83 (1976) 59.
3 E. Kokufuta, S. Kokubo, M. Hirata and S. Iwai, Chemistry Associations Union Tohoku District Meeting, Preprint 2DO1 (1975).
4 A. Mizote, H. Odagiri, K. Tôei and K. Tanaka, Analyst (London), 100 (1975) 822.

Analytica Chimica Acta, 89 (1977) 391—395

Short Communication

THE USE OF A PERIODATE-SENSITIVE PERCHLORATE-SELECTIVE ELECTRODE IN THE KINETIC ULTRAMICRODETERMINATION OF CHROMIUM(III) BASED ON ITS ACCELERATING EFFECT ON THE PERIODATE—ARSENITE REACTION

C. E. EFSTATHIOU and T. P. HADJIIOANNOU*

Laboratory of Analytical Chemistry, University of Athens, Athens (Greece)

(Received 29th July 1976)

Perchlorate-selective electrodes respond quantitatively to periodate and can be used in the potentiometric determination of vicinal glycols [1]. The present communication describes the application of the perchlorate electrode for monitoring another periodate reaction. Trace amounts of chromium(III) accelerate the reaction between periodate and arsenite in neutral solution

$$IO_4^- + H_3AsO_3 \rightarrow HAsO_4^{2-} + IO_3^- + 2H^+ \quad (1)$$

The reaction can be monitored with a perchlorate electrode, and under controlled conditions a linear relation exists between the increase in electrode potential within a fixed period of time and the amount of chromium(III) present. A kinetic method for the ultramicrodetermination of chromium(III) can be based on this accelerating effect of chromium(III). Submicrogram amounts of chromium(III) in the range 40—300 ng can be determined with relative errors and precision of about 2—3 %.

Experimental

Apparatus. An Orion perchlorate-selective electrode, Model 92-81, was used as the indicator electrode, in conjunction with a double-junction silver—silver chloride electrode, Orion Model 90-02-00, as the reference electrode. The behaviour and maintenance of the electrode, and the reaction cell, have been described elsewhere [1]. The electrode potential was measured and printed with an Orion Ionanalyzer (Model 801A digital pH/pIon meter) coupled to an Orion Digital Printer (Model 751) which was adjusted to print the potential every minute. A pH/pIon Electrometer (Heath-Schlumberger Model EU-200-30) was used to sample the electrode potential. A potentiometric recorder (Heath-Schlumberger Model EU-205B) was used to monitor the output from the electrometer and record the reaction curve.

Reagents. All solutions were prepared with deionized twice-distilled water and reagent-grade substances.

Chromium(III) standards. For the stock solution, dissolve 0.7073 g of

*To whom correspondence should be addressed.

$K_2Cr_2O_7$ in 100 ml of 2 M H_2SO_4 and add 5 g of $NaHSO_3$ in small portions with vigorous stirring. Boil the solution to complete the chromium(VI) reduction to chromium(III) and expel the SO_2, and dilute to 1 l. This solution contains 250 p.p.m. of chromium(III). Prepare working standards containing 0.5—5.0 p.p.m. of chromium(III) from the stock solution by dilution.

Composite 0.0200 M arsenite—0.050 M phosphate buffer solution. Dissolve 2.60 g of $NaAsO_2$ in 800 ml of water, adjust the pH to about 6 with 5 M H_2SO_4, add 6.80 g of $NaH_2PO_4 \cdot H_2O$, adjust the pH to 6.6 with 5 M NaOH and dilute to 1 l.

Sodium periodate, $8.0 \cdot 10^{-4}$ M. Prepare fresh when needed from a 0.0500 M stock $NaIO_4$ solution, store in an amber bottle and protect from organic materials.

Procedure. Draw 0.100 ml of chromium(III) standard or sample solution into a 0.1-ml Hamilton microliter syringe. Into the thermostated reaction cell (kept at 28 °C) pipet 15.00 ml of $8 \cdot 10^{-4}$ M $NaIO_4$ solution and 5.00 ml of the composite arsenite-buffer solution. Immerse the electrodes into the solution, start the stirrer, press the "start" switch of the printer after a pre-measurement period of 20—30 s to print the initial electrode potential E_0, and immediately inject the chromium solution into the cell. After exactly 60 s, the new electrode potential E_{60} is automatically printed. Empty the cell with suction, rinse the electrodes and the cell with water and dry by suction. Repeat the procedure for each analysis including a blank.

Calculations. Working curves are prepared to read p.p.m. of chromium(III) by plotting ΔE values ($\Delta E = E_{60} - E_0$) against the chromium concentration of the standards.

Results and discussion

Chromium(VI) compounds have no influence on the rate of reaction 1, which demonstrates that the acceleration by chromium(III) occurs only in the initial stage of reaction 1 because of the simultaneous oxidation of chromium(III) by periodate

$$3\,IO_4^- + 2\,Cr^{3+} + 5\,H_2O \rightarrow 3\,IO_3^- + 2\,CrO_4^{2-} + 10\,H^+ \qquad (2)$$

The pH strongly affects the accelerating action of chromium(III) on reaction 1, since reactions 1 and 2 are both influenced by pH, both being faster in more alkaline solutions. Figure 1 shows the accelerating effect of Cr(III) at various pH values.

The addition of EDTA in excess over chromium(III) inhibits its accelerating effect. Since chromium(III) reacts very slowly with EDTA, it is quite possible that other chromium species are involved. Chromium species of intermediate oxidation state between III and VI are known to form complexes readily with EDTA [2]. Therefore the accelerating effect is probably due to one of these species. The role of chromium(III) may be considered as that of promoter rather than catalyst and the catalytically active species slowly disappear according to the following scheme

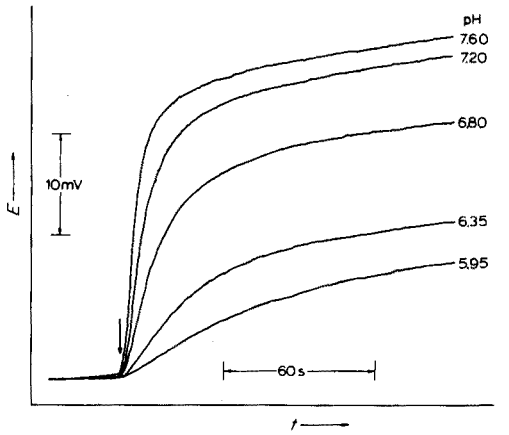

Fig. 1. Effect of pH on the accelerating effect of Cr(III) on the periodate—arsenite reaction. Initial concentrations: $NaIO_4$, $8.2 \cdot 10^{-4}$ M; H_3AsO_3, $2.7 \cdot 10^{-3}$ M; Cr(III) (after injection), $1.58 \cdot 10^{-6}$ M (0.082 p.p.m.). pH adjusted with NaH_2PO_4—NaOH mixture; total H_3PO_4, 0.082 M.

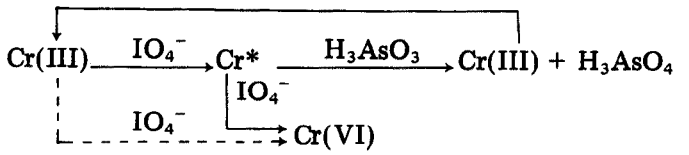

(3)

where Cr* is a chromium species of intermediate oxidation state easily complexed by EDTA.

Figure 2 shows typical recorded curves and the corresponding working curve. Although linearity is fairly good up to 5 p.p.m. Cr, satisfactory preci-

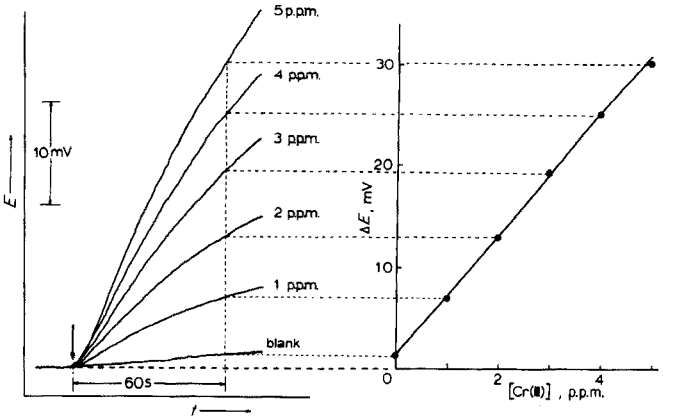

Fig. 2. Recorded curves of cell voltage vs. time for the periodate—arsenite reaction in the presence of Cr(III), and the corresponding working curve. Initial concentrations: $NaIO_4$, $6.0 \cdot 10^{-4}$ M; H_3AsO_3, $5.0 \cdot 10^{-3}$ M; Cr(III) (after injection), $9.6 \cdot 10^{-8}$—$4.8 \cdot 10^{-7}$ M (5—25 p.p.b. Cr). pH 6.6; total phosphate, 0.012 M.

sion is not obtained for samples containing more than 3 p.p.m. Cr. The lower limit should not be smaller than 0.4 p.p.m. Cr since the ΔE value has an absolute uncertainty of ± 0.1 mV which corresponds to a relative uncertainty of about ± 3 % for a 0.4 p.p.m. Cr sample.

Analysis of aqueous chromium(III) solutions of known concentrations gave the results shown in Table 1. The data indicate that ultramicro amounts of chromium(III) in the range 40—300 ng in a total volume of 20.1 ml can be determined with relative errors of about 3 %. Twelve replicate determinations were made with a 2.5 p.p.m. Cr solution. The average ΔE value was 16.9 mV (range = 1.1 mV) and the relative standard deviation was 1.8 %.

Table 2 shows the effects of various ions on the determination of chromium(III). These ions in the stated ratios caused a relative error of less than 10 %; in all cases the error was negative. Manganese and copper interfered most seriously.

The proposed kinetic method is simple and fast but certain precautions must be taken to ensure reliability. Each sample must be introduced uniformly. Sample injection should be as fast as possible with the maximum possible stirring without formation of air bubbles. Otherwise, local excesses of chromium(III) may result in the formation of basic phosphate precipitates with a concomitant negative error. Further, standards and samples should contain chromium(III) species in the same form. Good results are obtained if standards and samples contain 0.01 M H_2SO_4 and have been equilibrated by boiling or prolonged standing. If chromium(III) is introduced from strongly alkaline solution, the promoting effect appears to decrease by about 80 %. This effect is perhaps due to another oxidation path of chromium(III) by periodate where the active chromium species is not formed (path shown by the interrupted line in the reaction scheme).

TABLE 1

Results for the determination of chromium(III) in dilute solutions

$\Delta E = E_{60} - E_0$ (mV)	Cr(III), ng per 0.100 ml sample		Error, %
	Taken	Found	
1.3	0	—	—
3.8	40	42	+5.0
6.9	100	95	−5.0
11.0	160	163	+1.9
15.3	230	233	+1.3
18.6	300	290	−3.3
			Av. 3.3

TABLE 2

Effect of various ions on chromium(III) determination at a concentration of $2.88 \cdot 10^{-5}$ M (1.50 p.p.m.)

Ion	Molar ratio Ion: Cr(III)	Ion	Molar ratio Ion: Cr(III)
Mn^{2+}	0.1	Pb^{2+}	200
Cu^{2+}	0.7	Cr(VI) as CrO_4^{2-}	300
Co^{2+}	5	Al^{3+}	350
Ni^{2+}	12	Mg^{2+}	350
Fe^{3+}	20	Zn^{2+}	350
		Ca^{2+}	1000

The authors are grateful to H. Freiser, University of Arizona (U.S.A.) and J. D. R. Thomas, UWIST (U.K.) for helpful discussions made possible by NATO Research Grant No. 1000.

REFERENCES

1 C. E. Efstathiou and T. P. Hadjiioannou, Anal. Chem., 47 (1975) 864.
2 H. B. Mark and G. A. Rechnitz, Kinetics in Analytical Chemistry, Wiley-Interscience, N.Y., 1968, p. 307.

Analytica Chimica Acta, 89 (1977) 397—398

Short Communication

EXTRACTION—SPECTROPHOTOMETRIC DETERMINATION OF THORIUM WITH ALIQUAT-336 AND XYLENOL ORANGE

M. CONTARINI, P. PASQUINELLI and L. RIGALI

Centro Applicazioni Militari dell'Energia Nucleare, S. Piero a Grado, Pisa (Italy)

(Received 28th July 1976)

The direct extraction—spectrophotometric determination of elements offers the advantages of increased rapidity and sensitivity and may be useful in solving particular problems. In previous work [1] the quaternary ammonium compound Aliquat-336, a strong and selective solvent for thorium [2], was used for the separation of thorium followed by its determination in aqueous stripping solutions. Xylenol orange has been employed with success in the colorimetric determination of zirconium in solutions of tri-n-octyl amine [3] and its use has now been extended to the determination of thorium in Aliquat-336 solutions.

Experimental

Reagents. Commercial grade Aliquat-336 (monomethyltricaprylammonium chloride; General Mills Inc.) was used in xylene solution (5 % w/v) and converted to the nitrate form by equilibration with 4 M nitric acid. Xylenol orange (Fluka) was dissolved (0.2 % w/v) in A.C.S.-grade methanol (C. Erba). All other chemicals were reagent grade. The standard solution of thorium ($2 \cdot 10^{-3}$ M) was prepared by dissolving thorium nitrate in 4 M nitric acid.

Procedure. Dilute aliquots of the standard thorium solution to 25 ml with 4 M nitric acid and extract twice (5 min each) with equal volumes of the Aliquat-336 solution. Combine the organic extracts, mix and transfer a 5-ml portion to a 50-ml volumetric flask. Add 10 ml of absolute ethanol, 2 ml of glacial acetic acid and 10 ml of the xylenol orange solution. Dilute to volume with absolute ethanol and leave for 20 min to obtain complete development of the colour. Read the absorbance at 540 nm against a reagent blank containing 5 ml of the extractant.

Colorimetric measurements were performed with a Beckman DU spectrophotometer.

Results

Since Aliquat-336 exhibits maximum extraction coefficients ($E_a^o \simeq 50$) in the range 2—5 M nitric acid, solutions of thorium in 4 M nitric acid were used for the extractions. Although a single equilibration gave about 98 %

recovery of thorium from the aqueous solution, two successive equilibrations with equal volumes of organic and aqueous phases were necessary for complete extraction.

The maximum absorption of the thorium—xylenol orange complex in the extractant solution is close to 535 nm and colorimetric measurements were made at 540 nm. Beer's law was followed up to 5 p.p.m. of thorium (absorbance 0.8 units) and the colour was stable for 24 h.

The effect of some foreign ions was investigated by determining thorium extracted from 4 M nitric acid solutions containing different amounts of these ions. The results are listed in Table 1.

Ions of Group IVA, e.g. zirconium and hafnium, interfere strongly with the determination of thorium (a Zr:Th ratio of 6.5 gave an error of + 10 %). These interferences can be substantially reduced by scrubbing the organic extracts with a 0.5 volume of 4 M nitric acid.

TABLE 1

Maximum tolerable weight ratio of foreign ion to thorium, in the initial aqueous solution (Initial aqueous thorium concentration, $4 \cdot 10^{-4}$ M.)

Foreign ion (Me)	Me:Th	Foreign ion (Me)	Me:Th
Ce(III)	30	U(VI)	50
La(III)	30	Mn(II)	100
Fe(III)	120	Cu(II)	100
Cr(III)	112	Ni(II)	100

REFERENCES

1 M. Cospito and L. Rigali, Anal. Chim. Acta, 57 (1971) 107.
2 P. Gerontopulos and L. Rigali, Radiochim. Acta, 3 (1964) 122.
3 E. Cerrai and C. Testa, Anal. Chim. Acta, 26 (1962) 204.

Analytica Chimica Acta, 89 (1977) 399—402

Short Communication

REDUCTION OF TRACE METAL LEVELS IN ANALYTICAL-GRADE ACTIVATED CARBON

B. VANDERBORGHT and R. VAN GRIEKEN

Department of Chemistry, University of Antwerp (U.I.A.), B-2610 Wilrijk (Belgium)

(Received 4th August 1976)

The problem of removing trace amounts of metals from analytical-grade activated carbon (AC) arises in connection with its use as an adsorber to enrich chelated metal ions from aqueous solutions before analysis [1].

Reduction of trace metal levels in AC is largely a problem of the removal of the ash. In view of the possible adverse effects of the ash material on the adsorption properties, several demineralization procedures have been studied [2]; extraction with aqua regia, water, acetic acid, and acetone appeared to be inefficient. Korver [3], relying on earlier work by Miller [4], developed a procedure in which HF is allowed to act for several days at room temperature on the AC, which is then washed with HCl to remove insoluble fluorides, and with water. In a comparative study, Blackburn and Kipling [5] found this, in a slightly modified form, to be the best method.

The present communication discusses the influence of this procedure on the adsorption characteristics, ash content, and trace metal levels of analytical-grade AC. Hitherto there was no evidence that application of such a treatment might decrease further the trace metal levels in the purest commercial AC presently available without affecting the adsorption properties. Also quantitative information was not available on the concentration of the individual elements in the AC, although this information is essential in defining the sensitivities of analytical techniques applied to an AC matrix.

Experimental

Purification procedure. Commercial analytical grade AC with a very low ash content (0.4 %) was obtained from Baker Chemical Co. (no. 1991). Weighed AC samples (500 g) were put in polyethylene flasks together with a threefold excess of 48 % HF (Baker analytical grade no. 6013). The mixtures were continuously shaken for 72 h. After decantation of the HF, 1500 ml of 12 M HCl (p.a., Merck) was added and the samples were again shaken for 72 h to remove insoluble metal fluorides. After filtration of the HCl, the AC was washed with 20 l of cold deionized and doubly distilled water and subsequently with 40 l of hot water. The AC was finally dried at 110 °C for 48 h.

Results and discussion

Ash content. Ash contents were determined by ashing a given aliquot of AC in a low-temperature asher. The ash level of 0.4 % in the original commercial product appeared to be reduced by a single treatment to 0.05 %. Since inorganic matter is mainly contained in the ash of the AC, the ash content is an important criterion for the overall effectiveness of the purification.

Trace metal levels. Trace element concentrations in the AC before and after treatment were determined by neutron activation analysis in the reactor Thetis at Ghent (Belgium). Treated and untreated AC samples (1 g) were irradiated in a thermal neutron flux of 10^{12} n s^{-1} cm^{-2} together with suitable standards; the induced activities were measured by Ge(Li) γ-ray spectrometry (a) a few minutes after irradiation for 5 min, and (b) a few weeks after irradiation for 18 h. Detection limits for the analysis of short-lived isotopes in the treated AC were rather high because of the enlarged Compton scattering from Cl peaks. For some elements, only an upper limit of concentration can be given. The long-lived spectrum of the treated AC was characterized by several Br peaks. Results are given in Table 1.

To obtain optimal conditions of thickness and detection limits for analysis with x-ray fluorescence spectrometry, samples were ashed at low temperature, the ash was dissolved in ultrapure HNO_3, and evaporated on a Whatman filter. The filters were irradiated with Mo K_α and K_β x-rays. The induced characteristic x-rays were resolved and integrated by a Si(Li) semiconductor detector and multichannel analyzer. Results are included in Table 1.

Analysis by spark-source mass spectrometry was performed to obtain semi-quantitative information on the ratio of contamination before and after treatment. AC (300 mg) was ashed at low temperature, the ash was dissolved in ultrapure HNO_3, and mixed with suprapure graphite. The graphite mixture was pressed to form electrodes. Mass spectra were recorded photographically on Ilford Q2 photoplates. Manual analysis of the twelve different exposures on each plate gave an estimate of concentration ratios. These results are also given in Table 1. The impurity concentration ratios before and after the treatment are in reasonable agreement, and the absolute analyses by n.a.a. and x.r.f. compare well, except for the results for Fe and Zn which may suffer from some minor contamination.

Cl and Br concentrations appear to be higher in the treated than in the untreated AC through insufficient washing with water. The As impurity has been elevated, probably because of As contamination in analytical-grade HCl. For all other elements, a reduction of trace metal level, up to a factor of 200, is observed. On average, the proposed treatment appears to allow an impurity reduction by a factor of 5.

Adsorption properties. Although some authors (e.g. Frey, [6]) postulate some changes in physicochemical characteristics of the AC after treatment with strong acids (e.g. pore size enlargement, changes in surface complexes), alterations were not observed in this study. The CH_3COOH adsorption isotherms from water were measured before and after HF—HCl treatment. Both

TABLE 1

Trace metal levels (p.p.b.) in activated carbon before and after purification

Element	Neutron activation analysis (precision ≈ 10 %)			X-ray fluorescence (precision ≈ 20 %)			S.s.m.s.[a]
	Before	After	Before/ After	Before	After	Before/ After	Before/ After
Ag							7
Al	53000	<600	>88				
As	47	140	0.34	86	170	0.51	0.4
Au	0.2	0.2	1				
Ba	11900	4400	2.7				3
Br	341	3800	0.09				
Ca				149000	48000	3.1	3
Ce	300	230	1.3				
Cl	8800	730000	0.01				
Co	122	120	1				
Cr	1551	625	2.5	341	142	2.4	
Cs	7	5	1.4				
Cu	5500	<3600	>1.5	8100	1800	4.5	3.5
Eu	10.3	4.3	2.4				
Fe	178000	126000	14.2	95000	8400	11.4	
K				79000	4100	19	15
La	290	180	1.6				
Lu	2.4	1.4	1.7				
Mg	115000	<140000	>0.82				
Mn				29500	5900	5	6
Na	<2000	<4000					
Ni				1800	880	2	3
P							200
Pb				380	123	3.1	4
Rb				232	65	3.6	
Sb	57	51	1.1				
Sc	30.7	1.4	21.7				
Si							10
Sm	31	18.3	1.7				
Sr				2900	1100	2.6	3
Ti				11800	820	14	10
Th	21.6	17.7	1.2				
V	150	<43	>3.5				
Zn	1600	377	4.3	1400	700	2.0	3
Zr							3

[a] Spark-source mass spectrometry.

appeared to be identical. The specific surface, determined by N_2 adsorption from the gas-phase in a BET adsorption apparatus, also remained unchanged at 900 $m^2 g^{-1}$ after purification. Probably the reduction by 0.3 % of the already low ash content is not sufficient to cause physicochemical changes.

Conclusion

Without deterioration in the physicochemical properties of the AC, the proposed purification results in a reduction in the trace metal content of the purest commercially available charcoal by about a factor of 5 (except for Cl, Br and As). This purification will permit further reduction of the detection limits of analysis of trace metals after enrichment on AC.

The authors thank Prof. J. Hoste (Institute for Nuclear Sciences, Ghent State University) and Dr. R. Dewolfs (Department of Chemistry, University of Antwerp), for enabling the neutron activation analyses and specific surface determinations to be made.

REFERENCES

1 B. Vanderborght and R. Van Grieken, submitted to Anal. Chem.
2 J. J. Kipling, Q. Rev. Chem. Soc., 10 (1956) 1.
3 J. A. Korver, Chem. Weekbl., 46 (1950) 301.
4 E. J. Miller, J. Phys. Chem., 30 (1926) 1031.
5 A. Blackburn and J. J. Kipling, J. Chem. Soc., (1955) 4103.
6 H. Frey, Proc. Roy. Soc., A, 228 (1955) 510.

Analytica Chimica Acta, 89 (1977) 403—406

Short Communication

AIR SAMPLING METHODS FOR THE DETERMINATION OF SELENIUM

A. D. SHENDRIKAR* and PHILIP W. WEST

Environmental Sciences Institute, Coates Chemical Laboratories, Louisiana State University, Baton Rouge, La. 70803 (U.S.A.)

(Received 6th July 1976)

In an earlier study, selenium was found to be a common contaminant in filter papers [1]. This observation led to investigations of selenium concentration in cigarette papers and tobacco [2]. The presence of selenium in cigarette smoke was confirmed and must be considered a possible health hazard because of the known toxicity of selenium and its compounds [3]. Admittedly, selenium is also known to be an essential trace element. Inhalation, however, may produce toxic effects and should be contrasted with beneficial effects associated with ingestion. Further, it has been noted that vegetation has the ability to assimilate and in many cases concentrate selenium from soils [4]. Investigations of various plant materials have indicated that selenium is a common constituent of vegetation [5] and, therefore, it is present in most wood and wood products. Thus, wood burning, forest fires and incineration of trash can be sources of selenium emissions to the atmosphere.

The collection of air samples for selenium monitoring is a significant problem because of the known volatility of selenium compounds. Although not as volatile, generally, as the sulfur analogues, selenium compounds may exist as gases, liquids or solids. The solids are expected to have sufficient vapor pressures in many cases, to negate the use of filtration as a method of sample collection.

The literature provides relatively few reports of air sampling for measuring selenium levels [6]. In the past, electrostatic precipitators [7], filters [8] and liquid impingers [9] have been used to collect airborne selenium. Neutron activation methods [8] have been employed to determine selenium from air samples (via filters and aqueous bubblers) as well as from snow and rain. Pillay et al. [10], have used sequential tape samplers for collecting airborne selenium, and found that, on average, 56 % of the selenium was lost from filter material that retained nearly 100 % of other particulate species with diameters of 0.1 μm or greater.

*Present address: The Oil Shale Corporation, 18200 West Highway 72, Golden, Colo. 80401 (U.S.A.).

For about two years, air samples were collected routinely by passing the smoke resulting from trash burning into an impinger containing water which was subsequently analyzed for selenium. Concentrations as high as 273 $\mu g\ m^{-3}$ (expressed as selenium dioxide) were found when wood chips were burned [11]. Extended experiments showed that this method of trapping airborne selenium was very efficient. However, when samples were collected with high-volume samplers, serious losses of selenium occurred. The following results substantiate the fact that intolerable losses of selenium occur when filtration methods are employed.

Experimental

Samplers. A high-volume sampler equipped with an 8 × 10-in. filter holder was employed, together with a parallel system consisting of a Telematic sampler coupled with a 47-mm holder for membrane filters. The sampling rate for the high-volume sampler was 100 cu. ft. min^{-1} (2.83 $m^3\ min^{-1}$) while the rate for the Telematic sampler and the membrane filter was 0.0028 $m^3\ min^{-1}$. Fiber glass filters were used for the high-volume sampler studies, and Millipore filters for the low-velocity filtration experiments. Telematic samplers equipped with midget impingers were used for sampling studies involving scrubbing processes.

Procedure. The catalytic method developed by West and Ramakrishna [12] was used for the determination of selenium in smoke samples [11].

Results and discussion

In a series of smoke studies, selenium was sampled simultaneously by placing a high-volume sampler between two Telematic samplers. These experiments were performed to compare the efficiency of collection of the two sampling techniques. At the end of the sampling time, aliquots from the impingers were analyzed and yielded values of 67 and 49 $\mu g\ m^{-3}$ of selenium dioxide. An areal aliquot (weighed) of the fiber glass filter was equilibrated with 25 ml of deionized water for 30 min and filtered. The filtrate was boiled, cooled and made to a known volume, and selenium was determined. Based on the value obtained for selenium on this portion of the filter, the mass on the whole filter was calculated. The two fiber glass filters were found (each sampled for 15 min) to contain only 0.37 and 0.84 $\mu g\ m^{-3}$ of selenium dioxide.

On the basis of the discrepancies noted above, further studies of filtration versus solution impingement were undertaken. A mobile laboratory (Kem-Tech Laboratories, Inc., Baton Rouge) was equipped with the desired sampling devices. The mobile laboratory included a series of impingers which were capable of pulling smoke at the rate of 0.004 $m^3\ min^{-1}$. Three impingers were used in such a way that smoke would first pass through Millipore filters and then into impingers which contained water. At the end of the sampling time (30 min), the filters as well as aliquots from the impingers were analyzed. No selenium was found on any of the three filters by the catalytic method [12]

which has a sensitivity of 0.1 μg, while the impingers were found to contain 16.2, 15.4 and 6.1 $\mu g\ m^{-3}$ of selenium dioxide, respectively. The experiments clearly indicated that losses of selenium occurred if filtrations were used for its collection.

These initial findings led to a detailed investigation of the nature and rate of selenium losses during air sampling. The inlet to the impinger on a Telematic sampler was connected (by 8 in. of Tygon tubing) to a Millipore filter holder. The smoke which entered the nozzle of the holder was filtered and then bubbled through water to absorb the remaining selenium. At the end of the sampling time, the filter and the water from the impinger were analyzed for selenium. The data obtained (Table 1) indicate that selenium (as its oxides) is passed through the pores of the filters. The losses ranged from about 19 to 35 %, even with the low flow rate used for filtration for these studies.

The variation (Table 1) in the percentage loss of selenium oxides from the filter media may have been due to variations in the temperature of the smoke, the distance between the sampling unit and burning point source and resultant wind effects, densities of smoke or, obviously, variations in the selenium content of materials being combusted. It may also be assumed that initially a portion of the smoke containing selenium oxides was passing through the pores of the filter and subsequently was being trapped in the water. As the sampling time advanced, the pores of the filter paper became clogged (by dust and soot), thus restricting the amount of selenium that could escape. Alternatively, selenium oxides might be effectively collected on the surface of the filter paper, but because of their relatively high vapor pressure, they could be expected to volatilize during continued sampling. The problem of volatilization would be especially critical in the case of high-volume sampling.

To verify the latter thinking, experiments were run in which smoke samples were collected as described above, by filtration followed by scrubbing. After a fixed sampling period, the water from the scrubber was analyzed for selenium. The impinger was next recharged with fresh water and clean labora-

TABLE 1

Loss of selenium dioxide during low-velocity field sampling
(Sampling rate, 0.0028 $m^3\ min^{-1}$. Samples were collected by allowing the smoke (resulting from trash burning) to pass through Millipore or fiber glass filters in front of the Telematic impinger that contained water.)

Nature of filter	Total $\mu g\ SeO_2 m^{-3}$ on the filter	Total $\mu g\ SeO_2 m^{-3}$ in 10 ml water	Loss from filter (%)
Millipore	8.48	3.38	28
Fiber glass	11.49	2.67	19
Millipore	32.39	16.99	34
Fiber glass	29.97	11.16	27
Millipore	36.18	16.80	32
Millipore	21.92	11.66	35

tory air was pulled through the filters and scrubbed for 4 h. These experiments showed that selenium oxides do in fact come off the filters. It is especially significant that the use of impingers imposed a restriction on the rate of air flow used. However, even with an air flow through the filters and bubblers of only approximately a thousandth of that which passes through filters when high volume samplers are used, the losses averaged 40 %. Increasing the air flow a thousand-fold would obviously increase substantially the losses of volatile species, such as SeO_2, and invalidate any data based on high-volume sampling for selenium.

Conclusions

Selenium, an inorganic carcinogen can be present in the atmosphere, and should be monitored regularly. The conversion of selenium oxides to selenous or selenic acids in the humid atmospheres in the moist tissues of respiratory tracts must be regarded as a definite health hazard. Care must be taken in selecting sampling techniques since filtration has been shown to be ineffective. Impingement techniques are strongly recommended with water as an absorbent.

This investigation was supported in part by the U.S. Public Health Service Grant No. AP 00128, National Center for Air Pollution, Bureau of State Service and NSF Grant No. 138-99-833.

REFERENCES

1 P. W. West and C. Cimerman, Anal. Chem., 36 (1964) 2013.
2 P. W. West, S. L. Sachdev and A. D. Shendrikar, Environ. Lett., 2 (1972) 225.
3 E. P. Painter, Chem. Rev., 28 (1941) 179.
4 J. W. Hamilton and O. A. Beath, Agric. J., 55 (1963) 528.
5 I. Rosenfeld and O. A. Beath, Selenium, Academic Press, New York, 1964.
6 U.S. Department of Health, Education and Welfare, Preliminary Air Pollution Survey of Selenium and Its Compounds, 1969.
7 F. A. Patty (Ed.), Industrial Hygiene and Toxicology, Vol. II, 2nd edn. Interscience, New York, 1963, p. 887.
8 Y. Hashimoto and J. W. Winchester, Environ. Sci. Technol., 1 (1967) 338.
9 M. Kawamura and K. Matsumoto, Japan Analyst (Tokyo), 14 (1965) 789.
10 K. K. Sivasankara Pillay, C. C. Thomas Jr. and J. A. Sondel, Environ. Sci. Technol., 5 (1971) 74.
11 A. D. Shendrikar and P. W. West, Environ. Lett., 5 (1973) 29.
12 P. W. West and T. V. Ramakrishna, Anal Chem., 40 (1968) 966.

Analytica Chimica Acta, 89 (1977) 407—408

Short Communication

DETERMINATION OF PYRUVIC AND GLYOXYLIC ACIDS IN THE PRESENCE OF ACETALDEHYDE

H. A. SOKOL

Materials and Molecular Research Division, Lawrence Berkeley Laboratory, University of California, Berkeley, Calif. 94720 (U.S.A.)

(Received 3rd August 1976)

In the radiolysis of alanine and its derivatives, pyruvic acid, glyoxylic acid and acetaldehyde are often formed. These compounds are often measured by trace colorimetric methods. In one such procedure, carbonyl groups are treated with 2,4-dinitrophenylhydrazine (DNPH) under aqueous acidic conditions; when the solution is made alkaline, a quinoidal hydrazone derivative is formed. This chromophore has a characteristic maximum absorption at 450 nm which follows Beer's law. DNPH concentrations of 0.1—1 % in dilute aqueous HCl or methanol are usually used. These concentrations give complete reaction of carbonyl groups with DNPH, but high concentrations of DNPH reagent cause other problems. Some compounds are oxidized by DNPH. For example, amino-carbonyl compounds are oxidized to dicarbonyls [1]; aminoacetaldehyde is oxidized to glyoxal in this way. Further, the instability of the methanolic DNPH reagent solution, which is used by Lappin and Clark [2], probably indicates the formation of oxidized products. Another reason for avoiding high concentrations of DNPH is that organic acids and derivatives form hydrazides with DNPH [3] which interfere with carbonyl determinations by depleting reagent and forming hydrazide chromophores. In addition, DNPH in alkaline solutions gives undesirable high reagent backgrounds. Finally, if chloroform extracts are used in paper chromatography for carbonyl detection, the DNPH reagent is also extracted. The resulting DNPH-streaks on paper obscure the carbonyl spots. Identification of the spots is thus made much more difficult.

Efforts have been made in this laboratory to reduce DNPH concentrations after reactions with carbonyl compounds. Solvent extractions were tried, but separation of reagent from derivative was poor. Recently, it was found that much lower DNPH concentrations could be used for the assay of pyruvic and glyoxylic acids than was earlier believed possible. If the DNPH reagent solution were kept at 0.012 % rather than 0.1—1 %, Beer's law was followed for DNPH/carbonyl ratios of 3 : 1 and greater. Calibration curves for glyoxylic and pyruvic acid in this low reagent procedure were essentially identical. The molar absorptivity coefficient was 10 500 for each. Under

these conditions acetaldehyde reacted only slightly. Actually, the DNPH and NaOH concentrations and the aqueous media favor fading and instability of the acetaldehyde derivative [4—9]; its molar absorptivity coefficient here is 1500. (Formaldehyde does not interfere because it reacts very slightly with DNPH reagent at these low concentrations and its alkaline chromophore fades very rapidly.) In practice, the acetaldehyde content of a sample can be determined by the method of Johnson and Scholes [9] in which pyruvic and glyoxylic acids do not interfere and a correction for acetaldehyde can then be made.

If identification of the carbonyl—DNPH derivatives is desired, the extractions with chloroform are done in the usual way, but in this case the contamination by excess reagent will be greatly reduced.

A typical procedure for the determination of pyruvic and glyoxylic acids in a sample containing acetaldehyde, with 0.012 % DNPH reagent is as follows.

Procedure. To a 1-ml sample containing 0.03—0.2 μmol of pyruvic acid and acetaldehyde in 2 M HCl, and to a 1-ml carbonyl-free sample blank in 2 M HCl, add 1 ml of 0.012 % ($6 \cdot 10^{-4}$ M) DNPH in 2 M HCl. Leave the reaction mixture for 3 h at room temperature, and then add 6 ml of aqueous 10 % KOH. Measure the sample absorption versus the blank at 450 nm 5 min after the alkali addition.

On a separate aliquot of the sample, measure the acetaldehyde content of the sample by the Johnson—Scholes method [9]. Calculate the corresponding absorbance by the present low reagent procedure and subtract this from the total obtained by this same procedure. The resultant absorbance is used with a calibration curve for pyruvic or glyoxylic acid. The presence of pyruvic and/or glyoxylic acid can be confirmed by paper chromatography of the hydrazones.

The author is grateful to Dr. Warren M. Garrison for his helpful suggestions.

REFERENCES

1 W. C. Taylor Jr. and C. W. Moeller, Inorg. Chem., 4 (1965) 398.
2 G. R. Lappin and L. C. Clark, Anal. Chem., 23 (1951) 541.
3 W. J. P. Neish, Methods Biochem. Anal., 5 (1957) 107.
4 J. D. Roberts and C. Green, J. Am. Chem. Soc., 68 (1946) 214.
5 T. W. Goodwin and G. R. Williams, Biochem. J., 51 (1952) 708.
6 C. F. Wells, Tetrahedron, 22 (1966) 2685.
7 H. Böhme and O. Winkler, Z. Physiol. Chem., 296 (1954) 274.
8 H. Böhme and O. Winkler, Z. Anal. Chem., 142 (1954) 1.
9 C. R. A. Johnson and G. Scholes, Analyst (London), 79 (1954) 217.

Analytica Chimica Acta, 89 (1977) 409—412

Short Communication

INVESTIGATIONS ON THE REDOX CHARACTER OF DITHIZONE BY VOLTAMMETRIC METHODS
PART III. APPLICATION OF DITHIZONE AS AMPEROMETRIC TITRANT

L. TOMCSÁNYI

Research Institute for Non-Ferrous Metals, 1509 Budapest-XI (Hungary)

(Received 5th Janaury 1976)

The electrochemical redox properties of dithizone are governed by its thiol group and formazan structure, hence it can be both reduced and oxidized electrochemically. The electrochemical reduction of the azo group to hydrazo [1] and the electrochemical oxidation of thiol and formazan to a tetrazolium compound [2] can be utilized to follow the concentration of dithizone in aqueous solutions by polarographic or voltammetric methods. As dithizone forms complexes with 18 different metal ions [3], its electrochemical activity can be utilized in amperometric titrations of these metal ions. The "dithizone metals" can thus be determined simply and quickly; amperometric end-point detection requires less rigorous conditions than polarographic or voltammetric determinations of dithizone.

Because the solubilities of metal dithizonates in aqueous solutions are very small (about 10^{-8} M), these methods are very sensitive. End-point detection can be done in various ways depending on the electrode reaction selected (reduction or oxidation of dithizone), the electrode used, and the electrode potential, as well as on the electrochemical behaviour of the metal ion to be determined. The dropping mercury electrode (DME) or different carbon electrodes can be applied.

Titrations are done in aqueous solutions, but the dithizone solutions must be prepared in organic solvents which are miscible with water. Ethanol, propanol, propylene carbonate and acetonitrile were examined as solvents. The most suitable solvent is acetonitrile; $5 \cdot 10^{-3}$ M dithizone solutions can be prepared, whereas only 10^{-3} M solutions can be made with ethanol.

Experimental

Titrations were carried out automatically with a Radiometer PO4 polarograph combined with a Radiometer SBU1 microsyringe burette. The burette was driven through its flexible cable by the chart drive motor of the polarograph. A specially made ground-glass burette with a volume of about 10 ml was used to ensure a suitable titrant volume-chart length ratio. The prepar-

ation of the different electrodes has been described [2]. A stirring propeller was attached to the rotated CPE, to ensure thorough mixing.

All chemicals used were of analytical grade. For the preparation of the metal ion solutions, at least 4N-quality metals were dissolved in acids. Twice-distilled water was used for dilution. Dithizone solutions were prepared with deaerated solvents.

Amperometric titrations at the DME

As Kolthoff and Miller reported [4], mercury ions can be determined polarographically; the limiting current is proportional to the mercury concentration up to $2 \cdot 10^{-3}$ M. Several amperometric determinations of ions or compounds that form precipitates or complexes with mercury have been developed on this basis [5]. Obviously, mercury ions can also be determined with dithizone, different types of titration curve are obtained depending on the electrode potential selected, as dithizone is also electroactive.

If the electrode potential is such that dithizone is not electroactive, the titration curve is similar to Curve 1 of Fig. 1; only the mercury concentration is followed. At a more negative potential, the azo group of dithizone is also reduced and Curve 2 is recorded. At more positive potentials, the total current recorded comprises the anodic oxidation current of the dithizone thiol group and the cathodic mercury reduction current (Curve 3, Fig. 1). In all three cases, the end-point can be evaluated easily from the inflection points. Mercury(II) can be determined in the range $2 \cdot 10^{-6}$ M—$5 \cdot 10^{-5}$ M with relative errors less than ±5 %.

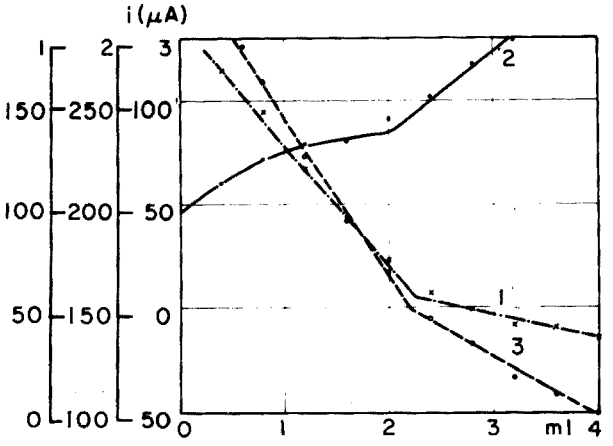

Fig. 1. Amperometric titration of mercury(II) at the DME. Curve 1, only Hg^{2+} is reduced. Curve 2, Hg^{2+} and dithizone (azo group) are reduced. Curve 3. Hg^{2+} is reduced and dithizone oxidized.

Other metal ions which form insoluble complexes with dithizone can be determined similarly. The time required for a titration is about 15 min, including the deaeration procedure needed with the DME.

Amperometric titrations at the rotating carbon paste electrode (RCPE)

The CPE can also be used for end-point detection, as the concentration of dithizone can be followed by this electrode [2]. The voltammogram for the oxidation of dithizone at the RCPE is shown in Fig. 2.

Over a considerable positive potential range, only the oxidation current of dithizone is measured, as dissolved oxygen and most metal ions are not electroactive; no deaeration is needed.

The titrations can be carried out continuously as the propellers attached to the RCPE stir the mixture effectively; thus the method can be automated very easily. A typical titration curve is shown in Fig. 3.

Mercury(II), zinc(II) and copper(II) were determined by such titrations; the media chosen to improve selectivity were 1 M H_2SO_4, 0.2 M sodium acetate, and 0.02 M HCl, respectively. Generally, the reproducibility (s_r) of the titrations was better than 5 % in the 10^{-5}—$2 \cdot 10^{-6}$ M range. A titration required only 3 min.

As practical examples, the mercury and zinc concentration of gallium and aluminium were determined. The results are summarized in Table 1. As aluminium and gallium do not react with dithizone, the "dithizone metal" content of these matrixes can be determined. The mercury content of gallium can be determined to a minimum of 0.5 %, and the zinc content of aluminium can be determined down to 0.05 %.

Methods of increasing the sensitivity of the titrations, and applications to other metals, are currently under study.

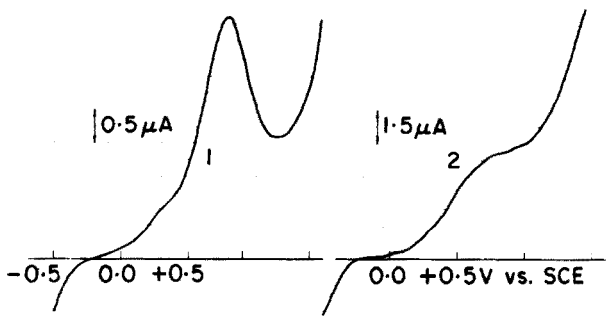

Fig. 2. Dithizone voltammograms at the CPE and RCPE in 0.2 M sodium acetate media.

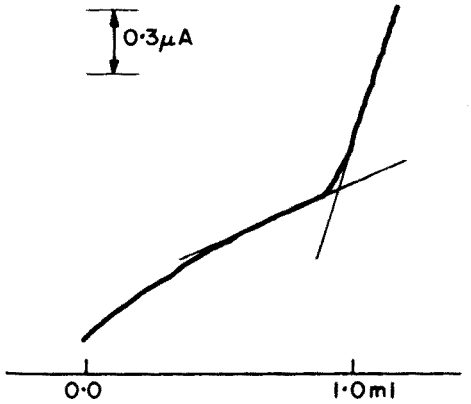

Fig. 3. Amperometric titration of zinc(II) at the RCPE.

TABLE 1

Amperometric titrations with dithizone at the RCPE

Ion	Range (M)	Matrix ion and conc. (M)	s_r (%)
Hg(II)	$5 \cdot 10^{-5}$	—	2
	$5 \cdot 10^{-5}$—$2 \cdot 10^{-5}$	—	5
	$5 \cdot 10^{-5}$—$2 \cdot 10^{-6}$	Ga 10^{-2}	5
Zn(II)	$5 \cdot 10^{-6}$	—	2
	10^{-5}	Al 10^{-2}	5
Cu(II)	$5 \cdot 10^{-6}$	—	2

REFERENCES

1 L. Tomcsányi, Anal. Chim. Acta, 70 (1974) 411.
2 L. Tomcsányi, Anal. Chim. Acta, 88 (1977) 371.
3 G. Iwantscheff, Das Dithizon und seine Anwendung in der Mikro- und Spuren-analyse, 2.Auflage, Verlag Chemie, Weinheim, 1972.
4 I. M. Kolthoff, and C. S. Miller, J. Am. Chem. Soc. 63 (1941) 2732.
5 J. T. Stock, Amperometric Titrations, Interscience, New York, 1965.

Analytica Chimica Acta, 89 (1977) 413—417

Short Communication

STOICHIOMETRY OF THE U_3O_8 PHASE FORMED DURING CALCINATION OF AMMONIUM URANATE

S. A. EL-FEKEY, M. Y. FARAH and N. H. ROFAIL

Nuclear Chemistry Department, Atomic Energy Establishment, Cairo (Egypt)

(Received 3rd May 1976)

Of the common non-stoichiometric oxides of uranium UO_2 and U_4O_9 have been widely studied [1] but U_3O_8 has been less extensively investigated [2]. A knowledge of the exact composition of the U_3O_8 phase, produced by calcination in air, is essential for (a) the determination of uranium in pure uranyl nitrate solutions [3, 4], ammonium uranates [5] and the crude uranium concentrate [6] known commercially as "yellow cake", (b) the determination of O/U in uranium dioxide powders [7], and (c) preparation of UO_2 pellets of controlled densities [8].

The physico-chemical properties of ceramic UO_2 nuclear fuel are governed by the history of ammonium uranate preparation, calcination and reduction [9—14]. The aim of this investigation was to study the effect of calcination regimes on the stoichiometry of the U_3O_8 phase produced by the thermal decomposition of ammonium uranate, which was prepared by precipitation with ammonia or urea at various solution pH.

Experimental

Uranate preparation via ammonia gas. Nuclear-pure uranyl nitrate solution, refined from crude uranium concentrate by counter-current extraction through tributyl phosphate [15], and containing 70 g U/L and 0.02—0.04 M free nitric acid, was heated to 80 °C. Air-diluted ammonia gas was bubbled through the solution for 20 min while stirring the slurry vigorously. After stirring for an additional 15 min, the pH was adjusted to 6.0, 7.0, or 8.0 with ammonia gas or AnalaR ammonia liquor. The precipitate was collected on a Buchner funnel and washed with distilled water, alcohol, and acetone, respectively, then dried at 45 °C for 24 h.

Uranate preparation via urea. Ammonia solution was added to the uranyl nitrate solution to increase the pH to 2.8. The solution was stirred vigorously and heated to 95 °C. Uranium was precipitated by adding one volume of urea solution (500 g l^{-1}), to two volumes of uranyl nitrate solution (145 g uranium l^{-1}). The temperature was kept at 95 °C throughout. Precipitation was allowed to continue to pH 6. The precipitate was filtered off immediately, washed with water, alcohol, and acetone, then dried at 45 °C for 24 h. The

mode of preparation of the five ammonium uranate preparations is given in Table 1.

Calcination. A sample layer, 0.3 or 1.5 cm thick, was placed on a stainless steel tray and ignited in a muffle furnace at temperatures ranging from 400 to 900 °C for different durations.

O/U ratio determination. The stoichiometry of the U_3O_8 phase was determined titrimetrically with cerium(IV) sulphate. A precisely weighed quantity (ca. 250 mg) of oxide powder with a mean particle diameter below 30 μm, as determined by the Andreason pipette [9], was dissolved in an excess of acidified 0.1 M cerium(IV) ammonium sulphate in 1.5 M sulphuric acid; the excess was determined by back-titration with freshly prepared iron(II) ammonium sulphate solution, using ferroin as indicator [16]. Three to eight determinations were performed on each sample.

Results and discussion

Table 2 shows that the O/U ratio of the intermediate uranium oxides, formed during thermal decomposition of samples 1 and 5 (0.3- and 1.5-cm thick layers), at temperatures ranging between 400 and 900 °C in air, varied between 2.961 and 2.618. The temperature of 400 °C was used as a starting temperature for calcination because in the vicinity of this temperature a sharp drop in the concentration of ammonia in the solid occurs with a simultaneous increase in the concentration of the reduced uranium [17]. On heating the uranate in air, an appreciable part of the ammonia is retained by the solid and a little ammonia is evolved [17]. The amount of U(IV) formed depends on the rate of heating, amount of occluded nitrate ions, atmosphere, thickness of uranate on trays, cooling, etc. [8, 18]. Table 2 indicates that more than 25 % of the uranium is reduced, even during heating of thick layers of different uranates at 400 °C for 1 h at a heating rate of 20 °C min^{-1}; this results from the incomplete oxidation of ammonia with atmospheric oxygen. By infrared spectra Price explained the detailed interaction steps that might occur in this stage [18],

The amount of reduced uranium in thick calcined layers is generally greater than in thin ones, presumably from cracking of the liberated ammonia retarded from evolution within the thicker layer. Reduction of UO_3 by

TABLE 1

Classification of samples

Sample	Mode of preparation
1	Precipitation by ammonia gas up to pH 8
2	Precipitation by ammonia solution up to pH 8
3	Precipitation by ammonia solution up to pH 7
4	Precipitation by ammonia solution up to pH 6
5	Precipitation by urea up to pH 6

TABLE 2

Effect of calcination temperature on the O/U ratio[a] of the U_3O_8 phase

Class of sample	Thickness of layer (cm)	Temp. ±10 °C	O/U ratio of oxides after			
			1 h	3 h	6 h	9 h
1	1.5	400	2.827	2.773	2.761	2.713[b]
5	1.5	400	2.961	2.940	2.789	2.765
1	0.3	500	2.816	2.771	2.761	2.764
1	1.5	500	2.781	2.658	2.690	2.682
5	0.3	500	2.809	2.761	2.755	2.750
5	1.5	500	2.782	2.715	2.688	2.679
1	0.3	600	2.682	2.669	2.662	2.662
1	1.5	600	2.668	2.663	2.666	2.644
5	0.3	600	2.644	2.671	2.666	2.665
5	1.5	600	2.651	2.653	2.663	2.668
1	0.3	700	2.634	2.627	2.627	2.634
1	1.5	700	2.628	2.644	2.635	2.645
5	0.3	700	2.652	2.645	2.645	2.636
5	1.5	700	2.645	2.618	2.618	2.619
1	0.3	800	2.651	2.650	2.633	2.618
1	1.5	800	2.651	2.645	2.642	2.619
5	0.3	800	2.640	2.640	2.634	2.624
5	1.5	800	2.641	2.639	2.633	2.615
1	0.3	900	2.649	2.647	2.648	2.648
1	1.5	900	2.649	2.649	2.643	2.646
5	0.3	900	2.643	2.645	2.641	2.648
5	1.5	900	2.642	2.648	2.648	2.649

[a]Average of 3 independent estimations. [b]The standard deviation on the average = ± 0.004.

evolved ammonia was also proposed by Notz et al. [19]. Above 700 °C, the U_3O_8 phase is significantly oxygen-deficient; below 500 °C the U_3O_8 phase is oxygen-rich with an O/U ratio greater than 2.667, a result which agrees with that of other workers [2].

The UO_3 used as a starting material for U_3O_8 preparation in the experiments reported in Table 3 was prepared by heating the different uranate samples slowly up to 350 °C for 9 h to allow reaction of the ammonia with atmospheric oxygen before auto-reduction, i.e. before reaction of the retained ammonia with the UO_3 [18]. The NH_4/U ratio in this oxide does not exceed 0.016 [15], while the value of x in the original uranate samples represented by the molecular formula $UO_2(OH)_{2-x}(ONH_4)_x zH_2O$ continuously varies, according to precipitation and washing conditions [17, 18] within the limits of 0—0.7. The method of preparation of β-UO_3 by calcining the uranate at 520 ± 5 °C as reported by Ramakrishnan [16] was not used because it is generally agreed that β-UO_3 decomposes around this temperature to give U_3O_8 [20]. Calcination of the present UO_3 at temperatures varying between 600 and 800 °C leads to U_3O_8 oxides in which the difference between

TABLE 3

Calcination effect on O/U ratio[a] of the U_3O_{8-z} phase formed by decomposing UO_3 of various origins in a stream of air

Starting material	Layer thickness (cm)	O/U ratio of oxides formed at					
		600° 3 h	600° 9 h	700° 3 h	700° 9 h	800° 3 h	800° 9 h
Sample 1	0.3	2.663	2.662	2.670	2.662	2.668	2.670
Sample 1	1.5	2.663	2.662	2.662	2.663	2.666	2.662
Sample 2	1.5	2.665	—	2.666	—	2.666	—
Sample 3	1.5	2.671	—	2.668	—	2.666	—
Sample 4	1.5	2.666	—	2.662	—	2.663	—
Sample 5	1.5	2.668	2.667	2.671	2.668	2.662	2.665

[a]Average of 3 independent estimations.

the average and the true $UO_{2.667}$ is not more than ±0.005. This confirms that during calcination of uranates (in one step) the ammonia present in the original uranate samples induces self-reduction to varying extents depending on the nature of the uranate used. This leads to non-stoichiometric products.

On heating uranate layers, 1.5-cm thick, containing 10 and 20 % by weight of solid ammonium nitrate, after mixing well at temperatures varying between 600 and 800 °C, $UO_{2.667}$ is formed through the oxidation of ammoniates (Table 4). The work of many investigators [2, 16, 21] shows that the stoichiometry of the U_3O_8 phase depends strongly on temperature and as the surface area of this oxide decreases from ca. 7 $m^2 g^{-1}$ at 600 °C to

TABLE 4

Effect of ammonium nitrate addition on O/U ratio[a] of intermediate uranium oxides

Starting material	Temp. ±10 °C	O/U ratio after addition of	
		10 % NH_4NO_3	20 % NH_4NO_3
Sample 1	600	2.666 ± 0.0022	2.666 ± 0.0022
Sample 1	700	2.665 ± 0.0024	2.666 ± 0.0022
Sample 1	800	2.665 ± 0.0022	2.666 ± 0.0022
Sample 2	600	2.666 ± 0.0022	2.666 ± 0.0023
Sample 3	600	2.666 ± 0.0024	2.666 ± 0.0022
Sample 4	600	2.666 ± 0.0022	2.666 ± 0.0022
Sample 5	600	2.666 ± 0.0022	2.666 ± 0.0023
Sample 1	900	2.660 ± 0.0023	2.661 ± 0.0022
Sample 3	900	2.659 ± 0.0022	2.659 ± 0.0022
Sample 5	900	2.658 ± 0.0022	2.659 ± 0.0022

[a]Average of 6—8 independent estimations; the precision compares favourably with that of Ramakrishnan [16].

ca. 1 m^2 g^{-1} at 900°C because of micro-sintering [15], its reactivity also decreases and non-stoichiometric U_3O_8 is formed at 900 °C. When this U_3O_8 is reheated with 10 % ammonium nitrate for 3 h, $UO_{2.666 \pm 0.002}$ is obtained.

There is some doubt concerning the actual composition reported in previous studies. The removal of occluded nitrate from uranate by washing with distilled water, alcohol, and acetone, followed by drying, is necessary before gravimetric estimation in order that an exact dry weight of uranate, free from impurities, can be taken. The procedure recommended implies the addition of 10 % by weight of solid AnalaR ammonium nitrate and subsequent calcination to 600—800 °C for 3 h, instead of the conventional gravimetric procedure involving calcination at 1070—1270 K [22].

REFERENCES

1 Thermodynamics and Transport Properties of Uranium Dioxide and Related Phases, International Atomic Energy Agency: Vienna, Technical Reports Series No. 39 (1965).
2 R. J. Ackermann and A. T. Chang, J. Chem. Thermodyn., 5 (1973) 873.
3 Springfields Works, PG Reports 133S (1960), 213S (1961) and 261S (1962).
4 O. A. Vita, C. R. Walker and E. Litteral, Anal. Chim. Acta, 64 (1973) 239.
5 Springfields Works, SCS-M-9A Report (1959) and PG Report 219S (1963).
6 Springfields Works, PG Reports 128 (1960), 1020 (1971).
7 T. M. Florence, Analytical Methods in the Nuclear Fuel Cycle, IAEA-SM-149/64 (1972).
8 M. Y. Farah, S. A. El-Fekey and F. H. Hammad, A. F. Bishay, 1st European Nuclear Conference TANSAO 20, Paris (1975) 607.
9 M. Y. Farah and S. A. El-Fekey, Arab J. Nucl. Sci. Appl., 8 (1975) 67.
10 M. R. Zaki, M. Y. Farah and S. A. El-Fekey, 8th International Mineral Processing Congress, P.E-3, Leningrad (1968).
11 M. Y. Farah, M. R. Zaki and S. A. El-Fekey, Thermal Analysis, 2, Academic Press, New York, 1969, 1475.
12 M. Y. Farah et al., 4th United Nations International Conference on the Peaceful Uses of Atomic Energy, A/CONF. 49/P/146 Geneva (1971).
13 M. Y. Farah and S. A. El-Fekey, Acta Chim. Acad. Sci. Hung., 85 (1975) 383.
14 M. Y. Farah and S. A. El-Fekey, Recent Advances in Science and Technology of Materials, 3, Plenum Press, New York, 1974, 343.
15 S. A. El-Fekey, M.Sc. and Ph.D. Theses, Cairo University (1967, 1972).
16 E. S. Ramakrishnan, Anal. Chim. Acta, 67 (1973) 209.
17 G. H. Price, J. Inorg. Nucl. Chem., 33 (1971) 4085.
18 G. H. Price and W. I. Stuart, AAEC/E 276 (1973).
19 K. J. Notz, M. G. Mendel, C. W. Huntington and T. J. Collopy, U.S. Rep. T.I.D. (1960) 6228.
20 J. L. Woolfrey, AAEC/TM 476 (1968).
21 A. R. Dharwadkar and M. S. Chandrasekaraiah, High Temp. Sci., 5 (1973) 5.
22 E. H. P. Cordfunke, The Chemistry of Uranium, Elsevier Publishing Company, New York, (1969) 233.

Analytica Chimica Acta, 89 (1977) 419—421

Short Communication

ADAPTATION OF THE SCHLIEREN OPTICAL SYSTEM OF A PREPARATIVE ULTRACENTRIFUGE TO 35-mm PHOTOGRAPHY

T. G. SMYRL, F. H. WOLFE and M. LeMAGUER

Department of Food Science, University of Alberta, Edmonton, Alberta (Canada)

(Received 19th July 1976)

The conversion of the schlieren optical attachment of a preparative ultracentrifuge to accommodate a 35-mm single lens reflex camera is described. The advantages of this adaptation lie in the very sharp photographs of the schlieren image, a precise method of analyzing the schlieren images, simultaneous capability of recording and observing the schlieren image, and rapid recording of successive photographs.

Construction

The adaptation to 35-mm photography is shown in Fig. 1. The optical tower of the schlieren attachment of the Beckman Model L2-65 Preparative Ultracentrifuge is represented by A. The tower attachment, B, is mounted on the tower with the existing facilities for the standard Polaroid attachment. The outer edge of B is threaded so that D, the camera adaptor, can be screwed onto and over B. A double convex lens, C, with a focal length of 20 cm is positioned between B and D. The outer side of B and the inner surface of D are tapered to accommodate the curvature of the double convex lens, C. The camera mount, E, slides horizontally onto the barrel of D. The right-hand

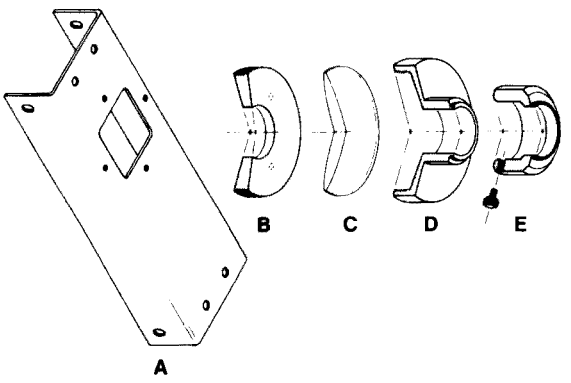

Fig. 1. Camera modification. A, optical tower; B, tower attachment; C, double convex lens; D, camera adaptor; E, camera mount.

section of the camera mount is threaded to accept a Miranda Sensorex 35-mm single lens reflex (s.l.r.) camera body, but any s.l.r. camera mount can be adapted. The camera mount can be securely fastened to D with the tightening nut on the camera mount.

Operation

During an experiment in which the schlieren patterns are monitored with time, the light source which is located in the base of the tower is kept illuminated at all times. One preliminary run is required to ascertain the correct camera shutter speed for the light sensitivity of the 35-mm film used. Generally it was found that a shutter speed of 1/8 s was suitable when Tri-X film (400 ASA) was used. To maximize the image sharpness as viewed through the camera viewer, the camera mount was moved horizontally along the barrel of D and then secured tightly onto D with the tightening nut. Once the correct shutter speed and camera position had been determined, no further adjustments were required unless a film of different ASA was used. Following a schlieren pattern with time consisted simply of advancing the film and taking photographs at the times desired.

Discussion

Conversion of the schlieren optical attachment of the Beckman Model L2-65B Preparative Ultracentrifuge to 35-mm photography offers several advantages over the standard Polaroid attachment. With the standard Polaroid attachment, the time of exposure of the film to the light is regulated by switching the light source on and off. When double sector cells are used, up to 10-s exposure time may be required [1]. Exposure times of this duration do not yield sharp photographic images of a rapidly changing schlieren pattern, e.g. the height of the schlieren peak may decrease by 5 % in a 10-s period in the diffusion of small molecules. However, when a fast film is used with the 35-mm adaptation, very short exposure times are required, and very sharp photographs of the schlieren image can be obtained. In addition, the only preparation required for the next photograph is to advance the film to the next frame. This time advantage is essential when D values of small molecules are measured.

Generally, measurements on the photographic images of optical patterns formed in the ultracentrifuge are carried out with an optical microcomparator [2] or analogously on tracings of the schlieren image made under an enlarger. According to Schachman [3], measuring schlieren patterns which have been enlarged by a factor of five is comparable to using a microcomparator. Since very clear and sharp images are obtained with the 35-mm system, magnifications of up to 40× yield very clear enlargements of the schlieren image with very little distortion. Magnifications to this extent were obtained by mounting the 35-mm negatives in glass slide mounts and using a commercial slide projector to project the images onto a vertical scale. Since the 35-mm negatives may be enlarged by a factor of 40 without serious distortion of the

schlieren image, the magnitude of the relative error on image measurements is minimized. The importance of precise peak height measurements in determining accurate and precise diffusion coefficients by the ultracentrifugal technique has been discussed by LeMaguer et al. [4].

The adaptation to 35-mm photography offers the convenience of being able to observe and record schlieren images simultaneously. Such a feature as constant viewing is useful, for example, to ensure that schlieren peaks are not recorded during a free diffusion experiment when the point of restricted diffusion is reached. With the unmodified system, if further viewing is desired once the Polaroid camera has been installed, the camera must be removed and replaced with the viewing apparatus.

The ability of the 35-mm s.l.r. camera to advance the film rapidly makes it possible to reduce the time between successive photographs to seconds. This has proved useful in monitoring boundary formation in the valve-type synthetic boundary cell and the double-sector capillary synthetic boundary cell [4].

The authors are grateful to the National Research Council of Canada for financial support and to the Photo Services Division of the University of Alberta.

REFERENCES

1 Beckman Instruction Manual, Spinco Division, Beckman Instruments, 1969.
2 C. H. Chervenka, A Manual of Methods for the Analytical Ultracentrifuge, Spinco Division, Beckman Instruments, 1969.
3 H. K. Schachman, in S. P. Colowick and N. D. Hepler (Eds.), Methods in Enzymology, Vol. 4, Academic Press, New York, 1957, pp. 32—103.
4 M. LeMaguer, F. H. Wolfe and T. G. Smyrl, AIChE, J., 22 (1976) 389.

Analytica Chimica Acta, 89 (1977) 423—426

Book Reviews

G. Svehla (Ed.), *Wilson and Wilson's Comprehensive Analytical Chemistry, Volume V. Emission Spectroscopy, Analytical Microwave Spectroscopy and Analytical Applications of Electron Microscopy*, Elsevier, Amsterdam, 1975, xiv + 374 pp., price U.S. $51.95; Dfl. 125.00.

This volume contains three chapters that deal with techniques which have been neglected to some extent in recent years. As is customary in this series, the aim is to provide a self-sufficient reference work with a blend of essential theory and applications, which should provide the reader with a suitable starting point for an analytical investigation.

The chapter on emission spectroscopy by T. Kantor occupies 193 pp. and gives 291 references; two of these are to work published in 1974, and there is reference to a book printed in 1973, but no other reference to original work is more recent than 1970. Analytical microwave spectroscopy is dealt with concisely by J. Sheridan in 42 pp.; none of the 70 references cited is more recent than 1971. The chapter on analytical applications of electron microscopy by J. Beretka occupies 122 pp. and presents 149 references, of which 7 are to work published in 1971. Features of this chapter are an 11-p. table which lists the electron microscopes, scanning electron microscopes and electron probe microanalyzers that are available commercially, and a large number of reproductions of plates showing transmission and scanning electron micrographs from a variety of sources.

In terms of the quality of its technical presentation and production, this volume maintains the high standards set by earlier volumes. There are two problems for the reviewer: how to comment on the price, which seems high even when viewed strictly in terms of hard currencies, and how to comment on the out-of-date appearance of the content of this book. The editor's preface is dated November 1974; the book was published late in 1975. Perhaps it is the old story of some chapters being submitted by a pre-arranged date, and being held up by the late submission of other chapters. Who knows? Probably only the editor and authors. Who cares? Probably only the subscribers. May the fact that the subscription price carries a discount of about 15 % prove sufficient solace! It seems unlikely that many who are not committed subscribers will contemplate purchase.

D. M. W. Anderson

G. Svehla (Ed.), *Wilson and Wilson's Comprehensive Analytical Chemistry, Vol. VI*, by K. Kiss Eröss, *Analytical Infrared Spectroscopy*, Elsevier, Amsterdam, 1976, xiv + 555 pp., price Dfl. 190; U.S. $76.50.

This book, the sixth volume of Comprehensive Analytical Chemistry, is devoted wholly to analytical infrared spectroscopy and is written by a single author. It begins with a short historical survey and a list of symbols and abbreviations. Thereafter there are chapters on Theory (78 pp.), Apparatus (77 pp.), Experimental Techniques (48 pp.), Qualitative Analysis (176 pp.), Quantitative Analysis (47 pp.), Possible Applications (39 pp.) and a guide to the literature.

It will be seen that the coverage is very wide, bearing in mind that most of these topics are themselves the subject of individual specialist monographs. The author is therefore restricted to a broad review and denied the opportunity to include much detail. For example, he is able to give only a very cursory treatment to interferometric or to far-infrared spectroscopy. Within these limitations, he and the editor have done a good job and the text is well written and clearly presented. Much of the material covered is dealt with in about the same depth in a number of earlier review volumes but the present text does include detailed specifications and optical diagrams of many commercial spectrometers and a substantial number of references to specific industrial applications. The book itself has a strongly familiar look. This is traceable to the use — with of course acknowledgements — of many illustrations and tables from earlier texts. Thus the chapter on Qualitative Analysis contains 28 illustrations of which 18 are reproduced from the text of Jones and Sandorfy and 10 others from three other texts. It also includes 50 pages of tables reproduced from Cross, and from Jones and Sandorfy. Similarly the chapter on Theory has 45 illustrations of which 41 come from other texts — in this case mainly from Herzberg.

The price of the book (over £40) is such as to put it beyond the reach of most students, and indeed of many of their teachers. The main customers must be librarians who must decide whether it is worth their while to spend so much on a review volume which contains little that is not already somewhere within the covers of books already on their shelves. I fear the decision of many will be that it is not worth their while, which is hard on the author who has worked hard to present a capable text.

L. J. Bellamy

H. Engelhardt, *Hochdruck-Flüssigkeits-Chromatographie (HPLC), Anleitungen für die chemische Laboratoriumspraxis, Band 14*, Springer Verlag, Berlin, 1975, x + 213 pp., price, DM 56.

This book appears in a series of monographs intended for practical chemists. It gives a survey of the possibilities and fields of application of high-pressure

liquid chromatography. This new technique permits the separation of nearly all soluble chemicals known, and is especially useful for products that are temperature-sensitive or have high melting points. Although the high speed of this technique is an advantage mainly on the analytical scale, preparative separations are also possible.

In line with the general aim of the series, the bulk of this book is concerned with practical considerations, and there is a minimum of theoretical treatment. The first two chapters (29 pp.) present a brief historical introduction, followed by a short exposition of the basic concepts of chromatography. The next two chapters (44 pp.) describe the apparatus needed for high-pressure liquid chromatography. The discussion of the different components is detailed, and provides guidelines to assist the reader in making the proper selection for his own needs. Twenty pages are devoted to detectors, emphasizing the importance and variety of these devices. Chapter 5 (16 pages) reviews the column packings, with a detailed examination of chemically modified and bonded phases, a topic which is a specialty of Saarbrücken University.

Chapters 6—12 (113 pp.) deal with the practical application of liquid chromatographic techniques. Adsorption, liquid-partition, ion-exchange, and molecular-sieve chromatography are discussed in detail and presented clearly enough that even a beginner should be able to choose the best method to solve his problem. A critical examination of the parameters which lead to errors or bad reproducibility helps the analyst to obtain rapid, convenient and precise analytical conditions. The illustrations of applications are carefully presented and chosen from various fields of chemistry. Other illustrations are sparse, but lists of recent references for each chapter provide good documentation.

Although, as the author states, "In a field with so many rapid new developments, nearly each page could be supplemented continuously", this book will remain for many years a good practical introduction to high-pressure liquid chromatography.

W. Haerdi

Bibliography of Electrophoresis, 1968—1972, and Survey of Applications, Z. Deyl, J. Kopecky, J. Davidek, M. Juricova and R. Helm (Eds.), Elsevier, Amsterdam, 1975, xiv. + 861 pp., price U.S. $83.50, Dfl. 200.

This book, another Supplementary Volume (Number 4 for 1975) of *Journal of Chromatography*, is quite simply a catalogue of authors' names, titles of papers, and references with complete indexes and a lot of cross-referencing. The details given below may help those able to propose its acquisition by a library that does not subscribe to the *Journal of Chromatography*; binding would be essential for the survival of this heavy, paper-backed book in a busy library.

This bibliography covers the electrophoretic procedures published in over 90 journals between January 1968 and December 1972. This massive task was undertaken by a Czechoslovakian team of editors and assistants; their introduction was dated April 1973, and so they wasted no time. The period thereafter, until publication late in 1975, was presumably involved in translation and production, both of which are superb.

For electrophoresis, the 1968—1972 period saw the publication of very little methodology and a great deal of applications which are listed under a sensible system of sub-divisions. Readers of this book will find the answers to questions such as: which studies were concerned with a specific separation of a group of substances or particular compound? Which papers were contributed by a particular author? Which solvents and/or media were used for a particular task?

There is no doubt that the editors, publishers, and all those concerned with this book deserve praise. The main question — apart from the vexed one of cost (and the people involved in digging this stuff out of the literature deserve reasonable financial recompense for their dreary task) is whether this sort of information on 1968—72 material is scientifically valuable in 1976. Were all the workers actively involved in electrophoresis in the interim waiting for a bibliography to appear? Perhaps a smaller, annual compilation, published not more than a year after the appearance of the original papers, would be more manageable production-wise and more viable economically. It would certainly be more useful scientifically. This is too much, too late.

Analytica Chimica Acta, 89 (1977) 427

ERRATA

M. Varadi, M. Gratzl and E. Pungor, Turbulent Hydrodynamic Voltammetry. Part II. Investigations of Turbulence Frequency in a Hydrodynamic Voltammetric Cell, *Anal. Chim. Acta*, 83 (1976) 1—8.

Equation (4) on page 6 of this paper should read:

$$\bar{i}_{df}(\nu) = \frac{A_R nFDC(E)^{1/2} p}{\pi(2)^{1/2} \delta_m^2} \nu^{-1}$$

D. R. Christmann and J. D. Ingle Jr., Problems with sub-p.p.b. Mercury Determinations: Preservation of Standards and Prevention of Water Mist Interferences, Anal. Chim. Acta, 86 (1976) 53—62.

On page 61, Table 4, between rows '10% (v/v) HNO_3 + 16 p.p.b. Au(III)' and '0.01% (w/v) H_2O_2 (pH_4)', aligned beneath '1 p.p.b. Hg solution', the heading '0.1 p.p.b. Hg solution' should be inserted.

ANALYTICA CHIMICA ACTA, VOL. 89 (1977)

AUTHOR INDEX

ANALYTICA CHIMICA ACTA, VOL. 89 (1977)

SUBJECT INDEX

(continued from page 4 of cover)

Short Communications

PRINTED IN THE NETHERLANDS

VOL. 89 No. 2 ANALYTICA CHIMICA ACTA APRIL 1977

CONTENTS

(continued on inside page of the cover)